University of Glasgow

Alshuwayer, Noha Ali (2024) *Elucidation of the role of methylarginine metabolism in regulation of nitric oxide production and inflammation.* PhD thesis.

https://theses.gla.ac.uk/84545/

Copyright and moral rights for this work are retained by the author

A copy can be downloaded for personal non-commercial research or study, without prior permission or charge

This work cannot be reproduced or quoted extensively from without first obtaining permission from the author

The content must not be changed in any way or sold commercially in any format or medium without the formal permission of the author

When referring to this work, full bibliographic details including the author, title, awarding institution and date of the thesis must be given

Enlighten: Theses
https://theses.gla.ac.uk/
research-enlighten@glasgow.ac.uk

Elucidation of the Role of Methylarginine Metabolism in Regulation of Nitric Oxide Production and Inflammation

Noha Ali Alshuwayer MBBS, M.Sc.

This thesis is submitted for the degree of Doctor of Philosophy

University of Glasgow

College of Medical, Veterinary and Life Sciences

January 2024

© N A Alshuwayer

Abstract

Atherosclerosis is a major global health issue, and inflammation is important in its pathogenesis. Many atherosclerosis risk factors lead to reduced nitric oxide (NO) bioavailability. Asymmetric dimethylarginine (ADMA), an independent cardiovascular disease risk factor and NO synthase inhibitor, is metabolised by dimethylarginine dimethylaminohydrolase (DDAH). DDAH2 is the isoform present in the immune system. A deeper understanding of ADMA metabolism could help reveal new therapies for atherosclerosis. However, it is debated if DDAH2 hydrolyses ADMA. There is evidence that DDAH2 has NO-independent cellular functions, and research in our group showed that DDAH2 regulates macrophage functions.

This thesis initially aimed to investigate the role of DDAH2 in regulating inflammation in atherosclerosis models. However, this was derailed by limitations imposed by the Covid-19 pandemic. Therefore, models of inflammation were used. Genes and mechanisms associated with inflammation and atherosclerosis were investigated.

RAW 264.7 murine macrophage cell line and bone marrow-derived macrophages (BMDM) were validated for suitability to study the DDAH-ADMA-NOS pathway. To better understand the functions of DDAH2, a macrophage-specific *Ddah2* null mouse model was re-derived and validated. RNA sequencing data previously generated by our group from peritoneal macrophages of the same model was re-analysed and revealed almost 5,000 genes to be DDAH-dependent and required for normal immune response. More than 200 Reactome pathways appeared enriched, with apoptosis being the most enriched. The *in silico* data was validated *in vitro* in DDAH2-knockout peritoneal macrophages from the macrophage-specific *Ddah2* null mouse model. Inferred hypotheses were investigated in DDAH2-Knockout BMDMs from the macrophage-specific *Ddah2* null mouse model with confirmatory studies on C57BL/6J BMDMs using ADMA.

The *in vitro* analysis in the BMDMs showed no conclusive evidence supporting the *in silico* data that DDAH2 regulates the investigated genes (except *Il17a*), nor did ADMA alter the gene response to LPS. *Il17a* was shown by the *in silico* analysis to be regulated by DDAH2 and was validated *in vitro* in peritoneal macrophages by

both RT-qPCR and ELISA. Given the significant role of IL17A in inflammation and its existing use in treating systemic inflammatory conditions such as psoriasis, this thesis proposes DDAH2 as a potential therapeutic target for inflammatory diseases in general and atherosclerosis in particular.

Table of Contents

Abstract		2
List of Tables		8
List of Figures		9
Publications		12
Acknowledgement		13
Author's Declaration		14
List of Abbreviations and Acronyms		15
Chapter 1	General Introduction	20
1.1	Atherosclerosis	20
1.1.1	Introduction	20
1.1.2	Historical perspective	20
1.1.3	Risk factors	22
1.1.4	Pathophysiology	22
1.2	Immune system	26
1.2.1	Types of immunity	27
1.2.2	Macrophages	28
1.2.3	Activation of the innate immune system	29
1.2.4	Macrophage classification	31
1.2.5	Macrophages in atherosclerosis	32
1.3	Nitric Oxide	34
1.3.1	Nitric oxide properties	35
1.3.2	Nitric oxide synthase pathway	36
1.3.3	Nitric oxide in atherosclerosis	38
1.4	Asymmetric dimethylarginine	39
1.4.1	ADMA synthesis and clearance	39
1.4.2	ADMA and disease	42
1.5	Dimethylarginine dimethylaminohydrolase	43
1.5.1	Isoforms	44
1.5.2	Activity	44
1.5.3	DDAH2 gene polymorphisms	45
1.5.4	Functional studies	46
1.6	Hypothesis and aims	51
1.6.1	Hypothesis	51

1.6.2 Aims 51
Chapter 2 Materials and methods 52
2.1 Materials 52
2.1.1 Mice 52
2.1.2 Cells 52
2.1.3 Reagents 53
2.2 Methods 55
2.2.1 Generation of the macrophage-specific Ddah2 null mouse model 55
2.2.2 Genotyping 56
2.2.3 Cell culture 57
2.2.4 Flow cytometry 60
2.2.5 RNA extraction and analysis 66
2.2.6 Protein extraction and western blot analysis 69
2.2.7 Greiss assay 72
2.2.8 RNA Sequencing analysis 72
2.2.9 Enzyme-linked immunosorbent assay 74
2.3 Statistical Analysis 75
Chapter 3 Results: Characterisation of the models for the study of the role of DDAH2 in inflammation 76
3.1 Introduction 76
3.2 Aims 79
3.3 RAW 264.7 characterisation 79
3.3.1 qPCR validates the use of *Rpl13* as a housekeeping gene in RAW 264.7 murine macrophage cell line 79
3.3.2 RT-qPCR validates RAW 264.7 cells expression of key genes of interest in the nitric oxide pathway 81
3.3.3 RAW 264.7 murine macrophage cell line expresses DDAH2 protein 83
3.3.4 RAW 264.7 cells synthesise iNOS protein in response to LPS stimulation 84
3.3.5 RAW 264.7 cells release nitric oxide in response to LPS stimulation 85
3.3.6 ADMA does not affect NO release in resting macrophages 86
3.3.7 High-variation in the response of RAW 264.7 to ADMA post- LPS-stimulation in high-arginine media 86
3.3.8 100 μM is the optimal concentration of arginine in the culture media to study the effect of ADMA on nitric oxide production 88

3.3.9 ADMA does not reduce iNOS gene expression 90
3.4 C57BL/6J bone marrow-derived macrophage characterisation 91
3.4.1 Bone marrow cells differentiate into macrophages after stimulation with recombinant macrophage colony-stimulating factor 91
3.4.2 Flow cytometry validates BMDM differentiation protocol 92
3.4.3 The yield of BMDM can be improved with the addition of pyruvate to the media used in the differentiation process 94
3.4.4 Flow cytometry confirms that the increased differentiation cell yield is due to an increase in BMDM numbers 96
3.4.5 Rpl13 is a reliable qPCR housekeeping gene regardless of the media used for differentiation 97
3.4.6 Target gene expression responds similarly to LPS stimulation and ADMA treatment in BMDM differentiated in High glucose media and Low glucose media 99
3.4.7 Nitric oxide production increases in response to LPS stimulation and decreases with ADMA pre-treatment in BMDM differentiated in either High glucose media or Low glucose media 100
3.4.8 Western blot confirms DDAH2 and iNOS protein expression in BMDM 101
3.5 Macrophage-specific Ddah2 null mouse model 103
3.5.1 DNA, RNA and protein expression confirm genotype 103
3.5.2 Third party testing validates genotype 108
3.5.3 DDAH2 does not regulate eNOS and iNOS gene expression in BMDM 108
3.5.4 Ddah2 knockdown causes a significant increase in spleen weight 109
3.6 Discussion 110
3.6.1 Brief Summary of chapter findings 110
3.6.2 RAW 264.7 characterisation 111
3.6.3 C57BL/6J bone marrow-derived macrophage characterisation 113
3.6.4 Macrophage-specific Ddah2 null mouse model 115
3.7 Chapter Summary 116
Chapter 4 Results: Effect of DDAH2 knockdown in LPS-stimulated peritoneal macrophages 117
4.1 Introduction 117
4.2 Aims 120
4.3 RNA sequencing in silico data analysis 120
4.3.1 Quality control and processing 121

4.3.2 Alignment 123
4.3.3 Normalised gene counts 125
4.3.4 Differentially expressed genes 128
4.3.5 Functional analysis 131
4.4 RT-qPCR validation of RNA sequencing data 134
4.4.1 Chemokines 135
4.4.2 Interleukins 138
4.5 Functional validation of IL17A response to LPS stimulation in peritoneal macrophages 141
4.6 Discussion 143
4.6.1 Brief summary of chapter findings 144
4.6.2 RT-qPCR In vitro validation of the in silico analysis in peritoneal macrophages 145
4.6.3 DDAH2 regulates IL17A expression in peritoneal macrophages 146
4.7 Chapter summary 148
Chapter 5: Effect of DDAH2 knockdown in LPS-stimulated bone marrow-derived macrophages 149
5.1 Introduction 149
5.2 Aims 150
5.3 DDAH2-dependent genes required for a normal immune response 150
5.3.1 Investigation in macrophage-specific Ddah2 null mouse model 151
5.3.2 Confirmatory study in C57BL/6J wild-type BMDM 154
5.4 DDAH2-dependent genes enriched in apoptosis 155
5.4.1 Investigation in macrophage-specific Ddah2 null mouse model 156
5.4.2 Confirmatory study in C57BL/6J wild-type BMDM 160
5.5 *Il17a* expression in bone marrow-derived macrophages 163
5.5.1 Confirmatory study in C57BL/6J wild-type BMDM 164
5.6 Discussion 165
5.6.1 Brief Summary of chapter findings 166
5.6.2 DDAH2-dependent genes required for a normal immune response 167
5.6.3 DDAH2-dependent genes enriched in apoptosis 168
5.7 Chapter Summary 169
Chapter 6 General Discussion 171
6.1 Introduction 171
6.2 Thesis aims 171

6.3 Summary of salient findings 172
6.4 Thesis insights and implications 174
6.4.1 The in silico analysis indicates that a substantial number of genes are regulated by DDAH2 174
6.4.2 Inflammation regulation is a crucial function of DDAH2 175
6.4.3 Unmasking the uniqueness: bone marrow-derived vs. peritoneal macrophages 176
6.4.4 DDAH2 regulates IL17A production in peritoneal macrophages 179
6.5 Future perspectives 181
6.6 Summary 181
List of References 183

List of Tables

Table 2-1 Cell culture reagents 53
Table 2-2 Molecular biology reagents 54
Table 2-3 Primer sequences for confirmation of mice genotype by qPCR 56
Table 2-4 PCR primers for genotyping 56
Table 2-5 PCR program for LysM-Cre 57
Table 2-6 PCR program for DDAH2 57
Table 2-7 Flow cytometry reagents 61
Table 2-8 Primer sequences used in qPCR during experiments 67
Table 2-9 Primary antibodies used in western blot 71
Table 2-10 Secondary antibodies used in western blot 71
Table 4-1 High alignment of the reads to the mm10 mouse genome via HiSat2 123
Table 4-2 There are many significantly Differentially Expressed Genes (DEG) in the four analysis groups, both up and down regulated 128
Table 4-3 Symbols and names of genes selected for the general validation of the RNA Sequencing data analysis 133
Table 4-4 Log_2 Fold Change (Log_2FC) and P-adjusted value (p-adj) for the selected chemokines 135
Table 5-1 *Olr1* and *Arg1* in silico results 153
Table 5-2 Apoptosis genes in silico results 158

List of Figures

Figure 1-1 Atherosclerotic plaque 26
Figure 1-2 Nitric oxide synthesis 38
Figure 1-3 Methylarginine synthesis 41
Figure 1-4 ADMA metabolism 42
Figure 1-5 DDAH-ADMA-NOS Pathway 50
Figure 2-1 Generation of macrophage-specific *Ddah2* null mouse model 55
Figure 2-2 Bone marrow-derived macrophage isolation and differentiation 59
Figure 2 -3 Fluorescence minus one (FMO) controls used to identify gate boundaries in bone marrow cells 63
Figure 2-4 Fluorescence minus one (FMO) controls used to identify gate boundaries in bone marrow-derived macrophages 64
Figure 2-5 Gating strategy utilised in flow cytometry analysis of differentiation efficiency of bone marrow Cells to BMDM using recombinant M-CSF 65
Figure 2-6 RT-qPCR primer melt curve 68
Figure 2-7 Pierce Detergent Compatible Bradford assay standard curve 70
Figure 2-8 Griess assay standard curve 72
Figure 2-9 In silico analysis in Galaxy software 73
Figure 2-10 IL17A ELISA standard curve 75
Figure 3-1 RT-qPCR validates the use of *Rpl13* as a housekeeping gene 80
Figure 3-2 RAW 264.7 murine macrophage cells express key target genes in NO-ADMA-DDAH pathway 82
Figure 3-3 DDAH2 protein is expressed in RAW 264.7 macrophage cell line 83
Figure 3-4 iNOS protein is synthesised in RAW 264.7 macrophage cell line in response to LPS stimulation 84
Figure 3-5 RAW 264.7 murine macrophage cells release nitric oxide in response to LPS stimulation 85
Figure 3-6 ADMA does not affect NO release in resting RAW 264.7 macrophages 86
Figure 3-7 Macrophages have a high variation in their levels of nitric oxide released in response to LPS-stimulation when they are pretreated with ADMA 87
Figure 3-8 100 μM L-arginine is the optimal concentration to study the effects of ADMA on NO production in LPS stimulated RAW 264.7 cells 89

Figure 3-9 ADMA does not alter candidate gene expression in LPS stimulated RAW 264.7 macrophages 90
Figure 3-10 BMDM after differentiation from bone marrow cells using M-CSF 92
Figure 3-11 Differentiation of bone marrow cells to BMDM using recombinant M-CSF yields a population of cells with double expression of F4/80 and CD11/b 93
Figure 3-12 The number of BMDM obtained post-differentiation is altered depending on the culture media used for differentiation 95
Figure 3-13 BMDM differentiation yield is increased by using low glucose media with added pyruvate during differentiation 95
Figure 3-14 Increased BMDM differentiation yield is due to an increased number of BMDM post-differentiation as confirmed by expression of macrophage markers CD11b and F4/80 97
Figure 3-15 *Rpl13* mRNA expression is stable at baseline and after stimulation with LPS with or without pre-treatment with ADMA, regardless of the media conditions used for differentiation 98
Figure 3-16 mRNA expression of target genes is comparable regardless of the media conditions used for differentiation 99
Figure 3-17 Nitric oxide is released in response to LPS stimulation and decreases in response to pretreatment with ADMA in BMDM regardless of the media conditions used for differentiation 101
Figure 3-18 DDAH2 protein is expressed in C57BL/6J BMDM 102
Figure 3-19 iNOS protein is synthesised in C57BL/6J BMDM in response to LPS stimulation 103
Figure 3-20 PCR genotyping validates *Ddah2* knockdown 104
Figure 3-21 qPCR validates *Ddah2* knockdown 106
Figure 3-22 DDAH2 protein expression in BMDM significantly decreases in DDAH2 macrophage-specific knockdown 107
Figure 3-23 DDAH2 does not regulate *eNOS* and *iNOS* gene expression in BMDM 108
Figure 3-24 DDAH2 knockdown causes a significant increase in spleen weight 109
Figure 4-1 RNA sequencing experiment workflow 119
Figure 4-2 Fast QC analysis confirms the high quality of the raw RNA sequencing data 122
Figure 4-3 Alignment percentage 124

Figure 4-4 DeSeq2 analysis results in four groups of significantly DEG groups 125
Figure 4-5 Distinct separation between the different sample groups displayed by a PCA Plot 126
Figure 4-6 Violin distribution plot of normalised read counts 127
Figure 4-7 Differentially expressed genes represented in volcano plots 129
Figure 4-8 Top 15 differentially expressed genes per comparison 130
Figure 4-9 4966 genes are DDAH2-dependent and required for a normal immune response 132
Figure 4-10 *In vitro* analysis of selected chemokines gene expression partially validates the in silico analysis 138
Figure 4-11 *In vitro* analysis of *Il17a* gene expression validates the *in silico* analysis 141
Figure 4-12 DDAH2 regulates IL17A production in LPS-stimulated peritoneal macrophages 143
Figure 5-1 DDAH2 does not regulate *Olr1* and *Arg1* gene expression in BMDM 153
Figure 5-2 ADMA does not alter *Olr1* and *Arg1* gene expression in BMDM 155
Figure 5-3 DDAH2 does not regulate selected apoptosis gene expression in BMDM 159
Figure 5-4 ADMA does not alter Caspase 3, Caspase 6 and Caspase 7 gene expression in BMDM 161
Figure 5-5 ADMA does not alter *Bcl2, Bcl2l1* and *Bax* gene expression in BMDM 162
Figure 5-6 DDAH2 does not regulate *Il17a* gene expression in BMDM 164
Figure 5-7 ADMA does not alter *Il17a* gene expression in BMDM 165
Figure 6-1 DDAH2 has an inhibitory role in the regulation of IL17A release in LPS-stimulated peritoneal macrophages 182

Publications

Dowsett, L., Higgins, E., Alanazi, S., **Alshuwayer, N.** A., Leiper, F. C. and Leiper, J. (2020) 'ADMA: a key player in the relationship between vascular dysfunction and inflammation in atherosclerosis', Journal of Clinical Medicine, 9(9), pp. 3026.

Abstract: Oral Presentations

N. Alshuwayer, G. Joudah, C. McAleese. LPS-stimulated mitochondrial fission in macrophages: Investigating the role of DDAH2. A Pilot Study. The 2nd SCMH Early Career Researcher Symposium, 2023. Glasgow, UK.

Abstract: Poster Presentation

N. Alshuwayer, L. Dowsett, B. Ahmetaj, F. Leiper, J. Leiper. Dimethylarginine dimethylaminohydrolase 2 (DDAH2) as a possible therapeutic target for inflammation in atherosclerosis. Novel and emerging targets in atherosclerosis. British Atherosclerosis Society 2022. Oxford, UK.

N. Alshuwayer, L. Dowsett, B. Ahmetaj, F. Leiper, J. Leiper. Dimethylarginine dimethylaminohydrolase 2 (DDAH2) as a possible therapeutic target for inflammation in atherosclerosis. Early Career Cardiovascular Scientists' Symposium, 2022. Manchester, UK.

Grants:

N. Alshuwayer, G. Joudah, C. McAleese. Elucidation of the role of Dimethylarginine dimethylaminohydrolase 2 (DDAH2) in LPS-stimulated mitochondrial fission in bone marrow-derived macrophages. ICAMS ECCR Pump priming scheme. Funded by the Welcome Trusts Institutional Strategic Support Fund (ISSF), 2022. University of Glasgow, 2022.

Acknowledgement

I want to thank the Government of The Kingdom of Saudi Arabia for their continuous support and generous funding of my PhD research.

Professor James Leiper, I sincerely thank you for your expert guidance and insights, which were instrumental in shaping my work. Thank you for your ongoing support and for providing me with the resources and facilities necessary to complete this project. It was a pleasure being part of the Leiper group.

Dr. John Mercer, I am deeply grateful for your valuable insights and continuous encouragement during my PhD studies. I highly appreciate how you always ensured I left our meetings feeling accomplished and motivated.

Fiona, thank you for helping me start on the right path with my research, the training in the lab, and continuous support. Zaniah, thank you for your patience with my million microscopy questions and long flow cytometry experiments. I will miss our genuine talks! Erin and Corey, it was great working with you. The help in the lab, chats and laughs are moments I will never forget.

Thank you to all the people who make SCMH. Special thanks to Simon for his help in the RNA Sequencing analysis, Ryszard for sharing his flow cytometry expertise, Wendy for her help with specimens and genotyping, Francisco for guiding me through the BMDM differentiation, Elaine for her help with genotyping, and the Salt Group, most of whom are dear friends. Dorothy, I'm grateful to you for always supporting us all in every way possible. Blair, thank you for your informative training and generous feedback.

Laura Dowsett, I am deeply grateful for your supervision and guidance throughout my PhD. Your support during the most challenging times of this learning journey, particularly during the pandemic, and writing up is much appreciated. Your dedication and kindness to all your students are admirable.

I give special thanks to Professor Gwyn Gould for his caring advice that shaped my PhD experience.

My utmost appreciation goes to my wonderful parents, who have always encouraged my passion for learning and been a source of unwavering support.

This thesis is dedicated to my great husband and amazing kids. My companions in this journey. Thank you for your endless patience, understanding and cheerful smiles. Raed, Mohammad, Dana and Jouri, this achievement is ours.

Author's Declaration

I, Noha Alshuwayer, hereby confirm that the work presented in this thesis is my own. Information derived from other sources has been referenced, and work done in collaboration has been cited.

January 2024

List of Abbreviations and Acronyms

Main abbreviations

ADMA	Asymmetric dimethylarginine
ANOVA	Analysis of variance
BMDM	Bone marrow-derived macrophage
CGM	Complete Growth Medium
DDAH	Dimethylarginine dimethylaminohydrolase
***Ddah2*$^{f/f}$ LysM-Cre$^{0/+}$ (KO)**	DDAH2 macrophage-specific knockout mouse
***Ddah2*$^{f/f}$ LysM-Cre$^{0/0}$ (WT)**	DDAH2 homozygous wild-type mouse
DEG	Differentially expressed gene
HGM	High glucose media without pyruvate
iNOS	inducible NOS (NOS2)
KO	DDAH2 macrophage-specific knockout mouse
LCCM	L929 cell-conditioned medium
LGM	Low glucose media with pyruvate
L-NMMA	N(G)-monomethyl-L- arginine
LPS	Lipopolysaccharides
M1	Proinflammatory macrophages
M2	Anti-inflammatory macrophages
M-CSF	Macrophage colony-stimulating factor
MMA	Monomethylarginine
nNOS	Neuronal nitric oxide synthase (NOS1)
NO	Nitric oxide
NO_2	Nitrogen dioxide
NO_2^-	Nitrite
NO_3^-	Nitrate
NOS	Nitric oxide synthase
PRMT	Protein arginine methyltransferase enzymes
ROS	Reactive oxygen species
RPL13	Ribosomal protein L13
SDMA	Symmetric dimethylarginine
SEM	Standard error of the mean
WT	DDAH2 homozygous wild-type mouse

Other abbreviations

ABCA1	ATP-binding cassette transporter
ABCG1	ATP-binding cassette sub-family G member-1
ACAT1	Acylcholesterol transferase 1
ADC	Arginine decarboxylase
AGAT	Arginine-glycine amidinotransferase
AGXT2	Alanine-glyoxylate aminotransferase
APC	Antigen-presenting cells
ARG1	Arginase 1
ARGII	Arginase 2
ATP	Adenosine triphosphate
BAM	Binary alignment map
BAX	Bcl-2 Associated X-protein)
Bcl-2	B-cell lymphoma 2
BCL2L1	BCL-2-like protein 1
BH4	Tetrahydrobiopterin
BSA	Bovine serum albumin
Casp3	Caspase 3
Casp6	Caspase 6
Casp7	Caspase 7
CaSR	Calcium sensing receptor
CCL2	(C-C motif) ligand 2
Ccrl2	C-C Motif chemokine receptor-like 2
CD11	Cluster of differentiation molecule 11B
CD36	Cluster of differentiation 36
CD68	Cluster of differentiation 68
CD86	Cluster of differentiation 86
cDNA	Complementary deoxyribonucleic acid
cGMP	Cyclic guanosine monophosphate
CIMT	Carotid intima-media thickness
CLR	C-type lectin receptors
CVD	Cardiovascular disease
Cxcl1	C-X-C Motif Chemokine Ligand 1
Cxcl2	C-X-C Motif Chemokine Ligand 2

DAMPs	Damage-associated molecular patterns
DCs	Dendritic cells
DMEM	Dulbecco's Modified Eagle's Medium
DMGV	α-keto-δ-(NG, NG-dimethylguanidino) valeric acid
DMSO	Dimethylsulfoxide
DNA	Deoxyribonucleic acid
DPBS	Dulbecco's Phosphate Buffer Saline
DRP1	Dynamin-related protein 1
ELISA	Enzyme-linked immunosorbent assay
eNOS	Endothelial nitric oxide synthase (NOS3)
ESRD	End-stage renal disease
FACS	Fluorescence-Activated Cell Sorting
FBS	Fetal bovine serum
FC	Fold change
FDA	The Food and Drug Administration
FDR	False discovery rate
FITC	Fluorescein isothiocyanate
FMO	Fluorescence minus one
GFF	General feature format
GM-CSF	Granulocyte macrophage colony-stimulating factor
GO	Gene Ontology
GSIS	Glucose-stimulated insulin secretion
GTP	Guanosine triphosphate
HDL	High-density lipoprotein
HEK	Human embryonic kidney
HMGB1	High-mobility group protein 1
HSP70	Heat shock protein 70
ICU	Intensive care unit
IDDM	Insulin-dependent diabetes mellitus
IL17A	Interleukin-17 A
IL1b	Interleukin 1 beta
IL6	interleukin-6
IFN-γ	Interferon-gamma
KLF2	Kruppel-like Factor 2
KLF9	Kruppel-like factor 9

LDL	Low-density lipoprotein
LOX1	Lectin-type oxidised LDL receptor 1
LXLRα	Liver X receptor alpha
MALT	Mucosal-associated lymphoid tissue
MAVS	Mitochondrial antiviral signalling
MCP-1	Monocyte chemoattractant protein-1
MESA	Multi-ethnic Study of Atherosclerosis
MHC	Major histocompatibility complex
NADPH	Nicotinamide-adenine-dinucleotide phosphate
NF-κB	Nuclear factor kappa B
NK	Natural Killer T cells
NLR	(NOD)-like receptors
NOD	Nucleotide-binding oligomerisation
OLR1	Oxidised low-density lipoprotein receptor 1
OVA	Ovalbumin
PAMP	Pathogen-associated molecular patterns
PBS	Phosphate buffer saline
PC1	First principal component
PC2	Second principal component
PCA	Principal component analysis
PCR	Polymerase chain reaction
PKG	Protein kinase G
PMSF	Phenylmethylsulfonyl fluoride
PPARs	Peroxisome proliferator-activated receptors
PRRs	Pathogen recognition receptors
PVDF	Polyvinylidene difluoride
RCF	Relative centrifugal force
RIG-1	Retinoic acid-inducible gene 1
RIPA	Radioimmunoprecipitation assay
RLR	RIG-I–like receptor
RNA	Ribonucleic acid
RPM	Revolutions Per Minute
RT-qPCR	Real-time quantitative PCR
SDS-PAGE	Sulphate-polyacrylamide gel electrophoresis
SLE	Systemic lupus erythematosus

SNP	Single-nucleotide polymorphism
TBE	Tris-borate-EDTA buffer
TBK1	TANK-binding kinase 1
TLR	Toll-like receptors
TNF	Tumour necrosis factor
TUNEL	Terminal deoxynucleotidyl transferase dUTP nick-end labelling

Chapter 1 General Introduction

1.1 Atherosclerosis

1.1.1 Introduction

Cardiovascular diseases (CVD) remain the first cause of mortality globally, causing around 17.9 million deaths in 2019 (WHO, 2023 Global Report, ISBN 978-92-4-007432-3). Atherosclerosis is the main underlying pathology in CVD (Frąk *et al.*, 2022) and one of the most common causes of morbidity and mortality worldwide (Abdolmaleki *et al.*, 2019; Libby *et al.*, 2019). While advances in medicine and health care have shifted the demographics and epidemiology of atherosclerotic disease, they have not reduced the cumulative global burden (Libby, 2021). Lack of access to healthcare and preventive medicine, lifestyle factors such as smoking, lack of physical activity, and mental stress all play a pivotal role in developing cardiovascular disease (Benjamin *et al.*, 2019). Other contributors to CVD generally, and atherosclerosis specifically, are the obesity epidemic and the spread of metabolic syndrome (Silveira Rossi *et al.*, 2022). Where communicable disease prevalence has decreased, leading to increased life expectancy, the ageing population suffers from the long-term effects of atherosclerosis, such as myocardial infarction, stroke and their complications. Although there have been advancements in therapies available to control some risk factors, such as hypertension and hyperlipidaemia, it still imposes a significant medical challenge.

1.1.2 Historical perspective

Interestingly, although many of the risk factors associated with atherosclerosis have been linked with a modern lifestyle and environmental impact, atherosclerosis has affected humanity for thousands of years (Thompson *et al.*, 2013). Evidence of plaques has been uncovered in mummies from different geographical populations, which leads one to wonder why. Could it be shared risk factors with our ancestors, such as inflammation secondary to infectious diseases, smoke inhalation, age-related pathology, genetic predisposition or

other risk factors we have not yet uncovered? (Thomas *et al.*, 2014; Clarke *et al.*, 2014; Wann *et al.*, 2019)

Arteriosclerosis (hardening of the arteries) was first described as early as 1575 by Fallopius as the "degeneration of arteries into bone", and although there were various reported descriptions over hundreds of years, the term "atherosclerosis" was coined by the pathologist Felix Marchand in 1904, from 'athero' meaning porridge-like and 'sclerosis' meaning hardening (McMillan, 1995). Some of the significant landmarks in atherosclerosis-related research include the introduction of inflammation as an initiating factor in atherosclerosis by Rudolf Virchow (1821–1902) and the opposing theory by Carl von Rokitansky (1804–1878) that inflammation is secondary to disease in the vessel. As for the involvement of cholesterol in the development of atherosclerosis, some of the first experimental associations were described in 1908 by Ignatowski (Ignatowski, 1908), while in 1910, Adolf Windaus showed the presence of a higher content of cholesterol in an atheromatous lesion compared to a normal arterial wall (Windaus, 1910). This was followed by the development of the first atherosclerosis animal model by feeding rabbits a high-cholesterol diet by Nikolai Anichkov in 1913 (Konstantinov *et al.*, 2006). Anichkov also described the various cell types within a lesion, including foam cells.

This was followed by more groundbreaking work, including the discovery of the low-density lipoprotein (LDL) receptor in 1973 by Michael S. Brown and Joseph L. Goldstein (Goldstein and Brown, 1973) and the discovery of a specific ß-Hydroxy ß-methylglutaryl-CoA (HMG-CoA) reductase inhibitor, paving the pathway to the development of statins (Endo, Kuroda and Tanzawa, 1976). A major contribution to understanding the pathogenesis of atherosclerosis was the "Response to Injury Hypothesis" by Russel Ross and John Glomset (Ross, Glomset and Harker, 1977). Therefore describing atherosclerosis as a chronic inflammatory disease resulting from an interaction of factors such as hypertension, atherogenic lipoproteins and a variety of cells in the vessel wall, including endothelial cells, immune cells and smooth muscle cells (Newby, 2000).

The term "Arteriosclerosis" is commonly used as an umbrella for several pathologies, including "Arteriolosclerosis", which affects only small vessels (Kashgarian, 1985), "Mönckeberg's arteriosclerosis", which is a form of

calcification that affects medium and large-sized arteries without lumen narrowing (Mönckeberg, 1903) and the topic of this thesis “Atherosclerosis”. The term atherosclerosis refers to a chronic progressive inflammatory disease that affects the intima of medium and large-sized arteries and is characterised by the “atheromatous plaque” due to the accumulation of lipids and a variety of immune cells and smooth muscle cells (Ross, 1993; Linton *et al.*, 2019). The American Heart Association has suggested an elaborate subclassification of atherosclerosis in relation to both pathology and clinical features (Virmani *et al.*, 2000). However, the more practical and routinely used classification as early, intermediate and advanced lesions will be used here.

1.1.3 Risk factors

Many of the risk factors for atherosclerosis are intertwined. One strong example of this is the ‘Metabolic Syndrome”, which is associated with a doubling of risk for plaque formation (Grundy *et al.*, 2005). The metabolic syndrome is the concomitant occurrence of obesity, hypertension, dyslipidaemia and insulin resistance (Lanktree and Hegele, 2017). Each of these factors has been linked to atherosclerosis. Various underlying pathologies and mechanisms have linked obesity to atherosclerosis, including underlying dyslipidaemia, inflammation and altered gut microbiome (Lovren, Teoh and Verma, 2015); however, obesity comorbidities such as hypertension and insulin resistance show ethnic disparity, which likely implicates different genetic predispositions (Cossrow and Falkner, 2004). Several studies, such as the Framingham heart study, Suita study and MESA (multi-ethnic Study of Atherosclerosis), have linked hypertension with an increased risk of adverse cardiovascular events (Poznyak *et al.*, 2022). Although this increased risk is well established, the underlying mechanisms are still a matter of investigation. The altered shear stress and oxidative stress in the affected areas are probable contributors.

1.1.4 Pathophysiology

The earliest initiating event in the development of atherosclerosis occurs due to an insult to the endothelial cell layer, which borders the vessel lumen and overlies the intima, termed endothelial dysfunction. Atherosclerosis affects vessels in a focal, non-symmetrical, distinctive manner, mainly in areas that

exhibit turbulent blood flow, such as bifurcations (Glagov *et al.*, 1988). Initially, turbulence was thought to physically damage the endothelial lining or increase that vessel's exposure to lipoproteins, increasing their permeability into the vessel (Ross, Glomset and Harker, 1977; Caro, Fitz-Gerald and Schroter, 1971). Later, a large body of experimental evidence showed a link between haemodynamic force and transcriptional regulation of endothelial cells' genes, supporting the atheroprotective role of laminar shear stress (Traub and Berk, 1998; Topper and Gimbrone Jr, 1999). Laminar shear stress was found to mechanically stimulate the upregulation of atheroprotective genes, such as the positive effect on the transcription factor Kruppel-like Factor 2 (KLF2) (Gimbrone, Nagel and Topper, 1997; Dekker *et al.*, 2002; Parmar *et al.*, 2006). Several studies showed multiple atheroprotective functions for KLF2, including endothelial barrier function (Lin *et al.*, 2010), the stimulation of nitric oxide (NO) production (Wu *et al.*, 2019) and anti-thrombotic (Lin *et al.*, 2005) and anti-inflammatory effects (Das *et al.*, 2006). Therefore, one of the main reasons lesions appear in areas of turbulent flow is the absence of the positive regulation of atheroprotective genes due to laminar shear stress.

Another mechanism by which the type of flow in the vessel can affect the development of atherosclerosis is by influencing epigenetic changes, such as altered gene expression in response to disturbed flow as a result of upregulation of DNA methylation (Dunn, Thabet and Jo, 2015). Equally, the type of flow may influence the modulation of expression of microRNAs (miRNAs) at the site, which may eventually have either an atheroprotective effect (Chen *et al.*, 2012) or an atheroprone effect (Son *et al.*, 2013). Furthermore, disturbed blood flow activates signalling pathways such as nuclear factor kappa B (NF-κB), thus priming the endothelium to a pro-inflammatory state (Takahashi *et al.*, 1997).

One of the essential functions of the endothelium is the regulation of vascular tone. Nitric oxide (NO) is a paracrine factor synthesised in response to shear stress by endothelial nitric oxide synthase (eNOS) from L-arginine and released by endothelial cells. Due to its lipophilic properties, it diffuses readily to nearby cells. NO is a potent vasodilator and has anti-platelet aggregation properties. Most of the risk factors for atherosclerosis lead to a decrease in NO bioavailability either through inhibition of eNOS activity or enzyme uncoupling.

Hypercholesterolaemia leads to eNOS uncoupling (Stepp *et al.*, 2002), which can be worsened by cigarette smoking (Steffen *et al.*, 2012). Additionally, inflammatory mediators released during inflammation, such as monocyte chemoattractant protein-1 (MCP-1), interleukin-6 (IL-6), and interleukin-17 (IL-17) (Nguyen *et al.*, 2013; Hung *et al.*, 2010) and other atherosclerosis risk factors may also work at least in part by decreasing NO bioavailability (Shivkar and Abhang, 2014).

Therefore, endothelial dysfunction at atheroprone locations increases endothelial adhesiveness and permeability, procoagulant properties and the release of inflammatory factors, thus forming the earliest atherosclerotic lesion, the fatty streak, which may be present since childhood (Napoli *et al.*, 1997). The fatty streak is an inflammatory response which may be preceded in high-risk individuals with an accumulation of lipids on the arterial wall (Simionescu *et al.*, 1986). Increased recruitment of leukocytes coupled with increased endothelial adhesion is followed by migration of monocytes into the intima. Monocytes in the intima are influenced by cytokines and chemokines in the lesion area and differentiate into macrophages under the effect of local Macrophage colony-stimulating factor (M-CSF). Macrophages then take up oxidised low-density lipoprotein (ox-LDL) through phagocytosis or scavenger receptors and convert it to cholesterol, forming the characteristic foam cells. Macrophages efflux cholesterol using transporters; however, this process can become overloaded in the presence of risk factors. The fatty streak or initial stage is asymptomatic and reversible (Schillaci *et al.*, 2011), with control of both dyslipidaemia and inflammation leading to decreased cardiovascular disease risk (Pirro *et al.*, 2004; Ridker *et al.*, 2009).

On the other hand, the persistence of the offending agents leads to the continuation of the inflammatory response and progression of the atherosclerotic lesion to the intermediate/remodelling phase. This intermediate phase is mainly characterised by the migration of smooth muscle cells from the media into the intima and the infiltration of the atherosclerotic lesion. As the lesion progresses, there is increased macrophage infiltration, cholesterol accumulation and deposition. There is also an increase in foam cell formation, with the main contributors being macrophages and vascular smooth muscle cells (Gui, Zheng

and Cao, 2022). Thus forming the atherosclerotic plaque, which is initially supported by collagen released by the smooth muscle cells and fibroblasts. The lesion's growth thickens the arterial wall, compensating by gradual dilation, maintaining the arterial lumen size (Glagov *et al.*, 1987). The smooth muscle cells within the lesion lose their contractile ability and undergo phenotypic switching. They may develop macrophage-like phagocytic function and contribute further to foam cell formation (Wamhoff *et al.*, 2004; Allahverdian *et al.*, 2014).

Continued inflammation leads to a progression of inflammatory and smooth muscle cell migration and proliferation within the lesion, the release of cytokines, chemokines and hydrolytic enzymes (Ross, 1999). This leads to the development of the advanced lesion, characterised by a core of necrotic tissue and lipids covered by a fibrous cap that protrudes into and narrows the lumen (Ross, 1999) (Figure 1-1).

Atherosclerosis is a chronic disease, and both healing and progression are dynamic and rely largely on local or systemic inflammation episodes. Symptoms and complications are related to the stage and status of the disease. Narrowing of the lumen due to the thickening of the plaque may lead to decreased blood flow and angina or peripheral arterial disease, particularly with exercise. If a lesion ruptures, it may result in clots, which could block the blood flow, leading to myocardial infarction or stroke.

The innate and adaptive immune systems play a role in the inflammatory response in atherosclerotic disease (Hansson and Hermansson, 2011; Shimada, 2009). The main cells responsible for all disease stages are monocyte-derived macrophages and T and B lymphocytes (Shimada, 2009; Jonasson *et al.*, 1986; Das *et al.*, 1989; Moore and Tabas, 2011). Mast cells and eosinophils may contribute to disease progression (Abdolmaleki *et al.*, 2019; Wang, Cheng and Shi, 2011).

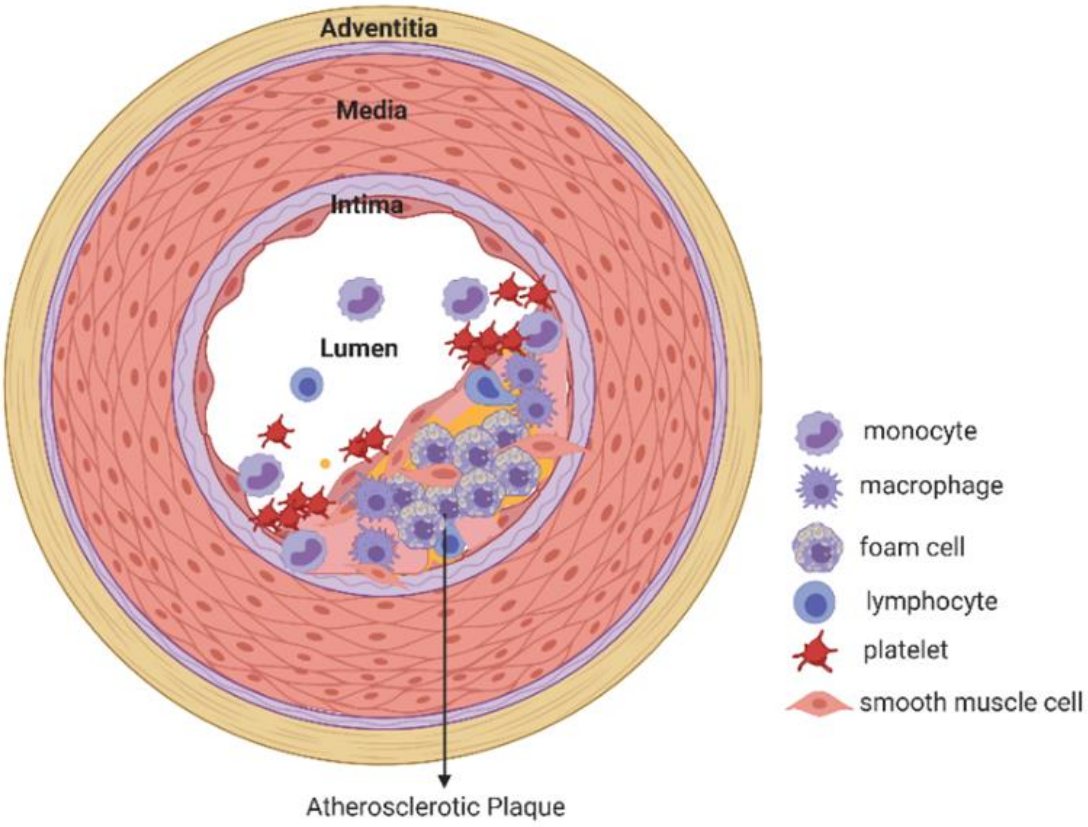

Figure 1-1 Atherosclerotic plaque
Many cell types are involved in the development of an atherosclerotic plaque in the intima of medium and large-sized arteries. Endothelial dysfunction leads to increased platelet adhesion, leukocyte recruitment and lipid accumulation in the intima. Monocytes migrate into the intima and differentiate into macrophages, which, along with vascular smooth muscle cells migrating from the media, contribute to the development of foam cells. Advancement of the atherosclerotic disease leads to enlargement of the atherosclerotic plaque, narrowing of the vessel lumen, and development of a necrotic core and thin fibrous cap, which may lead to low plaque stability and disease complications. The illustration was created with BioRender.com.

1.2 Immune system

The immune system is responsible for detecting, identifying and protecting the body against pathogens, debris and tumour cells. It is composed of a complex network of organs, cells and chemicals. The immune organs include the primary immune organs, bone marrow and thymus, which are the sites of maturation of T and B cells and the secondary immune organs, where the T and B cells reside after maturation and include the spleen, tonsils, lymph nodes, Peyer's patches, and other mucosal-associated lymphoid tissue (MALT). The immune cells are collectively called white blood cells or leukocytes, and they all originate from

haematopoietic stem cells in the bone marrow (Cooper, 2011). There are many different types of leukocytes with distinct functions and roles in the immune response. The types of immune responses are classified into innate and adaptive immunity.

1.2.1 Types of immunity

1.2.1.1 Innate immunity

The innate immune response produces a rapid, immediate, non-specific response to a pathogenic insult. Its main aim is to stop the spread and proliferation of the pathogen while stimulating the more specific adaptive response. Leukocytes involved in the innate immune response include granulocytes (polymorphonuclear cells), mast cells, natural killer T cells, dendritic cells and macrophages.

Granulocytes include neutrophils, eosinophils and basophils and are all short-lived. Neutrophils form the majority of circulating leukocytes. They are fast-acting and destroy pathogens by both phagocytosis and capturing them using extracellular structures called neutrophil extracellular traps (NETs) (Medina, 2009). Neutrophils also release various cytokines and chemokines that modulate the immune response and attract more neutrophils and leukocytes to the injury site (Gasperini *et al.*, 2000). Eosinophils and basophils play a role in allergic response. Basophils are the scarcest leukocyte cell type and are mainly in circulation (Yamanishi and Karasuyama, 2016; Ravin and Loy, 2016). They release histamine and various cytokines; further functions are still under investigation (Voehringer, 2017; Falcone, Haas and Gibbs, 2000).

Mast cells have a vital role through their interaction with the vasculature to attract neutrophils and eosinophils through a variety of mechanisms, including increasing vascular permeability and release of cytokines, histamine and heparin; therefore, they contribute to both initiating an inflammatory and allergic response (Marshall and Jawdat, 2004). Characteristically, they have a long life span and retain the ability to proliferate and self-renew (Yamanishi and Karasuyama, 2016). A population of lymphocytes that play a role in the innate immune response are Natural Killer T cells (NK cells), which release cytolytic

granules and function mainly in defence against tumours and viral infections (Vivier *et al.*, 2008). Dendritic cells have both phagocytic ability and are antigen-presenting cells. After engulfing the pathogen, they migrate to lymphoid tissue to prime T cells and initiate an adaptive immune response (Bobryshev, 2010). Another population of leukocytes with phagocytic and antigen-presenting functions are macrophages, which will be discussed in section (1.2.2).

1.2.1.2 Adaptive immunity

Antigen-presenting cells (APC) like macrophages and dendritic cells internalise the pathogen and degrade it, generating peptides that are flagged or presented on receptors on the surface of the APC called the major histocompatibility complex class II (MHC-II). The MHC-II interacts with receptors of lymphocytes within lymphoid tissue and, along with the action of secreted co-stimulatory molecules, stimulates the naive lymphocytes. Lymphocytes composed of B cells and subtypes of T cells initiate the adaptive immune response. Although it takes a longer time for the adaptive immune response to be initiated, it produces a more targeted response and builds memory for a faster, more robust response in case of future exposure. If an APC only presents the MHC-II but does not release co-stimulatory molecules, they are called non-professional APCs (unlike professional APCs). Examples of non-professional APCs are fibroblasts and vascular endothelial cells, and they are unable to stimulate naive lymphocytes but can reactivate memory lymphocytes.

1.2.2 Macrophages

Macrophages are a heterogeneous group of cells that form an essential part of the innate immune system. In the bone marrow, multipotent haematopoietic stem cells mature into myeloid progenitor cells under the influence of transcription factors. Myeloid progenitor cells develop into monocytes and granulocytes (neutrophils, eosinophils and basophils). Monocytes are released into the circulation, and if they migrate into tissues, they differentiate into macrophages. Circulating monocytes are small, round cells with a kidney-shaped nucleus. When they mature into macrophages, they generally increase in size and can assume different shapes depending on the tissue in which they reside and their polarisation state. They also have surface or cellular markers to

identify them, but some are shared with other cells of common ancestry, e.g. cluster of differentiation molecule 11B (CD11b), F4/80 and cluster of differentiation (CD68).

The migration of circulating monocytes into different body tissues and, thus, the differentiation into tissue-resident macrophages occurs during gestation. This is due to the influence of their surrounding environment and the supportive and homeostatic functions needed specifically in that location. This variation may be explained by the effects of various transcription factors. During the homeostatic state, macrophages play an important role in wound healing, tissue repair, and muscle regeneration. While in the presence of tissue injury, inflammation or infection, macrophages play a vital role in the innate immune response. They are recruited to the injury site by chemokines, where they internalise the pathogens by phagocytosis. By presenting the MHC-II molecules, they stimulate the adaptive immune response.

1.2.3 Activation of the innate immune system

For the immune system to fulfil its functions in protecting the body from pathogens, it must be able to identify them and differentiate them from self. This might fail, leading to immunodeficiency diseases, hypersensitivity or autoimmune disorders. Here, the activation of the innate immune response will be discussed.

Innate immune cells identify pathogens (infectious agents, debris, tumour cells) using pathogen recognition receptors (PRRs). PRRs recognise pathogen-associated molecular patterns (PAMPs) and damage-associated molecular patterns (DAMPs). PAMPs contain conserved structures that have a vital function in pathogen survival, are shared among the class of pathogens and are essentially absent in self or host cells. Examples of PAMPs are lipopolysaccharide and teichoic acid in the cell walls of Gram-negative and Gram-positive bacteria, respectively. Other examples of PAMPs are flagellin protein present in a variety of bacteria, ß-glucan in the inner wall of fungi (Erwig and Gow, 2016) and double-stranded ribonucleic acid (dsRNA) in viruses (Alexopoulou *et al.*, 2001). DAMPS, on the other hand, are released by the host cell in pathological conditions such as inflammation, infection or cell death and thus considered

danger signals such as uric acid (Shi, Evans and Rock, 2003), heat shock protein 70 (HSP70) (Junprung *et al.*, 2022) and high-mobility group protein 1 (HMGB1) (Kazama *et al.*, 2008).

The PRRs on the host cell that detect PAMPs and DAMPs can be transmembrane or cytosolic. There are different subtypes of PRRs. Retinoic acid-inducible gene 1- (RIG-1)-like receptors (RLR) recognise viral RNA in the cytoplasm. Nucleotide-binding oligomerisation (NOD)-like receptors (NLRs) are cytoplasmic and can sense bacterial cell-wall peptidoglycan (Kaparakis *et al.*, 2010; Babamale and Chen, 2021). C-type lectin receptors (CLRs) are transmembrane and recognise carbohydrate structures on pathogens.

Toll-like receptors (TLRs) are a family of widely distributed and well-studied PRRS recognising extracellular or endosomal PAMPs. There are 10 TLRs identified in humans and 12 in mice; while some are transmembrane, others are intracellular (Kawasaki and Kawai, 2014). One of the first TLRs discovered in mammals is Toll-like receptor 4 (TLR4) (Medzhitov, Preston-Hurlburt and Janeway Jr, 1997), which is conserved between humans and mice. It was first identified to sense lipopolysaccharides (LPS) in mammals in 1998 by Poltorak *et al.* as they showed that mice with TLR4 mutations fail to respond to LPS stimulation (Poltorak *et al.*, 1998). TLR4 is a transmembrane receptor structurally composed of three domains: a transmembrane domain, an extracellular domain and an intracellular domain. The extracellular domain facilitates LPS recognition (Zanoni *et al.*, 2011). The binding of LPS with the TLR4 complex (composed of TLR4 and facilitating proteins) and their interactions induce conformational changes that initiate the intracellular domain-mediated downstream signalling through the action of adaptors, finally leading to the activation of two different signalling pathways. This leads to interactions with several adaptor proteins and transcription factors and, eventually, the expression of proinflammatory cytokines such as interleukin-6 (IL-6) and tumour necrosis factor α (TNF-α) (Lu, Yeh and Ohashi, 2008; Ciesielska, Matyjek and Kwiatkowska, 2021) or to the release of anti-inflammatory mediators such as interleukin-10 (IL-10) (Chanteux *et al.*, 2007). The TLR4 subsequently undergoes lysosomal degradation, which facilitates the control of the inflammatory response to LPS (Husebye *et al.*, 2006). Other TLRs also act through one or both

of the aforementioned signalling pathways, leading to the release of different cytokines.

Cytokines are polypeptides of various structures and functions, released by both immune and non-immune cells, with the shared role of communication with and between immune cells (O'Shea, Gadina and Siegel, 2019). Cytokines may be grouped according to the receptor they target. One example is the TNF cytokine family, which includes a large number of cytokines and ligands, including TNF, which activates phagocytes, stimulates its own production as well as other cytokines and upregulates MHC-I and II expression in response to TLR4 activation by LPS in bacterial infection. Interferon-gamma (IFN-γ) is another example of a member of the TNF cytokine family with pro-inflammatory and macrophage-activating effects. A family of cytokines that share the activation of receptor tyrosine kinases include macrophage-colony stimulating factor (M-CSF), which functions in the differentiation of monocytes. Chemokines are a large family of cytokines that bind to seven transmembrane domain receptors and function in leukocyte recruitment, including Cxcl1 and Cxcl2. An example of pro-inflammatory cytokines implicated in immune-mediated disease is the IL-17 cytokine family. Some hematopoietic cytokine receptor superfamily members have anti-inflammatory effects, such as IL-27, which stimulates the upregulation of IL-10, another anti-inflammatory cytokines of the same family.

As cytokines have many functions, may target one or more receptors, act on various cells and may be induced by multiple factors, some of the cytokines may be more specific than others. Agents targeting some of the cytokines has been approved for therapeutic use, such as the specific inhibition of TNF-α for the treatment of rheumatoid arthritis (Ma and Xu, 2013; Moelants *et al.*, 2013), which results in decreased inflammation and the modulation of macrophages to an anti-inflammatory phenotype (Degboé *et al.*, 2019).

1.2.4 Macrophage classification

Macrophages are classically divided into M1 (proinflammatory) and M2 (anti-inflammatory) macrophages, each exhibiting different phenotypes and biomarker expression (Shapouri-Moghaddam *et al.*, 2018). Macrophages polarise in response to external stimuli (Shapouri-Moghaddam *et al.*, 2018; Trus, Basta and Gee,

2020). They also exhibit plasticity, thus switching from one phenotype to another (Sica and Mantovani, 2012). Macrophage polarisation and plasticity play an important role in atherogenesis. Polarisation towards M1 occurs under the influence of oxidised LDL, IFN-y and IL-1 cytokines and towards M2 under the influence of IL-4 (Colin, Chinetti-Gbaguidi and Staels, 2014). M1 are pro-atherogenic, while M2 have an anti-inflammatory effect, and plasticity from one phenotype to another is possible (Shapouri-Moghaddam *et al.*, 2018). M1 and M2 phenotypes have been identified in human and mouse atherosclerotic lesions.

1.2.5 Macrophages in atherosclerosis

Circulating monocytes patrol the vessel wall by intermittent crawling phases on the endothelial cells' luminal side to maintain homeostasis (Auffray *et al.*, 2007). Under homeostatic non-inflammatory conditions, circulating monocytes may be recruited into a vessel but with low efficiency (Geissmann, Jung and Littman, 2003). The migration of circulating monocytes into the vessel wall and across the endothelial cell layer is an active process. It requires communication between cell types, including chemokines released secondary to inflammation, such as chemokine (C-C motif) ligand 2 (CCL2) (Trogan *et al.*, 2006) and endothelial cells' overexpression of adhesion molecules (O'Brien *et al.*, 1996). If the disease regresses, the recruitment of circulating monocytes is suppressed (Potteaux *et al.*, 2011).

In the intima layer of blood vessels, monocytes differentiate into macrophages under the effect of local colony-stimulating factor (CSF) released by local endothelial and smooth muscle cells (Sinha *et al.*, 2021). The subtype of CSF affects the polarisation state of the differentiated macrophages. Macrophage colony-stimulating factor (M-CSF), expressed in healthy vessels, promotes the M2 anti-inflammatory macrophage phenotype. On the other hand, GM-CSF (GM-CSF) expression increases with the progression of atherosclerosis, and it induces an M1 pro-inflammatory phenotype (Haghighat *et al.*, 2007; Brochériou *et al.*, 2011). The macrophages are also exposed to a multitude of stimuli that influence their functional phenotype, including polarisation factors released by the T cells in the plaque. Type II helper T cells (Th2) cytokines, including interleukin-4 (IL-4) and interleukin-13 (IL-13), induce an M2 phenotype which

induces the release of interleukin-10 (IL-10), thus downregulating pro-inflammatory cytokine release. M2 macrophages facilitate plaque regression by promoting the phagocytic removal of apoptotic cells (efferocytosis) and tissue repair (Bi *et al.*, 2019). M1 phenotype, on the other hand, is induced under the influence of cytokines released by Th1, such as Interferon-gamma (IFN-γ) and tumour necrosis factor-alpha (TNF-α), LPS from a leaky gut or infection or oxLDL. M1 produces a pro-inflammatory response, including the release of nitric oxide reactive oxygen species (ROS) production and induces apoptosis. M1 is associated with advanced lesions and unstable plaques and, therefore, worse outcomes (De Gaetano *et al.*, 2016).

Part of the homeostatic functions of macrophages is the clearance of oxidised LDL in three processes: uptake, esterification and efflux. LDL uptake is mediated by scavenger receptors such as lectin-type oxidised LDL receptor 1 (LOX1), scavenger receptor 1 (SR-A) and the cluster of differentiation 36 (CD36). LDL is hydrolysed in lysosomes within the macrophage and converted to free cholesterol. Free cholesterol undergoes re-esterification by acylcholesterol transferase 1 (ACAT1) into cholesterol ester and stored as lipid droplets. For cholesterol to be effluxed, cholesterol esters are first converted back to free cholesterol, which then is effluxed outside the cell by active transporters such as adenosine triphosphate (ATP)-binding cassette transporter 1 (ABCA1) and ATP-binding cassette sub-family G member-1 (ABCG1). These transporters are regulated mainly by peroxisome proliferator-activated receptors (PPARs) and liver X receptor alpha (LXLRα) (Chinetti *et al.*, 2001). The cholesterol is then carried by extra-cellular high-density lipoprotein (HDL) to the liver for clearance. This process aids in clearing LDL in the endothelium. PPARs also decrease monocyte recruitment by downregulating monocyte chemoattractant protein-1 (MCP-1) (Barish *et al.*, 2008).

However, with increased LDL retention and oxidisation, more macrophages are recruited into the vessel with a decreased ability to clear LDL, resulting in foam cell formation. Multiple factors further worsen the outcome. The increased macrophage recruitment by chemokines released by the foam cells such as MCP-1, the release of pro-inflammatory cytokines such as IL-6 and TNF-α and ROS causing further injury. Also, the increased lipid accumulation activates Toll-like

receptor 4 (TLR4), thus promoting more inflammation (Singh *et al.*, 2020). Inflammatory modulators lead to the upregulation of scavenger receptors LOX-1, SR-A and CD36, leading to increased uptake and, thus, more foam cell formation. Risk factors such as a leaky gut and infections lead to increased circulating LPS, which decreases cholesterol efflux by reducing the expression of scavenger receptor B1 (SR-B1), ABCA1 and ABCG1 (Maitra and Li, 2013).

The increase in ox-LDL uptake induces foam cell formation and leads to apoptosis by sustained accumulation of cytosolic calcium (Salvayre *et al.*, 2002), dysfunction of proteases (Vieira *et al.*, 2000), and the activation of the caspase cascade (Salvayre *et al.*, 2002; Wintergerst *et al.*, 2000). The inability to effectively clear the apoptotic cells contributes to the necrotic core formation (Puylaert *et al.*, 2022). Cell death leads to the release of DAMPs, which further contributes to the inflammation in the lesion.

In the core of the advanced lesion, the number of macrophages increases mainly by proliferation rather than further recruitment of circulating monocytes (Robbins *et al.*, 2013). As the inflammation is sustained and efferocytosis is less sustainable, more macrophages die, contributing to the increased size of the necrotic core (Yurdagul *et al.*, 2017; Thorp *et al.*, 2008). The active inflammation also stimulates the macrophages to release metalloproteinase proteolytic enzymes that degrade the collagen and elastin in the fibrous cap of the necrotic core, leading to its thinning (Gong *et al.*, 2021). The increased size of the necrotic core and thinning of its cap render the lesion more susceptible to rupture; thus, the patient is at higher risk of complications (Shin, Edelberg and Hong, 2003).

The atherosclerotic plaque structure and, thus, its severity are under the continuous influence of the different phenotypes of macrophages and their modification due to the surrounding stimuli (Abdolmaleki *et al.*, 2019).

1.3 Nitric Oxide

Macrophages play an important role in the immune response. They release nitric oxide in response to stimulation with pro-inflammatory stimuli.

1.3.1 Nitric oxide properties

Nitric oxide (NO) is a radical gas, as it has one unpaired electron. It is considered a stable radical because although it can interact with other radicals, such as superoxide ions, it does not dimerise at standard temperature and pressure. However, it may dimerise under low temperatures or long exposure under high pressure, leading to the formation of toxic gases such as nitrous oxide and nitrogen dioxide (Hughes, 2008). It is slightly soluble in water (Wink *et al.*, 1996). When NO reacts with oxygen in water, multiple molecules are produced, including other radicals such as nitrogen dioxide (NO_2) and stable products, nitrite (NO_2^-) and nitrate (NO_3^-). The oxidation of NO to its stable end products, nitrite and nitrate, leads to its rapid inactivation. The measurement of these end products is the basis of the Greiss assay, often used to measure NO production (Griess, 1858). A reverse pathway occurring in biological systems, whereby nitrate and nitrite can be reduced back into NO, was discovered in the 90s (Zweier *et al.*, 1995; Lundberg *et al.*, 1997; Benjamin *et al.*, 1994). Here, nitrate's initial reduction into nitrite depends on bacterial reductase enzymes (Sasaki and Matano, 1979). Other processes by which nitrate can then be reduced to NO *in vivo* include reduction by deoxyhemoglobin (Huang *et al.*, 2005), deoxymyoglobin (Shiva *et al.*, 2007) and Xanthine oxidoreductase (Li *et al.*, 2001; Millar *et al.*, 1998), with all these processes being especially active in hypoxic conditions. Thus, these processes offer alternative sources of NO when conditions are not as favourable for the classical pathway of NO synthesis, which depends on nitric oxide synthase enzymes, which will be discussed later in this section.

NO has a half-life of several seconds. One of its important features is its high lipophilicity, which, along with its small size, contributes to its efficiency in diffusing from one cell to another (MacMicking *et al.*, 1997) and thus, its effects are not limited to the cells it is produced in. In the target cell, classically, NO binds to the heme group of soluble guanylate cyclase (sGC), leading to its activation and the conversion of cellular guanosine triphosphate (GTP) to cyclic guanosine monophosphate (cGMP) (Kang *et al.*, 2019). cGMP then activates cGMP-dependent protein kinases, ion channels, and phosphodiesterases, and downstream signalling leads to the control of vascular tone and other physiological functions (Derbyshire and Marletta, 2012). One of the protein

kinases is protein kinase G (PKG), which, when activated, leads to the sequestration of intracellular calcium in smooth muscle, the dephosphorylation of myosin light chains, and finally inhibits its contraction and reduces vascular muscle tone (Shah *et al.*, 1994). This pathway is controlled by the hydrolytic activity of phosphodiesterase enzymes. Other physiological effects of NO include vascular endothelium protection through inhibition of leukocyte and platelet adhesion (Kubes, Suzuki and Granger, 1991; Radomski, Palmer and Moncada, 1987), regulation of mitochondrial respiration (Cleeter *et al.*, 1994), neuronal signalling (Garthwaite, 2019), modulation of insulin secretion (Bahadoran *et al.*, 2021) and immune functions.

1.3.2 Nitric oxide synthase pathway

The primary source of NO synthesis occurs under the influence of nitric oxide synthase enzymes. Nitric oxide synthases (NOSs) are a family of enzymes that catalyse the oxidation of L-arginine to nitric oxide (NO) and citrulline (Figure 1-2). This reaction requires the cofactors nicotinamide-adenine-dinucleotide phosphate (NADPH), tetrahydrobiopterin (BH4), flavin adenine dinucleotide and flavin mononucleotide (Förstermann and Sessa, 2012)

There are three isoforms of nitric oxide synthase, named according to the order of their purification, the tissue they were purified from, and their characteristics. The first isoform to be isolated, thus named “NOS1”, was purified in 1990 from rat brain and thus named neuronal NOS (nNOS) (Bredt and Snyder, 1990; Bredt, Hwang and Snyder, 1990; Schmidt *et al.*, 1991). Shortly after, the second isoform, “NOS2”, was purified from mouse macrophages after stimulation with lipopolysaccharide, thus termed inducible NOS (iNOS) (Stuehr *et al.*, 1991a; Hevel, White and Marletta, 1991). “NOS3” was purified from endothelial cells and thus named endothelial NOS (eNOS) (Pollock *et al.*, 1991; Busse and Mülsch, 1990).

However, the expression of the different isoforms is not limited to the tissues they were initially purified from (Förstermann *et al.*, 1995). eNOS is found in endothelial cells and releases NO that stimulates the relaxation of vascular smooth muscle cells and inhibits its proliferation, thus maintaining it in a relaxed state. Inhibition of eNOS leads to vasoconstriction and increased blood

pressure. It is also expressed in many other cell types, including blood platelets, cardiac myocytes and macrophages. nNOS releases NO in peripheral nerves and stimulates the relaxation of vascular and non-vascular smooth muscle cells. Furthermore, it is expressed in other cell types, including endothelium and smooth muscle cells. The third isoform, iNOS, is widely distributed in many cell types. iNOS is transcriptionally regulated, releases NO in some cells at physiological levels, and characteristically generates a large amount of NO when stimulated by toxins or cytokines. eNOS and nNOS are constitutively expressed with activity dependent on intracellular calcium. In contrast, iNOS is not sensitive to calcium levels (MacMicking *et al.*, 1997; Piazza, Guillemette and Dieckmann, 2015), which contributes to its ability to sustain the production of NO for several days if stimuli are maintained (Vodovotz *et al.*, 1994).

The sources of L-arginine, the substrate for NOS, are protein breakdown, endogenous synthesis and dietary intake. The average physiologic concentration of L-arginine is around 100 μM, and as NOS has a high affinity for L-arginine, under physiological conditions, L-arginine substrate availability is not a rate-limiting step for NOS activity. L-arginine K_m values for the different NOS isoforms are eNOS=2.9 μM (Pollock *et al.*, 1991), nNOS=1.5 μM (Bredt and Snyder, 1990) and iNOS=2.3-10 μM (Furfine *et al.*, 1993; Stuehr *et al.*, 1991b).

L-arginine is also a substrate for other enzymes, such as arginase, which hydrolyses L-arginine to L-ornithine and urea (Munder, 2009). Arginase has two isoforms: arginase I (ARGI) and arginase II (ARGII); however, arginase has a much lower affinity for L-arginine than NOS. L-arginine K_m values for the different arginase isoforms range between 20-20,000 μM (Wu and Morris Jr, 1998). However, arginase can still compete with NOS for L-arginine as the two enzymes have demonstrated similar rates of L-arginine consumption at physiological states (Wu and Morris Jr, 1998). Arginase isoform expression in macrophages is influenced by the inflammatory state. ARGI is linked with the M2 phenotype and has been shown to decrease L-arginine bioavailability and, thus, decrease NO synthesis and contribute to the anti-inflammatory response (Munder *et al.*, 1999).

Other enzymes metabolising L-arginine but having a lower affinity than NOS are arginine-glycine amidinotransferase (AGAT) and arginine decarboxylase (ADC). L-

arginine is transported into the cells using cationic amino acid transporters (CAT).

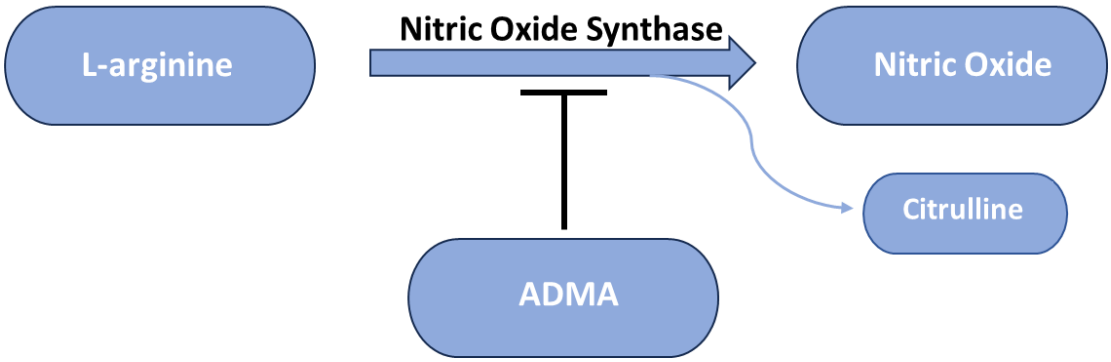

Figure 1-2 Nitric oxide synthesis
Nitric oxide synthase (NOS) enzyme utilises L-arginine as a substrate for the production of nitric oxide and citrulline. Asymmetric dimethylarginine (ADMA) is a competitive inhibitor of NOS. (Adapted from Leiper, J. and Nandi, M. 2011).

1.3.3 Nitric oxide in atherosclerosis

In atherosclerosis, endothelial dysfunction leads to the impairment of NO release from endothelial cells. This leads to decreased NO release, inhibiting NO-dependent relaxation and reducing NO-anti-thrombotic and anti-inflammatory effects. Reduced NO bioavailability also leads to an increase in vascular oxidative stress. The uncoupling of NOS secondary to endothelial dysfunction leads to the favoured production of peroxynitrite instead of NO. At high levels, peroxynitrite is toxic as it forms peroxynitrous acid, which is cytotoxic due to its ability to modify proteins by nitration (Ischiropoulos and Al-Mehdi, 1995).

Persistence of oxidative stress secondary to atherosclerotic risk factors and reduced NO bioavailability lead to the initiation of monocyte recruitment, migration, differentiation to macrophages and their polarisation, including M1 phenotype. The expression of iNOS by M1 macrophages leads to a surge in NO release (MacMicking *et al.*, 1997). The initial increase in NO is a compensatory mechanism for the decreased NO bioavailability. However, sustained NO release by iNOS leads to the production of reactive oxygen and nitrogen species.

The interaction between NO and the surrounding atherosclerotic microenvironment leads to tissue injury. The protective mechanism initiated to combat injury exerts destruction and advances the atherosclerotic lesion to an irreversible symptomatic stage. Therefore, eNOS is mainly described as protective or anti-inflammatory. Conversely, iNOS is described as inflammatory or atherosclerotic. As risk factors are sustained, endothelial dysfunction worsens, oxidative stress and inflammation are amplified, and a vicious circle continues, leading to an atherosclerotic plaque and its advancement.

The pharmacological use of nitric oxide is hindered by its low therapeutic window due to its short biological half-life and its significant side effects due to the breadth of its biological functions. Thus, targeting regulators of NOS has become of interest as a therapeutic strategy in atherosclerosis. Due to its critical role in maintaining cardiovascular homeostasis, it is not surprising to find that NO synthesis is regulated at many levels, including the distribution of the different isoforms as mentioned above, intracellular calcium levels, activation or inhibition of the phosphorylation sites and competitive inhibition by Asymmetric dimethylarginine (ADMA).

1.4 Asymmetric dimethylarginine

Asymmetric dimethylarginine (ADMA) is a naturally occurring methylarginine with the important role of regulating nitric oxide synthesis. ADMA and two other endogenous methylarginines, symmetric dimethylarginine (SDMA) and monomethyl arginine (L-NMMA) were first identified in 1970 in human urine (Kakimoto and Akazawa, 1970). Vallance et al. observed its accumulation in chronic renal failure and identified its role as an endogenous nitric oxide synthase inhibitor (Leone *et al.*, 1992).

1.4.1 ADMA synthesis and clearance

Methylarginines are synthesised via post-translational modifications of proteins containing arginine residues. The methylation of protein arginine occurs due to the addition of one or two methyl groups to its guanidino terminus (Gary and Clarke, 1998) in a two-step reaction (Figure 4-3). This reaction is catalysed by a

group of highly conserved protein arginine methyltransferase enzymes (PRMT) (Gary and Clarke, 1998). All nine currently known isoforms of PRMT expressed in humans (Morales *et al.*, 2016; Tain and Hsu, 2017) can generate protein-incorporated monomethylarginine (MMA). Human PRMT isoforms are divided into three groups according to their ability to catalyse an additional methylation step (Morales *et al.*, 2016). Type I (PRMT 1,2,3,4,6 and 8) generates NG,NG-asymmetric dimethylarginine (ADMA), Type II (PRMT 5 and 9) generates NG,N'G-symmetric dimethylarginine (SDMA) whilst Type III (PRMT 7) can only generate MMA. Protein arginine methylation is currently accepted to be irreversible (Teerlink, 2005).

Target protein arginine methylation regulates numerous cellular processes such as RNA processing, signal transduction and DNA repair (Bedford and Richard, 2005). There is no known evidence of *in vivo* direct synthesis of free ADMA from free arginine (Teerlink, 2005). There is an unknown degree of contribution of dietary intake as an exogenous source of ADMA (Schlesinger *et al.*, 2016).

Free ADMA is released via proteolysis of methylated protein arginine (Figure 1-3) (Teerlink, 2005). Here, it is either degraded by dimethylarginine dimethylaminohydrolase (DDAH) or exported to the plasma via the bidirectional cationic amino acid transporters (CAT)(Teerlink, 2005) (Figure 1-4). CATs are bidirectional, which highlights the importance of ADMA intercellular and interorgan transport in health and disease. Normal physiologic plasma concentrations of ADMA are around 0.5μM (Horowitz and Heresztyn, 2007; Teerlink, 2007) with sex and age-dependent variability (Schulze *et al.*, 2005). The clearance of ADMA is approximately 80% by DDAH enzymes and 20% excreted renally (Teerlink, 2005). A second pathway, "alanine-glyoxylate aminotransferase" (AGXT2), plays a minor role in ADMA turnover (Leiper and Nandi, 2011; Rodionov *et al.*, 2010). AGXT2 catalyses the deamination of ADMA and produces α-keto-δ-(NG, NG-dimethylguanidino) valeric acid (DMGV)(Ogawa, Kimoto and Sasaoka, 1990) (Takada and Noguchi, 1982).

ADMA and L-NMMA inhibit nitric oxide synthase activity by competitive inhibition due to their structural similarity with NOS substrate L-arginine, while SDMA is incapable of this direct competitive inhibition. Furthermore, the interaction of ADMA with the cationic amino acid transporters may compromise L-arginine

availability. On the other hand, high concentrations of L-arginine, for example, when added exogenously, may affect the inhibitory effect of ADMA on NOS activity.

Notably, although physiologic levels of ADMA in the plasma range between 0.4-0.6µmol/L (Horowitz and Heresztyn, 2007), they have been documented to increase by two times in conditions such as hypertension or hypercholesterolaemia (Horowitz and Heresztyn, 2007) and around three times in chronic renal failure (Kielstein *et al.*, 2002).

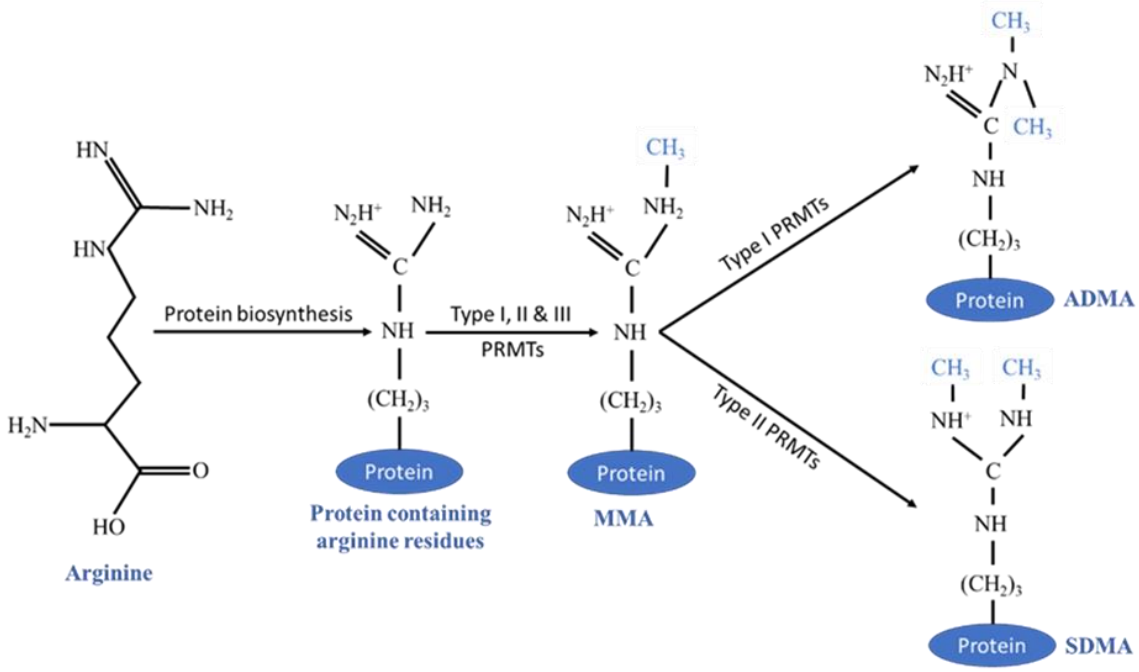

Figure 1-3 Methylarginine synthesis
Protein Arginine methyl transferases (PRMT) types I, II and III add one methyl group to proteins containing arginine residues, producing monomethylarginine (MMA). Type I and II PRMT catalyse a further methylation step generating NG,NG-asymmetric dimethylarginine (ADMA) and NG,NG-symmetric dimethylarginine (SDMA) respectively. (Adapted from Gary and Clarke,1998.)

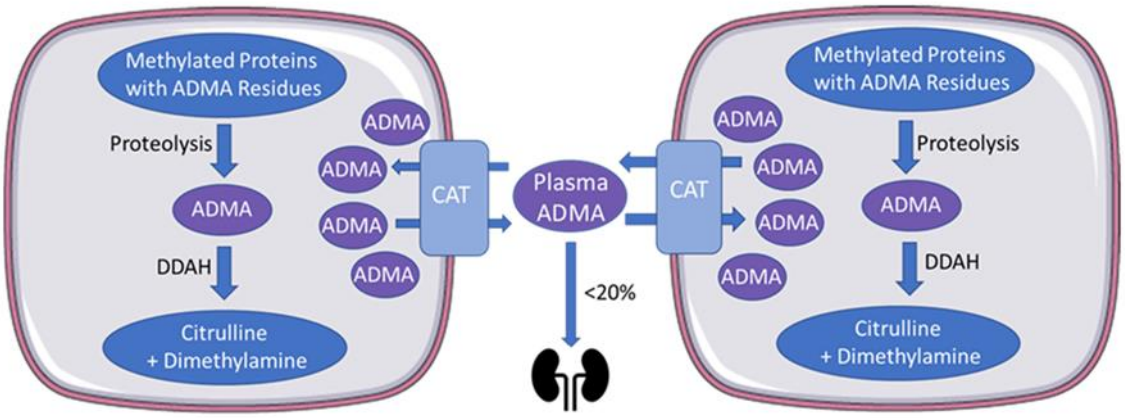

Figure 1-4 ADMA metabolism
Methylated proteins containing arginine residues release free methyl-arginines (including ADMA) intracellularly via proteolysis. ADMA is metabolised mainly by DDAH to citrulline and dimethylamine. Some ADMA may be transported by cationic aminotransferases to the plasma (or from the plasma to another cell or organ). Renal excretion is responsible for less than 20% of ADMA metabolism. (Adapted from Teerlink, 2005).

1.4.2 ADMA and disease

The accumulation of ADMA in chronic renal failure and its role as an endogenous inhibitor of nitric oxide synthase was first observed by Vallance et al. (Leone *et al.*, 1992). Fliser et al. noted that although ADMA was only slightly elevated in the early stages of renal disease, its levels increased with disease progress, and ADMA was an independent marker of kidney disease progression (Fliser *et al.*, 2005). Further studies conducted on patients with end-stage renal disease (ESRD) showed higher ADMA levels in subjects with manifest atherosclerotic disease than in patients without signs of atherosclerotic disease (Kielstein *et al.*, 1999) and a significant relationship to the extent of carotid atherosclerosis and identified ADMA levels as a strong predictor of cardiovascular mortality in patients with ESRD (Boger *et al.*, 2000).

Further clinical studies showed associations between ADMA and known atherosclerotic risk factors. Interestingly, increased ADMA levels were evident in hypercholesterolaemic - clinically asymptomatic adults and were associated with impaired NO-mediated vasodilation (Böger *et al.*, 1998). Also, Cooke et al. described increased intracellular levels of ADMA and impaired endothelium-

dependent vasodilation after balloon injury (Cooke, 2000; Masuda *et al.*, 1999), confirming findings in other studies which link increased ADMA levels to endothelial dysfunction (Sydow and Münzel, 2003).

A non-invasive method used to predict atherosclerotic development in subclinical patients involves the measurement of the carotid intima-media thickness (CIMT) (Bots *et al.*, 1996). Increased CIMT was found to be strongly associated with increased levels of ADMA in the absence of other risk factors (Miyazaki *et al.*, 1999; Furuki *et al.*, 2007), and even in the presence of various risk factors, ADMA levels were found to be an independent predictor of CVD risk (Murakami, Mizuno and Kaku, 1998). On the other hand, the Shimane Center for Community-Based Healthcare Research and Education (CoHRE) study found the arginine/ADMA ratio to be associated with increased CIMT. In contrast, no association was found with either ADMA or arginine alone and thus was suggested as a predictive marker (Notsu *et al.*, 2015). Conversely, CIMT and ADMA levels were found to be inversely related by Zsuga et al., and they suggested a possible selective inhibition of iNOS by ADMA, thus inducing an atheroprotective effect (Zsuga *et al.*, 2007). Furthermore, multiple studies showed a positive correlation between increased ADMA levels and endothelial dysfunction (Antoniades *et al.*, 2009; Perticone *et al.*, 2005; Päivä *et al.*, 2002).

Although several association studies have found significant positive correlations between plasma ADMA and atherosclerosis, and ADMA can be considered a main risk factor for atherosclerosis, causal relationships and mechanisms have yet to be identified. Since an increase in ADMA has been associated with many cardiovascular diseases (Dowsett *et al.*, 2020), and ADMA is a competitive inhibitor of NOS, it has been of interest to investigate the effect of modulating DDAH enzymes in diseases with perturbed NO.

1.5 Dimethylarginine dimethylaminohydrolase

Asymmetric dimethylarginine (ADMA) is metabolised mainly by Dimethylarginine dimethylaminohydrolase (DDAH), first described by Ogawa et al. as an enzyme that intracellularly catalyses the hydrolysis of ADMA and NG-monomethyl-L-arginine (L-NMMA) to L-citrulline and dimethylamine or monomethylamine

respectively (Ogawa *et al.*, 1987). The identification of the co-localisation of DDAH and nitric oxide synthase (NOS) in different anatomic sites in the rat kidney led to the hypothesis of DDAH as a regulator of NOS through ADMA metabolism regulation (Tojo *et al.*, 1997). Two isoforms of DDAH have been identified in humans, DDAH1 and DDAH2 (Leiper *et al.*, 1999).

1.5.1 Isoforms

DDAH is expressed in many tissues, including the kidney, liver, heart, brain and lung. In humans, two isoforms exist with overlapping but also distinct tissue distribution (Leiper *et al.*, 1999). DDAH1 is more diffusely distributed, colocalising with neuronal nitric oxide synthase (nNOS), while DDAH2 mainly co-localizes with endothelial NOS (eNOS) and inducible NOS (iNOS). Both DDAH isoforms colocalise in cardiovascular tissue (Leiper and Nandi, 2011). In immune cells, only DDAH2 is expressed (Tran *et al.*, 2000). The two human isoforms share 50% homology in their amino acid sequences (Anderssohn *et al.*, 2012).

Ddah1 and *Ddah2* have been localised in humans to chromosomes 1p22 and 6p21.3, respectively (Tran *et al.*, 2000). Susceptibility to diseases in which NO is altered, such as rheumatoid arthritis and insulin-dependent diabetes mellitus (IDDM), has been linked to the MHC-III region of 6p21.3 (Weinberg *et al.*, 1994). The expression of the DDAH2 isoform in the immune system (Tran *et al.*, 2000) and the location of *Ddah2* in the genomic region of MHC-III suggest a role for DDAH2 in immune-related disorders. Furthermore, elevated inducible NOS has been implicated in the pathology of autoimmune diseases such as rheumatoid arthritis and IDDM (Spanjaard *et al.*, 1997), thus adding a functional link.

1.5.2 Activity

DDAH has been successfully purified from rat kidneys and has been shown to be stable at 37°C for an hour (Ogawa, Kimoto and Sasaoka, 1989). No required cofactors have been identified for the activity of DDAH. Stoichiometry analysis of the hydrolysis of ADMA shows an equimolecular reaction. Therefore, one molecule of ADMA is broken down by DDAH to produce one molecule of citrulline and one molecule of dimethylamine (Ogawa, Kimoto and Sasaoka, 1989).

As for the regulation of DDAH activity, given that the DDAH1 Km value for ADMA is 69-170 μM (Hong and Fast, 2007; Arrigoni, Ahmetaj and Leiper, 2010) and ADMA's normal physiologic intracellular levels, DDAH is not saturated at normal physiologic conditions. Therefore, it is unlikely that DDAH function is regulated by methyarginine levels. Research suggests that DDAH may be regulated by the sensitivity of its activity to oxidative stress secondary to damage to the sulfhydryl group in the enzyme's active site (Stühlinger *et al.*, 2001). Examples of this are the reduction of DDAH activity by known cardiovascular disease risk factors such as ox-LDL, TNF-α (Ito *et al.*, 1999), homocysteine (Stühlinger *et al.*, 2001) hyperglycemia (Lin *et al.*, 2002) and infection (Weis *et al.*, 2004). In 2002, Leiper et al. showed evidence of a negative feedback loop mechanism by which high levels of nitric oxide lead to the reversible nitrosylation of the DDAH enzyme, thus decreasing its enzymatic activity and leading to the accumulation of ADMA, which in turn competitively inhibits nitric oxide synthase activity and leads to the reduction of NO produced (Leiper *et al.*, 2002). In 2021, Huang et al. demonstrated, in the context of anti-viral immunity and specifically "RIG-I-like receptor- mitochondrial antiviral signalling" (RLR-MAVS), the ability of TANK-binding kinase 1 (TBK1) to phosphorylate and inhibit DDAH2, thus establishing TBK1 as a DDAH2-regulator (Huang *et al.*, 2021).

The earlier resolution of the crystal structure of DDAH from the bacterium Pseudomonas aeroginosa enabled the confirmation of the catalytic site formed of a triad containing a cysteine residue (Cys-249, His-162, and Glu-114) (Murray-Rust *et al.*, 2001). Cys-249 has been identified as the nitrosylation site (Leiper *et al.*, 2002), and the active site is conserved across species (Murray-Rust *et al.*, 2001). The corresponding residues in mammalian (bovine) species were identified by analogy to be (Cys-273, His-172, and Asp-126) (Knipp *et al.*, 2003). The crystal structure of human DDAH1 was resolved in 2007, and the catalytic triad was composed of (Cys-273, His-172 and Asp-126) (Leiper *et al.*, 2007).

1.5.3 DDAH2 gene polymorphisms

In the previous section, ADMA levels were discussed in normal and pathologic states, and the normal ADMA levels varied between individuals. As the DDAH2 isoform is highly expressed in endothelial cells, a link between *Ddah2* variants and ADMA levels has been investigated. In 2003, six polymorphisms in the *Ddah2*

gene were identified with at least one functional variant (at DDAHII -871) showing increased activity of DDAH2 and reduced levels of ADMA (Jones *et al.*, 2003). Further studies on variants were conducted. The variant DDAH II -449 (single-nucleotide polymorphism (SNP) ID rs805305) was associated with increased requirement of vasopressors after cardiac surgery (Ryan *et al.*, 2006), while in septic patients, it was associated with increased ADMA levels, which is associated with the extent of organ damage (O'Dwyer *et al.*, 2006). Although the findings in these studies appear opposite to each other, they may indicate a high level of specific ADMA effect on NOS isoform regulation in a sterile vs. infectious disease background (O'Dwyer *et al.*, 2006). Another *Ddah2* variant, the rs9267551 C allele has been associated with higher expression of DDAH2 and reduced ADMA levels (Andreozzi *et al.*, 2012) leading to better insulin sensitivity than individuals with rs9267551 G allele (Andreozzi *et al.*, 2012), decreased prevalence of chronic kidney disease (Sesti *et al.*, 2013), lower risk of myocardial infarction in type 2 diabetic patients (Mannino *et al.*, 2019) and protection from increased arterial stiffness and rigidity (Averta *et al.*, 2022). *Ddah2* polymorphisms may have a prospective role to be used as biomarkers.

1.5.4 Functional studies

Although the role of DDAH1 in the metabolism of ADMA is widely accepted, the role of DDAH2 has been controversial due to conflicting studies regarding its enzymatic activity.

On the one hand, the polymorphism studies described above are in line with an ADMA-hydrolysing role for DDAH2. Furthermore, studies on DDAH2 knockout mice demonstrated increased ADMA levels (Lambden *et al.*, 2015; Lange *et al.*, 2016). These findings support that in the absence of DDAH2, ADMA metabolism was affected, leading to an increase in its levels. Furthermore, the overexpression of DDAH2 has been shown to be associated with reduced plasma ADMA and also to produce a phenotype resistant to exogenously administered-ADMA induced-hypertension (Hasegawa *et al.*, 2007). Reduced ADMA plasma levels were also reported in the lentivirus-induced DDAH2-overexpressing diabetic rat model (Zhu *et al.*, 2019). Therefore, an increase in DDAH2 levels was associated with increased ADMA metabolism.

On the other hand, other studies, mainly using siRNA techniques to evaluate the functions of the two DDAH isoforms, did not demonstrate an ADMA-dependent role for DDAH2. Wang et al. showed that isolated *Ddah1* silencing increased ADMA levels but did not affect endothelium-dependent vascular relaxation (Wang *et al.*, 2007). However, isolated *Ddah2* silencing, although not affecting plasma ADMA levels, substantially decreased endothelial-dependent relaxation. That supports the conclusion that endothelial-dependent relaxation is impaired with loss of DDAH2 even with normal plasma ADMA levels and indicates an ADMA-independent mechanism of action for DDAH2 (Wang *et al.*, 2007).

Furthermore, Pope et al. investigated the contribution of each of the DDAH isoforms to the total DDAH activity through siRNA inhibition studies and found that although DDAH1 contributed three times more than DDAH2 to DDAH enzymatic activity, both play an important role in methylarginine metabolism. Evidence from the concomitant silencing of both DDAH isoforms supports the presence of other metabolic pathways for methylarginine metabolism (Pope et al., 2009). The functional effects of *Ddah* silencing were also assessed in relation to eNOS activity. Isolated *Ddah1* or *Ddah2* silencing led to a 48% and 31% decrease, respectively, in endothelial NO production (Pope et al., 2009). Supplementation with 100 μM L-arginine was used to determine if it would be effective in overcoming the competitive eNOS inhibition by the elevated ADMA levels secondary to *Ddah* silencing. A partial reversal was noted in the case of *Ddah1* silencing, while no change was observed in the case of *Ddah2* silencing. Therefore, Pope et al. demonstrated that both DDAH isoforms regulate eNOS, but only DDAH1 is ADMA dependent (Pope, Karuppiah and Cardounel, 2009).

Furthermore, other studies detected DDAH activity in DDAH1-abundant tissues but not DDAH2-abundant tissues (Altmann *et al.*, 2012); thus, they questioned the extent of DDAH2's role in metabolising ADMA, if any. Also, DDAH activity was not detected in DDAH1 KO mice, even in DDAH2-rich tissues (Hu *et al.*, 2011).

Significantly, attempts to assess the enzymatic activity of DDAH2 towards ADMA directly have been limited by technical challenges in expressing and purifying the DDAH2 enzyme, and the crystal structure of DDAH2 has yet to be resolved, as so far homology models have been used to predict its active site and its ability to bind to ADMA.

From another perspective, there is supportive evidence of roles for DDAH2 beyond ADMA-hydrolysis. *Ddah2* variant rs2272592 is associated with type 2 diabetes but is not associated with ADMA plasma levels (Seo *et al.*, 2012), and Chen et al. implicated DDAH2 in the development of gestational diabetes via its interaction with transcription factor Kruppel-like factor 9 (KLF9) (Chen *et al.*, 2022). Although the DDAH-ADMA-NOS pathway (figure 1-5) was implicated in the protective role of DDAH2 from myocardial fibrosis in diabetic cardiomyopathy (Zhu *et al.*, 2019), DDAH2 was shown to have beneficial effects in type 2 diabetes by improving glucose-stimulated insulin secretion (GSIS) through the activation of secretagogin expression in an ADMA/NO independent fashion (Hasegawa *et al.*, 2013).

Multiple studies have shown a role for DDAH2 in the immune system. Some of the characteristics critical to macrophage immune functions are their motility and phagocytic ability. Interestingly, genetic disruption of DDAH2 in murine peritoneal macrophages led to a significant decrease in both functions, thus demonstrating a key role for DDAH2 in regulating the immune system (Ahmetaj-Shala, 2013).

Lambden et al. studied the role of DDAH2 in NO regulation and outcome in microbial sepsis using global DDAH2 knockout and macrophage-specific DDAH2 knockout murine models. Although plasma ADMA was not altered, there were increased ADMA levels in renal and myocardial tissues and increased ADMA urinary concentrations in the global DDAH2 knockouts compared to wild-type animals (Lambden *et al.*, 2015). Furthermore, after caecal ligation and puncture to induce sepsis, there was a significant reduction in survival in the DDAH2 global knockout and the DDAH2 macrophage-specific knockout murine models compared to the wild-type controls (Lambden, 2019). Thus, it was concluded that DDAH2 regulates NOS activity and increases survival in polymicrobial sepsis (Lambden *et al.*, 2015).

As mentioned previously, bacterial infection leads to the activation of iNOS and a subsequent surge in nitric oxide release, which plays a key role in the immune response. This increase in NO has been demonstrated in septic shock (Vincent *et al.*, 2000).

Furthermore, in a prospective clinical study on patients admitted to the intensive care unit (ICU), increased plasma ADMA levels were documented in septic patients and mRNA DDAH2 expression in peripheral blood mononuclear cells was inversely related to patients' disease severity (Winkler *et al.*, 2017). These findings were explained by the authors as a connection between the DDAH2-ADMA axis, decreased NO production in sepsis and the effect on the immune response (Winkler *et al.*, 2017).

Furthermore, DDAH2 was shown to play a NO-dependent vital role in the regulation of anti-viral immunity (Huang *et al.*, 2021). This study showed evidence of DDAH2 promoting mitochondrial fission and, therefore, suppressing the anti-viral immune response (Huang *et al.*, 2021).

While there has been controversy regarding the ADMA-hydrolysing effect of DDAH2, towards the end of this project, a multicentric consortium study showed evidence by negation against DDAH2 functioning in an ADMA-dependent matter (Ragavan *et al.*, 2023). However, the possibility of a DDAH1-supportive-function for DDAH2 in ADMA hydrolysis, in addition to the other important functions of DDAH2 involved in the immune response among others, highlights the importance of elucidating the role of DDAH2 in atherosclerosis.

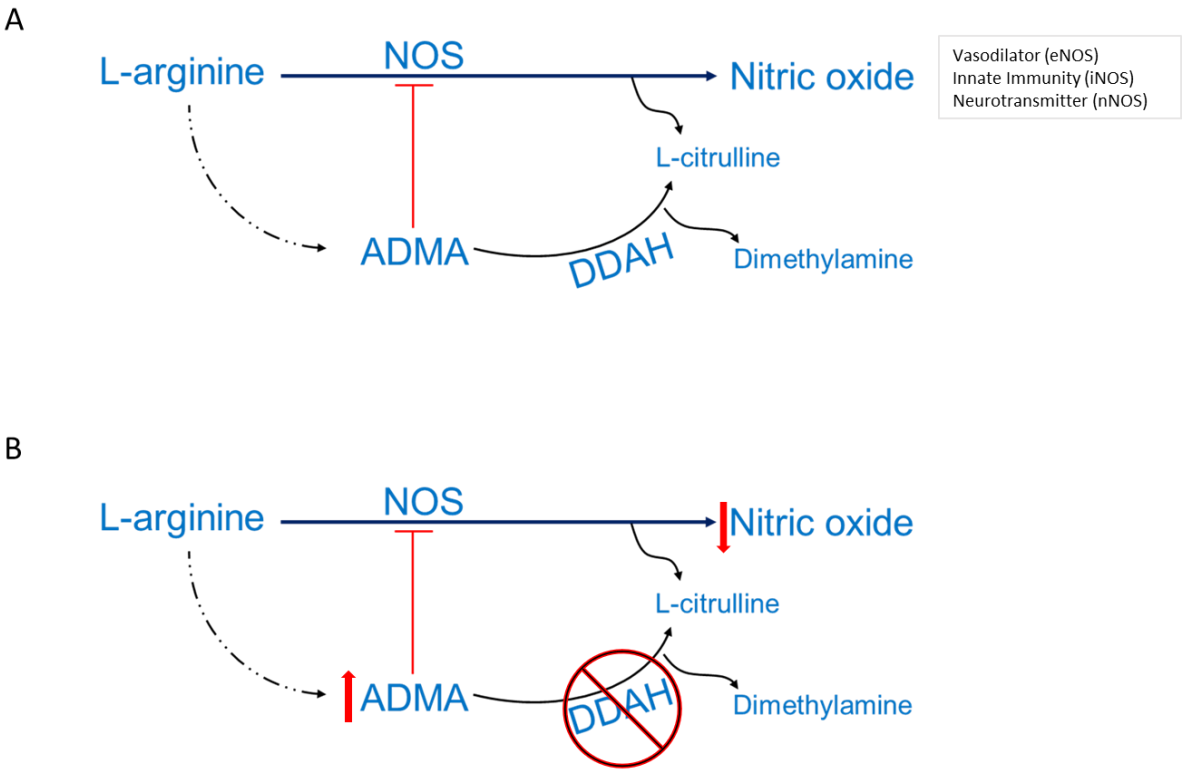

Figure 1-5 DDAH-ADMA-NOS Pathway
Nitric oxide synthases (NOSs) are a family of enzymes that catalyse the oxidation of L-arginine to nitric oxide (NO) and citrulline. There are three isoforms of nitric oxide synthase with different distribution and effect. Endothelial NOS (eNOS) is found in endothelial cells and releases NO that stimulates the relaxation of vascular smooth muscle cells and inhibits its proliferation, thus maintaining it in a relaxed state. Neuronal NOS (nNOS) releases NO in peripheral nerves and stimulates the relaxation of vascular and non-vascular smooth muscle cells. The third isoform, inducible NOS (iNOS), is widely distributed and characteristically generates a large amount of nitric oxide when it is stimulated by toxins or cytokines. Asymmetric dimethylarginine (ADMA) is mainly metabolised intracellularly by Dimethylarginine dimethylaminohydrolase (DDAH) to citrulline and dimethylamine. Inhibition of DDAH leads to increased levels of ADMA, which is an independent CVS disease risk factor). ADMA is a competitive inhibitor of NOS due to its structural similarity to L arginine, thus leading to decreased effects of nitric oxide. (Adapted from Leiper, J. and Nandi, M. 2011).

1.6 Hypothesis and aims

1.6.1 Hypothesis

Macrophages are an integral part of the innate immune response. They are responsible for initiating an immune response, recruiting other immune cells, releasing cytokines and releasing large amounts of nitric oxide in response to an inflammatory stimulus. Inflammation plays an important role in the development of many diseases such as atherosclerosis, which is of particular interest to our research group. Macrophages play a vital role in the development and progression of atherosclerosis.

The hypothesis of this project is:

" DDAH2 regulates NO production in the immune system through ADMA hydrolysis. Therefore, the knockdown of DDAH2 in macrophages reduces NO production and alters the immune response. DDAH2 also has roles beyond ADMA hydrolysis and affects cellular functions in a NO-independent manner."

1.6.2 Aims

1. Validate the suitability of using the murine cell line (RAW 264.7) and bone marrow-derived macrophages as a model to study the role of DDAH2 in inflammation.

2. Re-produce a macrophage-specific *Ddah2* null mouse model, characterise its genotype and phenotype, and use it as a model to study the role of DDAH2 in inflammation.

3. Identify DDAH2-dependent genes and pathways involved in atherosclerosis from RNA sequencing data on peritoneal macrophages and validate the *in silico* findings *in vitro*.

4. Investigate and validate the hypothesis generated from the *in silico* data in a bone marrow-derived macrophage (BMDM) model.

Chapter 2 Materials and methods

2.1 Materials

2.1.1 Mice

All animal procedures were conducted in accordance with the United Kingdom Home Office Animals Scientific Procedures act (1986) and the European Parliament directive on the protection of animals used for scientific purposes (2010/63/EU); approved by the University of Glasgow's institutional ethics review committee. ARRIVE guidelines were followed. PPL number is PP0895181.

C57BL/6J mice were obtained from The Jackson Laboratory Repository. The DDAH2 mouse was generated by Genoway for us in-house. The LysM-Cre mouse are from The Jackson Laboratory Repository (B6.129P2-Lyz2tm1(cre)Ifo/J) https://www.jax.org/strain/004781. The production of the macrophage-specific *Ddah2* null mouse is detailed in section (2.2.1). To avoid off-target effects, all Cre mice were maintained on a heterozygous background. The mice were housed with same-sex littermates in controlled humidity and temperature (22°C), on a 12-hour light/dark cycle and had access food and water *ad libitum*.

2.1.2 Cells

2.1.2.1 RAW 264.7 murine macrophage cell line

RAW 264.7 (ATCC® TIB-71™) Murine Macrophage adherent cell line was provided by Fiona Leiper. Cells were maintained in a complete growth medium (2.2.3.1) and passaged at or before they reached 80% confluency. No changes in phenotype were observed between the early and late passages other than a slight decrease in the doubling time.

2.1.2.2 Bone marrow-derived macrophages

Primary murine bone marrow-derived macrophages (BMDM) were differentiated from isolated bone marrow as in (2.2.3.2). BMDM were isolated from either C57BL/6J or the macrophage-specific *Ddah2* null mouse model.

2.1.2.3 Peritoneal macrophages

Murine primary peritoneal macrophages were isolated from peritoneal exudate as in (2.2.3.3) from the macrophage-specific *Ddah2* null mouse model .

2.1.3 Reagents

2.1.3.1 Cell culture reagents

Product	Company
Dulbecco's Modified Eagle's Medium (DMEM), High glucose, Glutamax.	Gibco, #61965
Dulbecco's Modified Eagle's Medium – low glucose, Glutamax, pyruvate	Gibco, #21885
*Dulbecco's Modified Eagle's Medium (DMEM), 4.5 g/L glucose, no L-Arginine, No L-Glutamine, No L-Lysine, No Sodium Pyruvate	Gibco, #A14431
L-homoarginine hydrochloride	Sigma, #A5131
L-lysine monohydrochloride	Gibco, #L5626
L-glutamine, 200mM (100X)	Gibco, #25030
Fetal bovine serum (FBS), Heat inactivated	Gibco, #10500
Penicillin/Streptomycin, 100 U penicillin, 0.1 mg/ml Streptomycin	Gibco, #15141
Dulbecco's Phosphate Buffered Saline (DPBS). Sterile, No CaCl2, No MgCl2	Gibco, #14190
Trypsin- Ethylenediamine tetraacetic acid (EDTA) Solution 0.05% (1X). Sterile, filtered, 0.5g porcine trypsin, 0.2g EDTA, 4Na/L of Hank's Balanced Salt Solution with Phenol Red	Gibco, #25300
Trypan Blue Solution, 0.4% liquid, sterile filtered	Sigma, T8154
Lipopolysaccharide Salmonella Typhosa (LPS) 1 mg/ml stock	Sigma, L-7895
Recombinant Murine Macrophage Colony Stimulating Factor (M-CSF)	Peprotech, #315-02
ADMA	Sigma, D4268
Ammonium-Chloride-Potassium (ACK) Lysis Buffer	Gibco, #A1049201

Table 2-1 Cell culture reagents
*Arginine deficient media (A14431) was used for Griess assay to test the effect of ADMA on NO production in LPS-stimulated cells. The media was supplemented with glutamine, lysine, arginine and 10% FBS.

2.1.3.2 Molecular biology reagents

Product	Company
RNeasy Mini Kit	Qiagen, #74104, 74106
High Capacity cDNA Reverse Transcription Kit	Applied Biosystems, #4368814
Fast Syber™ Green Master Mix	Applied Biosystems, #4385612
Griess Reagent kit	Invitrogen, G7921
RIPA Buffer	Sigma, #R0278
HaltTM Protease and Phosphatase Inhibitor Cocktail	ThermoScientific, #1861284
Phenylmethylsulfonyl fluoride (PMSF), 0.1M stock in ethanol	Sigma, #P7626
Dithiothreitol (DTT), 1M stock in water	Sigma, #D9779
Precast 4-15% Mini-Protean® TGX™ Gels	Biorad, #4561084
Precision Plus Protein™ All Blue Prestained Protein Standards ladder	Biorad, #1610373
Running Buffer: Ultrapure 10X Tris-glycine/SDS (0.25M Tris, 1.92M Glycine, 1% SDS)	Geneflow, #B9-0032
Transfer Buffer: Ultrapure 10X Tris-glycine (0.25M Tris, 1.92M Glycine)	Geneflow, #B9-0058
Immobilon®- polyvinylidene difluoride (PVDF) membrane	Millipore, #IPVH00010

Table 2-2 Molecular biology reagents

2.2 Methods

2.2.1 Generation of the macrophage-specific *Ddah2* null mouse model

Our group developed the original macrophage-specific *Ddah2* null mouse model, which was used to produce the RNA Sequencing experiment referred to in this thesis (Lambden *et al.*, 2015). However, the mice used in this thesis were from a recreation of the original model performed by Dr. Laura Dowsett. The model was obtained by crossing a floxed *Ddah2* mouse with a LysM-Cre aiming to obtain a homozygous floxed *Ddah2* expressing LysM-Cre for the experimental DDAH2 macrophage-specific knockdown mouse (*Ddah2*$^{f/f}$ LysM-Cre$^{0/+}$) and a homozygous floxed DDAH2 not expressing LysM-Cre (*Ddah2*$^{f/f}$ LysM-Cre$^{0/0}$) to be used as control (Figure 2-1).

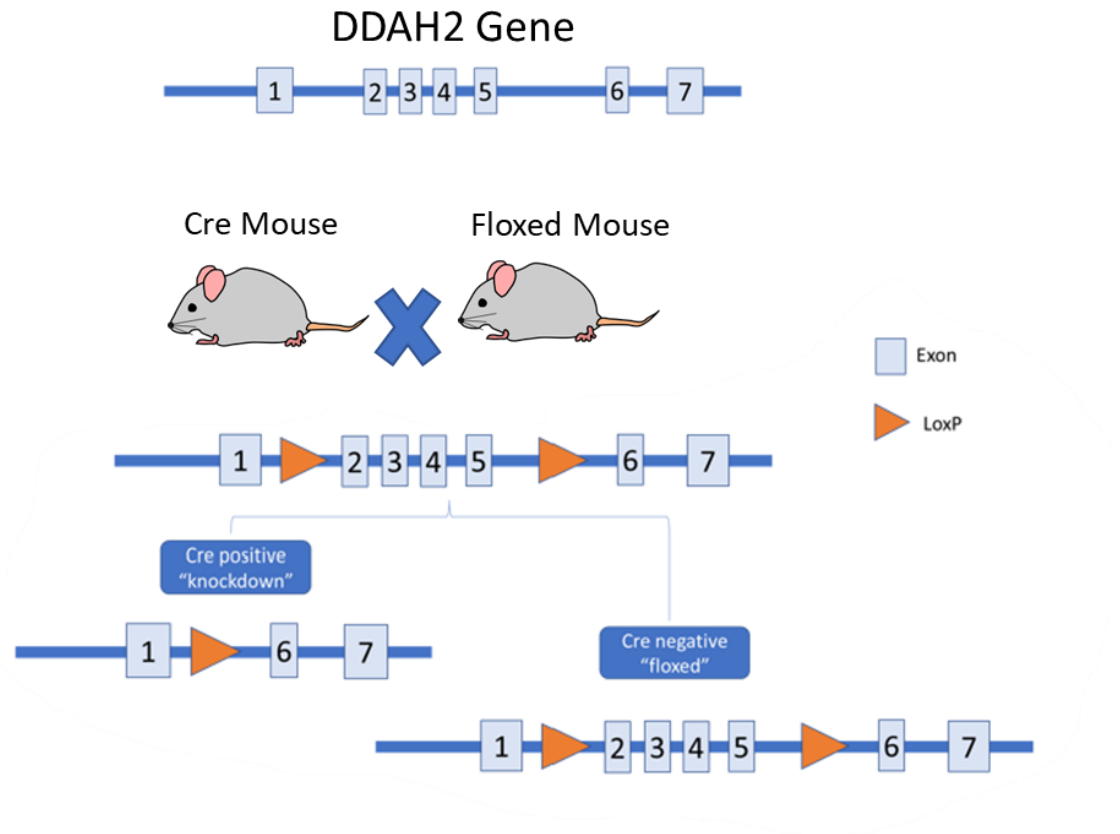

Figure 2-1 Generation of macrophage-specific *Ddah2* null mouse model
The *Ddah2* locus was floxed with LoxP recombination sites flanking exons 2-5. In the presence of Cre recombinase, exons 2-5 of *Ddah2* are excised in Lysozyme M expressing cells, resulting in *Ddah2* knockdowns (*Ddah2*$^{f/f}$ LysM-Cre$^{0/+}$). In the absence of Cre recombinase, *Ddah2* is floxed but not deleted, resulting in the experimental controls (*Ddah2*$^{f/f}$ LysM-Cre$^{0/0}$)

Gene	Forward Primer Sequence (5'-3')	Reverse Primer Sequence (5'-3')
DDAH2 Primer pair targeting exons 6 & 7	CCTGGTGCCACACCTTTCC	AGGGTGACATCAGAGAGCTTCTG
DDAH2-23 Primer pair targeting exons 2 & 3	AAGGAGACACGGCCCTAATC	GGTGAAGAGGACGTCGGTG
DDAH2-34 Primer pair targeting exons 3 & 4	TCCGAATTGTGGAGATGGGG	AGCTCCTCGATGATTGGTCC

Table 2-3 Primer sequences for confirmation of mice genotype by qPCR

2.2.2 Genotyping

The genetic identification of the macrophage-specific *Ddah2* null mice was conducted via three methods

2.2.2.1 In-house genotyping

In-house genotyping was performed by myself, Mrs. Wendy Beattie (Technician, University of Glasgow) and Mrs. Elaine Freil (Technician, University of Glasgow). Genomic DNA was isolated from ear biopsies using the "Extract-N-Amp™ Tissue PCR Kit (Sigma, #XNAT2R), which also contains a PCR ReadyMix™. PCR amplification for LysM-Cre recombinase expressing allele, the DDAH2 floxed allele, and the DDAH2 wild-type allele using the following primers (Table 2-4) and programs (Table 2-5 and 2-6). Then, samples were separated using gel electrophoresis in 1.5% agarose gel in 1X Tris-borate-EDTA buffer buffer (TBE) with added 1:33 1X Gel red nucleic acid stain (EMD Millipore, #SCT123). The samples were run along the molecular-weight marker, GeneRuler 100bp Plus DNA ladder (Thermofisher, #SM0323). The gel was run in the same TBE buffer (89 mM Tris, 89 mM boric acid, 2 mM EDTA) at 90 volts until PCR product separation was achieved. PCR products were visualised using a ChemiDoc+XRS UV system (BioRad). The expected band size for the wild-type DDAH2 PCR product was 495bp, and the floxed DDAH2 PCR product was 552bp. The expected band size for the Cre-recombinase PCR product was 720bp.

Gene	Forward Primer Sequence (5'-3')	Reverse Primer Sequence (5'-3')
DDAH2	GGGCAGGGCTATGGTGAAGG	ACCTCCTGGCTGTTGGGCAG
LysM-Cre	GCCTGCATTACCGGTCGATGCAACGA	GTGGCAGATGGCGCGGCAACACCATT

Table 2-4 PCR primers for genotyping

Step	Temperature	Time	# of cycles
Initial denaturation	95°C	5 minutes	
Denaturation	94°C	30 seconds	34 cycles
Primer Annealing	70°C	30 seconds	
Extension	72°C	1 minute	
Final Extension	72°C	10 minutes	

Table 2-5 PCR program for LysM-Cre

Step	Temperature	Time	# of cycles
Initial denaturation	95°C	3 minutes	
Denaturation	95°C	20 seconds	35 cycles
Primer Annealing	58.5°C	40 seconds	
Extension	72°C	1 minute	
Final Extension	72°C	10 minutes	

Table 2-6 PCR program for DDAH2

2.2.2.2 Third-Party Genotyping

Ear punches were genotyped via real-time PCR by Transnetyx for external validation.

2.2.3 Cell culture

All cell culture procedures were performed using aseptic techniques in class II laminar hoods. Non-sterile reagents were sterilised by using a 0.2 µm filter (Millipore). Viability assessment and cell counting were performed using a manual haemocytometer and an inverted light microscope (Eclipse TS100) after staining with Trypan Blue Solution (Sigma, #T8154) for non-viable cells.

2.2.3.1 RAW 264.7 murine macrophage cell line

RAW 264.7 cells ATCC® TIB-71™) were routinely cultured in 75 cm^2 corning tissue culture flasks in Dulbecco's Modified Eagle's Medium (DMEM) High Glucose with Glutamax (Gibco, #61965-02) supplemented with 10% v/v foetal bovine serum (FBS) (Gibco, #10500064) and 1% penicillin/streptomycin. This supplemented media is referred to as a "Complete Growth Medium" (CGM) moving forward. Cells were maintained in a humidified incubator at 37°C and 5% CO_2 and assessed for confluency, adherence, morphology and signs of contamination by an inverted light microscope.

RAW 264.7 cells were passaged every 48-72 hours at 80 % confluency using 0.05% v/v trypsin in Ethylenediamine tetraacetic acid (EDTA). Cell detachment was monitored by a light microscope and assisted by hand agitation. After neutralising trypsin enzymatic activity by diluting with Complete Growth Medium, the cells were centrifuged at 1500 revolutions per minute (RPM) for 5 min. The cells were subcultured at a 1:2 or 1:3 ratio as required.

To freeze RAW 264.7 cells, the cell pellet was resuspended in 1 ml in DMEM high glucose with glutamax supplemented with 10% v/v FBS and 5% v/v dimethylsulfoxide (DMSO) and transferred to sterile labelled cryogenic vials, then placed in a freezing chamber filled with isopropanol to achieve gradual cooling. Vials were transferred to liquid nitrogen for long-term storage.

The seeding density for RAW 264.7 cells for protein and Griess assay was $0.5X10^6$ cells per well in a 6-well plate and for RNA $0.25X10^6$ per well in 12-well plates.

2.2.3.2 Bone marrow-derived macrophages

Mice were euthanised, and hindlegs were supplied by Dr. Laura Dowsett and Mrs. Wendy Beattie.

Bone marrow-derived macrophages (BMDM) were isolated and differentiated according to the protocol developed by Rios et al. (2017). In short, the femur and tibia were dissected, sterilised with 70% ethanol, and then washed twice with sterile PBS. The ends (condyles) of each bone were cut with sterile scissors, and then the bone marrow was flushed with sterile, cold PBS using a 26G needle into a 70 µm filter into a falcon tube set on ice. Then, it was centrifuged at 500g for 10 minutes at 4°C. The supernatant was discarded, and the cell pellet was resuspended in 8 mL differentiation media (details below) supplemented with 20 ng/mL recombinant murine macrophage stimulating factor (M-CSF) (Peprotech, #315-02). Cells were incubated in 10 cm sterile non-tissue culture-treated dishes (37°C, 5% CO_2 and humid atmosphere). On day 3, an extra 8 mL of freshly M-CSF-supplemented media was added to each dish. On day 7, the M-CSF-containing media was replaced by media appropriate to each experiment (Figure 2-2).

Differentiation media: Dulbecco's Modified Eagle's Medium (DMEM) – low glucose, Glutamax, pyruvate (Gibco, #21885-025) supplemented with 10% v/v fetal bovine serum (FBS) (Gibco, #10500064) and 1% penicillin/streptomycin. During the optimisation of the differentiation process, two other media were tested:

a. Dulbecco's Modified Eagle's Medium (DMEM) high glucose with Glutamax (Gibco, #61965-02) supplemented with 15% v/v FBS and 1% penicillin/streptomycin

b. Dulbecco's Modified Eagle's Medium (DMEM) high glucose with Glutamax supplemented with 20% v/v FBS and 1% penicillin/streptomycin

The seeding density for BMDM cells for protein was $2X10^6$ per well in a 6-well plate, for RNA $0.2X10^6$ per well in 12-well plates and for flow cytometry $0.4X10^6$ per well in a 12-well plate.

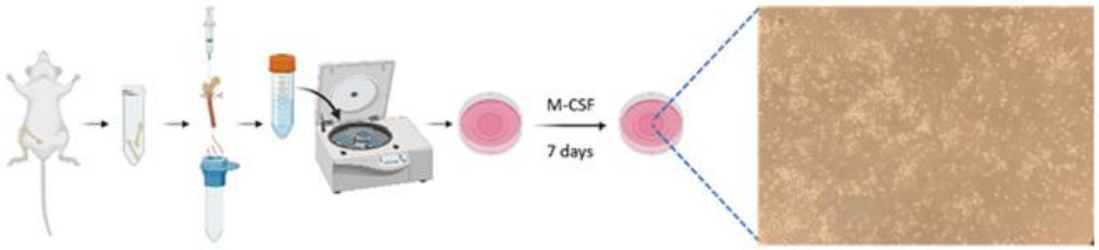

Figure 2-2 Bone marrow-derived macrophage isolation and differentiation
The femur and tibia of mice were isolated, and then the bone marrow was flushed into falcon tubes using PBS. After centrifugation, the cell pellet was resuspended in a supplemented M-CSF media. BMDM are differentiated in 7 days. The illustration was created with BioRender.com.

2.2.3.3 Peritoneal macrophages

Mice were euthanised, and peritoneal exudate was supplied by Dr. Laura Dowsett and Mrs. Wendy Beattie.

The protocol was based on Hirsch (1956). In short, after the mouse was euthanised, the abdomen was sterilised with 70% ethanol, and an abdominal incision was made to expose the intact peritoneal wall. 8ml ice-cold PBS (Ca^{2+}free, Mg^{2+} free) supplemented with 3% FBS was injected into the peritoneal cavity using a 25-gauge needle. The mouse belly was massaged for 10 seconds. The saline was withdrawn using a 19-gauge needle through the upper half of the peritoneal cavity. The extracted peritoneal exudate was dispensed into a 50 ml centrifuge tube on ice. The peritoneal exudate was centrifuged at 400 x g for 10 minutes at 4°C, the supernatant discarded, and the cells resuspended in cold DMEM High Glucose with Glutamax supplemented with 10% v/v FBS and 1% penicillin/streptomycin. 300,000-500,000 cells were plated in a 24-well plate and allowed to adhere for 1-3 hours. Non-adherent cells were removed by gently washing three times with warm PBS and fresh media was added. Adherent cells at this stage have been shown to be more than 90% macrophages.

2.2.4 Flow cytometry

Flow cytometry samples were analysed using the Fluorescence-Activated Cell Sorting (FACS) Canto II analyser (BD Biosciences), BD FACSDiva and FlowJo software.

2.2.4.1 Controls

For each cell type, the following controls were used. Blank unstained control, cells that were killed by heating and then stained with a viability stain to check for stain efficacy, single stained cells (compensation controls) and fluorescence minus one (FMO) controls (for gating) for each stain.

2.2.4.2 General protocol

Cells were detached by trypsinisation and then centrifuged at 500 x g for 5 minutes at 4°C. Each cell pellet was then resuspended in 3 ml PBS by repeated pipetting, then vortexed and stored on ice. To test viability, Zombie NIR™ dye, which is non-permeant to live cells and therefore detects dead cells by providing red fluorescence (excitation 633 nm, emission maximum 746 nm) was added. A master mix of Zombie stain was prepared by dilution in PBS at 1:1000. The samples were spun, the supernatant discarded, and 100 µl Zombie was added per sample and pipetted repeatedly to resuspend the pellet, vortexed and incubated in the dark for 15 minutes at room temperature. At the end of the incubation, the reaction was stopped by adding 3 ml 1% FBS in PBS per sample and centrifuging at 500 x g for 5 minutes at 4°C. The supernatant was discarded, and the pellet was dried. Samples were resuspended in 100 µl antibody solution per sample. Antibody master mixes were prepared by diluting antibodies 1:100 in 1% FBS in PBS. After the addition of the antibody solutions, the samples were vortexed and incubated on ice in the dark for 20 minutes. At the end of the incubation, the reaction was stopped by adding 3 ml 1% FBS in PBS per sample and centrifuging at 500 x g for 5 minutes at 4°C. The supernatant was discarded, and each sample was resuspended in 500 µl 1% FBS in PBS, vortexed and filtered. Samples were stored on ice until they were read on the machine.

Antibody	Conjugate	Company	Dilution
F4/80	Alexa Flour®647	BioLegend, #123121	1:100
CD11b	FITC	BioLegend, #101205	1:100
Zombie NIR™ Fixable Viability Kit	_	BioLegend, #423105	1:1000

Table 2-7 Flow cytometry reagents

2.2.4.3 Controls and gating strategy

The Zombie viability stain efficacy was tested by killing the cells by heating at 90°C for 2 minutes. The dead-control cells were stained at the lowest recommended dilution of Zombie NIR in PBS, 1:1000, and as that resulted in

efficient staining and clear separation of live and dead cells, this dilution was maintained for the protocol.

Fluorescence minus one (FMO) controls, which were stained with all stains and antibodies in a panel minus one, were used to guide the accurate placement of the gates (Figures 2-3 and 2-4). The FMO controls were repeated for each cell type and for each stain included in the panel. An unstained sample was used to define the unstained boundary gate. An FMO control was used to define the FMO-bound gate. In a fully stained sample, the gate used was the same as the FMO bound gate if it was different from the unstained bound gate.

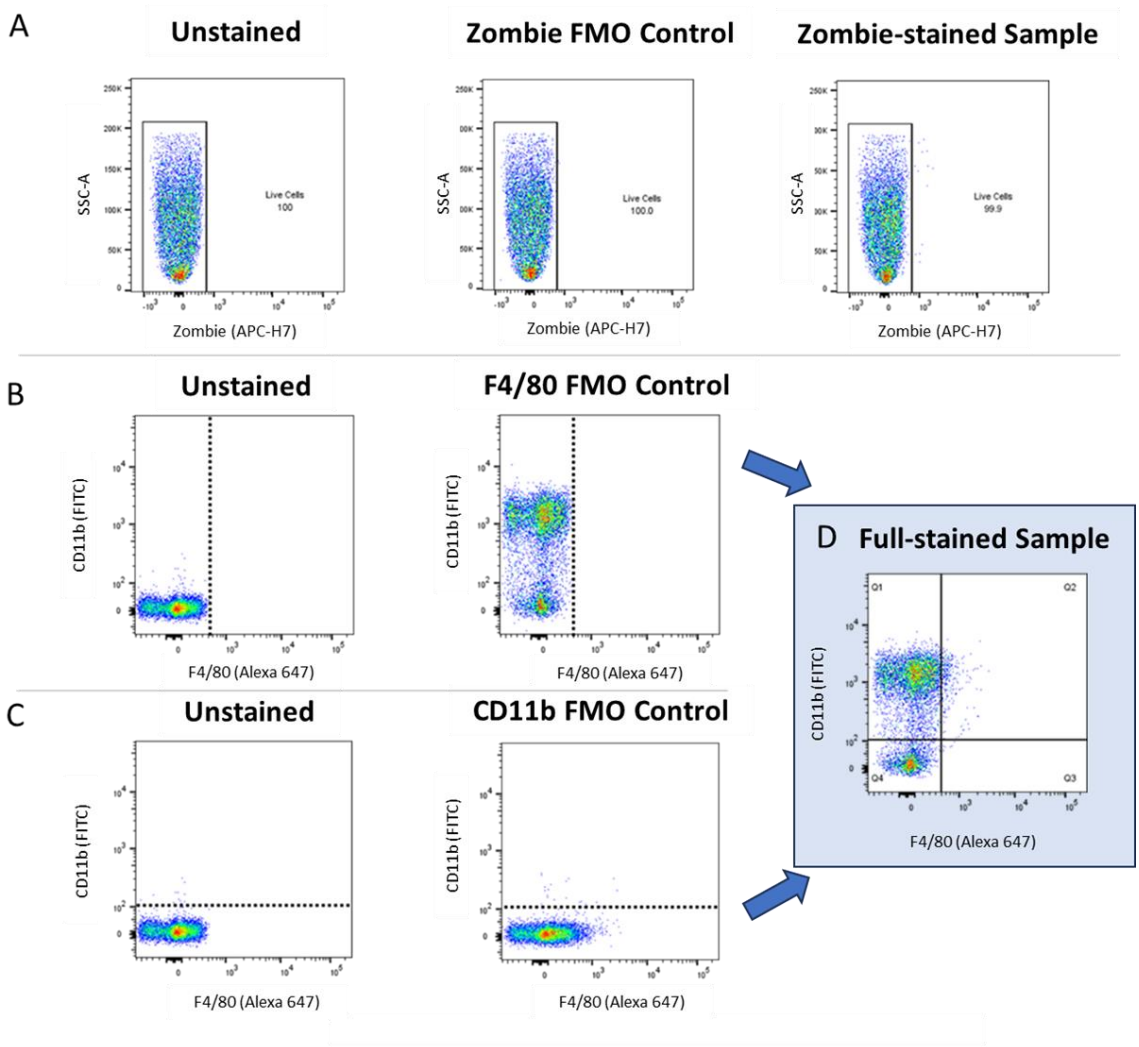

Figure 2-3 Fluorescence minus one (FMO) controls used to identify gate boundaries in bone marrow cells

The bone marrow cells were stained with all the fluorochromes in the panel except the one targeted to guide the accurate positioning of the gates. This was repeated for each fluorochrome in the panel.

(A) The Zombie NIRTM stain is positive in dead cells. In the first unstained sample, all cells inside the gate are Zombie-negative or alive, and this defines the unstained boundary gate. In the Zombie-FMO sample, the cells are stained with antibodies in the panel but not Zombie and here, all the samples in the gate are Zombie-negative or alive; this accurately defines the FMO-bound gate. In a fully stained sample, the gate used is the same as the FMO bound gate if different from the unstained bound gate.

(B) In the first unstained sample, all cells on the left of the gate are F4/80-negative, and on its right, F4/80 positive; this defines the F4/80 unstained boundary gate. In the F4/80-FMO sample, the cells are stained with all the antibodies in the panel except F4/80, and here, all the samples on the left of the gate are F4/80-negative and on its right F4/80 positive; this accurately defines the FMO bound gate. **(D)** In a fully stained sample, the gate used for F4/80 is the same as its FMO bound gate if different from the unstained bound gate**.**

(C) In the first unstained sample, all cells below the gate are CD11b-negative, and above the gate, CD11b positive; this defines the CD11b unstained boundary gate. In the CD11b-FMO sample, the cells are stained with all the antibodies in the panel except CD11b, and here, all the cells below the gate are CD11b-negative and above it are CD11b positive; this accurately defines the FMO bound gate. **(D)** In a fully stained sample, the gate used for CD11b is the same as its FMO bound gate, if different from the unstained bound gate.

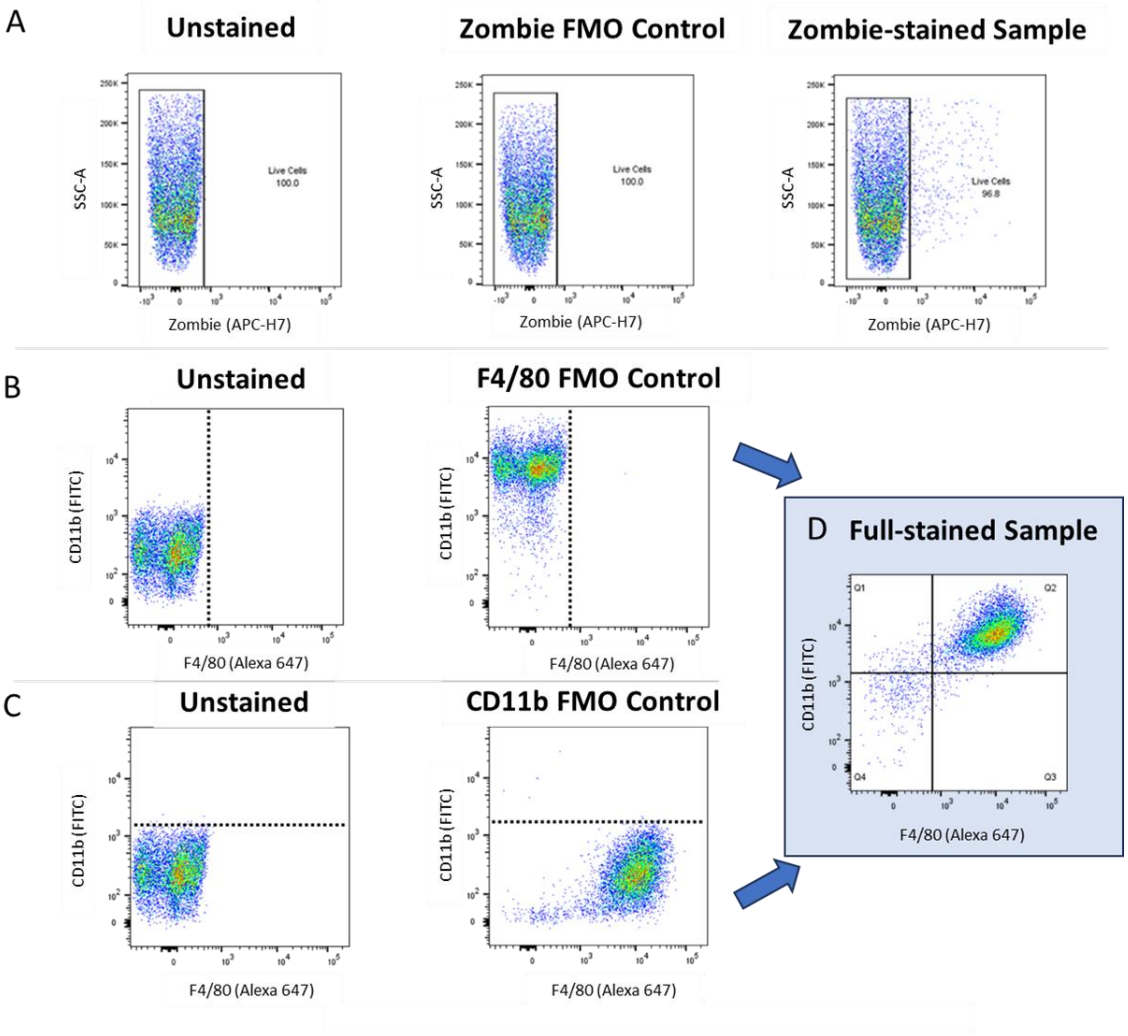

Figure 2-4 Fluorescence minus one (FMO) controls used to identify gate boundaries in bone marrow-derived macrophages

The bone marrow-derived macrophages were stained with all the fluorochromes in the panel except the one targeted to guide the precise positioning of the gates. This was repeated for each fluorochrome in the panel.

(A) The Zombie NIRTM stain is positive in dead cells. ()In the first unstained sample, all cells inside the gate are Zombie-negative or alive, and this defines the unstained boundary gate. In the Zombie-FMO sample, the cells are stained with antibodies in the panel but not Zombie and here, all the cells in the gate are Zombie-negative or alive; this accurately defines the FMO-bound gate. In a fully stained sample, the gate used is the same as the FMO bound gate if different from the unstained bound gate.

(B) In the first unstained sample, all cells on the left of the gate are F4/80-negative, and on its right, F4/80 positive; this defines the F4/80 unstained boundary gate. In the F4/80-FMO sample, the cells are stained with all the antibodies in the panel except F4/80, and here, all the cells on the left of the gate are F4/80-negative and on its right F4/80 positive; this accurately defines the FMO bound gate. **(D)** In a fully stained sample, the gate used for F4/80 is the same as its FMO-bound gate if it is different from the unstained-bound gate.

(C) In the first unstained sample, all cells below the gate are CD11b-negative, and above the gate, CD11b positive; this defines the CD11b unstained boundary gate. In the CD11b-FMO sample, the cells are stained with all the antibodies in the panel except CD11b, and here, all the cells below the gate are CD11b-negative, and all above it are CD11b positive; this accurately defines the FMO bound gate. **(D)** In a fully stained sample, the gate used for CD11b is the same as its FMO bound gate if different from the unstained bound gate.

2.2.4.4 Gating strategy

The gating strategy used for all the cell types was as follows: first cells only were included and debris was excluded. Next a gate was applied to include single cells only and thus exclude doublets. Next viable cells only were included. Lastly gates guided by the FMO controls were used to separate CD11b+ from CD11b- cells and to separate F4/80+ from F4/80- cells.

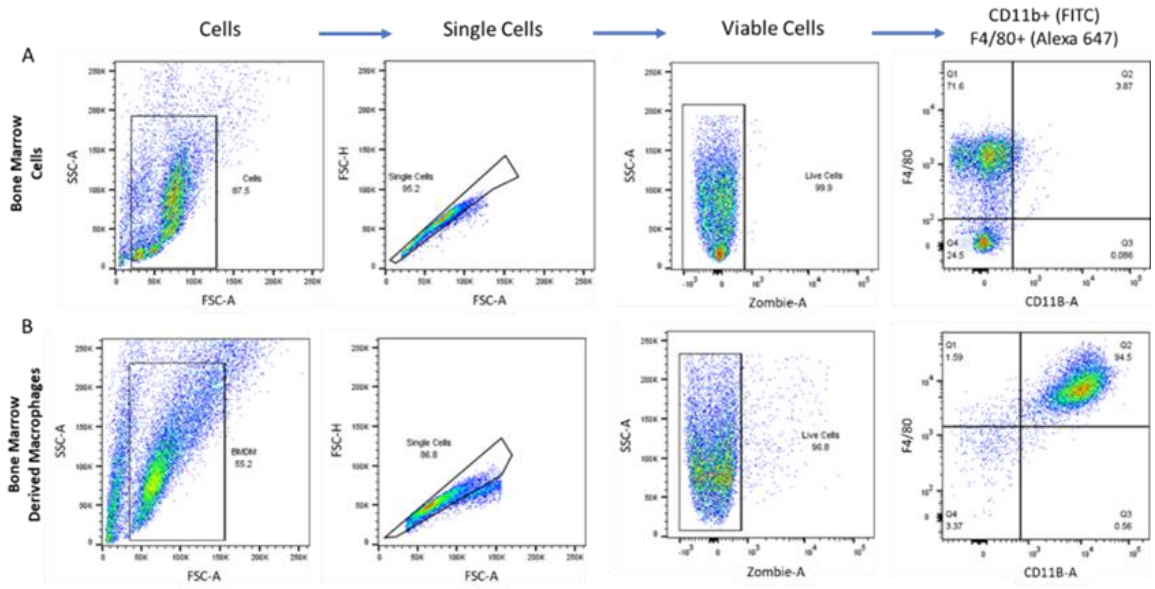

Figure 2-5 Gating strategy utilised in flow cytometry analysis of differentiation efficiency of bone marrow Cells to BMDM using recombinant M-CSF
(A) gating strategy for bone marrow cells (B) gating strategy for BMDM

2.2.4.5 BMDM differentiation validation

Bone marrow was isolated from the femurs and tibia of four C57BL/6J mice per protocol. The bone marrow cells from each mouse were depleted of erythrocytes by treatment with Ammonium-Chloride-Potassium (ACK) lysis buffer for 5 minutes. After resuspension, the depleted bone marrow cells were split into two halves. One half was frozen, and the other was differentiated using M-CSF. The frozen bone marrow cells were thawed at the end of the differentiation process. The expression of the macrophage markers F4/80 and CD11b was compared between each Bone marrow-derived macrophage and its corresponding Bone marrow stem cells. Details of the antibodies used and their dilutions are shown in table (2-7).

2.2.4.6 BMDM differentiation media comparison

For this aim, bone marrow was isolated from the femurs and tibia of four C57BL/6J mice per protocol and then treated with ACK lysis buffer. Bone marrow from each mouse was then split into two halves, one differentiated in Dulbecco's Modified Eagle's Medium (DMEM), high glucose, Glutamax media and the other half in Dulbecco's Modified Eagle's Medium – low glucose, Glutamax, with pyruvate media. At the end of the differentiation process, the flow cytometry protocol (2.2.2) was followed. F4/80 and CD11b expressions were compared between the two groups.

2.2.5 RNA extraction and analysis

2.2.5.1 RNA extraction and cDNA synthesis

Total RNA was extracted from cell cultures using the RNeasy Mini kit (Qiagen, #74104, 74106) following the manufacturer's protocol. Sample concentration and purity were determined using a Nanodrop 1000 Spectrophotometer. RNA was reverse transcribed to cDNA using the High-Capacity cDNA Reverse Transcription Kit (Applied Biosystems™, #4368814) following manufacturer protocol.

2.2.5.2 Real-Time quantitative PCR

Real-time quantitative PCR (RT-qPCR) reactions were performed using the QuantStudio Real-time thermocycler and QuantStudio® 12K Flex Software v1.3. cDNA (5 ng/µL) was mixed with forward and reverse primers at 200µM (table 2-4) in a final 1 X Fast SYBR™ Green Master Mix (Applied Biosystems™, #4385612) in a 10 µL reaction per well.

Gene	Forward Primer Sequence (5'-3')	Reverse Primer Sequence (5'-3')
Arg1	GGGACCTGGCCTTTGTTGAT	TGTCAGTGTGAGCATCCACC
Bax	TGCTACAGGGTTTCATCCAGG	GCTCCATATTGCTGTCCAGT
Bcl2	GAGAGCGTCAACAGGGAGAT	ATCAAACAGAGGTCGCATGC
Bcl2l1	GGCCACCTATCTGAATGACC	CCACAGTCATGCCCGTCA
Casp3	TGGAGAACAACAAAACCTCAGT	GTCCAGATAGATCCCAGAGTCC
Casp6	ACCGATGGCTTCTACAAAAGT	CAGGTTGTCTCTGTCTGCGT
Casp7	TGACCGATGATCAGGACTGT	CCATGCGGTACAGATAAGTGG
Ccrl2	CTCTTGTCATAACGGGCGTG	AACAGGCTGCGAAGGTATCT
Cxcl1	CGCCTATCGCCAATGAGC	AGCTTCAGGGTCAAGGCAA
Cxcl2	CTGCCAAGGGTTGACTTCAA	TTTTGACCGCCCTTGAGAGT
Ddah2	CCTGGTGCCACACCTTTCC	AGGGTGACATCAGAGAGCTTCTG
eNOS	AAGACAAGGCAGCGGTGG	GCAGGGGACAGGAAATAGTT
Il1b	GCTGCTTCCAAACCTTTGAC	TGTCCTCATCCTGGAAGGTC
Il17a	CCGCAATGAAGACCCTGATAG	TCAGGCTCCCTCTTCAGGACC
Il6	CCGGAGAGGAGACTTCACAG	TTCTGCAAGTGCATCATCGT
iNOS	CTATCAGGAAGAAATGCAGGAGAT	GAGCACGCTGAGTACCTCATT
Olr1	ACCCTCACCTTGAAGCTGAA	TAAAGGGCCCATGGAAGAGG
Rpl13	CTCATCCTGTTCCCCAGGAA	TGGGTGGCCAGCTTAAGTTC
18s	GCTCAGCGTGTGCCTACC	GGCCTCACTAAACCATCCAA

Table 2-8 Primer sequences used in qPCR during experiments

2.2.5.3 Primer design

Transcript sequences of the target genes were obtained from Ensembl genome project website (https://www.ensembl.org) (Martin *et al.*, 2022). The online software Primer3 v.4.1.0 (https://primer3.org) (Untergasser *et al.*, 2012) was used to obtain the primer pair sequences. Guideline parameters used were: exon-spanning, amplicon length 80-150bp, primer size 18-25 base pairs, GC content 40-60%, low self-complementarity and self-3'-complementarity. The proposed primer sequence was then blasted using the National Center for Biotechnology Information online tool Primer Blast (https://www.ncbi.nlm.nih.gov/tools/primer-blast) (Ye *et al.*, 2012). The specificity of the primer annealing was achieved by analysing its melt curve (Figure 2-6).

In the case of targeting the *Ddah2* gene, the primer pair in Table (2-4) was used historically in our group and was used in this project for all the RT-qPCR reactions. However, in order to confirm the genotype of the macrophage-specific *Ddah2* null mouse model , two new primers were designed. The reason

behind this is that in this model, exons 2-5 of the *Ddah2* gene are knocked out. The original primer pair used targets exons 6 and 7 and, therefore, cannot differentiate between wild-type and knockout. Therefore, two new pairs were designed to target the floxed region. One pair was designed to target exons 2 and 3, and the other pair was designed to target exons 3 and 4 (Table 2-3).

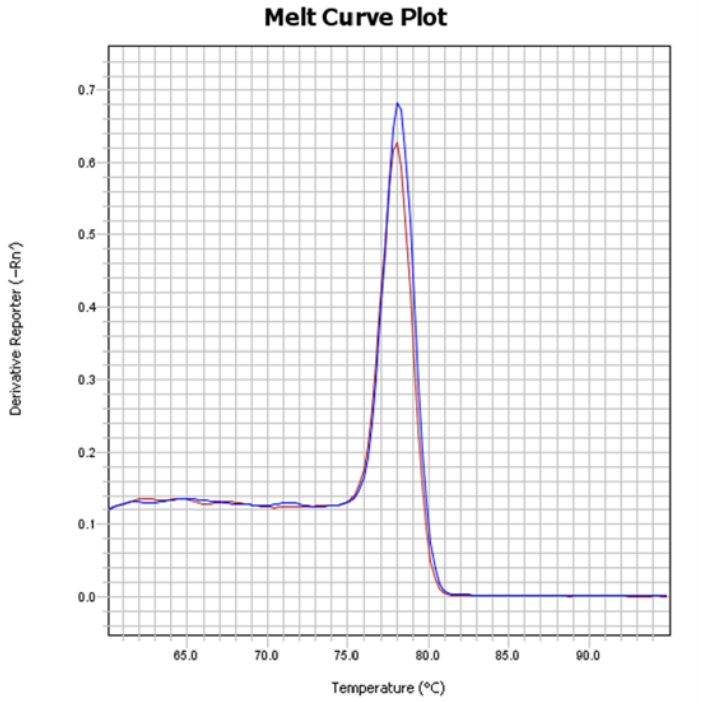

Figure 2-6 RT-qPCR primer melt curve
A representative melt curve was used to analyse the annealing specificity of a newly designed primer. A single peak is desirable as it indicates a single amplicon

2.2.5.4 RT-qPCR Data Analysis

The data was analysed using the delta-delta Ct method ($2^{-\Delta\Delta Ct}$ method) (Livak and Schmittgen, 2001). Ribosomal protein L13 (*Rpl13*) was used as the housekeeping gene.

2.2.6 Protein extraction and western blot analysis

2.2.6.1 Protein lysate and sample preparation

Total protein lysate was prepared while the culture plate was on ice, and all reagents were ice-cold. The media was discarded, and then the well was washed twice with PBS. Cells were scraped in radioimmunoprecipitation assay (RIPA) lysis buffer (Sigma, #R0278), supplemented with a final concentration of 1X Halt™ Protease and Phosphatase Inhibitor Cocktail (ThermoScientific, #1861284), 0.1 mM Phenylmethylsulfonyl fluoride (PMSF) (Sigma, #P7626), and 1 mM Dithiothreitol (DTT) (Sigma, #D9779).

Lysates were centrifuged at 14,000 relative centrifugal force (RCF), 4°C, for 20 minutes. An aliquot of the supernatant was used for protein concentration determination, and the remainder was diluted with 5X Laemmli buffer made in-house to a final 1X concentration. 5X Laemmli Buffer composition (5% ß-mercaptoethanol, 2.5 mM Tris, 19 mM glycine and 0.01 % SDS and bromophenol blue in dH_2O, pH 8.6). Samples were then heated to 95°C for 10 min and then either used directly or stored at -20°C.

2.2.6.2 Protein Concentration Determination

Extracted protein was quantified using the Pierce™ Detergent Compatible Bradford Assay Kit (Thermoscientific, # 23246). This assay is based on the binding of the Coomassie dye to the protein in an acidic medium, leading to a colorimetric reaction measured at 595nm on a Spark® Multimode Microplate Reader (Tecan). Protein concentrations of the unknown samples were determined using the standard curve generated by the bovine serum albumin (BSA) standards (Figure 2-7).

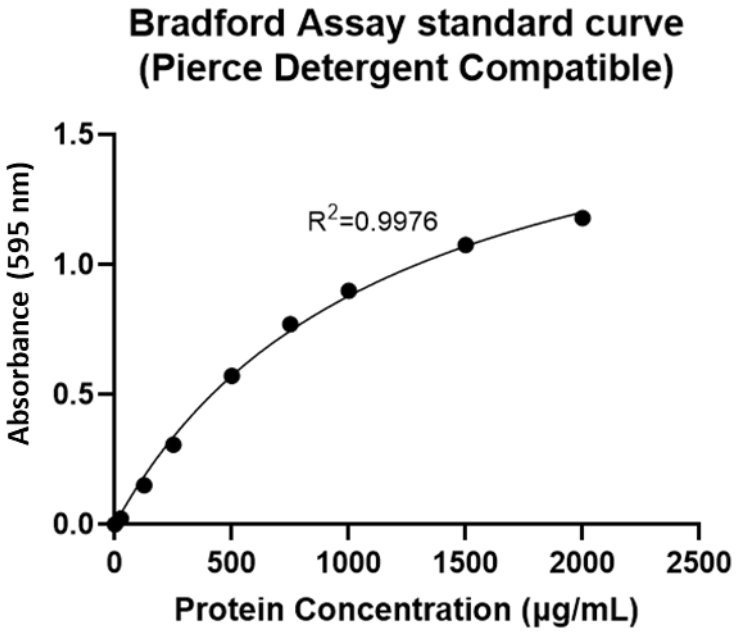

Figure 2-7 Pierce Detergent Compatible Bradford assay standard curve
A representative standard curve was generated for the Pierce Detergent Compatible Bradford Assay using bovine serum albumin (BSA) standards with concentrations ranging from 0-2,000 µg/mL

2.2.6.3 Western blot

After samples were prepared and denatured as 2.4.1, they were separated using Sodium dodecyl sulphate-polyacrylamide gel electrophoresis (SDS-PAGE), which was performed using precast 4-15% Mini-Protean® TGX™ Gels (Biorad, #4561084). The gels were loaded with equal amounts of protein for all the samples (max 20 µg) and 10 µl Precision Plus Protein™ All Blue Prestained Protein Standards ladder (Biorad, #1610373). The electrophoresis was conducted in 1X Tris-glycine-SDS running buffer in ddH_20 (prepared from Ultrapure 10X Tris-glycine/SDS, Geneflow,#B9-0032) at 80 volts for 20 minutes, then 110 volts until adequate separation of the target proteins was achieved. Next, proteins were transferred in 1X Tris-glycine transfer buffer in ddH_20 (prepared from Ultrapure 10X Tris-glycine, Geneflow,#B9-0058 by adding 2 part methanol and 7 part ddH_20). The transfer was conducted overnight at a constant of 50mA at 4°C onto an Immobilon®-PVDF membrane (Millipore, #IPVH00010).
After transfer, the membrane was stained with Revert™ 700 Total Protein Stain (Licor, #926-11010) according to manufacturer protocol and imaged using the LI-COR Odyssey scanner.

The membrane was blocked in 20% Sea block (Abcam, #166956) diluted in 0.1% Tween 20 in TBS (TBS-T) on a shaker at room temperature for one hour. The membranes were incubated overnight with the primary antibody (table 2-9) on a shaker at 4°C. The membranes were washed and incubated for one hour at room temperature in the suitable secondary antibody (table 2-10). ß-actin was used as a housekeeper protein.

Primary Antibody	Manufacturer/ product code	Source	Dilution	Dilution buffer
DDAH2	Abcam, #184166	Rabbit monoclonal	1:750	2% v/v sea block in 0.1%TBS-T
iNOS	Abcam, #283655	Rabbit multiclonal	1:1000	5% w/v BSA in 0.1%TBS-T
ß-Actin	Abcam, #170325	Mouse monoclonal	1:10,000	2% v/v sea block in 0.1%TBS-T

Table 2-9 Primary antibodies used in western blot

Secondary Antibody	Manufacturer/ product code	Dilution	Dilution buffer
Donkey anti-rabbit 800*	Invitrogen, #SA5-10044	1:10,000	***
Donkey anti-mouse 680**	Invitrogen, #SA5-10170	1:10,000	

Table 2-10 Secondary antibodies used in western blot
*for detection of DDAH2 and iNOS, **for Beta-actin, ***dilute in the same buffer as used with the corresponding primary antibody

2.2.6.4 Western Blot Analysis

A minimum of three biological replicates were used for each target protein per cell type. Beta-actin and Total Revert stain were used as internal loading controls. Target protein quantification was achieved by normalising to total protein via Empiria Studio 2.3. Image acquisition was via Odyssey CLx (LI-COR) and Image Studio software.

2.2.7 Greiss assay

Nitric oxide release was estimated by measurement of nitrite concentration in the cell media using the Griess Assay (Invitrogen, G7921) per manufacturer protocol. In brief, equal volumes of 0.1% *N*-(1- naphthyl)ethylenediamine dihydrochloride and 1% Sulfanilic acid in 5% phosphoric acid were mixed to form the Griess reagent. The reactions were prepared by mixing 20 µL of Griess Reagent, 130 µL of deionised water and 150 µL of the nitrite-containing sample or standard. Samples and standards (1-100µM Sodium nitrite) were prepared in duplicate in a 96-well plate. The mixture was incubated in the dark for 30 minutes at room temperature. The absorption of the azo dye generated from the reaction was measured at 548 nm by the VictorX3 spectrophotometer multilabel plate reader (PerkinElmer). Sample nitrite concentrations were interpolated from the standard curve generated by the known standards (Figure 2-8).

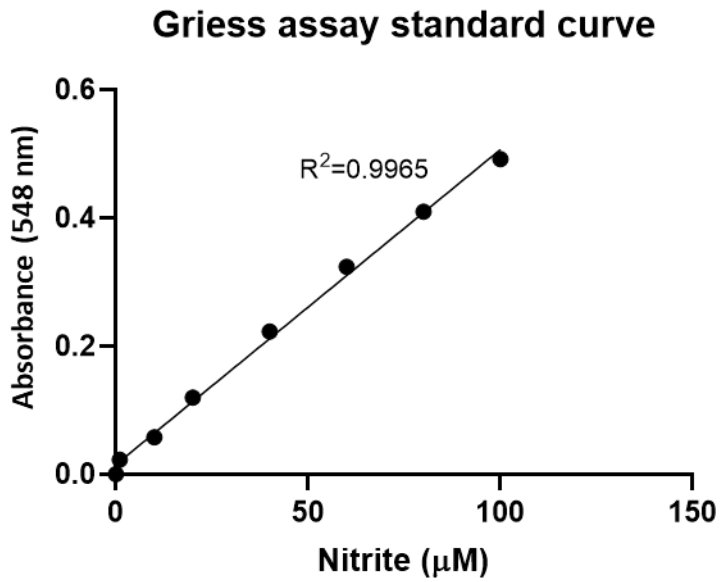

Figure 2-8 Griess assay standard curve
A representative standard curve was generated for the Griess assay using known sodium nitrite standards concentrations ranging from 0-100 µM

2.2.8 RNA Sequencing analysis

As the *in vitro* experiment for the RNA sequencing study and the RNA sequencing itself were conducted by a previous member of our group, details and references to them are included in the relevant results section (4.3) for context. This project started with the raw fastq files, and their analysis will be detailed here.

The analysis was conducted via a web-based platform, “Galaxy”, on the main public server (https://usegalaxy.org) (Figure 2-9).

First, raw reads were processed through FastQC (version 0.11.8) for quality control, and then, to improve the read quality, the data was processed using an all-in-one tool, Fastp (Version 0.20.1). This was followed by a second quality check by the FastQC tool (Version 0.11.8). Then, the paired files for each sample were aligned to the most recent Ensemble mouse genome (mm10) (mm10.ncbiRefSeq.gtf.gz) using the sensitive splice-aware Hisat2 alignment program (Galaxy version 2.1.0+galaxy7). The output binary alignment map (BAM) file was quality-checked using FastQC (version 0.72+galaxy1). Alignment statistics, including the numbers of mapped and unmapped reads (Table 4.1 a), were obtained using Samtool stats from which the Average Alignment Percentage was calculated for each sample group. Next, gene-based counts were generated using the HTSeq-count tool (Galaxy version 2.1.0 + galaxy7) using the same reference genome (mm10) in a general feature format (GFF) and the BAM files as input. These count tables were then taken forward as the input into the DESeq2 tool for the final identification of genes of interest. Each two groups of samples were compared across either treatment or genotype using DESeq2 (Galaxy version 2.11.40.6+galaxy1). The total significantly Differentially Expressed Genes were quantified with the cut-off point p-adj>0.05.

The upregulated and downregulated genes per group per their fold change (FC) were identified. Representative graphs were generated either using the Galaxy platform for the principal component analysis (PCA) plots or by Python using a code developed by Dr Simon Fisher in the school (violin and volcano plots). Gene Ontology (GO) software was used to identify the affected biological processes, and Reactome Pathways were identified per group.

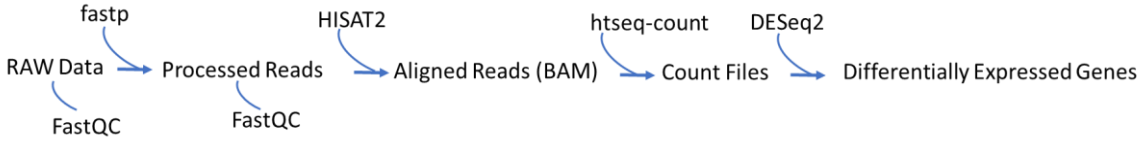

Figure 2-9 *In silico* analysis in Galaxy software

2.2.9 Enzyme-linked immunosorbent assay

Enzyme-linked immunosorbent assay (ELISA) was performed to detect interleukin-17 (IL17A) production by peritoneal macrophages using the Quantikine™ ELISA (R&D Systems, M1700) per manufacturer protocol. In short, after the isolation of peritoneal macrophages from the macrophage-specific *Ddah2* null mouse model, cells from the control and knockout mice were seeded in a 24-well plate at a density of 500,000 cells/well. For each mouse, two wells were prepared. After washing away the non-adherent cells per protocol (2.1.3), fresh media was added. In one well (untreated), 300 µl complete growth medium was added. In the other well (treated), 300 µl complete growth medium supplemented with LPS 10 µg/µL was added. The plate was incubated for 24 hours, and then the media was collected and stored in aliquots at -80°C to avoid IL-17A disintegration by freeze-thaw cycles. At the time of the assay, the reagents, samples, mouse IL17 standards (recombinant mouse IL17, ranging from 0-700 pg/mL, supplied with the kit) and the mouse IL-17A control (recombinant mouse IL17, range 76.7-128 pg/mL supplied with the kit) were prepared per manufacturer protocol. 50 µl of each of the samples and standards was processed in duplicate. At the end of the protocol, the plate was read within 30 minutes of the last step. Absorption was measured at 450 nm and 540 nm on the Spark® Multimode Microplate Reader (Tecan). For manual wavelength correction, the readings at 540 nm were subtracted from the readings at 450 nm. Sample concentrations were interpolated from the standard curve generated from the included standards (Figure 2-10).

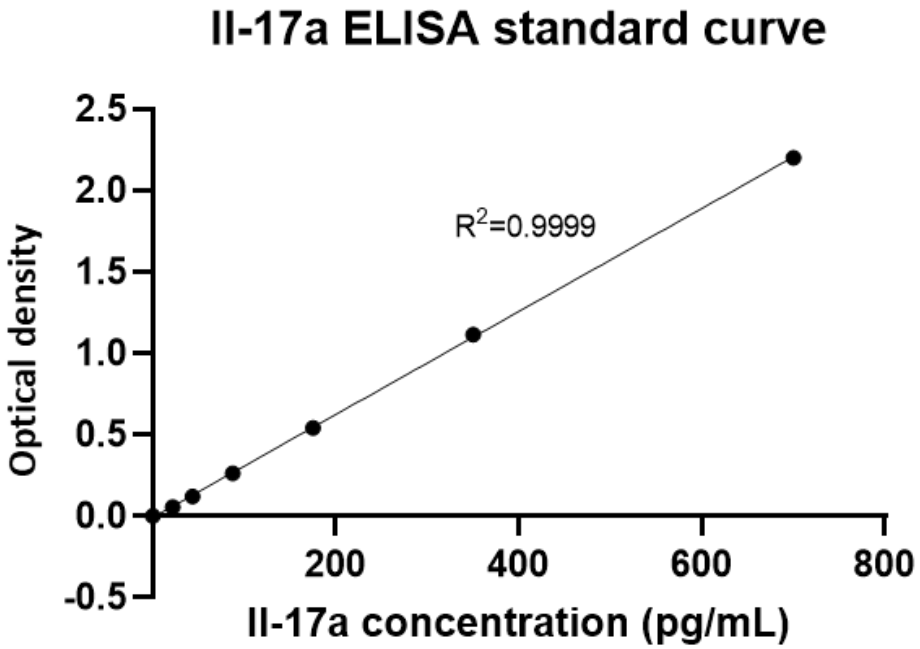

Figure 2-1 IL17A ELISA standard curve
A representative standard curve generated for the IL17A Enzyme-linked immunosorbent assay (ELISA) using the kit-supplied recombinant mouse IL17 standards ranging from 0-700 pg/mL. The readings were plotted after manual wavelength correction by subtraction of readings at 540 nm from the readings at 450 nm

2.3 Statistical Analysis

Data were analysed and plotted using GraphPad Prism version 9.3 for Windows, GraphPad Software, www.grahpad.com. Where $n \geq 3$, statistical tests in the form of Student's two-tailed t-tests, one-way and two-way analysis of variance (ANOVA) with post-hoc tests were performed as appropriate. P values equal to or less than 0.05 were considered significant. Data was plotted as Mean ± standard error of the mean (SEM).

Chapter 3 Results: Characterisation of the models for the study of the role of DDAH2 in inflammation

3.1 Introduction

This thesis initially aimed to study functions of DDAH2 in inflammation in an atherosclerotic mouse model. Atherosclerosis is a chronic progressive inflammatory disease that affects the intima of medium and large-sized arteries and is characterised by the "atheromatous plaque" due to the accumulation of lipids and a variety of immune cells and smooth muscle cells (Linton *et al.*, 2019; Ross, 1993). ADMA is an independent cardiovascular disease risk factor and a competitive inhibitor of nitric oxide synthase (Murakami, Mizuno and Kaku, 1998). ADMA is metabolised mainly by DDAH (Teerlink, 2005). Since DDAH2 is the isoform found in macrophages, we hypothesise that DDAH2 regulates NO production in the immune system through ADMA hydrolysis. We also hypothesise that DDAH2 has roles beyond ADMA hydrolysis and affects cellular functions in a NO-independent manner.

As mentioned previously, the initial aim of this project was to conduct the study on an atherosclerotic macrophage-specific *Ddah2* null mouse model. However, this was derailed by limitations caused by the Covid-19 pandemic. Therefore, the project aims were altered to study the inflammatory aspect of atherosclerosis and, specifically, the function of DDAH2. Hence, an inflammatory model was used in the form of a macrophage-specific *Ddah2* null mouse model and inflammation was induced *in vitro* by stimulation of extracted macrophages with LPS. Therefore, the macrophage cells used should express key genes of the DDAH-ADMA-NOS pathway and show a functional response to an inflammatory stimulus (Ludwig *et al.*, 2018). To better understand the DDAH-ADMA-NOS pathway in the immune system, it is crucial to investigate the mechanisms of action of DDAH2. As there is a debate surrounding the role of DDAH2 in ADMA hydrolysis, it would be beneficial to study the effects of short-term and long-term DDAH2 deletion. If DDAH2 does indeed hydrolyse ADMA, the effects of short-term DDAH2 deletion can be studied through pharmacological

administration of ADMA. However, the long-term effects of *Ddah2* deletion can be investigated by genetically manipulating it.

RAW 264.7 cell line was established from a tumour in a male BALB/c mouse induced with the Abelson murine leukaemia virus in 1978 by WC Raschke (1978). They are mainly adherent cells, but some are suspended and viable. They have a doubling time of 24 hours. RAW 264.7 is a macrophage cell-like cell line, as it was shown to have phagocytic, pinocytic and cytotoxic properties (Raschke, 1980; Taciak *et al.*, 2018; Raschke *et al.*, 1978). It responds robustly to lipopolysaccharide (LPS) stimulation as assessed by nitrite production by the Griess assay (Dunham *et al.*, 2023). The RAW 264.7 cell line has been extensively used to study nitric oxide biology, as a literature search in PubMed revealed more than 6,000 publications. RAW 264.7 cells have been shown to express genes relevant to the nitric oxide pathway, such as *eNOS* and *iNOS* (Noh *et al.*, 2006). ADMA has been shown to inhibit nitric oxide (NO) production (Pekarova *et al.*, 2013). Furthermore, more than 600 publications in PubMed have used it as a model to study atherosclerosis. LPS stimulation of RAW 264.7 in the presence of oxLDL induces inflammation and foam cell formation (Min, Cho and Kwon, 2012). Therefore, the first cells chosen as models in this project was the RAW 264.7 cell line, which was successfully used in NO studies and atherosclerosis. Furthermore, it is easily cultured, abundant, and cheaper than primary cells, and therefore, it is a practical choice to start experiments and train on methods.

Genetic modulation can be used to investigate the long-term effects of *Ddah2* deletion. One widely used specific gene modulation technique is the Cre-loxP system (Nagy, 2000). This system was developed in the early 1990s (Orban et al., 1992) and is based on the function of Cre recombinase, which is an enzyme derived from the P1 bacteriophage (Sternberg *et al.*, 1978; Sauer, 1998). It mediates the deletion of sequences between two lox-P sites, which are specific DNA sequences it can recognise (Sauer and Henderson, 1988; O'Neil, Hoess and DeGrado, 1990). Therefore, the Cre-loxP system relies on two components. A strain in which Cre recombinase is expressed, and if a tissue-specific promoter is used, the deletion is tissue-specific (Kim *et al.*, 2018). The second component is a strain which contains the gene of interest flanked by two lox-P sites (Kim *et al.*, 2018).

Mice expression of two lysozyme genes was harnessed to create macrophage-specific gene deletions. The P gene is expressed in Paneth cells, and the M gene is expressed in myeloid cells. Using LysM as a promotor, Clausen et al. created a highly macrophage-specific Cre-strain "LysM-Cre"(Clausen *et al.*, 1999). The use of the LysM-Cre strain showed high efficiency with 83-99% deletion in tissue-resident macrophages and around 80% deletion in developing *in vitro* differentiated bone marrow-derived macrophages. Therefore, deletion is more complete in fully differentiated cells (Clausen *et al.*, 1999). As Lys-M is expressed in myeloid cells, LysM-Cre mediated deletion was detected 80-99% in macrophages, partially in splenic or G-MCSF *in vitro* myeloid-derived dendritic cells (DCs) (Clausen *et al.*, 1999). However, it was not detected in peripheral DCs or T and B cells (Clausen *et al.*, 1999). LysM-Cre mice are available in the Jackson Laboratory (https://www.jax.org).

Our group used the LysM-Cre technology to generate a macrophage-specific *Ddah2* null mouse model (Lambden *et al.*, 2015). Although DDAH1 may compensate for DDAH function in the absence of DDAH2, macrophages only express DDAH2, and thus, that would not be a concern. Immune functions are frequently studied in peritoneal macrophages and bone marrow-derived macrophages. Peritoneal macrophages are tissue-resident macrophages extracted easily and accessibly from the peritoneal cavity (Hirsch, 1956). Albeit more challenging to isolate, bone marrow-derived macrophages, a naïve form of macrophages, are also used. They are differentiated from isolated bone marrow cells and differentiated *in vitro* (Rios, Touyz and Montezano, 2017). Although peritoneal macrophages are easier and faster to isolate, BMDMs have a much higher yield and can help increase the number of experiments conducted from one mouse.

Nitric oxide biology and immune functions have been studied in both peritoneal macrophages (Kobayashi *et al.*, 2018; Hrabák *et al.*, 2023; Abdelouhab *et al.*, 2012; Liu *et al.*, 2018) and BMDMs (Bailey *et al.*, 2020; Kresinsky *et al.*, 2016; Diotallevi *et al.*, 2022). Furthermore, both cell types have been used to study aspects of atherosclerosis, such as foam cell formation (Anzinger *et al.*, 2012; Guo *et al.*, 2023; Fujiwara *et al.*, 2018). Therefore, these cell types will be validated for this project.

3.2 Aims

1. Validate the suitability of using the murine RAW 264.7 macrophage cell line as a model to study the role of DDAH2 in inflammation.

2. Validate the suitability of using BMDM derived from Wildtype C57BL/6J mice as a model to study the role of DDAH2 in inflammation.

3. Validate the genotype and phenotype of the rederived macrophage-specific *Ddah2* null mouse model.

3.3 RAW 264.7 characterisation

3.3.1 qPCR validates the use of *Rpl13* as a housekeeping gene in RAW 264.7 murine macrophage cell line

The RAW 264.7 cell line was selected as a candidate model for the study due to its prior use as an *in vitro* model of atherosclerotic macrophage activation and is readily available. One of the analytical methods used throughout this project was evaluating gene expression through qPCR. Thus, the suitability of two candidate housekeeping genes for RT-qPCR was validated in the initial phase. The candidate housekeeping genes were two ribosomal genes, *18s* rRNA (18S ribosomal RNA) and *Rpl13* (60S ribosomal protein L13). Ribosomal proteins are commonly used as housekeeper genes as they are the most stably expressed genes, probably due to their fundamental role in replication (de Jonge *et al.*, 2007).

To validate their suitability in the planned experiments, RAW 264.7 cells were either left untreated as a control or stimulated with 1 µg/mL LPS, the inflammatory stimulus for future experiments. The expression of *18s* and *RPL13* (Figure 3-1) was evaluated by comparing their respective CT values between the control and LPS treatment. Both *18S* and *RPL13* showed stable expression throughout the experiments, as depicted by the number of cycles required for the fluorescent signal to cross the threshold in the qPCR analysis. A paired two-tailed T-test showed p-values higher than 0.05. Therefore, there was no

significant difference in the expression of either gene following treatment. Thus validating the use of either one for future analysis.

Rpl13 was selected for further validation for normalisation as its Ct value was closer to the target genes. Its expression was evaluated with LPS treatment across time points planned to be used in future experiments (2-24 hours).

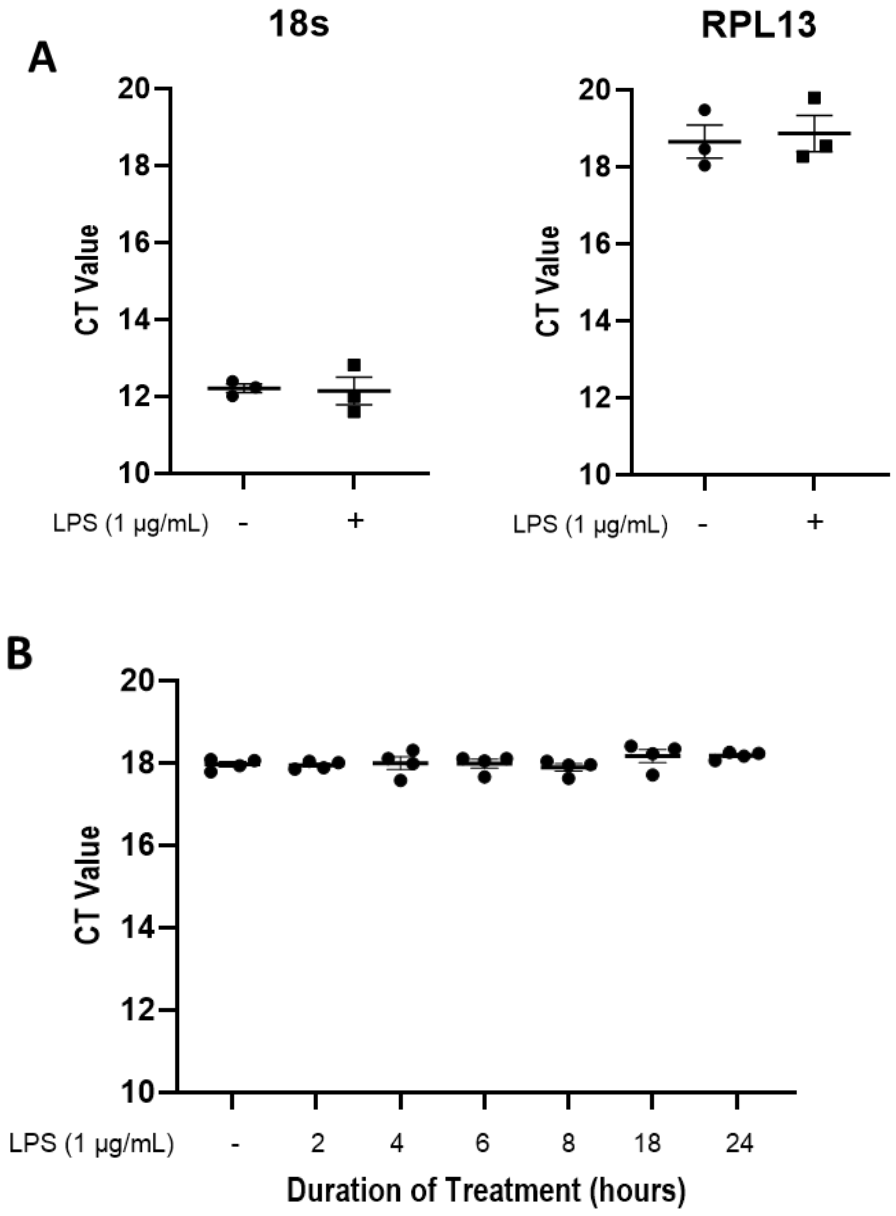

Figure 3-1 RT-qPCR validates the use of *Rpl13* as a housekeeping gene
(A) The cycle thresholds for *18S* and *Rpl13* were compared in RAW 264.7 murine macrophages untreated or treated overnight with 1 µg/mL LPS; (n=3) (B) Ct value for RPL13 only over 2-24 hours of LPS (1 µg/mL) stimulation; (n=4). Mean ± SEM. p>0.05. Unpaired two-tailed Student's t-test.

3.3.2 RT-qPCR validates RAW 264.7 cells expression of key genes of interest in the nitric oxide pathway

As the project revolves around studying the role of DDAH2 in atherosclerosis and DDAH2 has a well-established role in the metabolism of ADMA, a critical cardiovascular disease risk factor- it was of interest to establish the expression of genes involved in the DDAH-ADMA-NOS pathway in the RAW 264.7 murine macrophage cell line. Therefore, the expression of *Ddah2*, *iNOS*, and *eNOS* (Figure 3-2) was compared with and without activation with 1 µg/mL LPS for multiple durations.

Ddah2 expression showed a slight increase in expression after 4 hours of incubation and slightly further increased at 6 hours, then declined slightly at 8 hours before returning to control levels at 18 and 24 hours; however, changes were not statistically significant. *eNOS* expression follows the same pattern as *Ddah2* as it increased immediately in response to LPS exposure, reaching maximal expression at 6 hours, following which its expression fell slightly but remained above control levels for the entire 24-hour treatment. The changes in *eNOS* expression reached statistical significance at 4 hours (**** $p<0.0001$), at which the expression was doubled and remained significant for the 24-hour treatment duration. *iNOS* expression surged ~150 fold and reached statistical significance after only 2 hours of activation by LPS and continued to increase (>8,000 fold) and remained significant throughout the observed time points *(****$p<0.0001$)*.

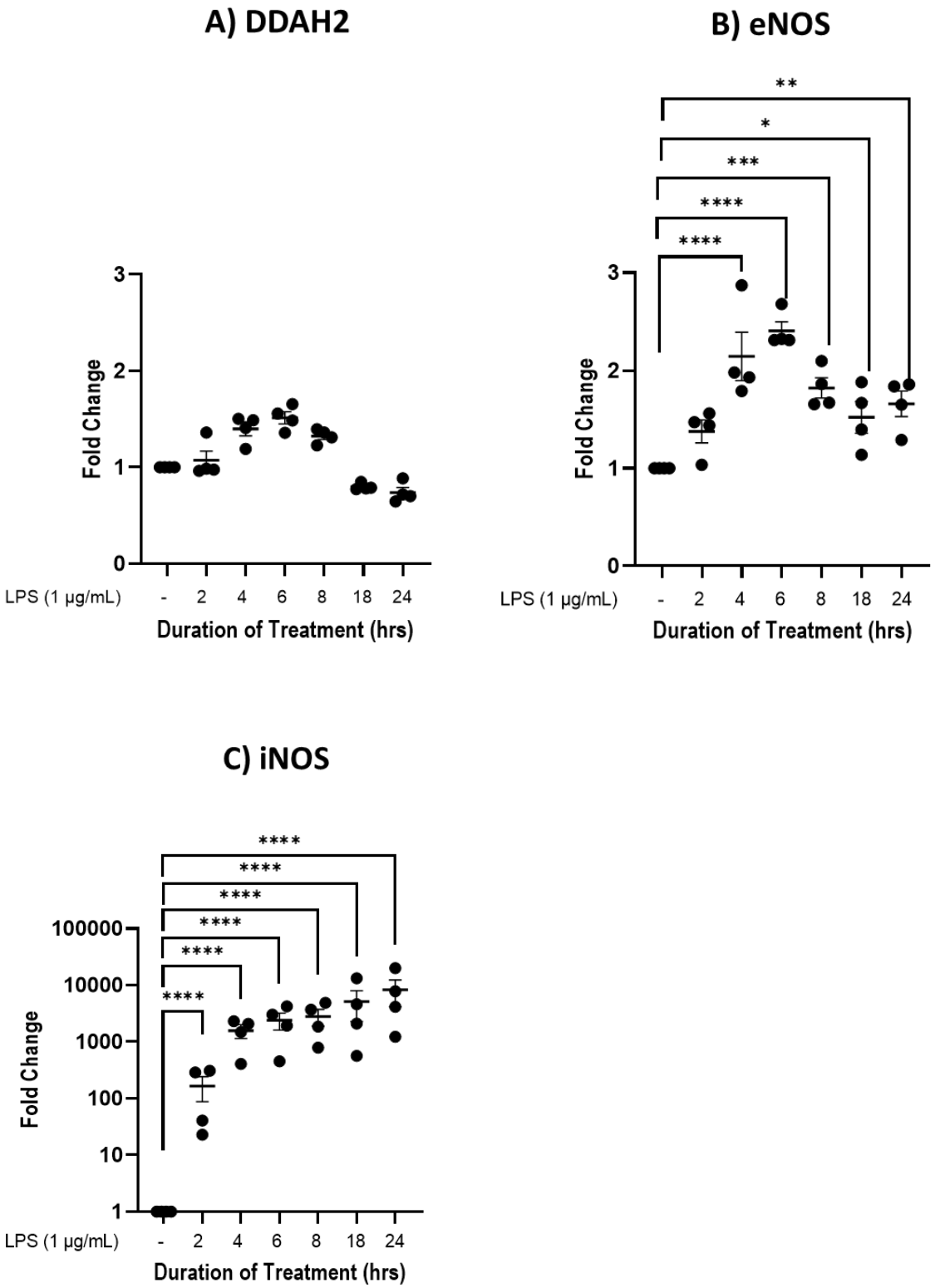

Figure 3-2 RAW 264.7 murine macrophage cells express key target genes in NO-ADMA-DDAH pathway

The mRNA expression of A) *Ddah2* in response to 1 µg/ mL was statistically not significant, B) *eNOS* expression increased with the treatment of LPS 1 µg/mL over 24 hours, reaching statistical significance at 4 hours, C) *iNOS* expression increased immediately significantly and continues to increase with time. n=4. Mean ± SEM. p>0.05. One-way ANOVA with Dunnett post hoc test. *(*p=0.012,** p=0.002, ***p=0.0003, ****p<0.0001)*.

3.3.3 RAW 264.7 murine macrophage cell line expresses DDAH2 protein

Since the gene expression of *Ddah2* in RAW 264.7 was confirmed at baseline and after stimulation with LPS for 24 hours by qPCR, the next step was to validate the DDAH2 protein expression by western blot analysis of lysates extracted at baseline and after stimulation with 1 µg/mL LPS for 24 hours (Figure 3-3). Although there appears to be a trend of increase in DDAH2 protein concentration after LPS stimulation similar to that noted with mRNA expression, the change was not statistically significant here either *(p=0.0982)*.

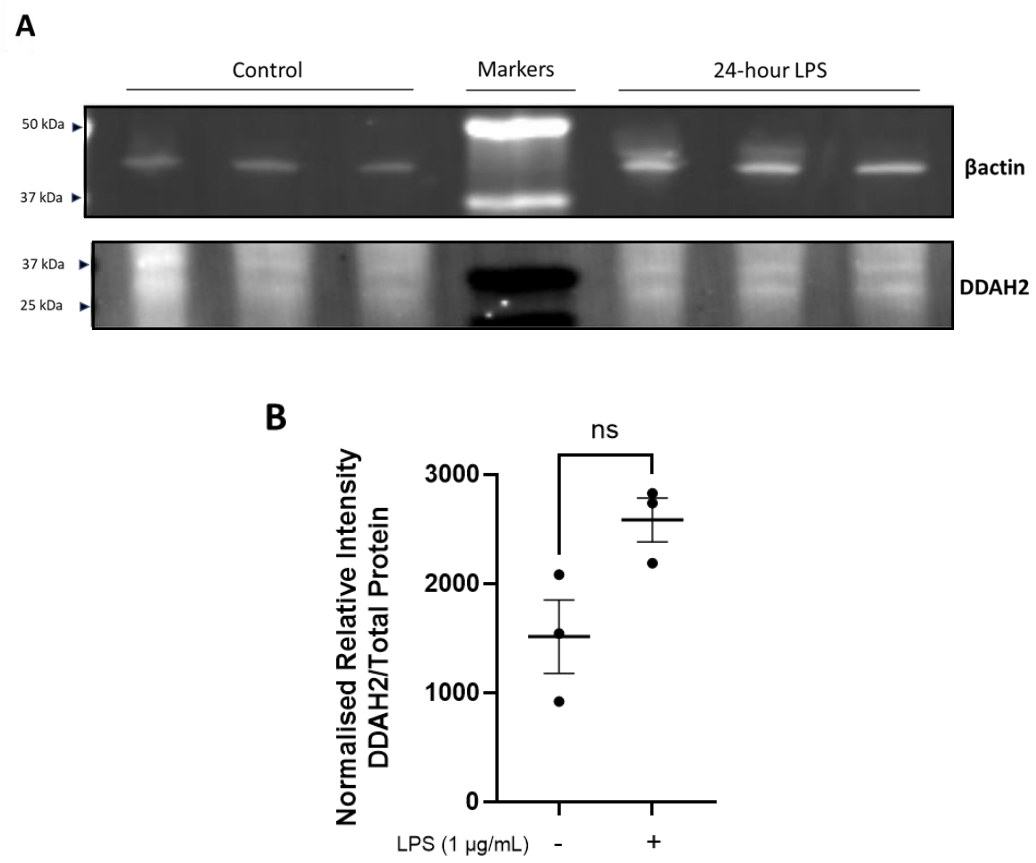

Figure 3-3 DDAH2 protein is expressed in RAW 264.7 macrophage cell line
Western blot analysis of RAW 264.7 protein lysates at baseline and after stimulation with 1 µg/mL LPS for 24 hours. (A) βactin antibody as internal loading control and anti-DDAH2 antibody. B) Densitometry analysis of DDAH2 protein expression showing increased trend of expression after LPS treatment. n=3. Mean ± SEM. p>0.05. Unpaired two-tailed Student's t-test

3.3.4 RAW 264.7 cells synthesise iNOS protein in response to LPS stimulation

To confirm that RAW 264.7 cells do not synthesise iNOS at baseline but the synthesis occurs as a result of activation with LPS, the protein expression was validated by western blot analysis of lysates extracted at baseline and after stimulation with 1 µg/mL LPS for 24 hours (Figure 3-4). There was no evidence of iNOS expression at baseline. However, there was a highly significant expression after stimulation with 1 µg/mL LPS for 24 hours *(p<0.001)*.

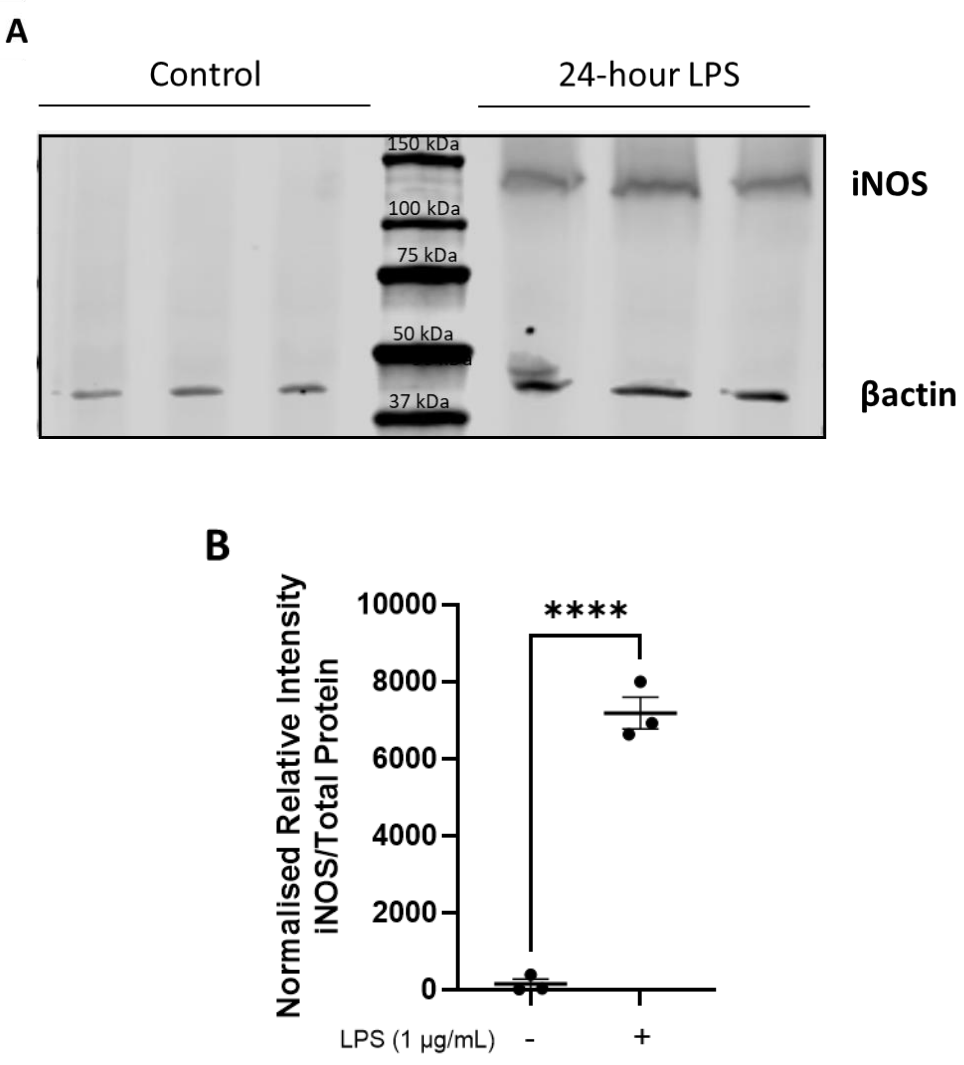

Figure 3-4 iNOS protein is synthesised in RAW 264.7 macrophage cell line in response to LPS stimulation
Western blot analysis of RAW 264.7 protein lysates at baseline and after stimulation with 1 µg/mL LPS for 24 hours. (A) βactin antibody as a qualitative internal loading control and anti-iNOS antibody. (B) Densitometry analysis of iNOS expression showing a statistically significant increase in expression after LPS treatment. n=3. Mean ±SEM. p>0.05. Unpaired two-tailed Student's t-test. *(****p<0.0001).*

3.3.5 RAW 264.7 cells release nitric oxide in response to LPS stimulation

To provide functional validation of the inflammatory response, the Griess assay was performed as an indirect measurement of nitric oxide (NO) released in the culture medium by RAW 264.7 cells in response to LPS stimulation. Culture media was collected from untreated (control) or LPS-treated RAW 264.7 cells from five passages over 2-24 hours. (Figure 3-5). The nitrite levels started to increase at 6 hours slightly, more at 8 hours, and continued to increase, reaching significance at 18 hours *(p=0.005)* and more so at 24 hours *(p=0.0001),* although variations within each time point exist.

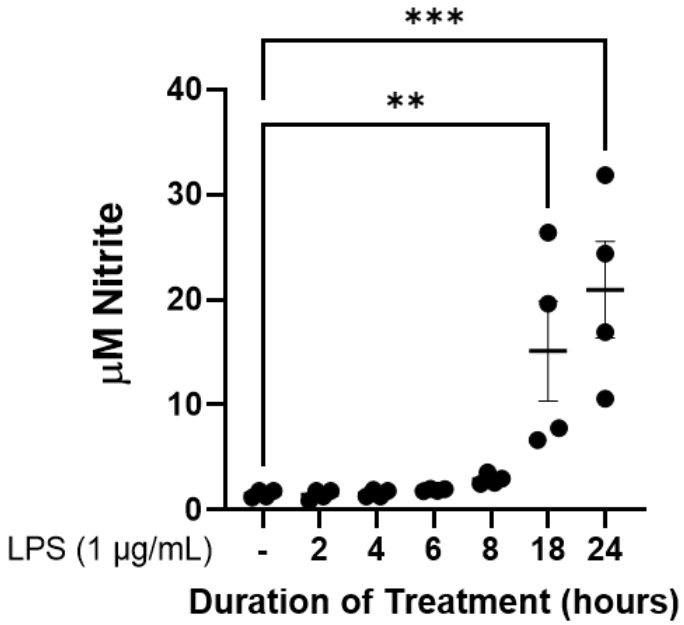

Figure 3-5 RAW 264.7 murine macrophage cells release nitric oxide in response to LPS stimulation
Nitrite levels released by RAW 264.7 into the culture medium after stimulation with LPS for 2-24 hrs. n=4. Mean ± SEM. p>0.05. One-way ANOVA with Dunnett post hoc test. *(**p=0.005, ***p=0.0001)*

3.3.6 ADMA does not affect NO release in resting macrophages

As ADMA is an established competitive Nitric Oxide Synthase inhibitor, we aimed to investigate if ADMA influences NO production in resting macrophages. RAW 264.7 macrophages were incubated for 24 hours in experimental media with different concentrations of ADMA (2,3,10,30 and 100 µM). NO production was then estimated by Griess assay (Figure 3-6). No significant change in NO level was noted in resting macrophages after treatment with ADMA.

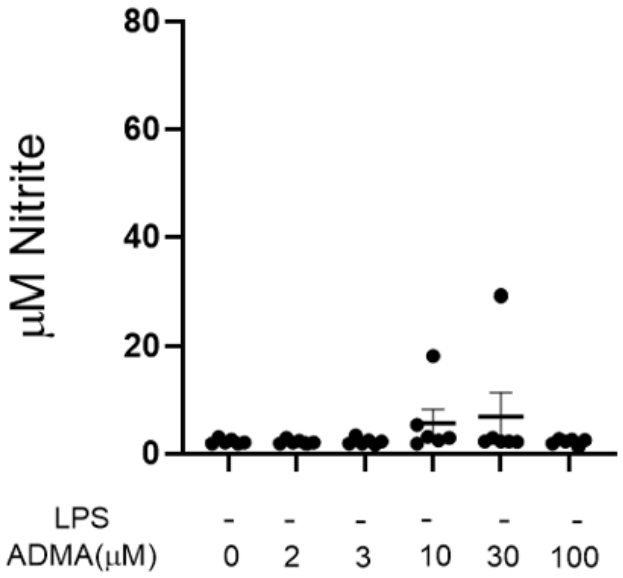

Figure 3-6 ADMA does not affect NO release in resting RAW 264.7 macrophages
Levels of nitrite released by RAW 264.7 into the culture medium after treatment with 2-100 µM ADMA for 24 hours were determined using Griess Assay. n=5. Mean ± SEM. $p>0.05$. One-way ANOVA with Dunnett post hoc test.

3.3.7 High-variation in the response of RAW 264.7 to ADMA post-LPS-stimulation in high-arginine media

As ADMA was found not to affect NO levels in resting macrophages, the effect of ADMA on NO levels in stimulated macrophages was investigated. Firstly, in an ADMA-dose finding experiment, the effect of treating RAW 264.7 macrophages with ADMA and LPS simultaneously vs pre-treatment with ADMA prior to

stimulation with LPS was investigated. RAW 264.7 cells were treated with 1 µg/mL LPS and ADMA (0, 2, 3, 10, 30, or 100 µM) simultaneously (Figure 3-7), or LPS was added 60 min after incubation with ADMA. In both conditions, the cells were treated in experimental media composed of Dulbecco's Modified Eagle Medium (DMEM) supplemented with 10% fetal bovine serum (FBS). The cells were incubated for 24 hours, then the medium was collected, and NO production was determined by the Griess assay. In both conditions, there appears to be a slight reduction of NO production with increased ADMA concentration, but the high variability in the data rendered comparison difficult.

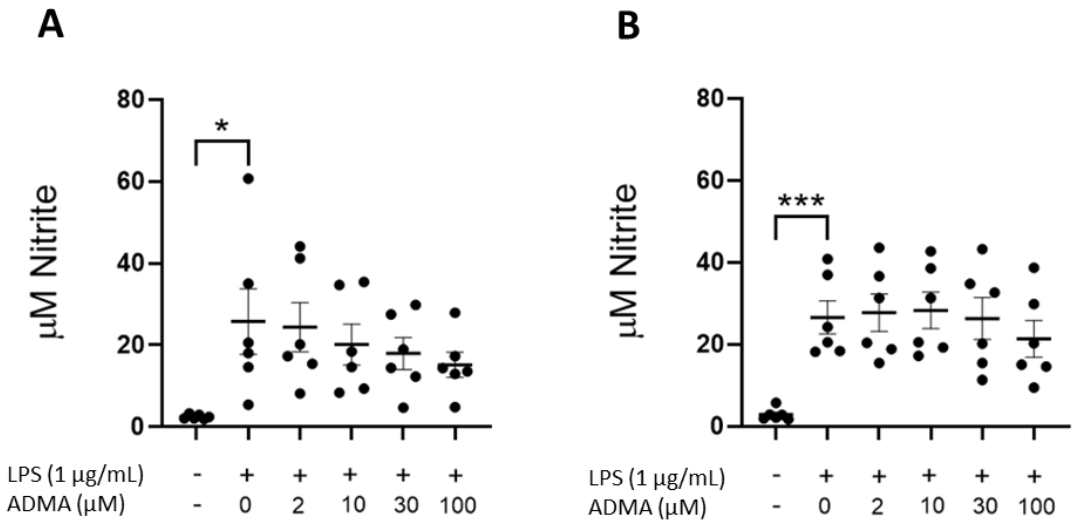

Figure 3-7 Macrophages have a high variation in their levels of nitric oxide released in response to LPS-stimulation when they are pretreated with ADMA

Levels of nitrite released by RAW 264.7 into the culture medium after treatment with ADMA for 24 hours were determined using Griess Assay (A)ADMA and LPS added simultaneously, (B) 60 min pretreatment with ADMA followed by LPS. n=6. Mean ± SEM. p>0.05. One-way ANOVA with Dunnett post hoc test. *(*p=0.0321, ***p=0.0009).*

3.3.8 100 µM is the optimal concentration of arginine in the culture media to study the effect of ADMA on nitric oxide production

As there was high variability in the results of the ADMA-dose-finding experiment run in standard DMEM (previous section), we looked at a specific component of the media – Arginine – and the likelihood that its concentration may be skewing the results. Arginine is one of the main substrates for NOSs, and the concentration of L-arginine in DMEM (400 µM) exceeds the physiological plasma levels estimated at an average of 100 µM, therefore depleting the concentration of arginine in the culture medium may enhance the NOS-inhibition effect of ADMA. This was examined by first seeding RAW 264.7 cells in complete growth medium. On the day of the experiment (at 50-70% confluency), the culture medium was replaced with arginine-deficient media supplemented with 100, 200, 300, or 400 µM L-Arginine monohydrochloride. The cells were then pre-treated for 1hr with 100 µM ADMA followed by 1 µg/mL LPS. Media was collected after 24 hours, and nitrite levels were determined by Griess assay (Figure 3-8).

When LPS-stimulated RAW 264.7 macrophages were treated with ADMA in media containing 100µM L-arginine, there was a gradual decrease in NO produced with increasing concentrations of ADMA reaching significance with 30 µM ADMA *(p=0.0188)* and more so at 100 µM ADMA *(p=0.0014)* in comparison to NO produced in response to LPS stimulation with no ADMA added. A decrease in the concentration of NO generated was noted with 10, 30 and 100 µM ADMA in media containing 200µM L-arginine, although not statistically significant, which might be explained by the higher variability of the readings throughout this data set. ADMA had no effect in cells grown in 300 and 400 µM L-arginine. However, the variability in the readings within each dataset seems to increase with increasing L-arginine concentration in the media. From this, it was concluded that further ADMA studies would be conducted in a culture medium containing 100 µM L-arginine.

Furthermore, although it has been reported that the Km of iNOS for L-arginine is 2.3-10 µM (Furfine *et al.*, 1993; Stuehr *et al.*, 1991a), this data shows a mean average production of 7.5 µM nitrite in 100 µM L-arginine media increasing to a

mean of around 30 µM in 200, 300 and 400 µM L-arginine media. This indicates that iNOS reached saturation with L-arginine concentration between 100-200 µM L-arginine.

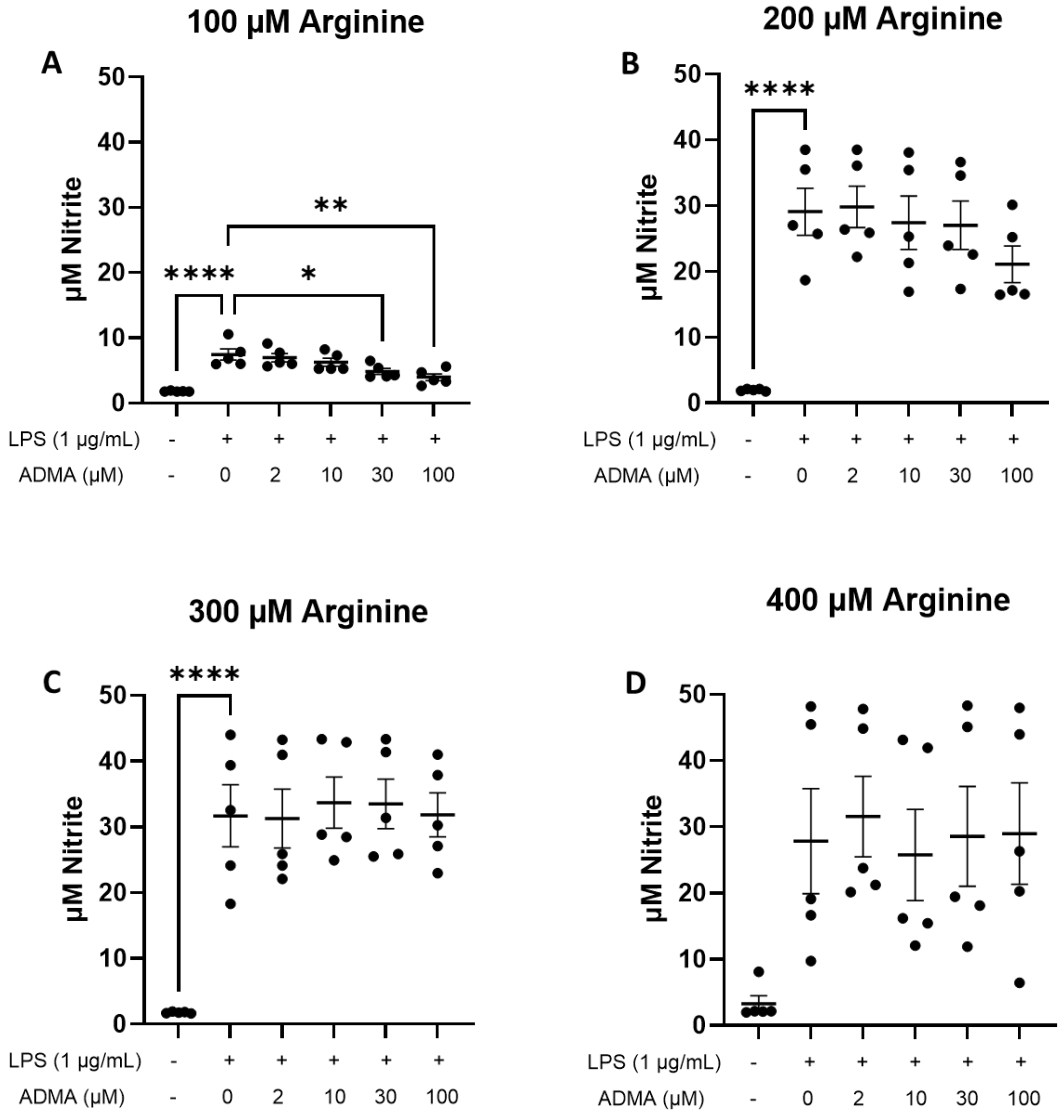

Figure 3-8 100 µM L-arginine is the optimal concentration to study the effects of ADMA on NO production in LPS stimulated RAW 264.7 cells
Nitrite levels post-treatment of stimulated RAW 264.7 with different concentrations of ADMA compared in Arginine-deficient media supplemented with different L-arginine concentrations. Levels of nitrite released by LPS-stimulated RAW 264.7 into the culture medium after treatment with 100 µM ADMA for 24 hours were determined using Griess assay. (A) 100 µM L-arginine, (B) 200 µM L-arginine, (C) 300 µM L-arginine and (D) 400 µM L-arginine. n=5. Mean ± SEM. p>0.05. One-way ANOVA with Dunnett post hoc test. (*$p=0.0188$, **$p=0.0014$, ****$p<0.0001$).

3.3.9 ADMA does not reduce *iNOS* gene expression

To investigate whether the effect of ADMA treatment on NO production in stimulated macrophages was in part due to a reduction in gene expression, RAW 264.7 cells were pre-treated with 10 or 100 µM ADMA for 1 hour and then stimulated with 1 µg/mL LPS in culture media containing 100 µM L-arginine. A 6-hour time point was chosen based on findings in the multiple time-point experiment (section 3.3.2). Changes in *Ddah2*, *eNOS,* and *iNOS* gene expression were determined by qPCR (Figure 3-9).

Treatment with ADMA showed no effect on *iNOS* gene expression at either 10 or 100 µM concentration in LPS-stimulated macrophages. This is in line with what is expected, as ADMA blocks the enzymatic activity of iNOS. No notable change in *DDAH2* and *eNOS* gene expression was seen when treated with 10 or 100 µM ADMA, but this requires further investigation due to variability in results.

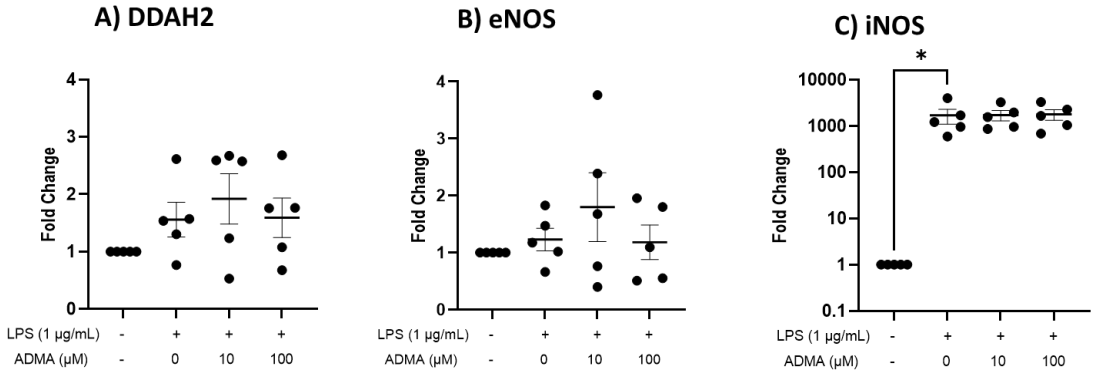

Figure 3-9 ADMA does not alter candidate gene expression in LPS stimulated RAW 264.7 macrophages
Effect of ADMA on Relative Gene Expression. Effect of 10 & 100 µM ADMA on candidate gene expression in 1µg/mL LPS-stimulated RAW 264.7 for 6hrs expressed as fold change (A) *Ddah2*, (B)*eNOS* and (C)*iNOS*. n=5. Mean ±SEM. p>0.05. One-way ANOVA with Dunnett post hoc test. (*$p=0.0382$).

3.4 C57BL/6J bone marrow-derived macrophage characterisation

3.4.1 Bone marrow cells differentiate into macrophages after stimulation with recombinant macrophage colony-stimulating factor

The second model chosen for use in this project was BMDM, as they are a naive form of macrophages. The initial step was to isolate bone marrow cells, differentiate them to BMDM and then validate the efficacy of the differentiation protocol. Bone marrow cells were isolated and then differentiated using Dulbecco's Modified Eagle's Medium (DMEM) High Glucose with Glutamax (HGM) supplemented with 15% v/v FBS and 1% penicillin/streptomycin and 20 ng/ml recombinant macrophage colony-stimulating factor (M-CSF) (2.2.1.2). The bone marrow cells at isolation appear rounded and are non-adherent. By the end of the differentiation process, the resultant BMDM are adherent cells with irregular shapes and varying numbers and lengths of processes extending from the cell body (pseudopodia). Some round cells may still be present depending on the degree of differentiation (Figure 3-10).

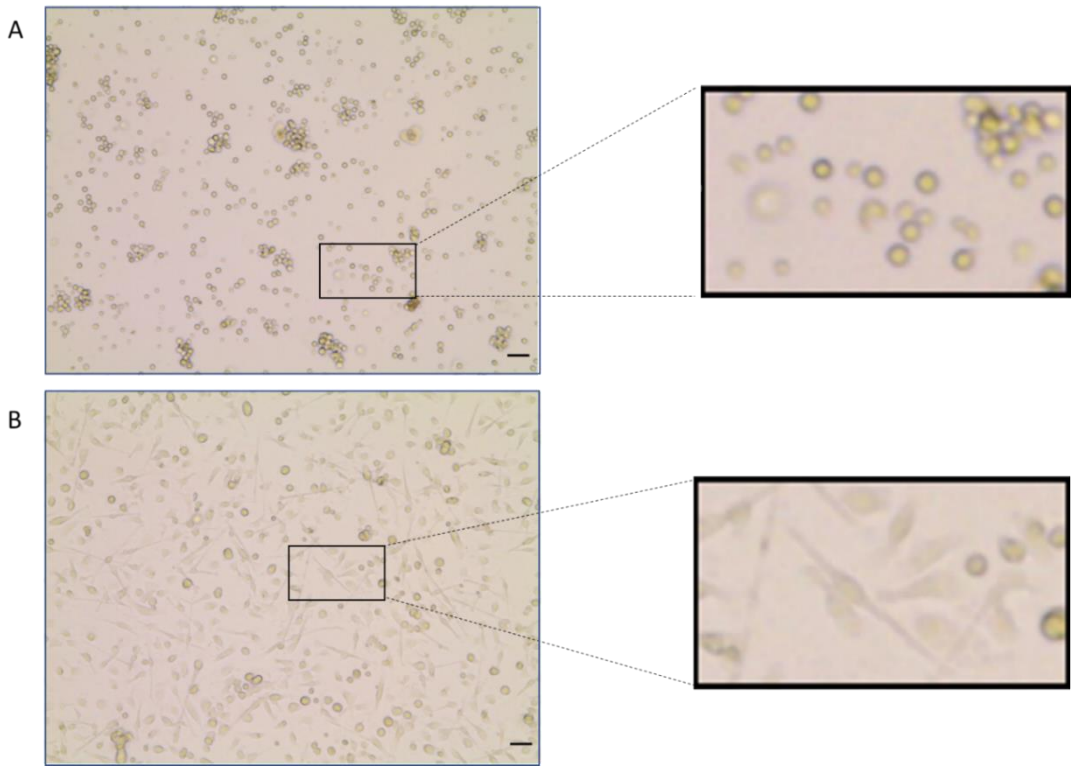

Figure 3-10 BMDM after differentiation from bone marrow cells using M-CSF
(A)Bone Marrow cells at extraction are rounded and non-adherent (B) Bone marrow-derived macrophages after differentiation are adherent, and morphology is heterogeneous, ranging from rounded cells to those with varying numbers and lengths of processes extending from the cell body. Images were taken using an EVOS XL Core microscope with a 20X objective lens.
Scale bar 50 µm.

3.4.2 Flow cytometry validates BMDM differentiation protocol

The expression of the macrophage markers F4/80 and CD11b in the obtained cells was investigated to validate the efficacy of the differentiation protocol used to derive macrophages from the bone marrow.

Bone marrow cells were isolated from four C57BL/6J mice. The macrophage markers F4/80 and CD11b expression were compared between the bone marrow-derived macrophage and the corresponding bone marrow (originating) cells using flow cytometric analysis . Following the differentiation process, there was a highly significant increase in the percentage of double-positive F4/80 and CD11b cells from 7% to 94% (Figure 3-11 A and B). Two-tailed unpaired t-test *(P<0.0001)*.

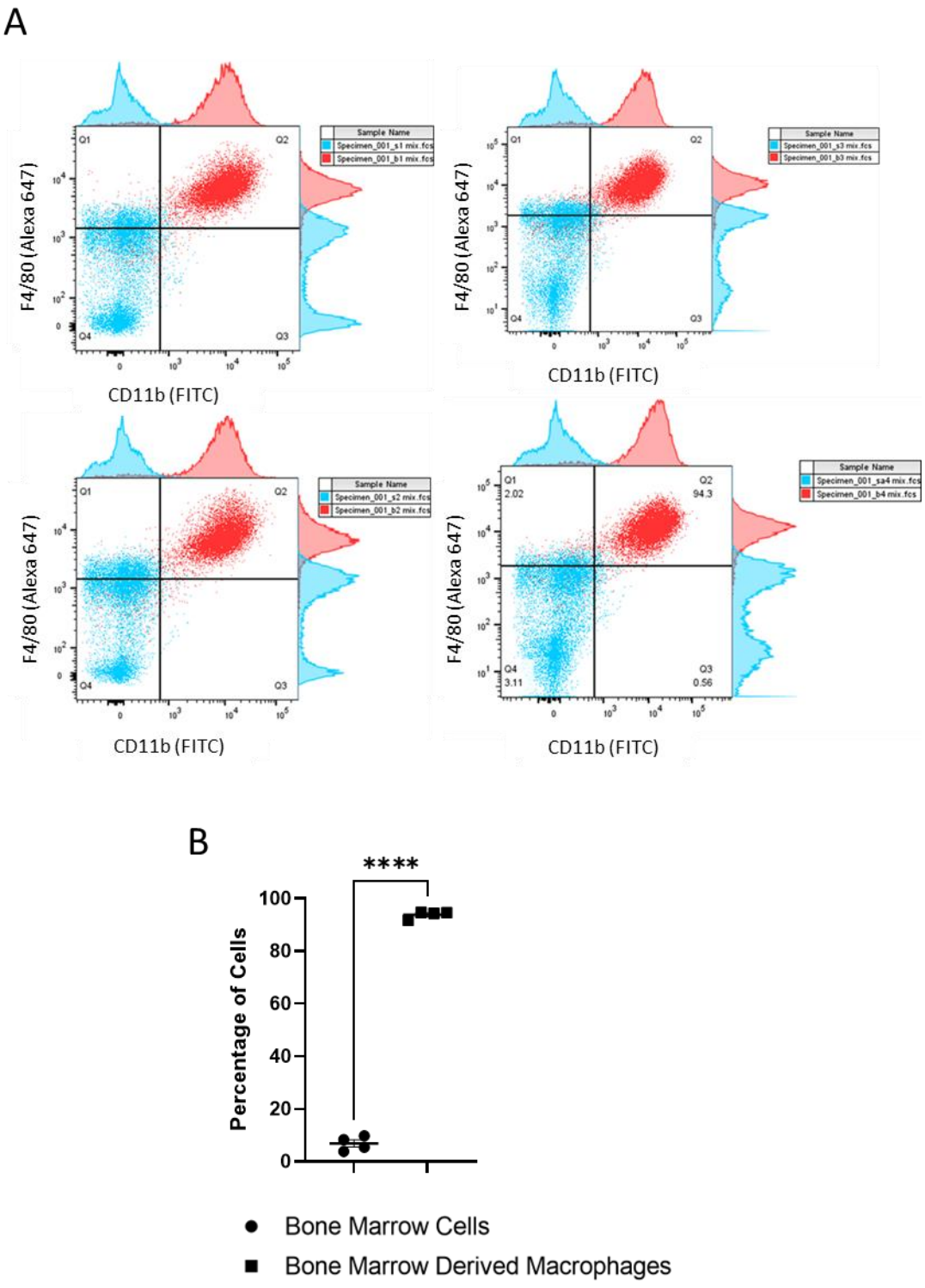

Figure 3-11 Differentiation of bone marrow cells to BMDM using recombinant M-CSF yields a population of cells with double expression of F4/80 and CD11/b

(A) Superimposition of the bone marrow cells and its BMDM final gates with an adjunct histogram showing the shift in F4/80 and CD11/b upon differentiation (B) the percentage of cells double positive for F4/80 and CD11/b per sample before and after differentiation with the average shifting from 7% to 94% respectively. n=4. Mean ± SEM. p>0.05. Unpaired two-tailed Student's t-test *(****P<0.0001).*

3.4.3 The yield of BMDM can be improved with the addition of pyruvate to the media used in the differentiation process

Although the BMDM differentiation using HGM and 15% FBS (3.4.1) was highly efficient (figure 3-11), the BMDM population was not confluent. As different protocols in the literature reported using varying culture media, changing the differentiation media's components was investigated in an aim to compare with them and increase the yield.

In review of the literature for BMDM differentiation media, they were all composed of a base medium which was supplemented with 10%-20% FBS, penicillin/streptomycin and a source of M-CSF. The source of M-CSF was either recombinant M-CSF or L929 cell-conditioned medium (LCCM). To limit the number of variables being changed during optimisation, the concentration of recombinant M-CSF was maintained throughout.

To control the number of variables tested, the first optimisation was to increase the amount of FBS used from 15% as in section (3.4.1) to 20% while maintaining the same base media as high glucose DMEM with no pyruvate. Since basic DMEM contains low glucose and pyruvate, while the media initially used in (3.4.1) was high glucose with no pyruvate, that was the second parameter for optimisation.

Therefore, bone marrow stem cells were isolated from four different C57BL/6J mice. The cells from each mouse were divided equally into three plates. One plate was differentiated in high-glucose no pyruvate media plus 15% FBS, the second plate was differentiated in high-glucose no pyruvate media plus 20% FBS and the third plate differentiated in low-glucose plus pyruvate media plus 15% FBS.

There was no noticeable increase in BMDM confluency when increasing the FBS percentage in the high glucose media (HGM) from 15 to 20%. However, the confluence of the obtained BMDM was visually, noticeably higher when changing the HGM-no pyruvate to low glucose media (LGM) plus pyruvate while maintaining the same amount of FBS added (Figure 3-12). Therefore, a quantitative comparison was performed by repeating the differentiation procedure in these two culture media. Then, the BMDM yield was calculated by

dividing the number of BMDMs obtained at the differentiation process's end by the starting number of bone marrow cells. This was repeated four times. The BMDM yield increased from 16% when using the high glucose – no pyruvate media to 26% when using the low glucose plus pyruvate media. For both media, 15% FBS was added, and the same concentration of M-CSF was used. The 10% increase in yield was statistically significant *(p=0.0019)* as determined by a two-tailed unpaired T-test (Figure 3-13).

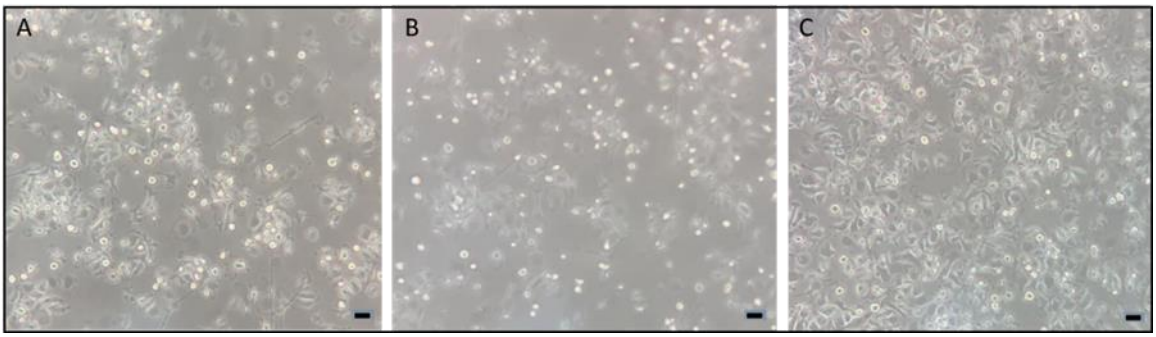

Figure 3-12 The number of BMDM obtained post-differentiation is altered depending on the culture media used for differentiation
High-glucose no pyruvate media plus 15% FBS was used in (A). The same media while increasing FBS to 20% was used in (B) and did not result in an obvious change in cell number. While in (C) the media was changed to low-glucose media plus pyruvate and 15% FBS and there was an obvious increase in BMDM confluency. Scale bar 100µm.

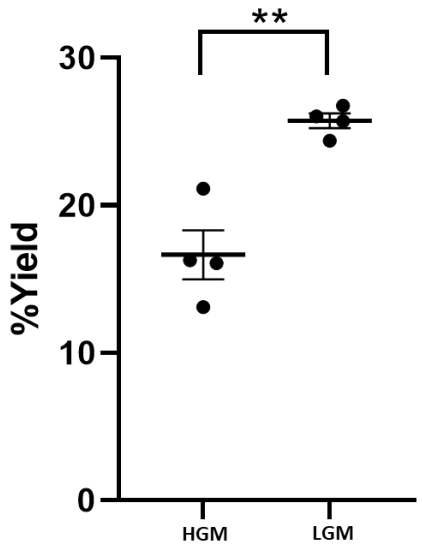

Figure 3-13 BMDM differentiation yield is increased by using low glucose media with added pyruvate during differentiation
The yield of BMDM is increased by 10% from 16% when using High glucose media to 26% when using Low Glucose media plus pyruvate while maintaining FBS at 15% in both conditions and using the same concentration of M-CSF. n=4. Mean ± SEM. p>0.05. Unpaired two-tailed Student's t-test. *(**p=0.0019)*

3.4.4 Flow cytometry confirms that the increased differentiation cell yield is due to an increase in BMDM numbers

The next step was to confirm that the increased confluency of cells was due to an actual increase in BMDM yield and not another cell type. To achieve that, the expression of macrophage markers on the obtained cells was examined via flow cytometry. Bone marrow cells from the same mouse were isolated and split into two. One half was differentiated using high glucose media (no pyruvate) supplemented with 15% FBS, and the second half was differentiated using low glucose media plus pyruvate supplemented with 15% FBS. M-CSF was added to both cultures and incubated for seven days. The cells were collected and prepared for flow cytometry at the end of the differentiation period. The percentage of cells isolated in culture after differentiation of bone marrow cells with M-CSF in (a) high glucose media (no pyruvate) or (b) low Glucose media plus pyruvate remains unchanged, with both being above 99%, confirming that the increased confluency in culture is due to an increased yield of BMDM indeed and not due to the introduction of a different cell type (Figure 3-14).

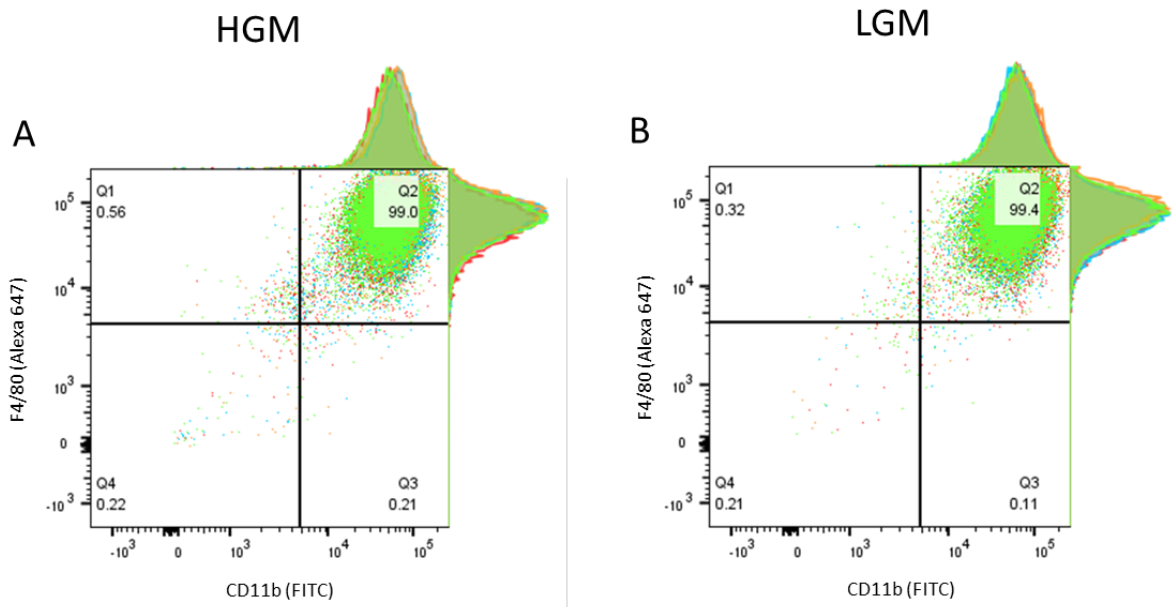

Sample	% F4/80+ CD11b+ cells
M1_BMDM_HGM	99.1
M2_BMDM_HGM	99.2
M3_BMDM_HGM	99.2
M4_BMDM_HGM	99.0
Average	**99.1**

Sample	% F4/80+ CD11b+ cells
M1_BMDM_LGM	99.3
M2_BMDM_LGM	99.6
M3_BMDM_LGM	99.4
M4_BMDM_LGM	99.4
Average	**99.4**

Figure 3-14 Increased BMDM differentiation yield is due to an increased number of BMDM post-differentiation as confirmed by expression of macrophage markers CD11b and F4/80
The percentage of cells isolated in culture after differentiation of bone marrow cells with M-CSF in (A) high glucose media (no pyruvate) or (B) Low Glucose media plus pyruvate remains unchanged at 97.5% and 98%, respectively, confirming that the increased confluency in culture is due to an increased yield of BMDM.

3.4.5 *Rpl13* is a reliable qPCR housekeeping gene regardless of the media used for differentiation

Next, the BMDM expression of target genes at baseline, after LPS stimulation with or without ADMA, was analysed and compared across the two populations. (Figure 3-15).

The mRNA expression of *Rpl13* (housekeeping gene) was compared. No significant difference in the expression of *Rpl13* was noted in response to LPS with or without pre-treatment with ADMA in either of the two populations of BMDM.

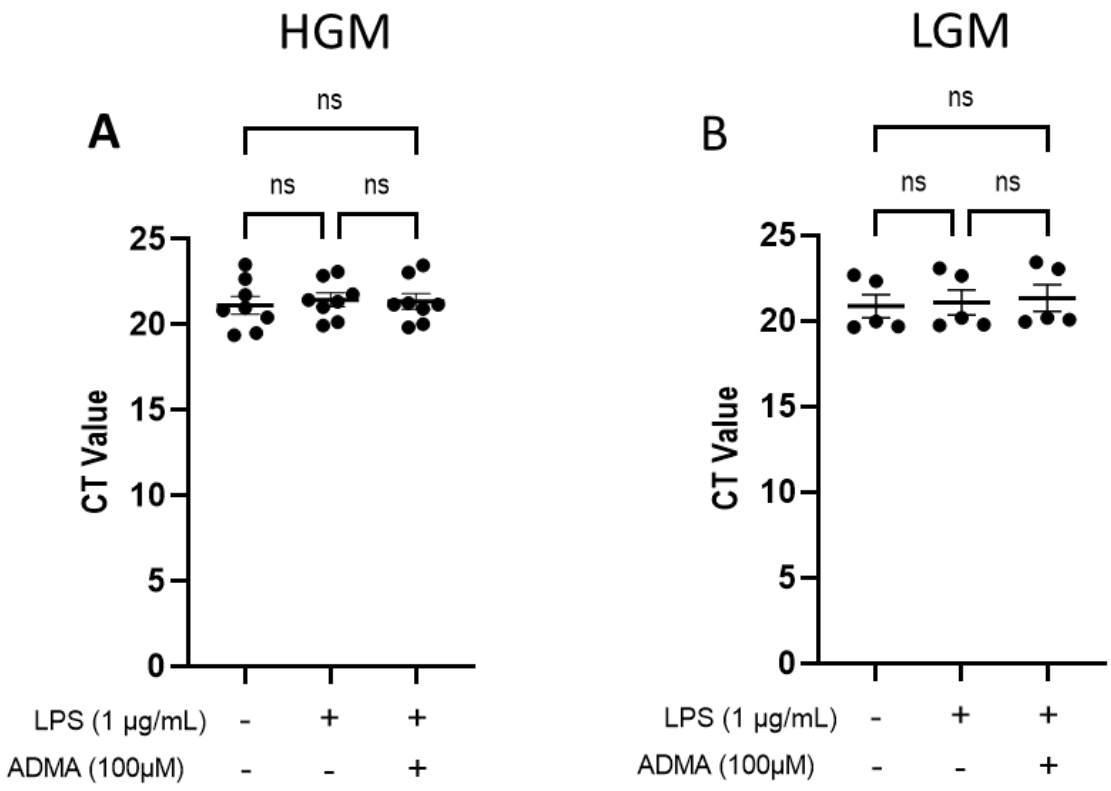

Figure 3-15 *Rpl13* mRNA expression is stable at baseline and after stimulation with LPS with or without pre-treatment with ADMA, regardless of the media conditions used for differentiation

The mRNA expression of *Rpl13* is stable in BMDM differentiated from bone marrow cells after the addition of M-CSF in (A) High glucose media with no pyruvate (n=8) and (B) Low Glucose media plus pyruvate (n=5) at baseline and after the stimulation with 1µg/mL LPS with or without pre-treatment with 100µM ADMA, confirming that it is a suitable housekeeping gene in either differentiation method. *Rpl13* has a mean Ct value of 20 with no significant change between treatments. Mean± SEM. $p>0.05$. One-way ANOVA with Tukey post hoc test.

3.4.6 Target gene expression responds similarly to LPS stimulation and ADMA treatment in BMDM differentiated in High glucose media and Low glucose media

Ddah2 expression in both conditions showed no significant change in response to LPS treatment with or without pretreatment with ADMA. *eNOS* expression in both conditions showed a trend to increase with LPS stimulation regardless of ADMA pretreatment, although not statistically significant. *iNOS* expression increased significantly in both conditions in response to LPS treatment *(p<0.0001) w*ith and without ADMA pretreatment before LPS stimulation (Figure 3-16).

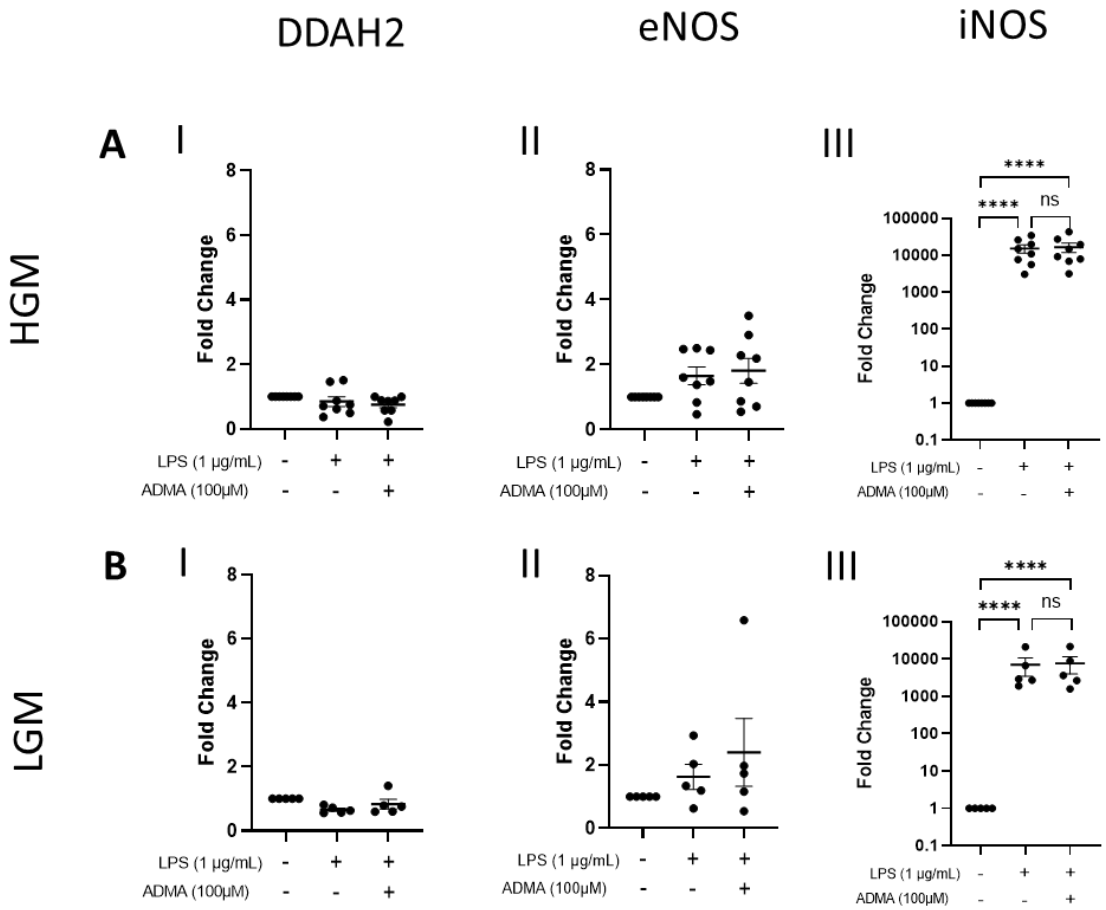

Figure 3-16 mRNA expression of target genes is comparable regardless of the media conditions used for differentiation
The mRNA expression of *Ddah2, eNOS, and iNOS*. Upper panel (A) cells differentiated in High Glucose media; n=8, and lower panel (B) cells differentiated in Low Glucose media with pyruvate; n=5. (I) *Ddah2,* (II) *eNOS* (II) i*NOS*. Mean ± SEM. p>0.05. One-way ANOVA with Tukey post hoc test. *(****p<0.0001)*

3.4.7 Nitric oxide production increases in response to LPS stimulation and decreases with ADMA pre-treatment in BMDM differentiated in either HGM or LGM

Furthermore, the functional ability of the differentiated BMDM to respond to LPS stimulation by releasing nitric oxide and whether that could still be inhibited by treating the cells with 100μM ADMA one hour before the stimulation with LPS was compared between the two differentiation media. To perform this comparison, Bone marrow cells from the same mouse were isolated and split into two. One half was differentiated using high glucose media (no pyruvate) supplemented with 15% FBS, and the second half was differentiated using low glucose media plus pyruvate supplemented with 15% FBS. M-CSF was added to both cultures and incubated for seven days. At the end of differentiation, the cells were stimulated with LPS with or without ADMA in low arginine high glucose media, and then the Griess assay was performed. (Figure 3-17).

There was an abundance of nitric oxide released in response to LPS treatment in BMDM differentiated in HGM increases from around 3.4 μM to 27 μM *(P<0.0001)*, while if treated with ADMA before LPS stimulation, increases only to 15 μM *(P=0.0006)*. BMDM differentiated in LGM show a similar pattern where nitric oxide released in response to LPS treatment in BMDM differentiated in HGM increases from around 3 μM to 26 μM *(P=0.0009)*. In comparison, if treated with ADMA before LPS, stimulation increases to only 12 μM, and the increase was statistically insignificant *(p=0.1789)*.

The differentiation of bone marrow cells into BMDMs, using either HGM or LGM, was confirmed by flow cytometry, and the differentiated BMDMs behaved similarly in response to LPS stimulation and ADMA treatment on both the genetic level and functional level per NO release. Therefore, the cells were differentiated in LGM plus pyruvate in future experiments to benefit from the increased BMDM yield.

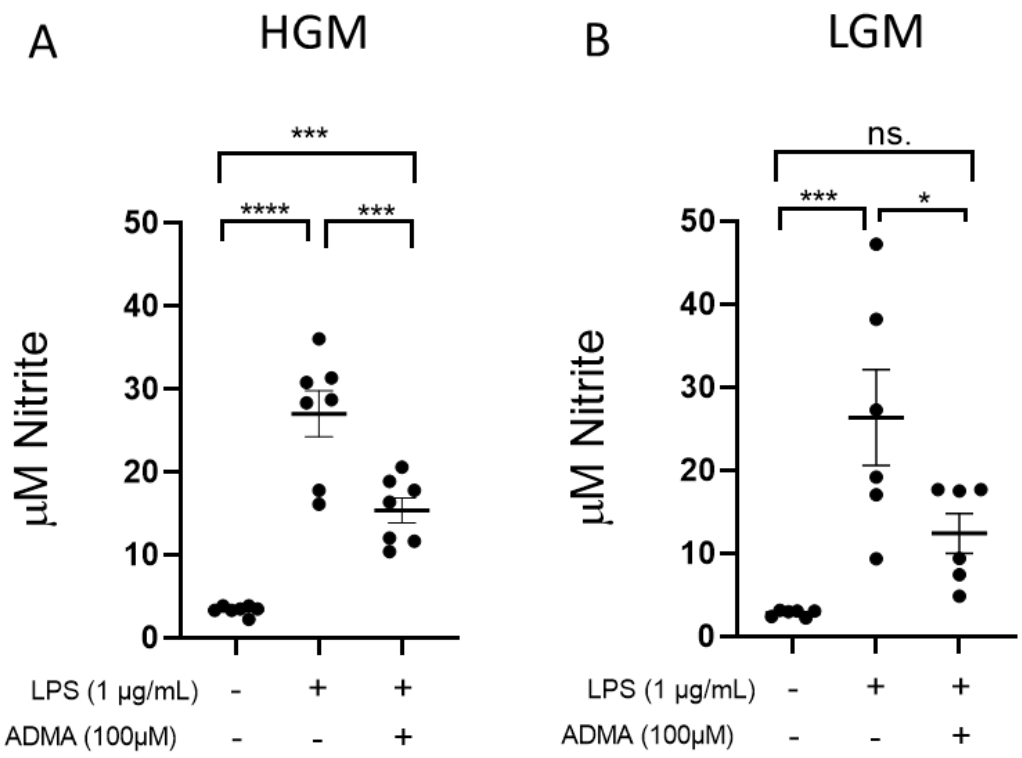

Figure 3-17 Nitric oxide is released in response to LPS stimulation and decreases in response to pretreatment with ADMA in BMDM regardless of the media conditions used for differentiation
Nitric oxide abundance- as reflected by nitrite measurement by the Griess assay- is increased significantly in (A) BMDM differentiated in High Glucose media; n=7 and (B) BMDM differentiated in low glucose media with pyruvate; n=6. Pre-treatment with 100 µM ADMA decreases the amount of nitrite released significantly in both conditions. Mean ± SEM. p>0.05. One-way ANOVA with Tukey post hoc test. HGM *(****p<0.0001, ***p=0.0006),* LGM *(*P=0.1789, ***p=0.0009)*

3.4.8 Western blot confirms DDAH2 and iNOS protein expression in BMDM

Having optimised and improved the yield of the BMDM differentiation protocol, the same conditions were used to look at DDAH2 and iNOS protein expression. Protein lysates extracted from BMDM differentiated in LGM with pyruvate and, after that, maintained in complete growth media composed of high glucose DMEM with added 10% FBS and 1% P/S (CGM) were left untreated or treated with LPS for 24 hours.

DDAH2 protein expression did not change significantly with 1 µg/mL LPS treatment for 24 hours (p=0.2424) (Figure 3-18). iNOS expression (Figure 3-19) was also compared across the same conditions and showed a significant increase with LPS stimulation (p=0.007) as it is not expressed in resting macrophages and surges with LPS stimulation. In both figure 3-18 and figure 3-19, each well or data point in the graph (n) represents a different mouse.

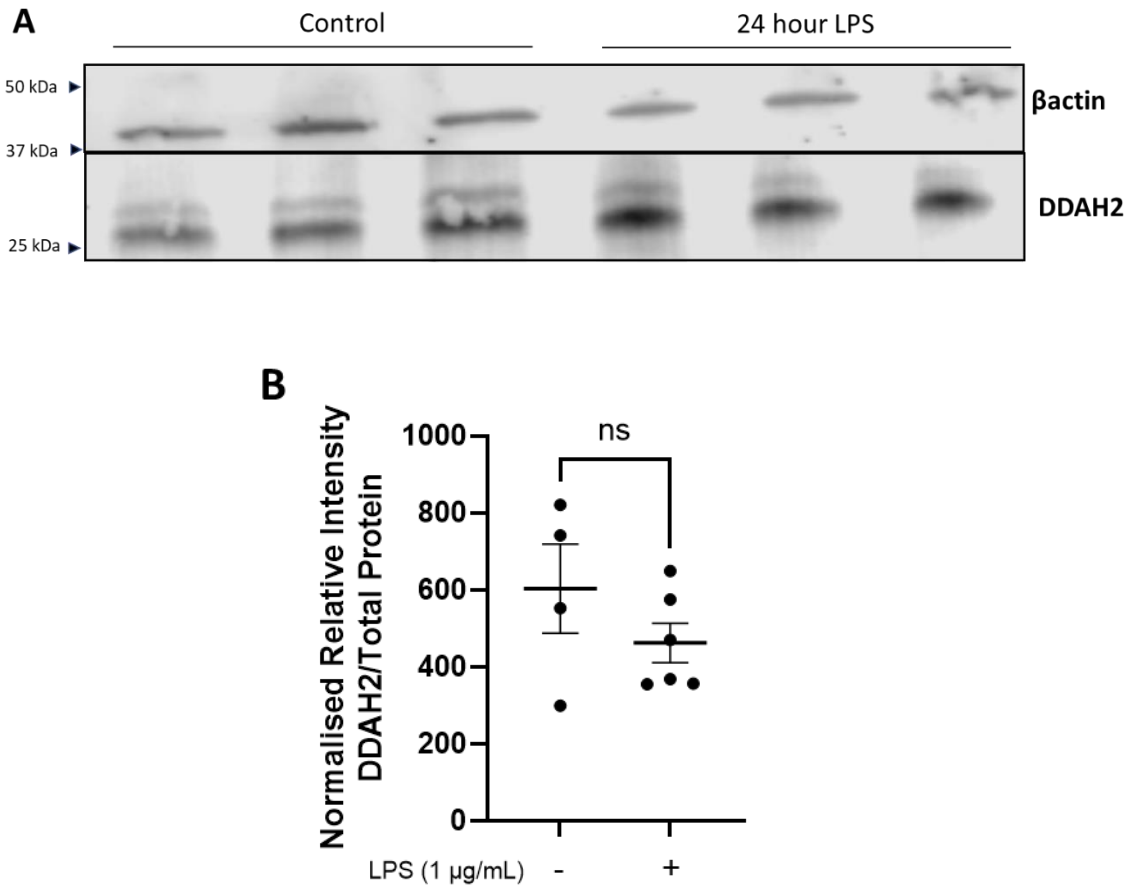

Figure 3-18 DDAH2 protein is expressed in C57BL/6J BMDM
Western blot analysis of C57BL/6J BMDM protein lysates at baseline and after stimulation with 1 µg/mL LPS for 24 hours. Equal amounts of protein (20µg) were loaded per lane. (A) The representative blot shows three different biological samples of the control and three of the LPS-stimulated samples. The blots were incubated with βactin antibody as a qualitative internal loading control and with an anit-DDAH2 antibody. (B) Revert total protein stain was used for quantitative normalization. Data from another blot was included in the quantitative analysis in B with Control:n=4, LPS-stimulated:n=6 . Mean ± SEM. Unpaired two-tailed Student's t-test.

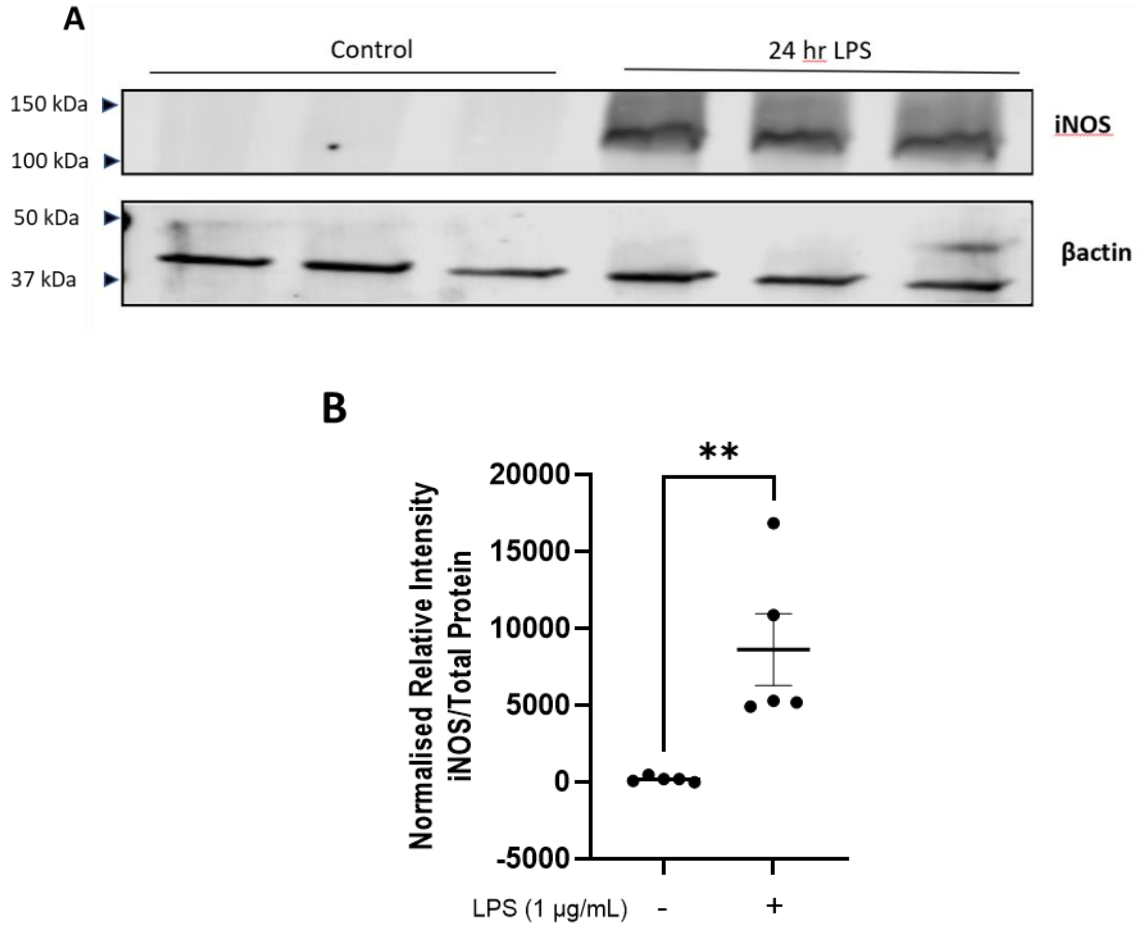

Figure 3-19 iNOS protein is synthesised in C57BL/6J BMDM in response to LPS stimulation
Western blot analysis of C57BL/6J BMDM protein lysates at baseline and after stimulation with 1 µg/mL LPS for 24 hours. Equal amounts of protein (20µg) were loaded per lane. (A) The representative blot shows three different biological samples of the control and LPS-stimulated samples. The blot was incubated with βactin antibody as a qualitative internal loading control and with an anti-iNOS antibody. (B) Revert total protein stain was used for quantitative normalization. Data from another blot was included in the quantitative analysis in B with n=5. Mean ± SEM. Unpaired two-tailed Student's t-test. *(**p=0.007).*

3.5 Macrophage-specific *Ddah2* null mouse model

3.5.1 DNA, RNA and protein expression confirm genotype

The macrophage-specific *Ddah2* knockdown mouse was first established by our group nearly ten years ago (Lambden *et al.*, 2015). This project uses a re-derived mouse model, hence the need to confirm the genotype and phenotype.

In order to do so, a combination of DNA PCR genotyping, mRNA expression by qPCR and protein analysis by western blot was performed.

PCR genotyping was performed in-house utilising ear punch tissue obtained from the mice at weaning. In the *Ddah2* PCR, wildtype (*Ddah2*$^{+/+}$) had a band size of 495bp, *Ddah2* homozygous-floxed mice had a single band size of 568 bp, while *Ddah2* heterozygous-floxed mice had two bands (495 and 568 bp). The mice were bred until litters composed of only *Ddah2* homozygous-floxed mice were obtained and used as experimental animals.

Cre PCR was also carried out similarly, with results showing either the absence (negative) or presence (positive) band of size 720bp. *Ddah2* homozygous-floxed mice not expressing Cre were used as experimental controls (*Ddah2*$^{f/f}$ LysM-Cre$^{0/0}$), while Cre-positive ones were the test animals as they were knockdowns (*Ddah2*$^{f/f}$ LysM-Cre$^{0/+}$). (Figure 3-20)

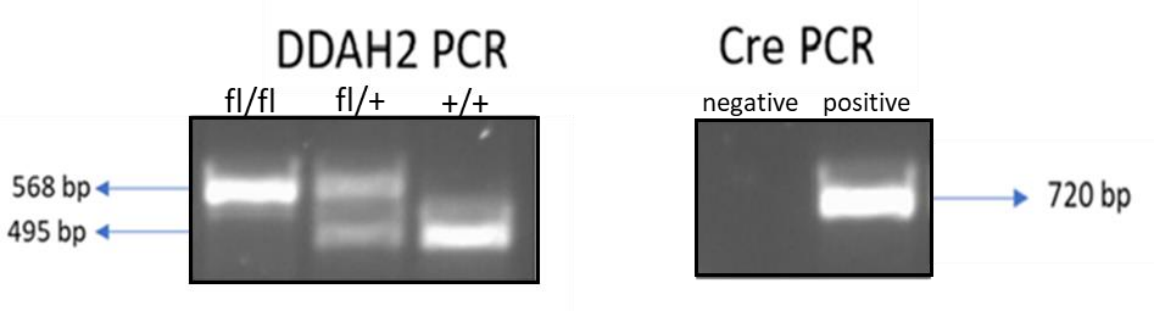

Figure 3-20 PCR genotyping validates *Ddah2* knockdown
Representative *Ddah2* PCR showing homozygous floxed, heterozygous floxed and wildtype. Cre PCR showing negative and positive bands. Litters used in experiments were all *Ddah2* homozygous – floxed either Cre-negative (controls) or Cre-positive (macrophage-specific *Ddah2* knockdown).

It is possible to utilise both BMDM and peritoneal macrophages from the knockdown mice, depending on the aim of the study, as they reflect different types of macrophages. Previously mentioned DNA PCR genotyping was performed in every mouse from ear notches. Furthermore, the genotype of each mouse used in an experiment was re-confirmed by RT-qPCR using RNA extracted from its peritoneal macrophages, BMDMs, or both. RNA was extracted and quantified

by RT-qPCR using three different newly designed sets of primers for DDAH2. The first primer pair targets exons 2 and 3, and the second pair targets exons 3&4. Exons 2,3, and 4 are within the sequence expected to be excised in the knockdown. The third set of primers targets exons 6 and 7, which fall out of the excised area and are expected to be expressed regardless of the mouse's genotype.

The results (Figure 3-21) show the mRNA expression for BMDM and peritoneal macrophages expressed as fold change. In both cell types, the expression of *Ddah2* as per primers targeting the excised region is ten times lower in *Ddah2*$^{f/f}$ LysM-Cre$^{0/+}$ in comparison to *Ddah2*$^{f/f}$ LysM-Cre$^{0/0}$ with a significance of $p<0.0001$. As expected, there is no significant change in expression when using the primers targeting beyond the floxed region. This confirms that the floxed region is excised with Cre expression, rendering a knockdown.

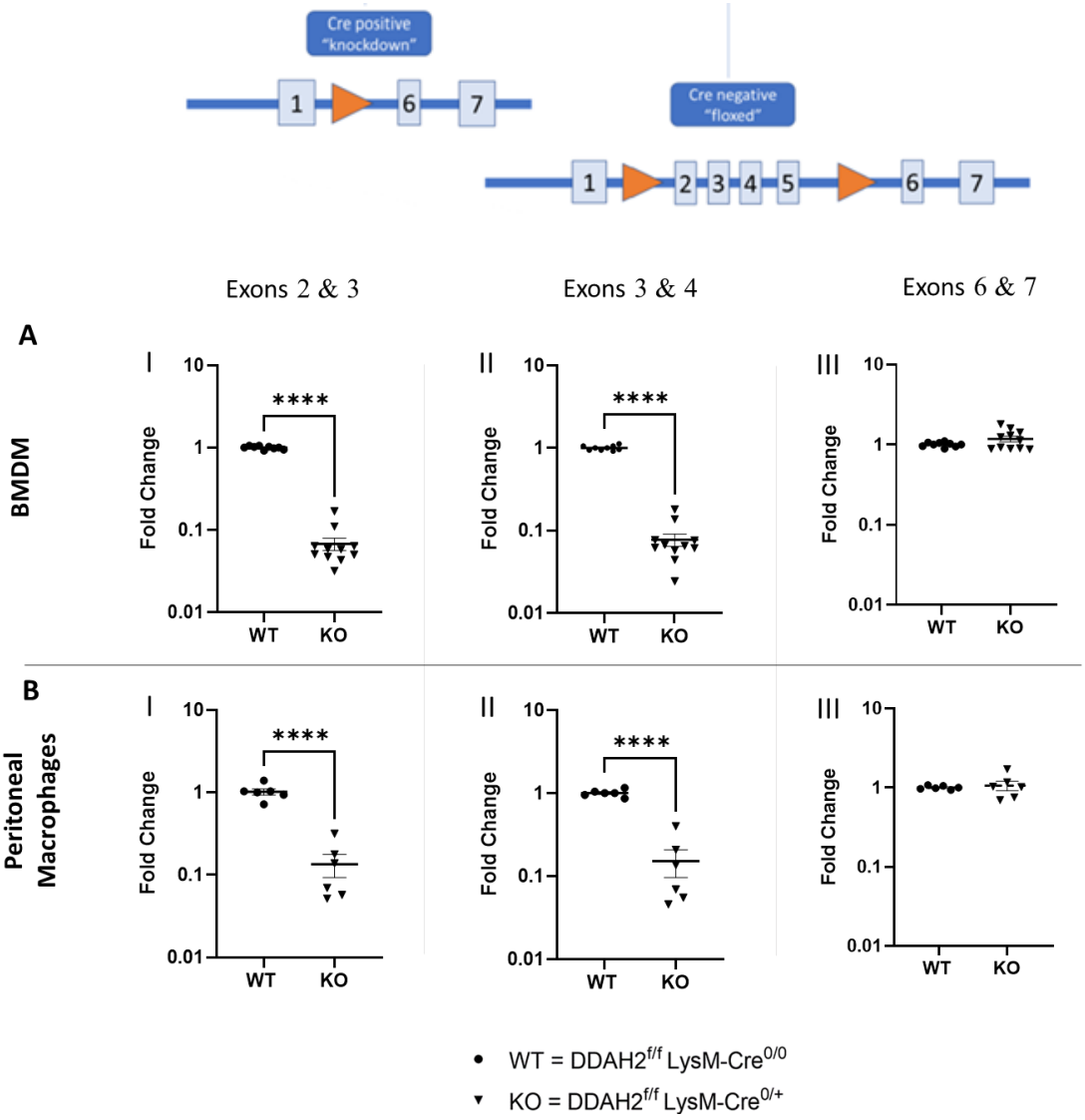

Figure 3-21 qPCR validates *Ddah2* knockdown
D*dah*2 RNA expression in upper panel (A)BMDM (n=11) and lower panel (B) peritoneal macrophages (n=6) isolated from *Ddah2*$^{f/f}$ LysM-Cre$^{0/0}$ and *Ddah2*$^{f/f}$ LysM-Cre$^{0/+}$ via qPCR using primers targeting *Ddah*2 exons (I) 2 &3 (II) 3&4 and (III) 6&7. Mean ± SEM. p>0.05. Unpaired two-tailed Student's t-test. *(****p< 0.0001).*

Furthermore, the effect on DDAH2 protein expression was validated. Protein lysates were extracted from BMDMs differentiated from *Ddah2*$^{f/f}$ LysM-Cre$^{0/0}$ and *Ddah2*$^{f/f}$ LysM-Cre$^{0/+}$ mice. DDAH2 protein expression was evaluated by western blot (Figure 3-22). Blotting for DDAH2 results in two bands, with the lower band being DDAH2, while the upper one is a non-specific band as the lower band only decreases in intensity in the knockout. *Ddah2*$^{f/f}$ LysM-Cre$^{0/+}$ protein

lysates from BMDM showed a highly significant ($p<0.0001$) decrease in the expression of DDAH2 protein in comparison to *Ddah2*$^{f/f}$ LysM-Cre$^{0/0}$. Thus further validating the knockdown model.

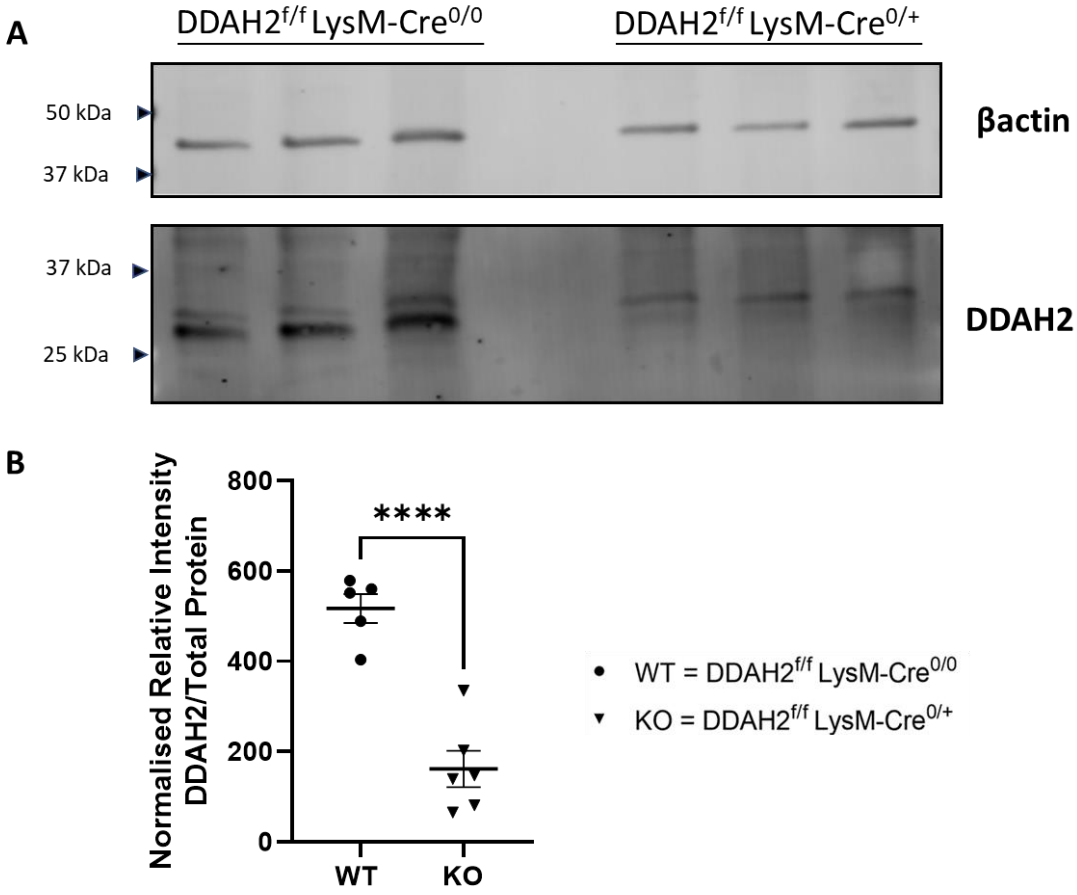

Figure 3-22 DDAH2 protein expression in BMDM significantly decreases in DDAH2 macrophage-specific knockdown

Western blot analysis of BMDM lysates from three biological replicas of *Ddah2*$^{f/f}$ LysM-Cre$^{0/0}$ and *Ddah2*$^{f/f}$ LysM-Cre$^{0/+}$ mice. Equal amounts of protein (20µg) were loaded per lane. (A) The representative blot shows three different biological samples of the control and KO samples. The blots were incubated with a βactin antibody as a qualitative internal loading control and an anti-DDAH2 antibody. (B) Revert total protein stain was used for quantitative normalisation. WT:n=5, KO:n=6. Mean±SEM. $p>0.05$. Unpaired two-tailed Student's t-test. *(****$p<0.0001$).*

3.5.2 Third party testing validates genotype

Transnetyx carried out genotyping via real-time PCR on ear punches taken at the time of culling for external validation, and their results validated the in-house genotyping performed by PCR and RT-qPCR.

3.5.3 DDAH2 does not regulate *eNOS* and *iNOS* gene expression in BMDM

In section 3.4.6, *eNOS* expression in C57BL/6J BMDM showed a trend to increase with LPS stimulation regardless of ADMA pretreatment, although not statistically significant. *iNOS* expression increased significantly in both conditions in response to LPS, with and without ADMA pretreatment before LPS stimulation. As DDAH is known to metabolise ADMA, the similarity of the effect of DDAH2 knockdown on *eNOS* and *iNOS* gene expression was evaluated. DDAH2 knockdown did not alter either gene expression (Figure 3-23). Therefore, it appears that DDAH2, like ADMA, does not regulate *eNOS* or *iNOS* gene expression in BMDM.

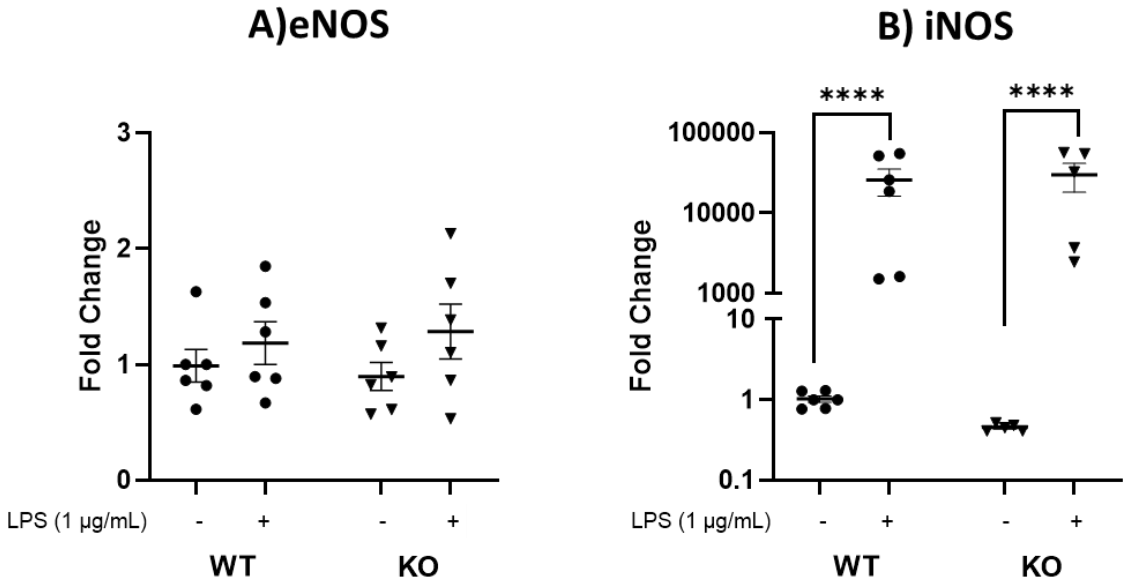

Figure 3-23 DDAH2 does not regulate *eNOS* and *iNOS* gene expression in BMDM
Effect of DDAH2 on (A) *eNOS* and (B) *iNOS* expression at baseline and in 1µg/mL LPS-stimulated *Ddah2*$^{f/f}$ LysM-Cre$^{0/0}$ and *Ddah2*$^{f/f}$ LysM-Cre$^{0/+}$ for 6hrs expressed as fold change. n=6. Mean ± SEM. p>0.05. Two-way ANOVA with Tukey post hoc test. (****$p<0.0001$).

3.5.4 *Ddah2* knockdown causes a significant increase in spleen weight

Previously, when the macrophage-specific *Ddah2* null mouse model was first created, there were non-quantitative reports of the knockdowns exhibiting enlarged spleens and having a lower resistance to infection.

Therefore, weights of spleens from *Ddah2*$^{f/f}$ LysM-Cre$^{0/0}$ and *Ddah2*$^{f/f}$ LysM-Cre$^{0/+}$ mice were compared at 7-9 weeks of age. There was a significant *p= 0.0281* increase in spleen weight (around 15%) in the knockdown mice (Figure 3-24).

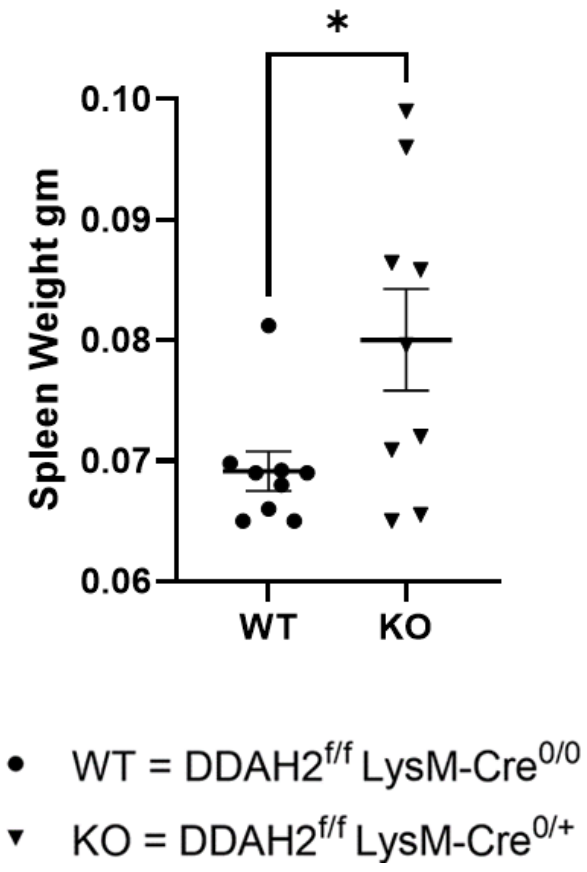

Figure 3-24 *Ddah2* knockdown causes a significant increase in spleen weight

Spleen weights were compared between *Ddah2*$^{f/f}$ LysM-Cre$^{0/0}$ and *Ddah2*$^{f/f}$ LysM-Cre$^{0/+}$ mice. n=9. Mean ± SEM. p>0.05. Unpaired two-tailed Student's t-test. *(*p=0.0281).*

3.6 Discussion

This project aimed to elucidate the role of DDAH2 in inflammation. The study in this chapter aims to confirm the suitability of different models to be used in it, including their expression of key genes in the DDAH-ADMA-NOS pathway and the response to LPS stimulation. It also includes the re-derivation and validation of a macrophage-specific DDAH2 null mouse model .

3.6.1 Brief Summary of chapter findings

In this chapter, the suitability of the murine macrophage cell line RAW 264.7 was investigated as a model for the role of DDAH2 in inflammation. The expression of *DDAH2, iNOS* and *eNOS* – key genes in the DDAH-ADMA-NOS pathway was confirmed, as was the protein expression of DDAH2. The validation of iNOS protein expression and NO release confirmed the activation of RAW 264.7 by 1 µg/mL LPS. The optimal level of arginine to study the effects of ADMA was investigated and found to be 100 µM, similar to the physiological levels. Furthermore, as is expected from previous literature, ADMA was found to inhibit the enzymatic activity of Nitric oxide synthase and not its gene expression. Hence, the RAW 264.7 cell line was found to be a suitable model to run the planned experiments. The concentration of arginine in the culture media was selected according to the above findings.

Furthermore, in this chapter, the suitability of using naïve primary macrophages, namely BMDM, was investigated. It was confirmed that bone marrow cells differentiate efficiently to BMDM using M-CSF, and the yield can be increased using a low glucose plus pyruvate medium. BMDMs were found to be a suitable model for this project as they express the genes of interest in the DDAH-ADMA-NOS pathway and respond to stimulation with LPS and release NO as a result, which was also shown to be decreased via pretreatment with 100 µM ADMA.

As mentioned, the macrophage-specific *Ddah2* null mouse model is re-derived, hence the importance of confirming the phenotype vs. using an ongoing model. This was confirmed using a variety of methods from both BMDM and peritoneal macrophages. Genotyping was performed at the first stage using agarose gel

electrophoresis of DNA PCR product, then confirmed using qPCR. Further confirmation of DDAH2 protein knockdown was obtained via protein detection using qualitative western blots. Third-party testing was used for further validation. Furthermore, the occurrence of enlarged spleens in the knockdowns noted by our lab group when previously using the initial model was confirmed quantitatively and was statistically significant.

3.6.2 RAW 264.7 characterisation

Initially, in this study, RAW 264.7 macrophages were characterised to ensure their suitability as a model cell line to study inflammation (figure 3-2). In response to LPS activation, iNOS showed an immediate surge in mRNA expression (more than 100 fold after 2 hours of stimulation). The change in *Ddah2* was not statistically significant, and only showed a mild increase at 4-6 hours then declined. *eNOS* started to increase at 2 hrs but only reached significance at 4 hours, increased more at 6 hrs then declined slowly. This aligns with previous evidence from studies on stimulation of Bone marrow-derived macrophages (BMDM) that eNOS is required to drive the high expression of iNOS (Connelly *et al.*, 2003; Connelly, Madhani and Hobbs, 2005). Another factor is that the high surge in NO inhibits the expression of eNOS (Schwartz *et al.*, 1997; Chauhan *et al.*, 2003). The delay in the increase in nitrite levels from the increase in iNOS mRNA expression is expected due to the lag time required for protein translation and nitrite accumulation to achieve detectable levels. This data shows evidence of expression of our targeted genes *Ddah2*, *eNOS* and *iNOS* and suggests an interplay between them after macrophage activation with LPS. These results were complemented with assessing DDAH2 and iNOS protein expression and its variation upon stimulation by LPS. This data indicates the suitability of RAW 264.7 as a model cell line for the initial phase of this project.

Furthermore, the effects of ADMA – a competitive NOS inhibitor – were tested on resting and stimulated RAW 264.7 macrophages. In resting macrophages, ADMA did not induce the production of NO, while in stimulated macrophages, ADMA appears to decrease NO production via inhibiting iNOS enzymatic activity (MacAllister *et al.*, 1996).

In another study, Pekarova et al. investigated the effect of ADMA on NO production in LPS-stimulated RAW 264.7 and alveolar macrophages (Pekarova *et al.*, 2013). Pekarova et al. conducted the experiments in a high arginine media (around 480 μM), used a lower dose of LPS (100 ng/mL) than in this project and ADMA concentrations ranging between 1-50 μM. Their results showed that 25 and 50 μM ADMA reduced NO production through its downregulation of iNOS mRNA and protein expression (Pekarova *et al.*, 2013). Therefore although in both their study and this project NO production in LPS-stimulated cells was inhibited by ADMA, we did not see an effect on *iNOS* mRNA expression and we did not test for iNOS protein expression. Interestingly they were also able to see this reduction in a culture media high in arginine, while in this project the inhibitory effect of ADMA on NO production was masked in media containing 200-400 μM arginine. Whether these differences could be explained by other components in the media, the timing of the addition of ADMA into the media in relation to LPS or the dose of LPS used would be interesting to follow up.

The data in this project also demonstrates the sensitivity of ADMA to L-arginine levels. This study shows that the reduction of L-arginine to near-plasma physiologic levels amplified the NO-inhibitory effect of ADMA and that despite the documented Km of iNOS to L-arginine (12.5) (Babu and Griffith, 1998), this study showed a saturation of iNOS with L-arginine concentrations between 100 and 200 μM. This may be due to the lack of correlation between plasma and intracellular levels of ADMA (Davids and Teerlink, 2013). Therefore, this study shows that, in line with previous literature, these cells express iNOS in response to LPS and extends the findings to show that the sensitivity to ADMA is arginine-dependent. Therefore, it highlights that by lowering exogenous arginine concentrations, ADMA becomes a more potent inhibitor of NO generation. This might be explained by the increased difficulty of exogenously administered ADMA to compete with the high arginine levels in the media for entry into the cells. Since a concentration of 100 μM arginine in the culture media was when the NO-inhibitory effect was evident in this project and is near physiologic levels, we established it as the condition under which the role of DDAH2 would be studied in the following chapters.

3.6.3 C57BL/6J bone marrow-derived macrophage characterisation

As the second aim in this chapter was to validate the use of BMDM as a cell model in this project. The expression of the key genes in the DDAH-ADMA-NOS pathway, including mRNA expression of *Ddah2*, *eNOS* and *iNOS,* was confirmed. LPS stimulation led to increased nitric oxide production, and the addition of ADMA attenuated the activity of NOS. iNOS protein expression in response to LPS stimulation was also validated in BMDMs via western blot. These findings validated the use of BMDMs in this project.

The protocol used in section (3.4.1) initially to differentiate BMDMs using recombinant M-CSF was highly efficient as the percentage of CD11b+ F4/80+ cells changed with differentiation from 7% to 94% (Figure 3-11). However, the BMDM population was not confluent. This observation, along with the variety of media used to differentiate BMDMs in different studies in the literature, encouraged the comparison of the compositions of the media used in the different protocols and the investigation of whether changing the composition would affect the final BMDM yield.

A literature review for BMDM differentiation media shows that they were all composed of a base medium supplemented with 10-20% FBS and penicillin/streptomycin. The source of utilised M-CSF was either recombinant M-CSF or L929 cell-conditioned medium (LCCM). The decision to use M-CSF and not LCCM in this project was based on literature demonstrating that differentiation using recombinant M-CSF produced more homogenous BMDM populations than LCCM (Zhao *et al.*, 2017; Zajd *et al.*, 2020). Furthermore, LCCM contains other factors besides M-CSF, and composition may differ between batches. The concentration of recombinant M-CSF was maintained throughout to limit the number of variables being changed during optimisation.

In the reviewed literature, the amount of FBS added varied between 10% (Chang *et al.*, 2013; Rios, Touyz and Montezano, 2017; El Bouhassani *et al.*, 2011; Xiao *et al.*, 2012; Robichaux III *et al.*, 2020; Toda *et al.*, 2021), 15% (Rios *et al.*, 2013) and 20% (Marim *et al.*, 2010). To control the number of variables tested,

the first optimisation was to increase the amount of FBS used from 15% as in (3.4.1) to 20% while maintaining the same base media as high glucose DMEM without pyruvate. However, the extra added FBS showed no apparent increase in the BMDM yield (Figure 3-12).

Furthermore, the base media used varied between DMEM high glucose (Robichaux III *et al.*, 2020; Rios, Touyz and Montezano, 2017; Toda *et al.*, 2021), DMEM (Xiao *et al.*, 2012; El Bouhassani *et al.*, 2011), RPMI (Chang *et al.*, 2013; Marim *et al.*, 2010; Davies and Gordon, 2005). Establishing the exact composition of the media used in papers was challenging as many did not include product codes. Since the original basic DMEM contained low glucose and pyruvate, while the media initially used in (3.4.1) was high glucose without added pyruvate, it was decided that was the second parameter for optimisation. Therefore, while maintaining 15% FBS, the base medium was compared between high glucose without pyruvate (HGM) and low glucose medium with pyruvate (LGM). There was an apparent increase in the yield when using LGM (Figure 3-12). This increase in BMDM yield demonstrated in this project aligns with a previous study also showing a positive effect of pyruvate on macrophage differentiation (Liu, Geng and Suo, 2009). Liu *et al.* reported increased macrophage differentiation from human pro-monocytic leukaemia U937 cell line in cultures with added pyruvate and uridine, demonstrated by increased adhesion of the cells to the culture plate (Liu, Geng and Suo, 2009). The differentiated cells showed morphologic features similar to macrophages, although the mechanism was not suggested (Liu, Geng and Suo, 2009).

This project extended this finding by quantifying the increased yield, from 16-26%, which was highly statistically significant (Figure 3-13) and validated the surplus cells' phenotype by flow cytometry (Figure 3-14). Enhanced macrophage differentiation in the presence of pyruvate may be explained by its proposed anti-apoptotic effect through scavenging hydrogen peroxide, which accumulates in culture media (O'Donnell-Tormey *et al.*, 1987) (Miwa *et al.*, 2000). Hydrogen peroxide is a reactive oxygen species released in the culture medium. Its accumulation causes oxidative stress; thus, lowering its levels in the media by pyruvate may provide a more favourable environment for cell differentiation. However, the degree of contribution of pyruvate to the increased yield would

need to be clarified by further testing. For example, maintaining the same glucose concentration and the pyruvate would be the only variable.

The glucose content was another essential difference between the two media used in this optimisation. HGM contains 4.5 g/L of D-glucose, while LGM contains 1 g/L. The results in this project indicate that the lower glucose levels in the media, in conjunction with the presence of pyruvate, had favourable outcomes on the BMDM differentiation yield. This may be supportive evidence of the more vital role of pyruvate in this enhanced yield. Pavlo *et al*. studied the effect of differentiating BMDM in normal glucose standard DMEM (5.5 mM glucose) vs. high glucose DMEM (same medium supplemented with additional 25 mM glucose). They saw no effect of the added glucose on the yield (Pavlou *et al.*, 2018). However, Pavlou *et al*. did note a decrease in phagocytic and bactericidal activity in BMDMs differentiated in the higher glucose medium, in addition to altered cytokine response to stimuli (Pavlou *et al.*, 2018). In this project, the mRNA expression of DDAH2, eNOS and iNOS were comparable between BMDM differentiated in HGM and LGM (Figure 3-16), as was average NO production in response to LPS stimulation (Figure 3-17). The comparison of other parameters, such as phagocytic activity, was out of the scope of this study, although it would be an exciting lead to investigate in the future.

The differences in the numbers of BMDM yield, the homogeneity of populations and their functional responses due to variation of the different components of differentiation media emphasise the importance of transparency of parameters used for reproducibility and comparability of results between researchers.

3.6.4 Macrophage-specific *Ddah2* null mouse model

It has been previously shown that DDAH2 is present in circulating immune cells. A previously validated approach was used to genetically remove the *Ddah2* gene. In line with previous observations using this approach, this study shows a significant decrease in *Ddah2* in peritoneal macrophages at the mRNA level. This study extends these findings to show that this approach also reduces DDAH2 in BMDMs at the mRNA level and, for the first time, also shows its decrease at the protein level. Whilst LysM expression has previously been demonstrated in BMDM (Cross and Renkawitz, 1990) and genetically modified LysM-Cre myeloid cell lines

can be used to study inflammatory diseases (Shi *et al.*, 2018), the ability of Cre to delete DDAH2 in these cells at the mRNA and protein level has not been shown previously. Therefore, this study demonstrates that and establishes this mouse as a suitable model to look at the role of DDAH2 in circulating immune cells.

A striking phenotype in the macrophage-specific *Ddah2* null mouse model was the enlarged spleen weight observed in the KO mice. There have been reports of Cre recombinase-expressing models exhibiting enlarged spleens compared to their Cre-negative controls (Torchia *et al.*, 2007). On the other hand, splenomegaly has been observed in patients with chronic inflammatory disease (Isomäki, Koivisto and Kiviniitty, 1971; Zhang *et al.*, 2020). Therefore, this may be suggestive evidence of an immune-regulatory role for DDAH2. Whether the splenomegaly noted in the KO mice is due to DDAH2 KO itself or due to Cre recombinase expression may be investigated by comparing spleen size between Cre-negative and Cre-positive mice in the absence of DDAH2 floxed regions. Another method would be to investigate if DDAH2 gene rescue in the KO mice would reverse the splenomegaly phenotype. It would also be interesting to investigate the cell composition difference between the spleens of WT and KO animals by flow cytometry. However, a more detailed investigation of the noted splenomegaly was out of the scope of this thesis and, therefore, was not pursued at the time. However, the following chapters investigate the role of DDAH2 in immune regulation.

3.7 Chapter Summary

This chapter demonstrated the suitability of the murine macrophage cell line RAW 264.7 and BMDMs for studying the role of DDAH2 in inflammation. The optimal level of arginine to study ADMA's effects was 100 µM, similar to physiological levels. As expected, ADMA was found to inhibit the enzymatic activity of Nitric oxide synthase, not its gene expression. The study also confirmed the efficiency of BMDM differentiation using M-CSF and increased yield using a low glucose plus pyruvate medium. The macrophage-specific *Ddah2* null mouse model was re-derived, and the phenotype and genotype were confirmed on mRNA and protein levels in-house and by third-party testing. The KO mice exhibited enlarged spleens compared to their WT littermates.

Chapter 4 Results: Effect of DDAH2 knockdown in LPS-stimulated peritoneal macrophages

RNA Sequencing Experiment: *In Silico* Analysis and *In vitro* Validation

4.1 Introduction

Dimethylarginine dimethylaminohydrolase (DDAH) catalyses the hydrolysis of ADMA to L-citrulline and dimethylamine intracellularly (Ogawa *et al.*, 1987; Tain and Hsu, 2017). ADMA is a well-established independent cardiovascular risk factor generally (Meinitzer *et al.*, 2007; Schlesinger *et al.*, 2016) and is associated with atherosclerosis specifically (Jacobi *et al.*, 2010; Miyazaki *et al.*, 1999). Two DDAH isoforms exist with overlapping but distinct tissue distributions (Leiper *et al.*, 1999). While both isoforms colocalise in cardiovascular tissue (Leiper and Nandi, 2011), DDAH1 is more diffusely distributed, colocalising with neuronal nitric oxide synthase (nNOS), while DDAH2 mainly co-localises with endothelial NOS (eNOS) and is the isoform present in the immune system. *Ddah1* and *Ddah2* have been localised in humans to chromosomes 1p22 and 6p21.3, respectively (Tran *et al.*, 2000). The role of DDAH1 in the regulation of ADMA is recognised by many studies (Abhary *et al.*, 2010; Amir *et al.*, 2018; Ding *et al.*, 2010; Liu *et al.*, 2013; Zhang *et al.*, 2013). On the other hand, DDAH2's role in ADMA metabolism has been debated, mainly limited by the inability to purify DDAH2 (Altmann *et al.*, 2012). Some of the supporting literature includes the identification of elevated ADMA in association with different DDAH2 genetic variants (Abhary *et al.*, 2010; Xuan *et al.*, 2016). Furthermore, DDAH2 knockout mice showed high ADMA levels in tissue (Lambden *et al.*, 2015; Lange *et al.*, 2016). On the other hand, other studies failed to find evidence to support that, including the inability to detect DDAH activity in DDAH1 knockout mice (Hu et al., 2011). Ragavan *et al.* showed the inability of ADMA to form a stable bond with DDAH2 in an *in silico* analysis and *in vitro* using recombinant DDAH2 (Ragavan *et al.*, 2023). They also showed that neither the knockdown nor the overexpression of DDAH2 affected total DDAH activity in human embryonic

kidney (HEK) cells (Ragavan *et al.*, 2023), although that is contradicted by other studies (Hasegawa *et al.*, 2007; Zhu *et al.*, 2019).

This controversy, along with evidence of a role for DDAH2 in the regulation of the immune response (Huang *et al.*, 2021) and the importance of the role of the immune system in the development of atherosclerosis (Engelen *et al.*, 2022; Roy, Orecchioni and Ley, 2022) establishes the importance of investigating the biological roles of DDAH2 targeting both possibly ADMA-dependent and independent effects which is made feasible with the use of RNA Sequencing.

High-throughput sequencing technologies have led to a better genomic understanding of disease and biological processes (Pan *et al.*, 2020). It allows the detection of known and new genomic sequences (Huang, Sherman and Lempicki, 2009) and the identification of sequence variations (Koch *et al.*, 2018). Bulk RNA Sequencing, a subtype of RNA Sequencing, although a relatively new technology (Emrich *et al.*, 2007; Lister *et al.*, 2008; Mortazavi *et al.*, 2008; Nagalakshmi *et al.*, 2008), has developed into a ubiquitous and almost routine technique with differentially expressed gene analysis (DEG) being its primary use (Stark, Grzelak and Hadfield, 2019). Previous studies have shown mRNA-level changes in atherosclerosis in humans and rabbits (Seo *et al.*, 2004; Tan, Wang and Li, 2018).

This project revolves around elucidating the role of DDAH2 in inflammation. The previous chapter showed the successful re-creation of a novel macrophage-specific *Ddah2* null mouse model created by our group, from which the group had conducted an RNA Sequencing experiment using peritoneal macrophages. The RNA Sequencing experiment started in the wet lab by extracting RNA from the experimental system, synthesising cDNA and converting it into a sequencing library (Figure 4-1). The library was then sequenced using a high-throughput system into reads, which were analysed by a computerised (*in silico*) system. Significantly differentiated genes under those experimental conditions were identified and were further analysed to determine enriched biological processes or pathways (Lambden *et al.*, 2015).

Since the initial analysis was almost ten years ago, there has been notable advances in the software tools utilised for *in silico* analysis leading to the

discontinuation of some of the software tools used previously and the availability of more precise and sensitive tools. Therefore, it was a valuable opportunity to re-analyse the data. Also, a common debate exists on whether RNA Sequencing data is reliable, mainly stemming from issues sometimes exhibited with the precursor technology, microarrays (Coenye, 2021). This has been investigated thoroughly, and many studies show a good correlation (Everaert *et al.*, 2017; Griffith *et al.*, 2010; Shi and He, 2014) for most of the analysed genes between the RNA Sequencing data and validation by RT-qPCR. It is usually not feasible to validate an entire set of genes by RT-qPCR; therefore, a selection can be made in correlation with the research question. In this study, it was found valuable to validate using a selection of genes related to the inflammatory aspect of atherosclerosis, especially since this validation will not be run on the same RNA extracted for the RNA Sequencing experiment. The validation in this study will allow testing on additional new samples from a new re-creation of the mouse model. In addition to the validation of the *in silico* analysis, new hypotheses related to atherosclerosis will be inferred such as identification of DDAH2-dependent genes involved in inflammation and DDAH2-dependent pathways involved in atherosclerosis .

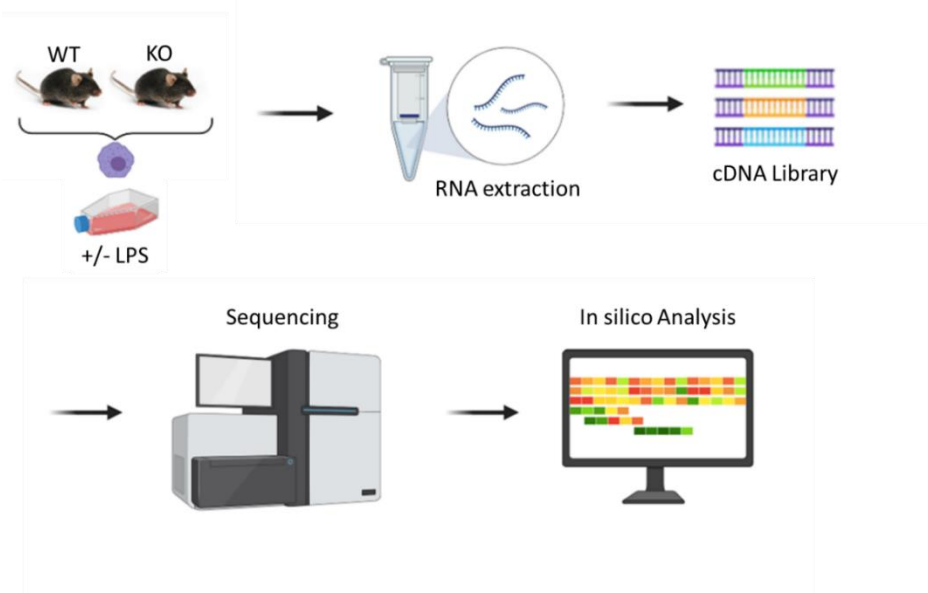

Figure 4-1 RNA sequencing experiment workflow
RNA extracted from peritoneal macrophages from the macrophage-specific *Ddah2* null mouse model were treated with 10 µg/mL LPS or left untreated. cDNA is synthesised and converted into a sequencing library. The library is sequenced using a high-throughput system into reads, which are analysed by a computerised *(in silico*) system**.** The illustration was created with BioRender.com.

4.2 Aims

1. Identification of significant differentially expressed genes in the macrophage-specific *Ddah2* null mouse model involved in inflammatory function

2. Identification of DDAH2-dependent pathways involved in atherosclerosis

3. *In vitro* validation of the *in silico* findings

4.3 RNA sequencing *in silico* data analysis

RNA sequencing raw data was kindly provided by Professor James Leiper. The raw data was the result of an experiment run previously by members of our research group while it was based at the London Institute of Medical Sciences, MRC, Imperial College of London. The group had created a novel macrophage-specific *Ddah2* null mouse model. Primary peritoneal macrophages from male wildtype *Ddah2*$^{f/f}$ LysM-Cre$^{0/0}$ (WT) and macrophage-specific *Ddah2* knockout mice *Ddah2*$^{f/f}$ LysM-Cre$^{0/+}$ (KO) were either treated with 10 µg/mL LPS for 6 hours or left untreated. The experiment included data from four untreated WT, four LPS-treated WT, three untreated KO and three LPS-treated KO mice. The library was prepared using the Illumina TruSeq™ RNA-Sequencing Library preparation kit (Lambden *et al.*, 2015). The data was provided as paired-end Fastq files.

Within this current project, the raw data was re-analysed to identify DDAH2-dependent genes and the atherosclerosis-relevant pathways in which they are involved. The analysis was conducted via a web-based platform, "Galaxy", on the main public server (https://usegalaxy.org). The previous analysis by our group was also analysed by galaxy, however in this study, the newer updated tools were used and alignment was to the currently and most recent mouse genome (mm10).

4.3.1 Quality control and processing

First, raw reads were processed through FastQC (version 0.11.8) for quality control. FastQC analyses multiple factors it flags in a traffic light system. The output was analysed, and then, to improve the read quality, the data was processed using an all-in-one tool, Fastp (Version 0.20.1). Fastp avoids bias as it internally analyses and then processes the reads as required, including trimming poor-quality reads and cutting off adaptors. This was followed by a second quality check by the FastQC tool (Version 0.11.8). The “Per Base Sequence Quality” graphs below show the positioning of the reads according to their quality: green (good), orange (medium) and red (poor). Almost all the reads in this data lie in the green zone, indicating high quality, with only the reads at the very end dipping into the orange (Figure 4-2A) or red zone (Figure 4-2B). However, it is normal for the quality of the read to drop at the end, which may be due to signal decay or phasing.

A

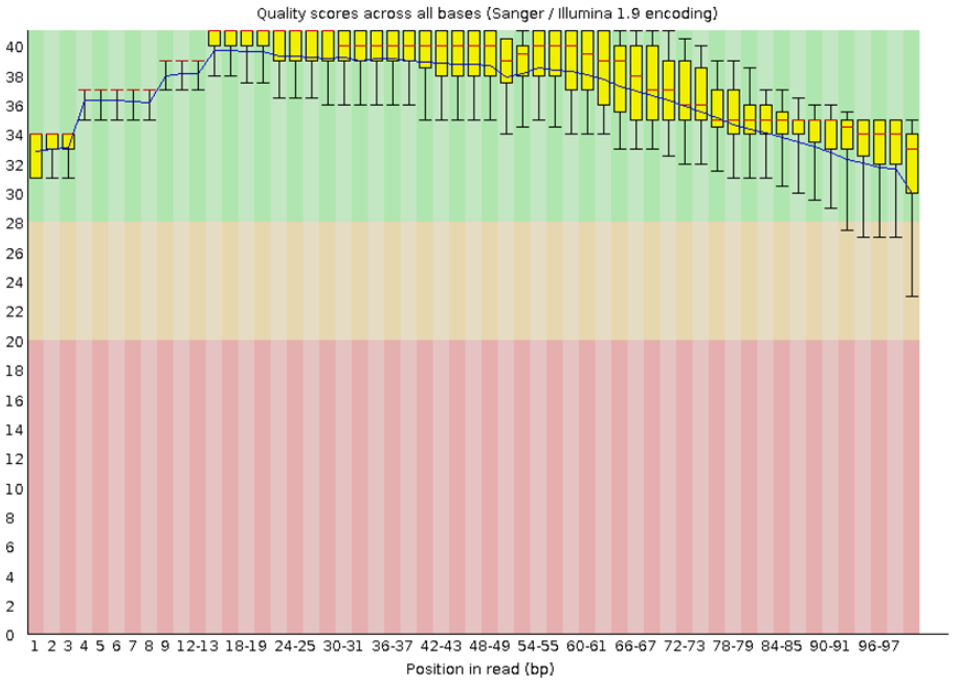

B

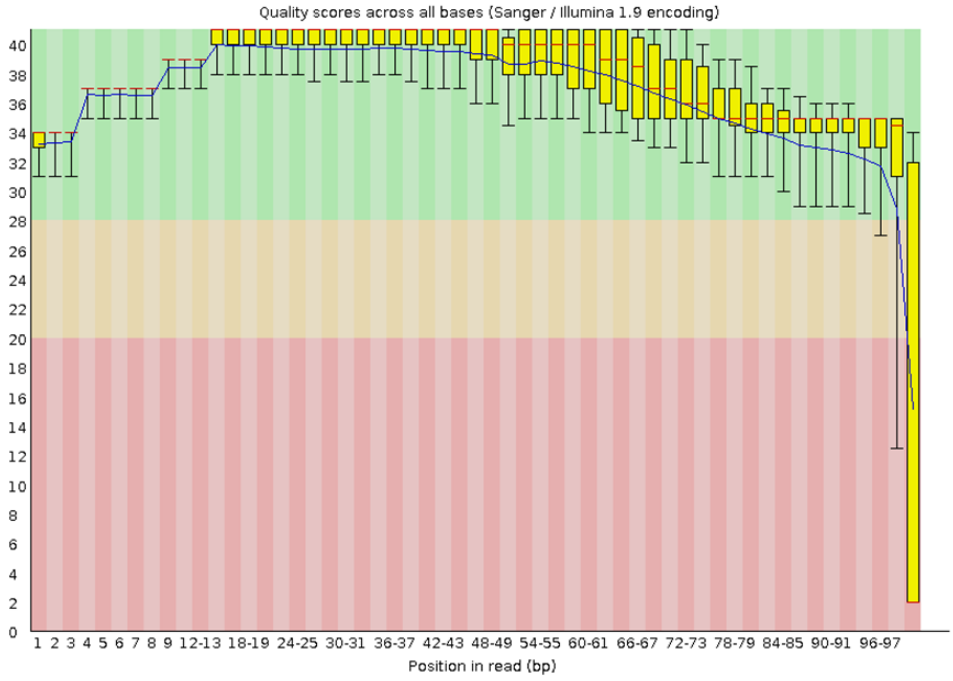

Figure 4-2 Fast QC analysis confirms the high quality of the raw RNA sequencing data

The graphs are representative of those obtained from the FastQC check post-Fastp processing run on our raw data showing Per Base Sequence Quality in Galaxy. The raw reads are of high quality, as the majority of the reads fall in the green zone. with only the reads at the very end dipping into the orange (Figure 4-2A) or red zone (Figure 4-2B).

4.3.2 Alignment

Following the second quality check, the paired files for each sample were aligned to the most recent Ensemble mouse genome (mm10) (mm10.ncbiRefSeq.gtf.gz) using the sensitive splice-aware Hisat2 alignment program (Galaxy version 2.1.0+galaxy7). The output BAM file was quality-checked using FastQC (version 0.72+galaxy1). Alignment statistics, including the numbers of total, mapped, unmapped reads and alignment percentage per sample (Table 4-1), were obtained using Samtool stats from which the Average Alignment Percentage was calculated for each sample group. All the sample groups showed a high and favourable alignment percentage -more than 97.5% (Figure 4-3).

Sample	Total Reads	Mapped Reads	Unmapped reads	Percentage Alignment
Wildtype_untreated_1	71531864	70915137	616727	99.1
Wildtype_untreated_2	39255376	38787248	468128	98.8
Wildtype_untreated_3	53670792	53174015	496777	99.1
Wildtype_untreated_4	54120826	53610125	510701	99.1
Wildtype_LPS-treated_1	49367820	48473272	894548	98.2
Wildtype_LPS-treated_2	58084428	57097810	986618	98.3
Wildtype_LPS-treated_3	32901582	32248352	653230	98.0
Wildtype_LPS-treated_4	24186928	23094865	1092063	95.5
Knockout_untreated_1	34076588	33251423	825165	97.6
Knockout_untreated_2	26897808	26534905	362903	98.7
Knockout_untreated_3	35883566	35225702	657864	98.2
Knockout_ LPS-treated _1	60443220	59686831	756389	98.7
Knockout_ LPS-treated _2	38624146	38119188	504958	98.7
Knockout_ LPS-treated _3	43670060	42998815	671245	98.5

Table 4-1 High alignment of the reads to the mm10 mouse genome via HiSat2

Statistics were obtained using Samtool stats. Numbers of total reads, mapped reads, unmapped reads and the alignment percentage for each sample.

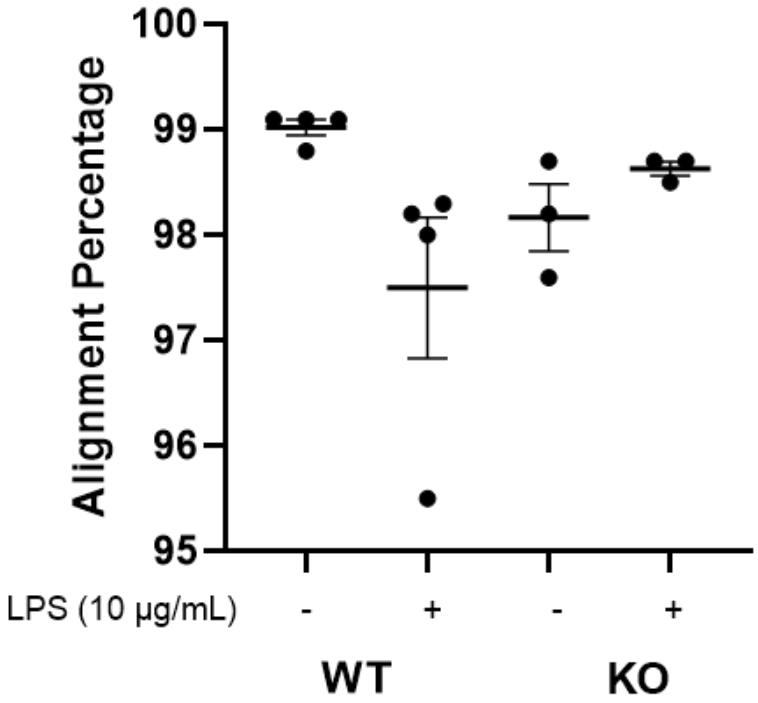

Figure 4-3 Alignment percentage
The alignment percentage per sample was calculated from the statistics obtained using Samtool stats. The average alignment percentage for the wildtype untreated group is 99%, the wildtype LPS-treated group 97.5%, the knockout untreated group 98.1%, and the knockout LPS-treated group is 98.6%. Mean ±SEM. One-way ANOVA with Tukey post hoc test.

4.3.3 Normalised gene counts

Gene-based counts were generated using the HTSeq-count tool (Galaxy version 2.1.0 + galaxy7) using the same reference genome (mm10) in a GFF format and the BAM files as input. These count tables are then taken forward as the input into the DESeq2 tool for the final identification of genes of interest. Each two groups of samples were compared across either treatment or genotype using DESeq2 (Galaxy version 2.11.40.6+galaxy1), resulting in four groups of significantly differentially expressed genes (DEG) (Figure 4-4).

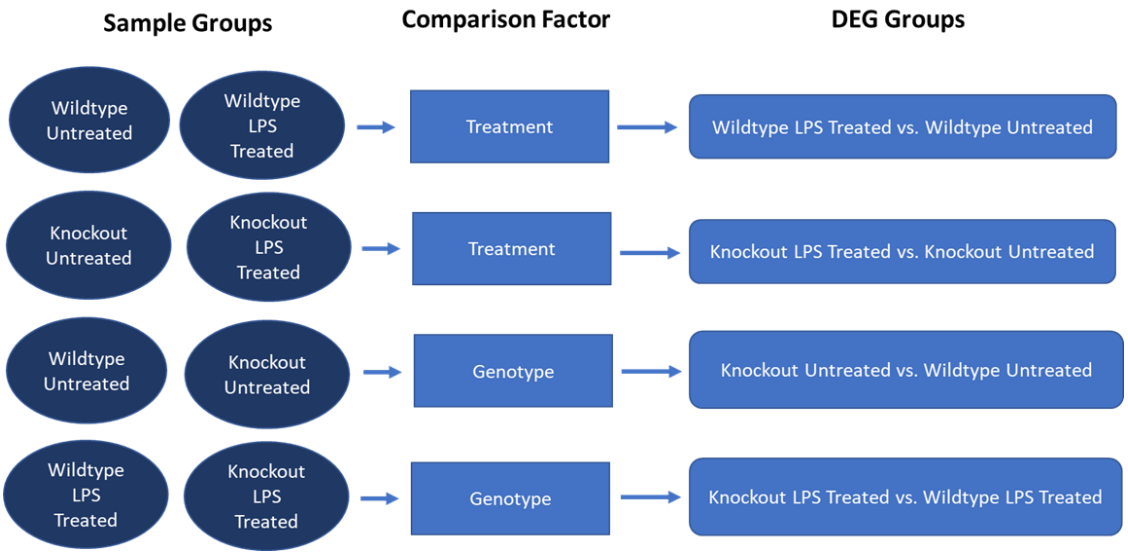

Figure 4-3 DeSeq2 analysis results in four groups of significantly DEG groups
Each two sample groups were compared across either treatment or genotype using DeSeq2, resulting in four groups of significantly differentially expressed genes.

The four experimental groups showed distinct separation while maintaining clustering within the samples of each group as shown in the Principal Component Analysis plot (Figure 4-5). This reinforces the good structure of the data with clear relationships between the different samples. Although one of the untreated knockout samples (KO_UNTR_3) is close to the cluster of wildtype untreated samples and one of the LPS-treated knockout samples (KO_LPS_3) is close to the cluster of wildtype LPS-treated samples, a dividing line can be drawn between the different groups.

Furthermore, there is a uniform general distribution of the genes in samples of the same experimental group with slight variation between different

experimental groups, as shown in the Violin graphs (Figure 4-6 A-I, B-I, C-I and D-I). This confirms that there is no difference in the quality of the samples as well as the high quality of all the samples.

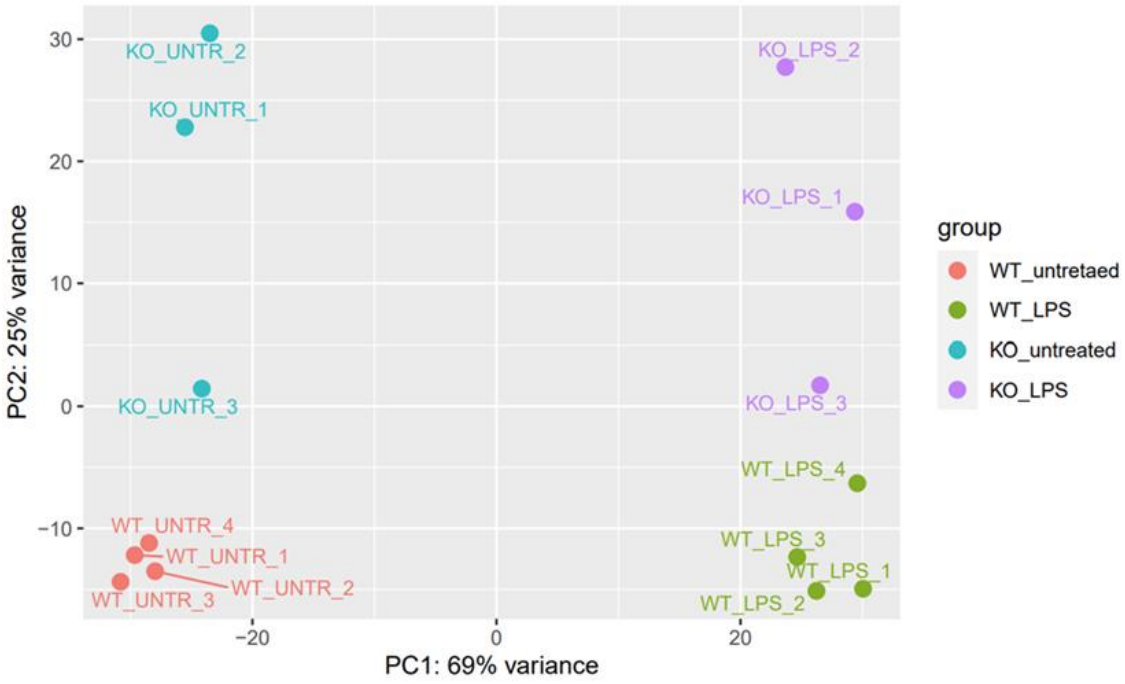

Figure 4-4 Distinct separation between the different sample groups displayed by a PCA Plot
The Principal Component Analysis plot shows the variance between the four different experimental sample groups and the individual samples within each group. WT untreated group (orange), WT LPS-treated (green), untreated DDAH2 KO (blue) and LPS-treated KO (purple). The first principal component (PC1) is displayed on the X-axis (69%) of variance, and the second principal component (PC2) is on the Y-axis (25%).

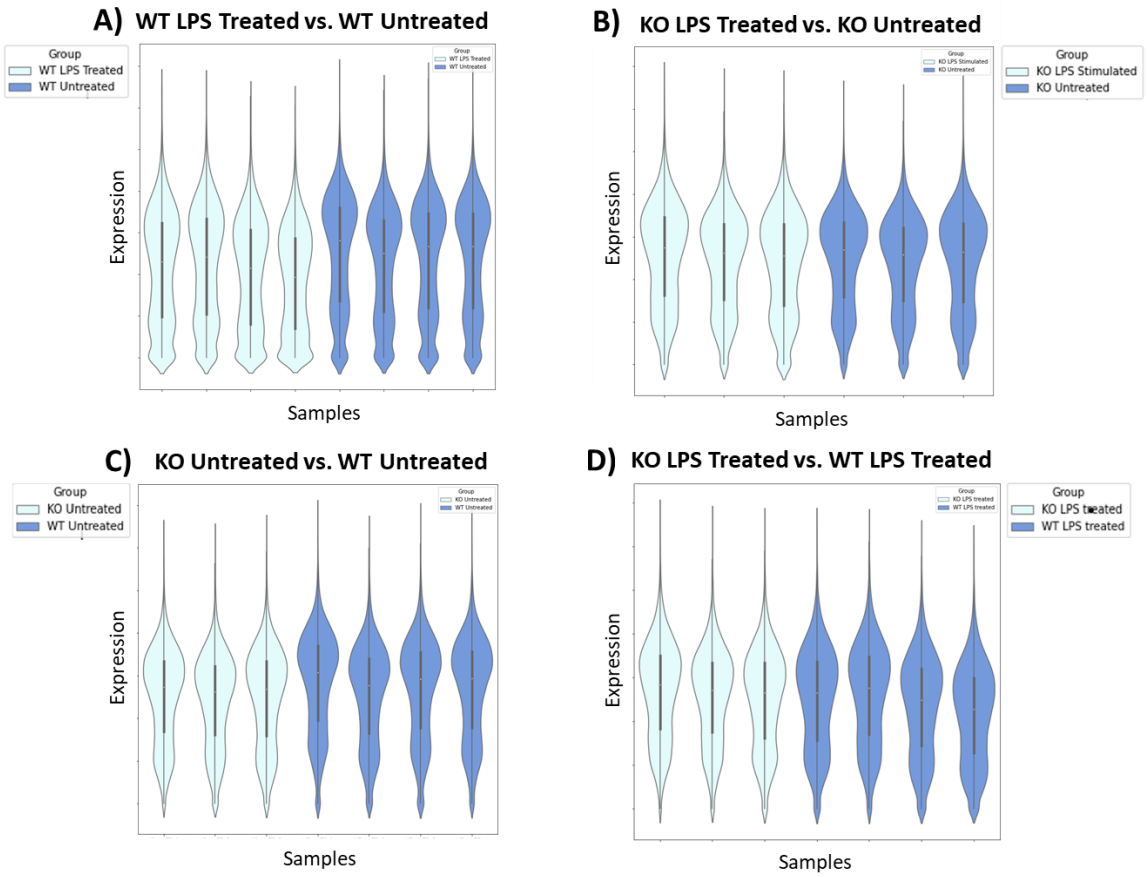

Figure 4-5 Violin distribution plot of normalised read counts
(A) Wild-type LPS-treated vs. Wild-type untreated (B) Knockout LPS-treated vs. Knockout untreated (C) Knockout untreated vs. Wild-type untreated (D) Knockout LPS-treated vs. Wild-type LPS-treated. The first group of samples per comparison is shown in sky blue, and the second group in the same comparison is shown in dark blue.

4.3.4 Differentially expressed genes

The total significantly differentially expressed genes (DEG) were quantified with the cut-off point p-adj>0.05. The upregulated and downregulated genes per group per their fold change were identified (Table 4-2). The highest number of DEG was seen in the wild-type groups after treatment with LPS (9,005 genes), with approximately half up and half downregulated. In comparison, only 4,684 DEGs were identified when the macrophage-specific DDAH2 knockout cells were treated with LPS. This displays the massive effect of LPS stimulation, which primes macrophages and initiates an immune response. Not all of these genes responded in the absence of DDAH2, making them DDAH2 dependent. As an effect of DDAH2 knockout, 3,547 genes were differentially expressed at baseline and 2,155 in the inflammatory state.

Comparison	Total significant DEG	Upregulated DEG	Downregulated DEG
WT LPS over WT UNTR	9,005	4,599	4,406
KO LPS over WT LPS	2,155	1,168	987
KO UNTR over WT UNTR	3,547	1,737	1,810
KO LPS over KO UNTR	4,683	2,346	2,337

Table 4-2 There are many significantly Differentially Expressed Genes (DEG) in the four analysis groups, both up and down regulated
The numbers of the total significant differentially expressed genes (p-adj<0.05), upregulated DEG (FC>0), and downregulated (FC<0). DEG per comparison between each two groups are displayed.

The high number of significant differentially expressed genes, with some upregulated and others downregulated per comparison, are shown in the volcano plots (Figure 4-7). The X-axis shows the $\log_2$ fold change in gene expression, and the Y-axis displays the negative $\log_{10}$ of the p-adjusted value (or false discovery rate (FDR)). The horizontal line displays the cutoff for significance at p-adj >0.05. Statistically not significantly differentially expressed genes are shown in blue and significantly differentially expressed genes in purple. Two vertical guidelines are set at fold change +1 and -1, indicating a doubling or decrease by 50% in expression. Upregulated genes appear on the right half of the plot, while downregulated genes appear on the left half of the plot. Both violin and volcano

plots were generated by Python using a code developed by Dr Simon Fisher in the school.

The top 15 DEGs identified from the *in silico* analysis using Deseq2 are displayed in figure 4-8. These top 15 significant DEGs per group are arranged top to bottom by descending significance level. Upregulated genes are displayed in green, while the downregulated ones are shown in red (Figure 4-8).

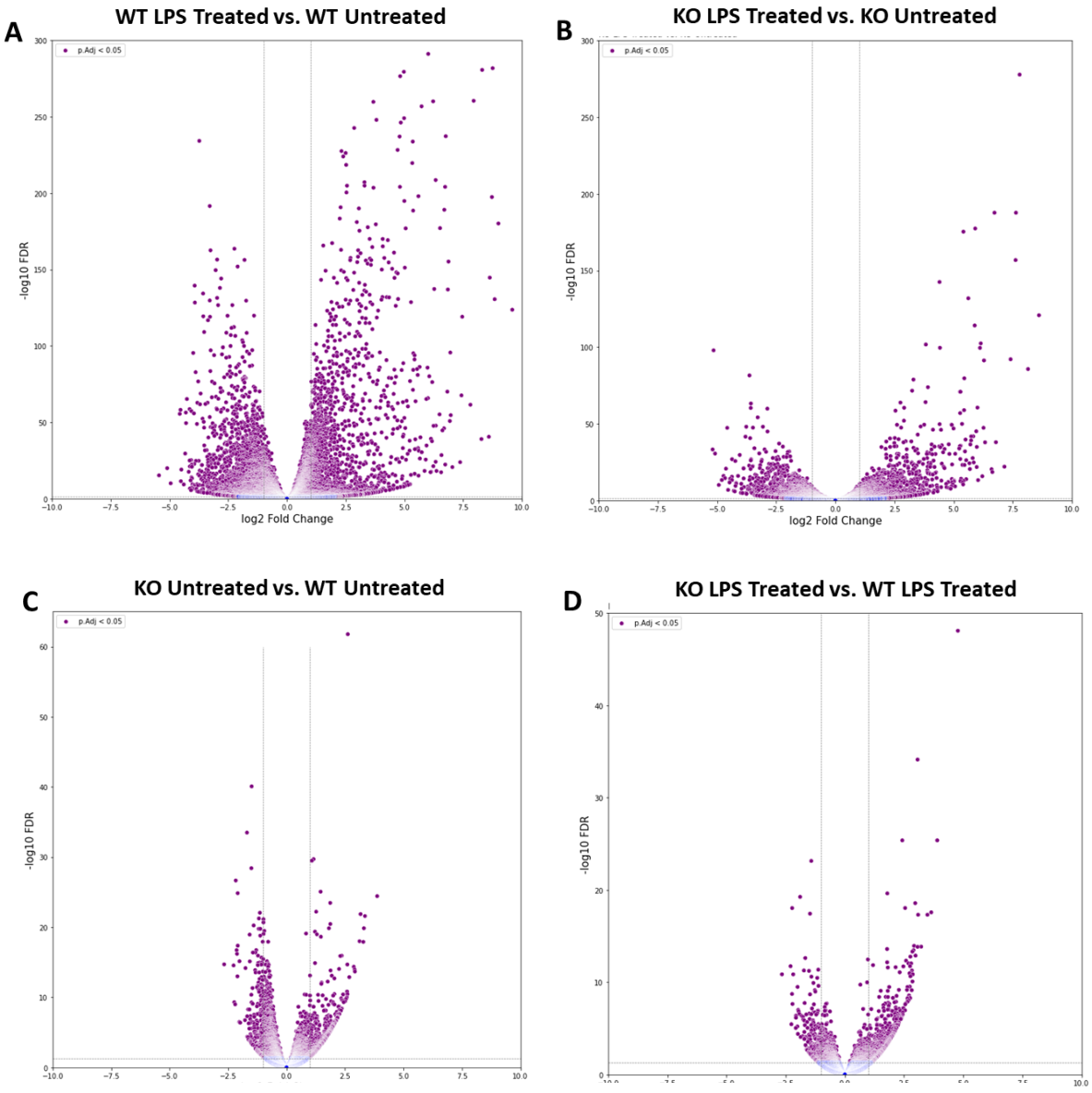

Figure 4-6 Differentially expressed genes represented in volcano plots Volcano plot of genes representing significantly DEG in purple and non-significantly differentially expressed genes in blue. Vertical guide bars at log2 fold change +1 and -1 and horizontal guide bar at significance p-adjusted value 0.05. Upregulated genes appear on the right half of the plot, and downregulated genes on the left half of the plot. (A) Wild-type LPS-treated vs. Wild-type untreated (B) Knockout LPS-treated vs. Knockout untreated (C) Knockout untreated vs. Wild-type untreated (D) Knockout LPS-treated vs. Wild-type LPS-treated.

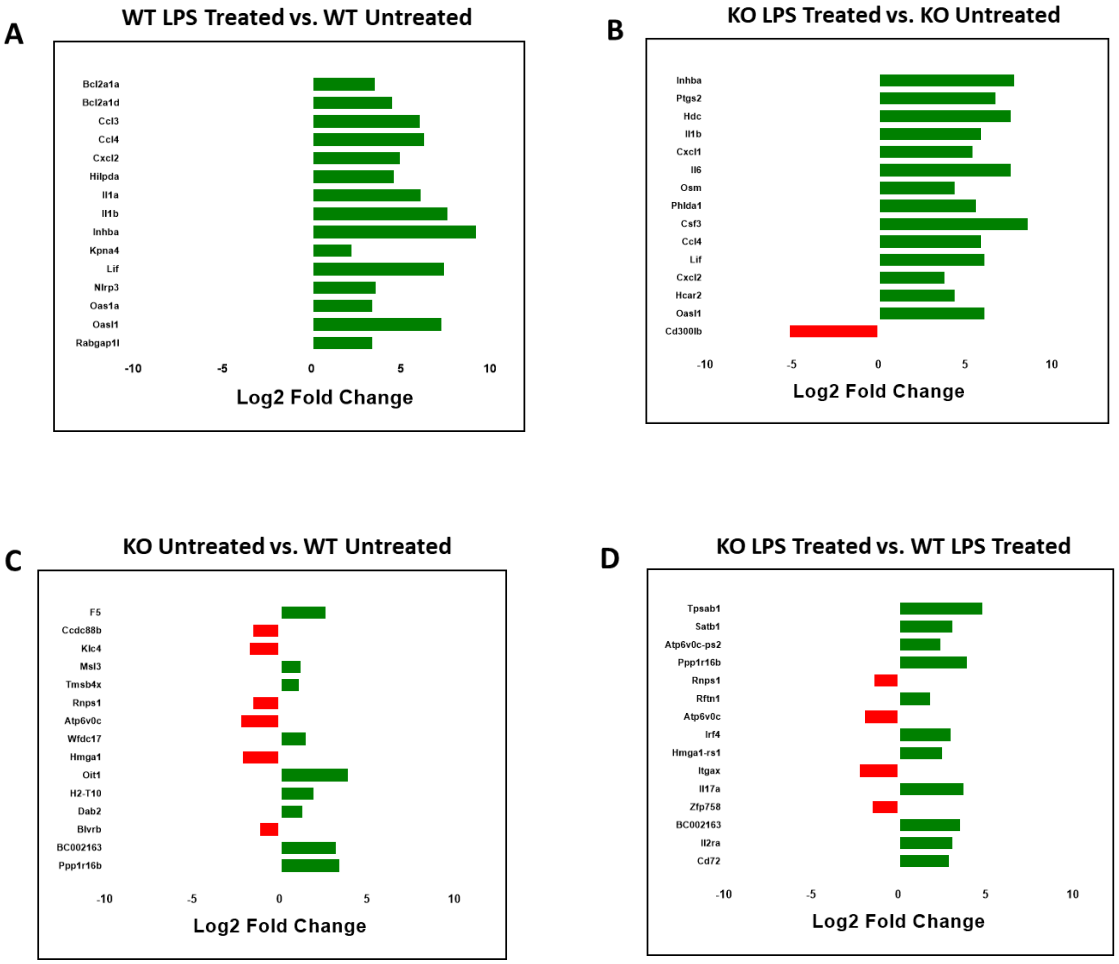

Figure 4-7 Top 15 differentially expressed genes per comparison
The top 15 DEG per comparison with the X-axis representing Log2FC. (A) Wild-type LPS-treated vs. Wild-type untreated (B) Knockout LPS-treated vs. Knockout untreated (C) Knockout untreated vs. Wild-type untreated (D) Knockout LPS-treated vs. Wild-type LPS-treated.

4.3.5 Functional analysis

The data from the DEGs (section 4.3.4) was analysed in combination with observations made previously by our research group. The phenotypic characterisation of the macrophage-specific *Ddah2* null mouse model used in the experiments to generate this data indicated the inability of the knockout mice to mount a normal immune response. Therefore, this information was used to identify genes likely to be DDAH2 dependent and required for a normal immune response. This was achieved by comparing the DEGs (total 9004) identified from comparing LPS-stimulated wild-type mice versus untreated wild-type mice (represented by the red Circle, Figure 4-7) with the DEGs (total 4683) identified from comparing LPS-stimulated Knockout mice vs. untreated knockout mice (represented by the green Circle) in the Venn diagram below (Figure 4-9).

The 4966 genes uniquely differentially expressed in the wild-type when LPS stimulated appear to be DDAH2 dependent as they do not change statistically significantly in the absence of DDAH2. Also they appear to be required to initiate a normal immune response as the knockout have less resistance to infection per the mentioned previous observations. These genes are represented in the red circle, excluding the yellow overlap area. This does not exclude the possibility of the remaining genes being DDAH2-dependent. This method was used to narrow down the number of genes in the follow-up analysis and relate it to the phenotypic description of the knockout mice.

The 4038 overlapping genes (represented in the yellow area) are differentially expressed in the wild-type and knockout upon LPS stimulation. The 645 genes uniquely differentially expressed in the knockout when LPS stimulated may be involved as an attempted compensatory mechanism in response to LPS stimulation but are not enough to produce a normal sufficient immune response.

Therefore, it was stipulated that the identified 4966 genes are both DDAH2 dependent and are required to achieve a normal immune response. Therefore, these genes may be used to elucidate the role of DDAH2 in the inflammatory aspect of atherosclerosis.

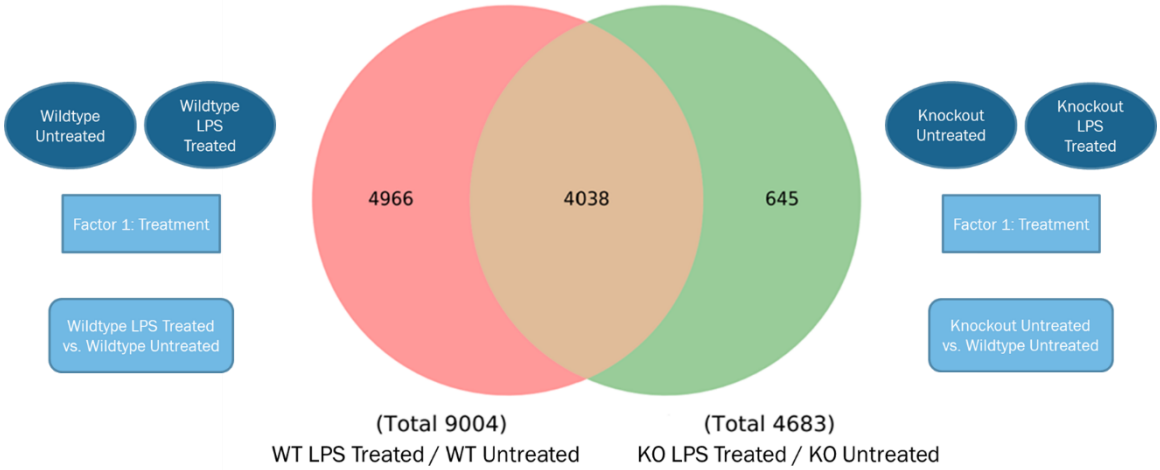

Figure 4-8 4966 genes are DDAH2-dependent and required for a normal immune response
Venn diagram of the 9004 DEG in WT upon LPS treatment (red circle) and 4683 DEG in KO upon LPS treatment (green circle).

The groups of DEGs were uploaded into Gene Ontology (GO) software, and hundreds of significantly affected biological processes and reactome pathways were identified per group. Due to the immense number of DEGs and enriched pathways identified, three aims were identified to proceed with the study.

The first aim was the general validation of the RNA Sequencing data. Since this project revolves around the inflammatory aspect of atherosclerosis, a group of genes shown in the literature to be generally related to inflammation and atherosclerosis specifically were selected. The chosen genes had varying profiles per their respective *in silico* response to LPS stimulation in the WT and the KO. The genes were the chemokines *Cxcl1*, *Cxcl2* and *Ccrl2* and the interleukins *Il1b*, *Il6* and *Il17a* (Table 4-3).

The second aim was to identify genes that are DDAH2-dependent and required for a normal immune response. Here, the selected genes are significantly differentially expressed upon LPS stimulation of the Wild-type but not in the macrophage-specific *Ddah2* null mice as illustrated in the Venn diagram (Figure 4-7). The genes selected for this aim were Oxidised low-density lipoprotein receptor 1 (*Olr1*) and arginase 1 (*Arg1*).

The third aim was to identify genes that are DDAH2-dependent and play a role in foam cell formation. Foam cells undergo various forms of programmed cell death including apoptosis. Interestingly when the 4966 DEGs uniquely in the LPS-stimulated wild-type were uploaded into Gene Ontology, the most highly enriched pathway was apoptosis (Cytochrome c-mediated apoptotic response) with fold enrichment 3.71 and FDR 4.53E-02. This indicates that the DEGs that were used as input are more likely to be associated with the apoptosis pathway than are likely to be by chance. The following genes were selected for validation from those enriched in the apoptosis pathway: Caspase 3, Caspase 6, Caspase 7, *Bcl2*, *Bcl2l1* and *Bax* (Table 4-3).

Gene Symbol	Gene Name
Cxcl1	C-X-C Motif Chemokine Ligand 1
Cxcl2	C-X-C Motif Chemokine Ligand 2
Ccrl2	C-C Motif Chemokine Receptor Like 2
Il6	Interleukin 6
Il1b	Interleukin 1 Beta
Il17a	Interleukin 17A
Olr1	Oxidized Low-Density Lipoprotein Receptor 1
Arg1	Arginase 1
Casp3	Caspase 3
Casp6	Caspase 6
Casp7	Caspase 7
Bcl2	B-cell lymphoma 2
Bcl2l1	Bcl-2-like protein 1
Bax	Bcl-2 Associated X-protein

Table 4-32 Symbols and names of genes selected for the general validation of the RNA Sequencing data analysis

4.4 RT-qPCR validation of RNA sequencing data

To validate the RNA Sequencing *in silico* results, the experimental conditions used to generate the RNA Sequencing Data were replicated in the macrophage-specific *Ddah2* null mouse model.

Peritoneal Macrophages extracted from *Ddah2*$^{f/f}$ LysM-Cre$^{0/0}$ (WT) and *Ddah2*$^{f/f}$ LysM-Cre$^{0/+}$ (KO) were treated with 10 µg/mL LPS for 6 hours or left untreated. RNA was extracted, and the expression of the selected genes was evaluated by RT-qPCR and then compared to the *in silico* results (Table 4-4).

The selected genes belong to either the chemokine or interleukin family as both are well established to be involved in inflammatory processes in general and in atherosclerosis specifically. Also some of the selected genes appear as part of the top DEG in the *in silico* analysis. *Cxcl1* is the 5th top most differentially expressed gene when the *Ddah2*$^{f/f}$ LysM-Cre$^{0/+}$ (KO) is LPS-treated in comparison with its unstimulated state while *Cxcl2* is the 5th top most differentially expressed gene when the WT is LPS-treated in comparison with its unstimulated state. Within the investigated interleukins, *Il6* is the 6th most significantly differentiated gene in the KO upon LPS stimulation in comparison with its non-stimulated state. *Il1b* is the 8th top most differentially expressed gene when the WT is stimulated compared to its unstimulated state and is also the 4th top most differentially expressed gene when the KO is stimulated compared to its unstimulated state. *Il17a* is one of the most (#327) significantly differentially expressed genes when the KO is stimulated compared to its unstimulated state and is the 11th most significant DEG when comparing the stimulated KO with the stimulated WT.

The expression in all the groups was analysed relative to the wild-type untreated controls in the same experiment and data will be displayed as fold change relative to the untreated WT. Litter mates were used in each experiment when possible. Both male and female 7-10 week-old mice were used for the *in vitro* experiments.

	WT_LPS/WT_unRx		KO_LPS/KO_unRx		KO_unRx/WT_unRx		KO_LPS/WT_LPS	
	Log2fc	p-adj	Log2fc	p-adj	Log2fc	p-adj	Log2fc	p-adj
Casp3	0.5	5.06E-05	-0.1	0.79	0.2	0.43	-0.4	0.12
Casp6	-1.1	1.97E-08	-0.4	0.2	-0.2	0.51	0.5	0.11
Casp7	1.7	2.43E-30	0.8	0.06	-0.6	0.01	-1.3	2.47E-06
Bcl2	-1.0	1.82E-09	-0.1	0.88	-0.5	0.13	0.4	0.25
Bcl2l1	-0.9	5.94E-07	0.5	0.13	-0.3	0.33	1.1	9.67E-06
Bax	-0.3	0.0012	0.2	0.52	-0.8	6.09E-06	-0.2	0.27

Table 4-4 Log_2 Fold Change (Log_2FC) and p-adjusted value (p-adj) for the selected chemokines
(*Cxcl1, Cxcl2* and *Ccrl2*) and Interleukins (*Il6, Il1b* and *Il17a*) from the *in silico* analysis of LPS-stimulated or untreated *Ddah2*$^{f/f}$ LysM-Cre$^{0/0}$ (WT) and *Ddah2*$^{f/f}$ LysM-Cre$^{0/+}$ (KO) peritoneal macrophages.

4.4.1 Chemokines

4.4.1.1 C-X-C motif chemokine ligand 1 (*Cxcl1*)

In the *in silico* analysis, when comparing *Cxcl1* gene expression in *Ddah2*$^{f/f}$ LysM-Cre$^{0/0}$ (WT) upon LPS stimulation with its unstimulated state, there is a statistically significant increase in expression with a 6.3 Log_2 fold change (corresponding to an increase by almost 79.4 times) and p-adj (5.40E-138). While when the LPS-treated *Ddah2*$^{f/f}$ LysM-Cre$^{0/+}$ (KO) is compared with its unstimulated state, there is a 5.4 Log_2 fold change (corresponding to an increase by 43 times) and p-adj (3.87E-176). There is no statistically significant difference in *Cxcl1* gene expression in the KO compared with the WT at baseline. However, when comparing *Cxcl1* gene expression in the KO in comparison with the WT while both are LPS-stimulated, there is a statistically significant (p-adj 0.026) decrease in gene expression at -0.5 log_2 fold change (corresponding to a reduction by 0.68 times) (Table 4-5).

In the *in vitro* analysis, *Cxcl1* gene expression increased statistically significantly in the WT with a mean fold change of 105 *(p<0.0001)* upon LPS stimulation. In the KO, *Cxcl1* increases statistically significantly with a mean fold change of 120 of *(p<0.0001)* upon LPS stimulation. There is no statistically significant difference in *Cxcl1* gene expression in the KO compared to the WT at baseline,

although there is an increase of around 1.4 fold. There is also no statistically significant difference when comparing *Cxcl1* gene expression in the LPS-stimulated KO in comparison with the LPS-stimulated WT. However, stimulated KO's gene expression levels are higher than WT (120 vs.105 fold) (Figure 4-10 A).

4.4.1.2 C-X-C motif chemokine ligand 2 (*Cxcl2*)

In the *in silico* analysis, there is a at a 4.9 Log_2 fold change (corresponding to a 25-fold increase) and p-adj (1.00E-300) when the LPS-treated WT is compared with its unstimulated state. When comparing *Cxcl2* gene expression in the KO upon LPS stimulation, the expression increased statistically significantly by 3.8 Log_2 fold change (corresponding to an increase of almost 14 times) and p-adj (1.79E-102). There is no statistically significant difference in *Cxcl2* gene expression in the KO compared with the WT at baseline. However, when comparing expression in the stimulated KO with the stimulated WT, there is a statistically significant decrease (p-adj 3.49E-07) in gene expression at -0.8 log_2 fold change (corresponding to a decrease by 0.6 times) (Table 4-5).

In the *in vitro* analysis, *Cxcl2* expression increased statistically significantly *(p<0.0001)* in the WT with a mean fold change of around 83 upon LPS stimulation. *Cxcl2* gene expression in the KO increased statistically significantly (p<0.0001) upon LPS stimulation with a mean fold change of around 95. There is no statistically significant difference in *Cxcl2* gene expression in the KO compared to the WT at baseline (mean fold change of 1.42). There is also no statistically significant difference in gene expression when comparing the stimulated KO with the stimulated WT (95 vs. 83 fold) (Figure 4-10 B).

4.4.1.3 C-C chemokine receptor-like 2 (*Ccrl2*)

In the *in silico* analysis, *Ccrl2* gene expression in the LPS-treated WT, when compared with its unstimulated state, shows a 2.3 Log_2 fold change (corresponding to a 4.98 fold increase) and p-adj 3.43E-95. However, when comparing *Ccrl2* gene expression in KO upon LPS stimulation with its expression at baseline, there is a statistically not significant increase in expression of 1.3 Log_2 fold change (corresponding to an increase by almost 2.5 times). There is no statistically significant difference in *Ccrl2* gene expression in KO compared to WT

at baseline, with a -0.6 log_2 fold change (corresponding to a decrease by almost 0.73 times). Also, when comparing *Ccrl2* gene expression in LPS-stimulated KO in comparison with LPS-stimulated WT, there is a statistically significant decrease (p-adj 0.03) in gene expression at -1.1 log_2 fold change (corresponding to a reduction by 0.54 times) (Table 4-5).

In the *in vitro* analysis, *Ccrl2* expression increased statistically significantly in the WT with a mean fold change of 11.3 *(p<0.0001)* upon LPS stimulation. When comparing *Ccrl2* gene expression in KO upon LPS stimulation with its expression at baseline, there is a statistically significant increase in gene expression with a mean fold change of around 12 *(p<0.0001)*. There is no statistically significant difference in *Ccrl2* gene expression in KO compared to WT at baseline with a 1.3 foldchange. Also, when comparing *Ccrl2* gene expression in LPS-stimulated KO with LPS-stimulated WT, there is no statistically significant difference in gene expression between the WT and the KO. *Ccrl2* expression is slightly higher in LPS-treated KO than in WT (12.1 vs. 11.3) (Figure 4-10 C).

In these three chemokines, the *in vitro* analysis validates the *in silico* analysis in terms of the effect of DDAH2 knockdown at baseline, as in all three genes, no statistically significant difference was seen between the WT and the KO. The *in vitro* analysis also validates the effect of LPS on the WT as in all three genes, the expression increased statistically significantly as expected from the *in silico* analysis. The *in vitro* analysis also validates the effect of LPS on the KO in *Cxcl1* and *Cxcl2* as gene expression increases statistically significantly per the *in silico* analysis. In *Ccrl2*, gene expression also increased *in vitro*, but it was statistically significant, unlike the statistically not significant rise seen in the *in silico* analysis. In all three genes, when comparing the KO and WT in the stimulated state, there was a statistically significant difference *in silico,* unlike the lack of significance seen *in vitro*. The degree of increase in gene expression in response to LPS was higher *in vitro* than *in silico*, especially in the KO, and that, coupled with the larger number of samples used *in vitro* than in the *in silico* analysis,

may have led to the differences in statistical significance. Therefore, the *in vitro* analysis partially validates the *in silico* analysis.

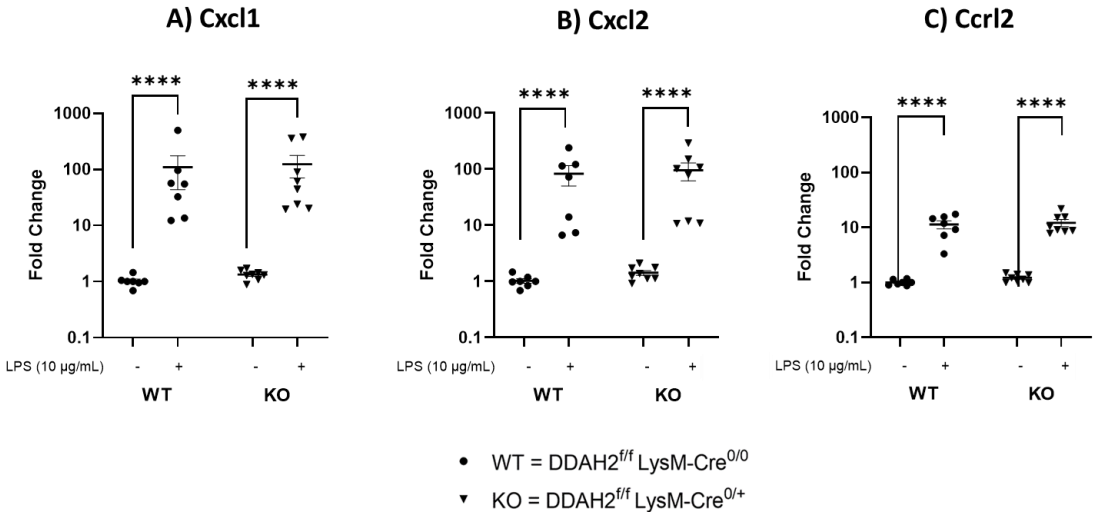

Figure 4-9 *In vitro* analysis of selected chemokines gene expression partially validates the *in silico* analysis
(A) *Cxcl1*, (B) *Cxcl2* and (C) *Ccrl2*. There is a highly significant increase in gene expression in both the WT and KO peritoneal macrophages in response to 10 µg/mL LPS stimulation for 6 hours. There is no significant difference between the gene levels in the WT and KO in either the unstimulated or LPS-stimulated state. Mean ± SEM. Two-way ANOVA with Tukey post hoc test. *(****p<0.0001).*

4.4.2 Interleukins

4.4.2.1 Interleukin 6 (*Il6*)

The *in silico* analysis shows a statistically significant (p-adj 1.35E-121) increase in *Il6* gene expression in the WT when it is LPS stimulated and compared to its unstimulated state at a $\log_2$ fold change of 10.3 (equivalent to 1291.5 times). There is a statistically significant (p-adj 1.36E-157) increase in *Il6* expression in the KO upon LPS stimulation compared with its unstimulated state at Log_2 fold change of 7.6 (corresponding to an increase of around 209 times). There is a highly statistically significant (p-adj 4.55E-08) increase in *Il6* expression in the untreated KO compared to the untreated wild-type at a 1.86 $\log_2$ fold change (equivalent to 3.6 times). There is also a statistically significant (p-adj=0.03) decrease in *Il6* gene expression in the stimulated KO compared to the stimulated WT with a $\log_2$ fold change of -0.64 (equivalent to 0.66 times) (Table 4-5).

In vitro, *Il6* expression increases statistically significantly (p<0.0001) in response to LPS stimulation by more than 7,180 fold compared to its unstimulated state. Also, *Il6* expression in the KO increases statistically significantly (p<0.0001) by 12,361 fold upon LPS stimulation compared to its unstimulated state. There is no statistically significant difference between the KO and WT at baseline, although there is a 4.3-fold increase in the KO. There is a statistically not significant increase in *Il6* expression in the stimulated KO compared to the stimulated WT (12,361 vs. 7,180 fold) (Figure 4-11 A).

4.4.2.2 Interleukin 1 beta (*Il1b*)

In silico, there is a statistically significant (p-adj 1.07E-300) increase in *Il1b* expression when the WT is stimulated in comparison to its unstimulated state at a 7.6 Log_2 fold change (corresponding to an increase by 182 times). When the KO is stimulated compared to its unstimulated state, there is a statistically significant (p-adj 3.2E-178) increase in *Il1b* expression at a 5.9 Log_2 fold change (corresponding to an increase by 58 times). There is a statistically significant (p-adj=2.04E-09) increase in *Il1b* gene expression in the KO compared to the WT at baseline at a 1.15 log_2 fold change (corresponding to an increase of 2.19 times). However, when comparing *Il1b* gene expression in the stimulated KO in comparison with the stimulated WT, there is a statistically not significant decrease in gene expression at -0.38 log_2 fold change (corresponding to a decrease by 0.76 times) (Table 4-5).

In the *in vitro* analysis, *Il1b* increases statistically significantly *(p<0.0001)* in the WT with a mean fold change of 891 upon LPS stimulation compared to its unstimulated state. *Il1b* expression also increases statistically significantly *(p<0.0001)* in the KO with a mean fold change of 1007 upon stimulation compared to its unstimulated state. There is a statistically not significant increase in *Il1b* gene expression in the KO compared with the WT at baseline by twofold. Also, there is a statistically not significant increase in gene expression in the stimulated KO compared to the stimulated WT (1007 vs. 891 fold) (Figure 4-11 B).

4.4.2.3 Interleukin-17a (*Il17a*)

In silico, *Il17a* gene expression shows a statistically not significant increase at a log_2 fold change of 1.65 (corresponding to an increase by 3.14 times) in the stimulated WT compared to its unstimulated state. However, when the KO is stimulated compared to its unstimulated state, there is a statistically (p-adj 1.86E-16) significant increase of 6.2 Log_2 fold change (corresponding to an increase by 75 times). At baseline, the comparison between KO and WT renders a Log_2 Fold Change as 0 reads, indicating very low values of both. However, when comparing the stimulated KO with the stimulated WT, there is a statistically significant (p-adj 2.65E-18) increase in expression with a 3.7 Log_2 fold change (corresponding to an increase of almost 12 times) (Table 4-5).

In vitro, *Il17a* expression in the stimulated WT increases by 1.9 times when compared to its unstimulated state and this increase is statistically not significant. However, *Il17a* shows a highly statistically significant *(p=0.0001)* increase in expression in the stimulated KO compared with its unstimulated state (4.7 vs. 0.99 mean fold change). At baseline, there is no statistically significant difference in gene expression between the KO and WT (0.99 vs. one log_2 fold change). However, *Il17a* increased statistically significantly (0.0339) *in* the stimulated KO compared to the stimulated WT (4.7 vs. 1.9 fold change) (Figure 4-11 C).

In the *in silico* analysis, *Il6* and *Il1b* gene expression increases statistically significantly in response to LPS stimulation in both the WT and the KO, and this is replicated *in vitro*. Also, in both genes, the knockdown of DDAH2 in the unstimulated state leads to a statistically significant increase in expression *in silico*. *In vitro,* gene expression follows the same trend but is statistically not significant. *In silico*, both genes show a decrease in expression when comparing the KO with WT in the stimulated state, although it is statistically significant only in the case of *Il6*. *In vitro*, the opposite trend occurs as expression in the LPS-stimulated KO is higher than in the stimulated WT. Therefore, in the case of *Il6* and *Il1b*, the *in vitro* analysis partially validates the *in silico* analysis. On the other hand, in the case of *Il17a*, the *in vitro* analysis fully validates the *in silico* analysis warranting further functional validation.

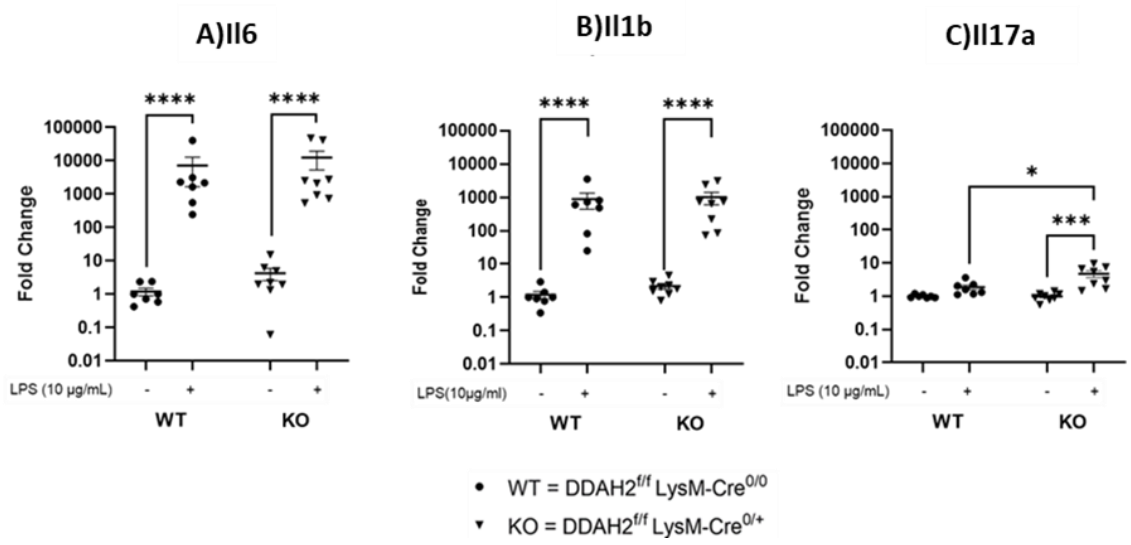

Figure 4-10 *In vitro* analysis of *Il17a* gene expression validates the *in silico* analysis
There is a highly statistically significant increase in gene expression in the KO in response to 10 µg/mL LPS stimulation for 6 hours. *Il17a* expression increased in the WT after LPS stimulation, but the increase was statistically not significant. There was no statistical significance in the difference in expression between the KO and WT at baseline. However, the expression in the stimulated KO is statistically significantly higher than in the stimulated WT. The data was analysed using the deltadelta CT method with normalisation of all the samples to the deltaCT average of the unstimulated-wildtype samples in the same PCR plate. Mean ± SEM. Two-way ANOVA with Tukey post hoc test. (**p=0.0339,***p=0.0001,****p<0.0001)*.

4.5 Functional validation of IL17A response to LPS stimulation in peritoneal macrophages

Given that *Il17a* was a highly concordant gene per the reproducibility of the *in silico* results between the analysis performed ten years ago by our research group (Lambden *et al.*, 2015) and the repeat *in silico* analysis performed in this study and the *in vitro* validation of the results by qPCR, it was of interest to follow up with a functional validation.

To determine the effect of DDAH2 Knockdown on IL17A cytokine production in inflammatory conditions, *Ddah2*$^{f/f}$ LysM-Cre$^{0/0}$ (WT) and *Ddah2*$^{f/f}$ LysM-Cre$^{0/+}$ (KO) peritoneal macrophages were either treated with 10 µg/mL LPS for 24 hours or left untreated. Stimulation of WT and KO with LPS caused an increase in IL17A released in the culture supernatant; 96 pg/mL (SEM=17.255) vs. 468 pg/mL(SEM=169.228) respectively.

A repeated measure two-way ANOVA run on the square roots of the concentrations (due to inherent skewness of data in the form of concentrations), comparing the four sample groups, showed that the LPS treatment produced a statistically significant increase in the concentration of the IL17A produced regardless of the genotype (p=0.0025). The genotype however, had no statistically significant effect at either baseline or after LPS treatment.

A detailed statistical comparison run on each comparison alone in the form of paired Students's t-test (for the effect of LPS treatment in the WT alone or in KO alone) and unpaired Student's t-test in the case of effect of genotype at baseline or after LPS treatment. These were followed by Bonferroni adjustment for multiple testing.

After the adjustment for multiple testing, all values were statistically non-significant except for the comparison of KO_untreated with KO_LPS-treated (p=0.0416). The lack of statistical significance in the WT may be explained by the low biological replicate numbers (n=3) and does not exclude the potential for there to be a biologically relevant difference (Figure 4-12).

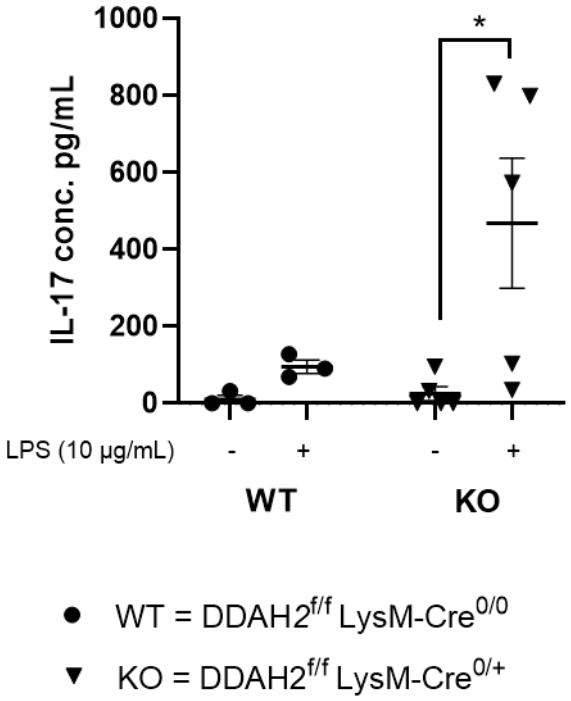

Figure 4-11 DDAH2 regulates IL17 production in LPS-stimulated peritoneal macrophages
The effect of 10 µg/mL LPS stimulation for 24 hours on IL17 release was evaluated in *Ddah2*$^{f/f}$ LysM-Cre$^{0/0}$ (WT) and *Ddah2*$^{f/f}$ LysM-Cre$^{0/+}$ (KO) peritoneal macrophages. There is a statistically significant increase in IL17A production in the KO in response to 10 µg/mL LPS stimulation for 24 hours. IL17A production increased in the WT after LPS stimulation but was not statistically significant. The difference in expression between the KO and WT at baseline or after LPS stimulation was not statistically significant. Mean ± SEM. WT (n=3), KO (n=5). Student's t-test with Bonferroni adjustment for multiple comparison *(*p=0.0406).*

4.6 Discussion

The macrophage-specific *Ddah2* null mouse model was re-created for this project. The RNA Sequencing experiment was conducted on samples from the original model around ten years ago. Due to the advances in software tools over the years, the *in silico* analysis was repeated using the latest recommended tools. To validate the *in silico* analysis, the same experiment was repeated using a larger number of new samples under the same conditions. Validation was by evaluating gene expression mainly using RT-qPCR with further validation by ELISA for the most concordant gene. For that aim, a number of genes belonging to either the chemokine or interleukin family and known to have a role in atherosclerosis were selected. Those genes also were some of the top DEG in the *in silico* analysis.

4.6.1 Brief summary of chapter findings

The *in silico* analysis of the RNA sequencing data confirmed the high quality of the raw data. Processing was run via a selection of unbiased tools using Galaxy software. The reads achieved a favourable high alignment against the mm10 mouse genome. Deseq2 was utilised to obtain DEGs while comparing every two data sets against either genotype or treatment. This resulted in four distinct groups of DEG with an apparent, distinct variance, as shown by the PCA plot.

Intersecting the DEGs when the wild-type samples are LPS stimulated with the DEGs when the knockout is LPS-stimulated, along with previous phenotypic observations, allowed the deduction of a hypothesis. A group of genes were identified as DDAH2-dependent and required for a normal immune response. GO analysis revealed a large number of affected biological processes and pathways either as the result of DDAH2 knockdown or LPS treatment. Further analysis firstly requires validation of the *in silico* analysis in the same model. Also, the other hypotheses may be investigated in the same or similar models.

Some of the RNA sequencing analysis results were reproducible, while others were not. It was noted that there was a variation in the gene response between *in vitro* replicate experiments, and although some of those experiments did indeed replicate the *in silico* analysis (n=3), that was not always the case, and the presented data represents the result of pooling the data of all these *in vitro* experiments together (n=8) to eliminate any bias. *In vitro, Il17a* gene expression showed full reproducibility and validation of the *in silico* analysis, and it was interesting to validate the observed results with a functional analysis such as ELISA which validated the production of IL17A by peritoneal macrophages and supports an inhibitory role for DDAH2 in the regulation of IL17A.

4.6.2 RT-qPCR I*n vitro* validation of the i*n silico* analysis in peritoneal macrophages

The *in vitro* validation of the *in silico* analysis of the selected genes in this study reveals a degree of concordance similar to that shown in previous literature. Everaert et al., in a benchmarking study of RNA sequencing workflows based on human samples, showed that 93% of genes that show discrepancies between RNA Sequencing and qPCR expression have a fold change of less than two in their *in silico* analysis (Everaert *et al.*, 2017).

In this study, in both the WT and the KO, all the selected genes replicated the LPS effect expected from the *in silico* analysis, as in the direction of change (all up-regulated) regardless of the fold change (ranging from 2.5-1,300 times increase *in silico*). However, the magnitude of increase in expression was different between the *in silico* and the *in vitro* analyses, leading in the case of *Ccrl2* to a discrepancy on whether it is a DEG in the KO when it is stimulated with LPS. *Ccrl2 in silico* was not identified as a DEG in the KO when it was LPS stimulated (p-adj=0.13), while *in vitro*, the increase was highly statistically significant *(p<0.0001)*.

When analysing the gene response as an effect of DDAH2 Knockdown at baseline, the genes differed in their concordance. In the case of the selected chemokines, the change was not statistically significant in both the *in silico* (change ranged between 0.73 - 1.24 times) and the *in vitro* analysis. The genes *in vitro* expression followed the same trend observed *in silico* in *Cxcl1* and *Cxcl2*, while *Ccrl2* followed the opposite trend. As for the interleukins, *Il6* and *Il1b* were both identified *in silico* as DEGs with a high degree of significance. However, *in vitro,* although they followed the same direction of change and magnitude, the change was not statistically significant. An increase in sample numbers may influence that factor. On the other hand, *Il17a*, was not highlighted as a DEG *in silico* and there was no evident difference in expression *in vitro* either. A low baseline expression of *Il17a* may explain this.

When analysing the gene response as an effect of DDAH2 Knockdown at in the LPS stimulated state (stimulated KO vs. stimulated WT), the only gene that

replicated the *in silico* analysis in this condition *in vitro* was I*l17a* (*in silico* fold change of 12). All the other genes had an *in silico* decrease in fold change between 0.55-0.79 times, and *in vitro*, they changed but the changes were statistically not significant, mainly in the opposite direction. *In vitro* expression in the stimulated KO compared to the stimulated WT was higher for I*l1b* and all the chemokines. *Il6* increased but the increase was statistically not significant.

Factors other than fold change, which were noted to play a role in the *in vitro* replicability of *in silico* data are the sizes of the genes and their levels of expression (Everaert *et al.*, 2017). Those aspects were not followed up in this study as it was outside the current scope of the project, but would be interesting to follow up in the future.

Some of the changes in the statistical differences between the *in silico* and *in vitro* analyses may be explained by the difference in magnitude of change and the larger sample size in the *in vitro* analysis. The increased number of samples plays a dual effect, causing either an increase in significance if results were close between the biological replicates or decreasing it when the opposite is the situation. In this study, as mentioned previously, individual *in vitro* experiments in some conditions mirrored the *in silico* data, while others did not. However, all the data was pooled to avoid investigator bias. *In vitro* results may be considered as having higher biological relevance due to the increased data set, but further functional analysis would be vital for translational purposes.

As for the role of DDAH2 in the regulation of inflammation, although the *in silico* data showed a statistically significant decrease in expression of *Cxcl1, Cxcl2, Ccrl2, Il6* and *Ill1b* in the stimulated KO compared to the stimulated WT, that was not reproducible *in vitro* within this study. Thus, DDAH2 may not play a role in their regulation. However, both *in silico* and *in vitro* analyses show a role for DDAH2 in regulating IL17A.

4.6.3 DDAH2 regulates IL17A expression in peritoneal macrophages

IL17A is primarily believed to be produced by Th17 cells, CD8 T cells, natural killer (NK) cells, T cells, and neutrophils and to form an essential link between

adaptive and innate immunity (Flierl *et al.*, 2008). However, it has also been documented to be released by non-T-cell sources (Reece *et al.*, 2021) and specifically alveolar macrophages where they play a role in the inflammatory allergic response (Song *et al.*, 2008; Zhang *et al.*, 2021). Peritoneal macrophages have been noted to produce IL17A in response to sensitisation with Ovalbumin (OVA) to produce an allergic reaction (Song *et al.*, 2008), in colitis-associated cancer (Zhang *et al.*, 2016) and in response to stimulation with either IL23 or Paclitaxel in a model of mechanical pain (Luo *et al.*, 2021).

Interestingly, Soudi et al. (2013) showed the production of IL17A by LPS-stimulated wild-type C57BL/6J peritoneal macrophages. They noted a concentration of 900 pg/mL after 24 hours of LPS stimulation. Our study shows lower concentrations in the *Ddah2*$^{f/f}$ LysM-Cre$^{0/0}$ (WT) and *Ddah2*$^{f/f}$ LysM-Cre$^{0/+}$ (KO) (around 100 vs.470 pg/mL). Some differences are noted between their study and this one beyond the essential point of this study being based on a DDAH2-KO model (although of the same genetic background). In their study, the mice were injected intraperitoneally with 4% w/v thioglycolate medium four days before they were sacrificed, while in this study, no pre-injection was used. Thioglycolate is an eliciting agent used to increase macrophage migration to the peritoneal cavity and thus increases the yield while also leading to contamination of the peritoneal lavage mainly by eosinophils (Misharin, Saber and Perlman, 2012). It also changes their metabolic state and increases their phagocytic activity (Pavlou *et al.*, 2017). In both studies, *in vitro* stimulation was by LPS; however the final concentration used was different. They used 1 µg/mL, while here, 10 µg/mL was used. The different LPS concentration is an interesting factor, as 1 µg/mL in their study was sufficient to produce around 20 µmol Nitric oxide at 24 hours as measured by the Griess Assay. However, experience in our research group found that dose to be insufficient in peritoneal macrophages and only achieved similar concentrations at the same time point either by increasing the dose of LPS by ten times or using an inflammatory cocktail of LPS/TNF-α/IFN-γ (Ahmetaj-Shala, 2013). This difference may be due to their use of thioglycolate. This current study highlights the role of DDAH2 in the regulation of IL17A. Although our LPS-stimulated WT mice did not produce IL17A at levels as high as the Sauodi study, the increase in the production in the LPS-stimulated KO was almost five-fold that in the WT and was statistically

significant. The fact that here, a floxed control was used as a WT control further aids in making this a reliable finding.

As the role of IL17A in inflammation is well established, and its blockade was found to have a protective effect in experimental sepsis (Flierl *et al.*, 2008), it is of interest to follow up the findings in this study documenting a possible role for DDAH2 in its regulation.

4.7 Chapter summary

This chapter aimed to identify DDAH2-dependent genes involved in inflammation and DDAH2-dependent pathways involved in atherosclerosis. This was achieved by the *in silico* analysis of an RNA sequencing experiment on primary peritoneal macrophages from *Ddah2*$^{f/f}$ LysM-Cre$^{0/0}$ and *Ddah2*$^{f/f}$ LysM-Cre$^{0/+}$ which were either treated with LPS or left untreated.

A substantial number of genes per the *in silico* analysis were affected by DDAH2 knockout both at baseline and post-LPS stimulation indicating that DDAH2 has many regulatory roles. *In vitro* validation of a selection of DDAH2-dependent genes revealed a degree of concordance aligning with studies in literature. The *in vitro* validation revealed a role for DDAH2 in the regulation of IL17A by RT-qPCR which was further supported by ELISA. Given the well-established role of IL17A in inflammation and the protective effect of its blockade in inflammatory disease, it is worth exploring the findings of this project that document a possible role for DDAH2 in regulating IL17A.

Chapter 5: Effect of DDAH2 knockdown in LPS-stimulated bone marrow-derived macrophages

5.1 Introduction

Macrophages are a part of the innate immune response, and the two most commonly used primary models for *in vitro* experiments are peritoneal and bone marrow-derived macrophages. There have been a variety of studies investigating the differences between these two types of macrophages. One of the major differences is the origin of these cells. Peritoneal macrophages are tissue-resident macrophages with homeostatic functions in the steady state. They originate during embryonic development and maintain themselves by self-renewal independent of circulating monocytes (Hashimoto *et al.*, 2013). Infection or chemical elicitation leads to transient recruitment and infiltration of circulating monocytes into the peritoneum (Yona *et al.*, 2013). The peritoneal macrophages used in this project are extracted from the peritoneal exudate directly without using any prior elicitation. The bone marrow-derived macrophages used in this project, on the other hand, are differentiated *in vitro* using macrophage colony-stimulating factor. Therefore, BMDMs are more naïve at the time of differentiation. This project revolves around the study of mechanisms and genes associated with inflammation generally and atherosclerosis, a pathological inflammatory state leading to vessel wall infiltration by macrophages originating from circulating monocytes (Ingersoll *et al.*, 2011). As the yield of circulating monocytes from mice is minimal (Argmann and Auwerx, 2006; Houthuys *et al.*, 2010), bone marrow-derived macrophages were selected as the representative model with the added advantage of a substantially higher yield.

The aim of the study discussed in this current chapter is to test the results (aims are detailed section 5.2) generated from the *in silico* analysis on a more-atherosclerosis relevant model, hence BMDM were utilised. Since previous studies have shown mRNA-level changes in atherosclerosis in humans and rabbits (Seo *et al.*, 2004; Tan, Wang and Li, 2018), this chapter will investigate the hypotheses by analysing mRNA expression using RT-qPCR. The investigated genes were those hypothesised to be DDAH2-dependent and required for a normal

immune response; *Olr1* and Arginase1 and genes that play a role in apoptosis and hypothesised to be DDAH2-dependent; caspase 3, caspase 6, caspase 7, *Bcl2, Bcl2l1* and *Bax*. Also, due to the evidence seen in peritoneal macrophages regarding the regulatory effect of DDAH2 on IL17A (sections 4.4 and 4.5), the investigation was extended to BMDMs.

5.2 Aims

1. Investigation of the genes identified in the *in silico* analysis as DDAH2-dependent and required for a normal immune response in a BMDM model

2. Investigation of the genes identified in the *in silico* analysis as DDAH2-dependent and play a role in foam cell formation in a BMDM model

3. Validation of expression of IL17A in BMDM in response to LPS stimulation

5.3 DDAH2-dependent genes required for a normal immune response

In the previous chapter (4.3.5), an analysis of the *in silico* data derived from the RNA sequencing experiment on LPS stimulated wildtype (*Ddah2*$^{f/f}$ LysM-Cre$^{0/0}$ or WT) and DDAH2 knockdown (*Ddah2*$^{f/f}$ LysM-Cre$^{0/+}$. Or KO) peritoneal macrophages, identified 4966 genes as DDAH2 dependent and required for a normal immune response. From those, two genes – *Olr1* and *Arg1*- were selected for further investigation as they have been previously related to atherosclerosis, and this study aims to investigate if DDAH2 plays a role in their regulation in an inflammatory BMDM model.

Oxidised low-density lipoprotein receptor 1 (OLR1) also known as LOX-1, is a scavenger receptor that plays an important role in the pathogenesis of atherosclerosis (Sharma, Romeo and Mehta, 2022). This scavenger receptor is expressed in endothelial cells and macrophages (Kume *et al.*, 2000). Its expression is upregulated in macrophages in proinflammatory states, leading to an increase in oxLDL uptake (Kattoor, Goel and Mehta, 2019), contributing thus to foam cell formation (Yang *et al.*, 2015).

Regarding Arginase 1 (Arg1), it is the enzyme driving the hydrolysis of arginine to ornithine and urea, the competing pathway to nitric oxide synthesis (Rath *et al.*, 2014). Arginase has been detected in human (Thomas *et al.*, 2007) and mouse atherosclerotic plaques (Khallou-Laschet *et al.*, 2010; Trogan *et al.*, 2006). It may promote tissue repair and help stabilise plaques (Khallou-Laschet *et al.*, 2010; Morris Jr, 2009) and thus its degree of expression is inversely associated with the severity of atherosclerosis (Teupser *et al.*, 2006). Furthermore, an increase in Arginase expression may be associated with atherosclerosis reversal (Pourcet *et al.*, 2011).

5.3.1 Investigation in macrophage-specific *Ddah2* null mouse model

In the RNA Sequencing experiment conducted previously by our group, extracted peritoneal macrophages from the WT and KO were either left untreated or treated with 10 μg/mL LPS for 6 hours, followed by RNA extraction and bulk RNA sequencing.

In the *in silico* analysis in this project (chapter 4), *Olr1* expression showed a 1.1 Log_2 fold change (corresponding to a 2.14 fold increase) statistically significant increase (p-adj 1.46E-19) in WT peritoneal macrophages in response to 10 μg/mL LPS stimulation in comparison to their unstimulated state, and this significant upregulation did not occur in the KO. There was no statistically significant effect of DDAH2 knockdown on *Olr1* expression at baseline. *DDAH2* expression was statistically significantly (p-adj 0.04) lower in the LPS-stimulated KO than the LPS-stimulated WT at a -0.6 Log_2 fold change (corresponding to a 0.59 fold decrease)(Table 5-1).

To investigate whether this remained true in our BMDM model, cells from WT and KO were stimulated with 1 μg/mL LPS for 6 hours, as 1 μg/mL is more widely used in BMDMs (Xiao *et al.*, 2012; Xaus *et al.*, 2000). *Olr1* expression increased statistically significantly in both WT (50 fold, p=0.0004) and KO (54 fold, p=0.0002) in comparison to their unstimulated states with no statistically significant differences between the two groups either at baseline or post-stimulation (Figure 5-1 -A). Thus, DDAH2, under these conditions does not seem to regulate *Olr1* expression in BMDM.

Arginase 1 in the *in silico* analysis showed a 1.0 Log_2 fold change (corresponding to a 2 fold) statistically significant increase (p-adj 0.04) in WT peritoneal macrophages in response to 10 µg/mL LPS stimulation in comparison to their unstimulated state. Although this increase in expression was not replicated in the KO, the baseline levels of *Arg1* were statistically significantly (p-adj 4.01E-05) higher in the KO than the WT at 1.7 Log_2 fold change (corresponding to a 3.16 fold increase) leading to a final statistically significantly (p-adj 1.07E-05) higher *Arg1* expression in LPS stimulated KO than in the WT at 1.9 Log_2 fold change (corresponding to a 3.74 fold increase) (Table 5-1).

In vitro, BMDMs stimulated with 1 µg/mL LPS showed a statistically significant *(p<0.0001)* increase in expression in *Arg1* in both the WT (22 fold) and the KO (16 fold). Although the difference in *Arg1* between the WT and KO was not statistically significant, the levels started at a slightly higher level at baseline in the KO, but post LPS-stimulation did not reach the same levels as the stimulated WT (Figure 5-1 B). Although there appears to be a trend of reduced *Arg1* expression upon LPS stimulation in the absence of DDAH2, due to the lack of statistical significance, it cannot be concluded from this data that DDAH2 significantly affects *Arg1* expression under these circumstances.

	WT_LPS/WT_unRx		KO_LPS/KO_unRx		KO_unRx/WT_unRx		KO_LPS/WT_LPS	
	Log2fc	p-adj	Log2fc	p-adj	Log2fc	p-adj	Log2fc	p-adj
Olr1	1.1	1.46E-19	0.1	0.8	0.3	0.36	-0.6	0.04
Arg1	1.0	0.04	0.4	0.69	1.7	4.01E-05	1.9	1.07E-05

Table 5-1 *Olr1* and *Arg1 in silico* results
Log_2 Fold Change (Log_2FC) and p-adjusted value (p-adj) for the selected genes Oxidised low-density lipoprotein receptor 1 (*Olr1*) and Arginase 1 (*Arg1*) from the in silico analysis of LPS-stimulated or untreated *Ddah2*$^{f/f}$ LysM-Cre$^{0/0}$ (WT) and *Ddah2*$^{f/f}$ LysM-Cre$^{0/+}$ (KO) peritoneal macrophages.

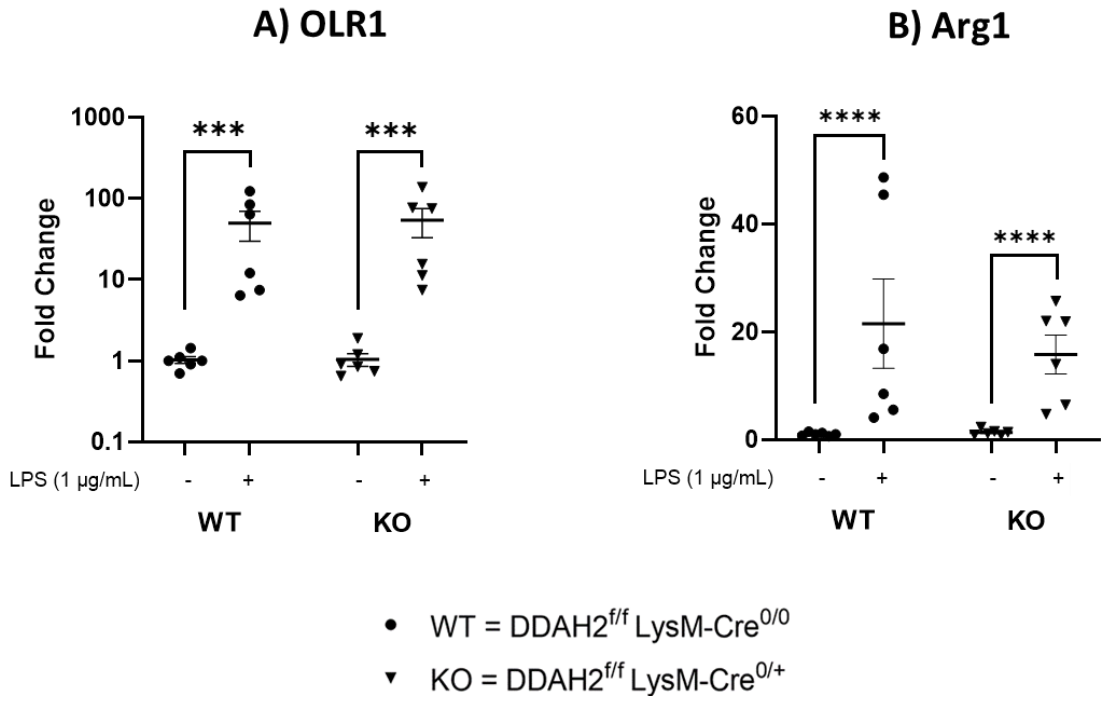

Figure 5-1 DDAH2 does not regulate *Olr1* and *Arg1* gene expression in BMDM
Effect of DDAH2 on *Olr1* and *Arg1* gene expression at baseline and in 1µg/mL LPS-stimulated *Ddah2*$^{f/f}$ LysM-Cre$^{0/0}$ and *Ddah2*$^{f/f}$ LysM-Cre$^{0/+}$ for 6hrs expressed as fold change. (A)*Olr1* and (B)*Arg1*. Mean ± SEM. Two-way ANOVA with Tukey post hoc test. *(***p=0.0004 (Olr1-WT) , ***p=0.0002(Olr1-KO)), ****p<0.0001).*

5.3.2 Confirmatory study in C57BL/6J wild-type BMDM

No regulatory effect was seen for DDAH2 on *Olr1* and *Arg1* in BMDMs from the knockout model. To confirm this, the experiment was repeated with ADMA as in immune cells ADMA is thought to be metabolised by DDAH2. BMDMs differentiated from wild-type C57BL/6J mice were stimulated with 1 μg/mL LPS for 6 hours after being treated with 100 μM ADMA for either 1 hour (Figure 5-2: I,II) or 24 hours (Figure 5-2: III, IV) or the cells were stimulated with 1 μg/mL LPS for 6 hours without pre-treatment with ADMA. *Olr1* expression increased statistically significantly *($p<0.0001$)* in response to LPS stimulation with no altered effect when ADMA was added for either treatment duration (Figure 5-2: A). Arg1 expression increased statistically significantly in response to LPS stimulation and prolonging the duration of pre-treatment with ADMA increased the statistical significance of the response to LPS stimulation to ($p=0.0027$) with, and ($p=0.0006$) without pretreatment with ADMA (5-2: B). Regarding *Arg1* expression, 1 hr pretreatment with ADMA followed by LPS stimulation replicated the effect of DDAH2 KO in the LPS stimulated BMDMs. In both, Arg1 expression increased statistically significantly but did not reach the higher levels as with LPS only or in WT respectively (Figure 5-2).

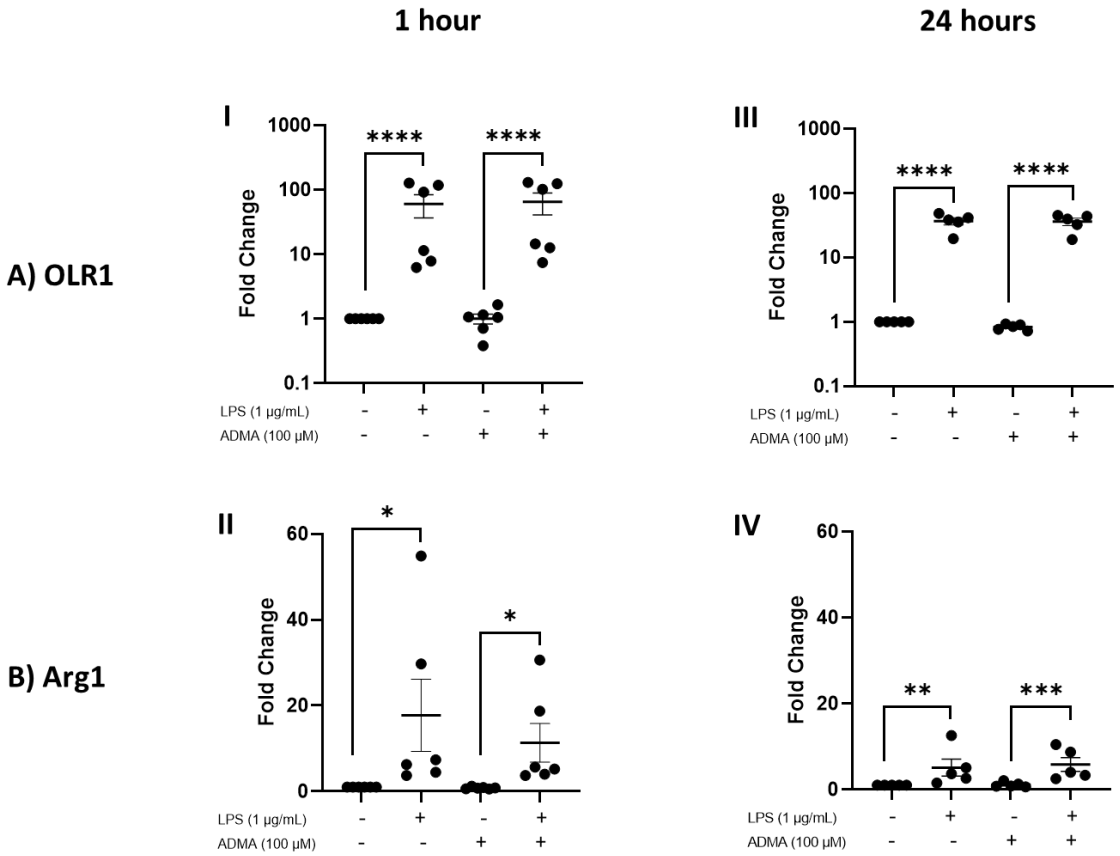

Figure 5-2 ADMA does not alter *Olr1* and *Arg1* gene expression in BMDM
Effect of 100 µM ADMA on (A) *Olr1* and (B) *Arg1* gene expression at baseline and in 1µg/mL LPS-stimulated WT C57BL/6J BMDM for 6 hours post-treatment with 100 µM ADMA for (I) 1 hour or (II) 24 hours expressed as fold change. Data was analysed using deltadelta CT method with all samples being normalised to the average delta CT of the control samples (no LPS, no ADMA). Mean ± SEM. One-way ANOVA with Bonferroni post hoc test. *(*p= 0.0.0279 (WT) , *p=0.0318 (KO)), **p=0.0027, ***p=0.0006 , ****p<0.0001).*

5.4 DDAH2-dependent genes enriched in apoptosis

The analysis (4.3.5), of the *in silico* data derived from the RNA sequencing experiment on *in vitro* 10 µg/mL LPS stimulated wildtype (*Ddah2*$^{f/f}$ LysM-Cre$^{0/0}$ or WT) and DDAH2 knockdown (*Ddah2*$^{f/f}$ LysM-Cre$^{0/+}$ Or KO) peritoneal macrophages, revealed apoptosis as the most highly enriched pathway by the genes identified as DDAH2-dependent as they were uniquely significantly differentially expressed in the WT when it was LPS stimulated and did not change statistically significantly in the absence of DDAH2.

Apoptosis is an integral part of the development of atherosclerotic disease and plays a dual role depending on its stage (Xie *et al.*, 2022). In early lesions, it appears to be athero-protective (Liu *et al.*, 2005) while in advanced lesions, it promotes plaque instability (Gautier *et al.*, 2009; Seimon and Tabas, 2009). Experimental evidence shows macrophage cell death by apoptosis and other mechanisms, such as necroptosis, may be a promising therapeutic target (Martinet *et al.*, 2019). However, apoptosis is a complex mechanism, and a deeper understanding of its pathways is needed.

Generally, apoptosis can be activated by extrinsic or intrinsic pathways. The extrinsic pathway involves the activation of tumour necrosis factor- alpha (TNFa) and the subsequent activation of a series of caspases (McArthur & Kile, 2018). The intrinsic or mitochondrial pathway is governed by members of the *Bcl2* family (Linton *et al.*, 2016). In this study, several genes involved in apoptosis and shown in the *in silico* analysis of the RNA sequencing experiment to respond to LPS stimulation only in the WT were selected to study the role of DDAH2 on apoptosis, including three genes from the caspase family (caspase 3, caspase 6 and caspase 7) and three genes from the *Bcl2* family (*Bcl2, Bcl2l1* and *Bax*).

5.4.1 Investigation in macrophage-specific *Ddah2* null mouse model

In the *In silico* analysis in this project (chapter 4) conducted on peritoneal macrophages from the macrophage-specific *Ddah2* null mouse model , all the selected genes to study the effect of DDAH2 on apoptosis statistically significantly changed in the WT upon 10 µg/mL LPS stimulation for 6 hours. Caspase 3 showed a 0.5 Log_2 fold change (corresponding to a 1.4 fold) statistically significant increase (p-adj 5.06E-05). Caspase 6 showed a -1.1 Log_2 fold change (corresponding to a 0.6 fold) statistically significant decrease (p-adj 1.97E-08). Caspase 7 showed a 1.7 Log_2 fold change (corresponding to a 3.17 fold) statistically significant increase *(*p-adj 2.43E-30). *Bcl2* showed a -1.0 Log_2 fold change (corresponding to a 0.5 fold) significant decrease (p-adj 1.82E-09). *Bcl2l1* showed a -0.9 Log_2 fold change (corresponding to a 0.54 fold) statistically significant decrease (p-adj 5.94E-07). *Bax* showed a -0.3 Log_2 fold change (corresponding to a 0.8 fold) statistically significant decrease (p-adj 0.0012).

However for none of these genes did the expression change statistically significantly in the KO upon LPS stimulation.

There was no effect of DDAH2 knockout on the expression of caspase 3, caspase 6, *Bcl2* and *Bcl2l1* at baseline while caspase 7 showed a -0.6 Log_2 fold change (corresponding to a 0.67 fold) statistically significant decrease (p-adj 0.01) and BAX showed a -0.8 Log_2 fold change (corresponding to a 0.57 fold) statistically significant decrease (p-adj 6.09E-06). Also, there was no statistically significant effect of DDAH2 knockout in the stimulated state in caspase 3, caspase 6, *Bcl2* and *Bax*, while caspase 7 decreased statistically *significantly (p*-adj 2.47E-06) at a -1.3 Log_2 fold change (corresponding to a 0.4 fold) and Bcl2l1 increased statistically significantly (p-adj 9.67E-06) at a 1.1 Log_2 fold change (corresponding to a 2.1 fold) (Table 5-2). This data indicated that DDAH2 may play a role in the regulation of apoptosis in peritoneal macrophages.

To investigate the role of DDAH2 in apoptosis, the effect of 1 µg/mL LPS stimulation on the selected apoptosis-related genes was tested on BMDM from the macrophage-specific *Ddah2* null mouse model . The genes had varying responses. Caspase 3 and *Bax* showed a statistically significant increase (p= 0.036, 0.043, respectively) in response to LPS stimulation in the WT only and although there was a similar degree of increase in the KO, it did not reach statistical significance. On the other hand, caspase 7 and *Bcl2l1* showed a statistically significant increase in both the WT and KO in response to LPS stimulation. Caspase 6 and *Bcl2* decreased (statistically not significant) in the WT and KO in response to LPS stimulation. None of the genes showed a statistically significant difference between the WT and the KO upon LPS stimulation; thus, from this data, a role for DDAH2 could not be concluded (Figure 5-3).

.

	WT_LPS/WT_unRx		KO_LPS/KO_unRx		KO_unRx/WT_unRx		KO_LPS/WT_LPS	
	Log2fc	p-adj	Log2fc	p-adj	Log2fc	p-adj	Log2fc	p-adj
Casp3	0.5	5.06E-05	-0.1	0.79	0.2	0.43	-0.4	0.12
Casp6	-1.1	1.97E-08	-0.4	0.2	-0.2	0.51	0.5	0.11
Casp7	1.7	2.43E-30	0.8	0.06	-0.6	0.01	-1.3	2.47E-06
Bcl2	-1.0	1.82E-09	-0.1	0.88	-0.5	0.13	0.4	0.25
Bcl2l1	-0.9	5.94E-07	0.5	0.13	-0.3	0.33	1.1	9.67E-06
Bax	-0.3	0.0012	0.2	0.52	-0.8	6.09E-06	-0.2	0.27

Table 5-2 Apoptosis genes *in silico* results
Log_2 Fold Change (Log_2FC) and p-adjusted value (p-adj) for the selected Caspases (Caspase 3, Caspase 6 and Caspase 7) and *Bcl-2* family (*Bcl2*, *Bcl2l1* and *Bax*) from the *in silico* analysis of LPS-stimulated or untreated *Ddah2*$^{f/f}$ LysM-Cre$^{0/0}$ (WT) and *Ddah2*$^{f/f}$ LysM-Cre$^{0/+}$ (KO) peritoneal macrophages

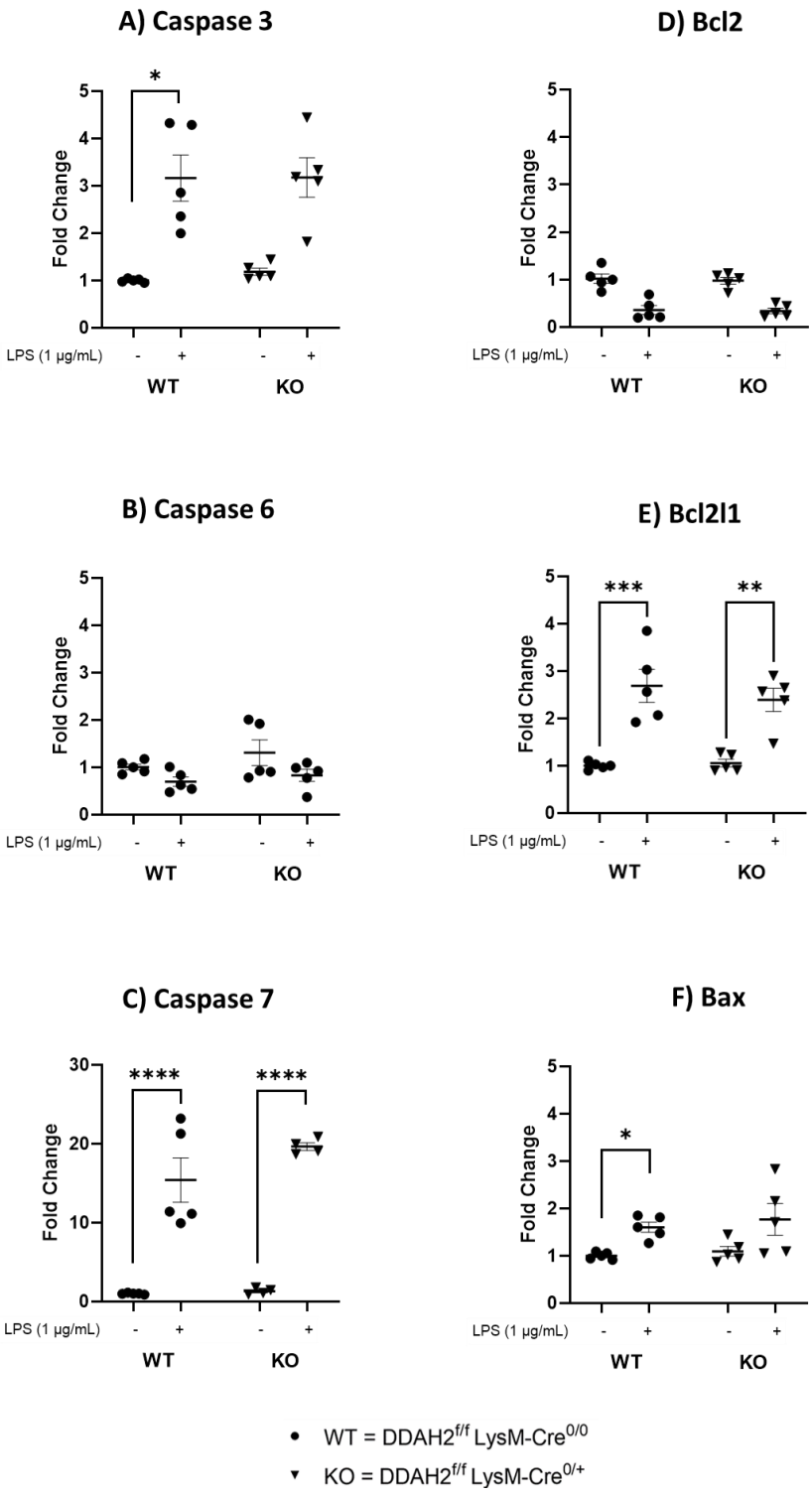

Figure 5-3 DDAH2 does not regulate selected apoptosis gene expression in BMDM

Effect of DDAH2 on apoptosis-genes expression at baseline and in 1µg/mL LPS-stimulated *Ddah2*$^{f/f}$ LysM-Cre$^{0/0}$ and *Ddah2*$^{f/f}$ LysM-Cre$^{0/+}$ for 6 hours expressed as fold change. (A) Caspase 3 (B) Caspase 6 (C) Caspase 7 (D) *Bcl2* (E) *Bcl2l1* (F) *Bax.* The data was analysed using deltdelta CT method with all samples being normalised to the average delta CT of the unstimulated wildtype samples. Mean ± SEM. p<0.05. Two-way ANOVA with Tukey post hoc test. (*caspase 3: *p=(0.0360), Bax: *p= (0.0434), **p=0.0023, ***p=0.0004 , ****p<0.0001*).

5.4.2 Confirmatory study in C57BL/6J wild-type BMDM

To confirm the lack of regulatory effect of DDAH2 on apoptosis gene expression in BMDM, the experiment was repeated with ADMA. BMDMs differentiated from wild-type C57BL/6J mice were stimulated with 1 µg/mL LPS for 6 hours after being treated with 100 µM ADMA for either 1 hour (Figure 5-4: I,II,III) or 24 hours (Figure 5-4: IV,V,VI) or the cells were stimulated with 1 µg/mL LPS for 6 hours without pre-treatment with ADMA.

All the genes changed in the same direction in response to LPS as in the macrophage-specific *Ddah2* null mouse model. The response to LPS was more uniform and evident than in the KO-model leading to a higher statistical significance. The treatment with ADMA for both time points did not alter the effect of LPS on gene expression, similar to what was observed with DDAH2.

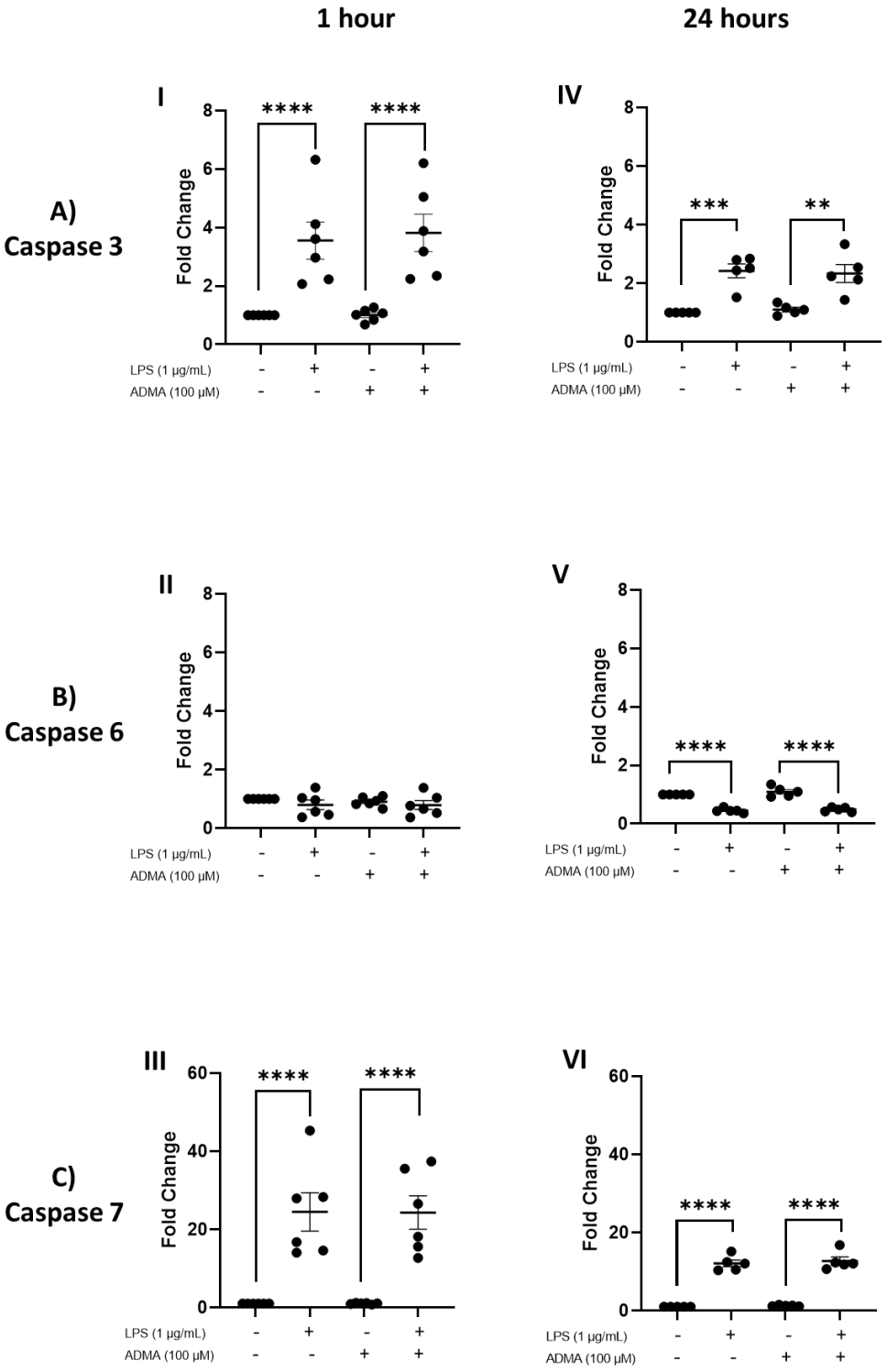

Figure 5-4 ADMA does not alter Caspase 3, Caspase 6 and Caspase 7 gene expression in BMDM

Effect of pretreatment with 100 µM ADMA on (A) Caspase 3, (B) Caspase 6 and (C) Caspase 7 gene expression at baseline and in 1µg/mL LPS-stimulated WT C57BL/6J BMDM for (I) 1hrs (n=6) or (II) 24 hours (n=5) expressed as fold change. The data was analysed using deltdelta CT method with all samples being normalized to the average delta CT of the control samples (no LPS, no ADMA). Mean ± SEM. $p<0.05$. One-way ANOVA with Bonferroni post hoc test. (***p=0.0017, ***p=0.0003, ****p<0.0001*).

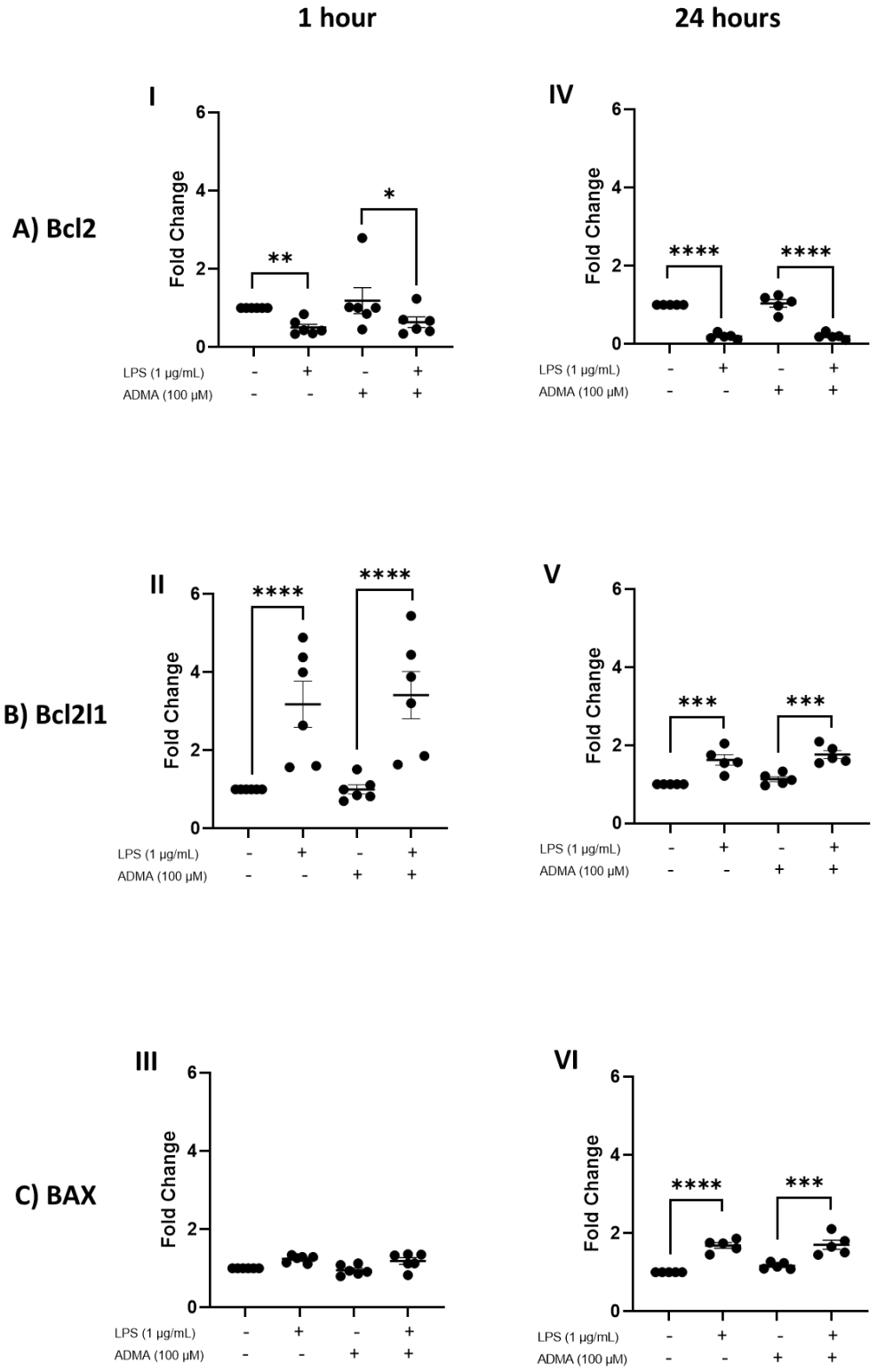

Figure 5-5 ADMA does not alter *Bcl2, Bcl2l1* and *Bax* gene expression in BMDM

Effect of 100 µM ADMA on (A) *Bcl2*, (B) *Bcl2l1* and (C) *Bax* gene expression at baseline and in 1µg/mL LPS-stimulated WT C57BL/6J BMDM for (I) 1hr or (II) 24 hours expressed as fold change. The data was analysed using deltdelta CT method with all samples being normalized to the average delta CT of the control samples (no LPS, no ADMA). Mean ± SEM. p<0.05. One-way ANOVA with Bonferroni post hoc test. (*p=0.0438, **p=0.0057,), *Bcl2l1*: ***p= 0.0001(WT), ***p= 0.0002(KO), *Bax* ***p=0.0007), ****p<0.0001).

5.5 *Il17a* expression in bone marrow-derived macrophages

The *in silico* analysis in chapter 4 showed a statistically significant (p-adj 1.86E-16) increase of 6.2 Log_2 fold change (corresponding to an increase by 75 times) in *Il17a* expression in response to 10 µg/mL LPS stimulation for 6 hours in peritoneal macrophages from the macrophage-specific *Ddah2* null mouse model while the increase in the WT was not statistically significant. This finding was validated *in vitro* using RT-qPCR on new peritoneal macrophage samples from the re-created macrophage-specific *Ddah2* null mouse model. There was a highly statistically significant *(p=0.0001)* increase in *Il17a* expression in the stimulated KO compared with its unstimulated state (4.7 vs. 0.99 mean fold change). Further validation was performed by using ELISA to measure IL17A production by peritoneal macrophages in the culture media after stimulation with 10 µg/mL LPS for 24 hours. In the KO there was a statistically significant increase in IL17A production upon LPS stimulation. That presented evidence of the role for DDAH2 in the regulation of IL17A expression in peritoneal macrophages.

As IL17A has an established role in inflammation and is upregulated in atherosclerosis (Nordlohne and von Vietinghoff, 2019), it was of interest to investigate the role of DDAH2 in regulating *Il17a* in BMDMs.

WT and KO BMDMs from the same macrophage-specific *Ddah2* null mouse model were stimulated with 1 µg/mL LPS for 6 hours and *Il17a gene* expression was compared. There was no statistically significant change in *Il17a gene* expression noted in either the WT or the KO upon LPS stimulation and furthermore, there was no difference in expression between them at baseline or after stimulation (Figure 5-6).

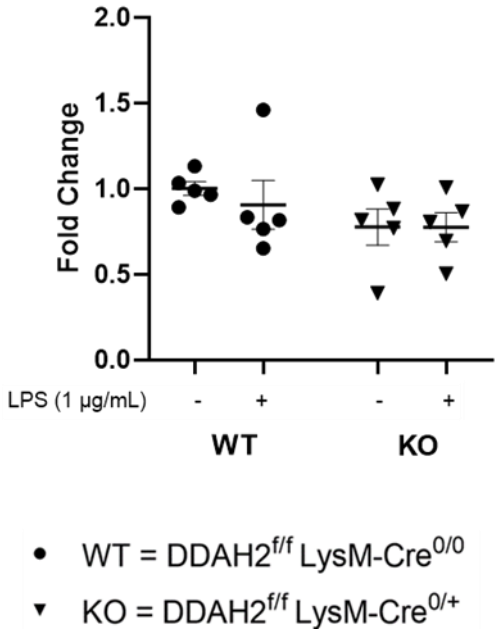

Figure 5-6 DDAH2 does not regulate *Il17a* gene expression in BMDM
Effect of DDAH2 on *Il17a* expression at baseline and in 1µg/mL LPS-stimulated *Ddah2*$^{f/f}$ LysM-Cre$^{0/0}$ and *Ddah2*$^{f/f}$ LysM-Cre$^{0/+}$ for 6 hours. Mean ± SEM. Two-way ANOVA with Tukey post hoc test.

5.5.1 Confirmatory study in C57BL/6J wild-type BMDM

As the change in *Il17a* expression in WT and KO BMDM upon 1 µg/mL LPS stimulation was not statistically significant, the experiment was repeated with ADMA treatment. Wild-type C57BL/6J BMDM were stimulated with 1 µg/mL LPS for 6 hours with or without pretreatment with 100µM ADMA for 1 hour. There was no statistically significant effect on *Il17a* gene expression noted between the different conditions (Figure 5-7).

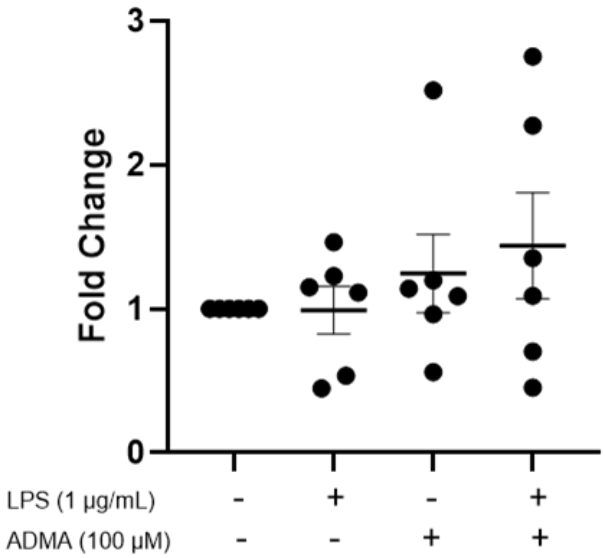

Figure 5-7 ADMA does not alter *Il17a* gene expression in BMDM
Effect of 100 µM ADMA on *IL/7a* gene expression at baseline and in 1µg/mL LPS-stimulated WT C57BL/6J BMDM for 6 hours expressed as fold change. Mean ± SEM. One-way ANOVA with Bonferroni post hoc test.

5.6 Discussion

The project in general aims to elucidate the role of DDAH2 in inflammation with a focus on pathways affected in atherosclerosis. As BMDMs may be closer to atherosclerotic plaque macrophages, this chapter aims to test the hypotheses inferred from the *in silico* analysis and the *in vitro* findings from peritoneal macrophages on BMDMs. Furthermore, the dose of LPS was reduced to a more commonly used dose in BMDM instead of the much higher LPS dose that was used on the peritoneal macrophages in the *in silico* analysis and replicated in its validation.

5.6.1 Brief Summary of chapter findings

From the *in silico* analysis of the RNA sequencing experiment on peritoneal macrophages from the macrophage-specific DDAH2 null mouse model , it was inferred that *Olr1* and *Arg1* are DDAH2-dependent genes. To test that in more closely atherosclerosis-related model, BMDMs from the same knockout model were treated with 1 μg/mL LPS and gene expression was compared across conditions. Furthermore, to confirm the results seen with DDAH2, BMDM from wild-type C57BL/6J were treated with the same dose of LPS with or without pretreatment with 100 μM ADMA. Although both *Olr1* and *Arg1* expression increased statistically significantly in both models in response to LPS stimulation, there was no statistically significantly altered effect due to either knocking DDAH2 out or treating it with ADMA. Therefore, this data demonstrates that, in BMDMs, *Olr1* and *Arg1* expression increased in response to 1 μg/mL LPS stimulation with no altered effect either due to DDAH2 knockdown or pre-treatment with 100 μM ADMA.

From the *in silico* analysis of the RNA sequencing experiment on peritoneal macrophages from the macrophage-specific *Ddah2* null mouse model , we inferred the hypotheses that the apoptosis pathway is highly altered in the absence of DDAH2. To test that in an atherosclerosis-related model, BMDMs from the same knockout model were treated with 1 μg/mL LPS and a selection of apoptosis-related gene expressions was compared across conditions. Furthermore, to relate DDAH2 and ADMA function, BMDM from wild-type C57BL/6J were treated with the same dose of LPS with or without pretreatment with 100 μM ADMA. Although all the selected gene expressions were altered (with varying statistical significance) in both models in response to LPS stimulation, there was no modified effect due to either knocking DDAH2 out or treating the BMDMs with ADMA.

In the previous chapter, the *in silico* analysis showed an effect of DDAH2 on IL-17A expression in peritoneal macrophages stimulated with 10 μg/mL LPS. This was validated *in vitro* by both RT-qPCR and ELISA. However, this was not the case when validating in BMDM from the same macrophage-specific DDAH2 null mouse model upon stimulation with 1 μg/mL LPS, nor did treating ADMA alter the response to LPS treatment in wild-type C57BL/6J BMDM. An interesting

follow up experiment for these findings in BMDM would have been to test IL17A release and compare to results Brobtained from the peritoneal macrophages (section 4.5), however this was not possible in this current project due to time limitations.

5.6.2 DDAH2-dependent genes required for a normal immune response

A large number of DDAH2-dependent genes were identified in the analysis (4.3.5) as they changed there was a statistically significant difference in the WT only and not in the KO upon LPS stimulation i.e. did not change in the absence of DDAH2. This was correlated with previous observations by our research group that the KO animals were more susceptible to infection and thus unable to mount a normal immune response. Therefore, those genes were hypothesised to be DDAH2-dependent and required for a normal immune response. From this large group of genes, two were selected for further investigation.

The first gene that was investigated in a BMDM model was Oxidized low-density lipoprotein receptor 1 (OLR1), which is a macrophage scavenger receptor that plays an important role in atherogenesis (Sharma, Romeo and Mehta, 2022). Previous studies have shown that 100 ng/mL LPS stimulation upregulates OLR1 expression in RAW 264.7 macrophages (Hossain *et al.*, 2015) and BMDM (Nomura *et al.*, 2019) which we confirmed here using 1 µg/mL LPS. However, in contrast to the *in silico* data, no effect of DDAH2 deletion was seen *in vitro*. Also, no effect of ADMA treatment was seen in this study on OLR1 expression. Other studies have seen an up regulatory effect of ADMA on *Olr1* expression, but these were carried out in different cells (macrophages differentiated from HL60) and using lower doses of ADMA than used in this study (Smirnova, Sawamura and Goligorsky, 2004; Smirnova *et al.*, 2004).

The other DDAH2-dependent gene and required for a normal immune response per the *in silico* analysis (4.3.5) which was selected for further investigation was Arginase1 (Arg1). Arg 1 is a critical enzyme in the competing pathway to nitric oxide synthase for the substrate arginine (Rath *et al.*, 2014). Arginase metabolises arginine to ornithine and urea. Since ADMA inhibits nitric oxide synthase (NOS) activity by competing with L-arginine for the catalytic binding

site on NOS, it can be hypothesised that ADMA may also regulate Arginase (Vallance *et al.*, 1992).

Furthermore arginase 1 been detected in atherosclerotic plaques (Khallou-Laschet *et al.*, 2010; Thomas *et al.*, 2007; Trogan *et al.*, 2006). *Arg1* expression has been shown to be stimulated by LPS in murine BMDMs and that was confirmed here (Corraliza *et al.*, 1995). Although some studies show a correlation between elevated ADMA and increased arginase activity (van den Berg, Meurs and Gosens, 2018; El Assar *et al.*, 2016), elevated ADMA has been described in patients with Arg1 deficiency (Huemer *et al.*, 2016). This study showed a trend of decreased *Arg1* expression in response to knocking down DDAH2 or treatment with 100 μM ADMA in LPS-stimulated BMDM. Although the effect was not statistically significant it still maybe biologically relevant.

5.6.3 DDAH2-dependent genes enriched in apoptosis

Apoptosis came up as the top enriched pathway in gene ontology in the *in silico* analysis (3.3.4), therefore there were a lot of genes affected by DDAH2 deletion. To investigate if DDAH2 regulates apoptosis in a more atherosclerosis-relevant model, six of those genes were selected for investigation and gene expression was evaluated in WT and KO BMDM in response to 1 μg/mL LPS stimulation. LPS has been shown to stimulate apoptosis in macrophages (Xaus *et al.*, 2000). Also, modulation of DDAH2 in endothelial cells has been documented to affect apoptosis as measured by annexin V- Fluorescein isothiocyanate (FITC) flow cytometry assay (Jia *et al.*, 2013). Moreover, increased ADMA concentrations in THP-1 macrophages have been shown to induce apoptosis as evaluated using Annexin V-propidium iodide (PI) double staining assay by flow cytometry (Hong *et al.*, 2015).

However, although the data in this project shows *in vitro* alteration of the apoptotic genes in response to LPS stimulation in BMDM which may be suggestive of an LPS effect on apoptosis in BMDM, it does not confirm a cumulative effect. Furthermore there was no statistical significance in the difference between the WT and KO response to LPS stimulation or with pretreatment with ADMA in the wildtype C57BL/6J BMDM.

There are many factors that may have played a role in the difference between the *in silico* and *in vitro* data. The difference in cell type (which will be elaborated on in 6.4.3), the difference in LPS dose used and the small changes in the Log_2 fold change of those genes *in silico* which is a factor that may be associated with less concordance (as discussed in section 4.6).

Since there were many genes in the apoptosis pathway affected by DDAH2 deletion in the *in silico* analysis with the majority having very small changes, each gene alone may be difficult to detect *in vitro* but there may be a cumulative effect on the whole pathway. Perhaps a better way to test this would have been to look at the degree of apoptosis in WT and KO cells rather than individuals points in the pathway for example by measuring the difference in DNA fragmentation using a terminal deoxynucleotidyl transferase dUTP nick-end labeling (TUNEL) assay (Huan *et al.*, 2021). More detailed assays can also be used such as flow cytometry detection of apoptosis proteins and specific Caspase Activity (Ludwig, Maxcy and LaBelle, 2019). However, in this current project time constraints were a limiting challenge in that aspect.

Although the *in vitro* data in this chapter did not show an effect of DDAH2 on apoptosis, the combination of evidence in the literature that LPS-induced early apoptosis in BMDMs occurs through TNFα activation (Jia *et al.*, 2013) and the *in silico* analysis in this project on peritoneal macrophages both flagging apoptosis as the top pathway affected by DDAH2 deletion and showing a decrease in TNFα expression when comparing LPS-stimulated KO vs. LPS-stimulated WT by a 1.99 log_2 fold change (p-adj 3.2E-10) are encouraging factors to follow up in the future.

5.7 Chapter Summary

This chapter aimed to validate hypotheses inferred from the RNA sequencing experiment on peritoneal macrophages as analysed in chapter 4, in BMDMs extracted from a macrophage-specific *Ddah2* null mouse model. This included the validation of DDAH2-dependent genes required for a normal immune response, DDAH2-dependent genes that play a role in foam cell formation and the expression of *Il17a* using RT-qPCR. However, the *in vitro* analysis showed no conclusive evidence that DDAH2 regulates any of the investigated genes in

BMDMs nor does treating with ADMA alter the gene response to LPS. This may be partially explained by differences between the two models from which the hypotheses were inferred and validated.

Chapter 6 General Discussion

6.1 Introduction

Dimethylarginine dimethylaminohydrolase 2 (DDAH2) is the dimethylarginine dimethylaminohydrolase (DDAH) isoform present in macrophages, which has a major role in the development and progress of atherosclerosis. Several studies on dimethylarginine dimethylaminohydrolase 2 (DDAH2) genetic variants have shown evidence of different DDAH variants with evidence of an inverse relationship between DDAH activity and ADMA levels (Jones *et al.*, 2003; O'Dwyer *et al.*, 2006; Andreozzi *et al.*, 2012). Furthermore, DDAH2 knockout mice have demonstrated increased ADMA levels (Lambden *et al.*, 2015), while DDAH2-overexpressing models were associated with decreased ADMA levels (Zhu *et al.*, 2019) and resistance to exogenous-ADMA induced-hypertension (Hasegawa *et al.*, 2007). As DDAH2 is the isoform expressed in the immune system and ADMA is a competitive inhibitor of nitric oxide, this suggests that DDAH2 regulates nitric oxide (NO) production in the immune system through ADMA hydrolysis. Therefore, the knockdown of DDAH2 in macrophages reduces NO production and alters the immune response. On the other hand, DDAH2 has been shown to have roles beyond ADMA hydrolysis and that it affects cellular functions in a NO-independent manner, such as the association of different variants with diabetes through its interaction with the transcription factor Kruppel-like factor 9 (KLF9) or the activation of secretagogin expression (Chen *et al.*, 2022; Seo *et al.*, 2012; Hasegawa *et al.*, 2013). Moreover, research in our group has shown the importance of DDAH2 for macrophage functions such as motility and phagocytic ability (Ahmetaj-Shala, 2013).

6.2 Thesis aims

The starting part of this thesis was to expand on the hypothesis that DDAH2 is a regulator of macrophage NO and the inflammatory response. The aims set to test this hypothesis were:

1. Validate the suitability of using the murine cell line (RAW 264.7) and bone marrow-derived macrophages as a model to study the role of DDAH2 in inflammation.

2. Re-produce a macrophage-specific DDAH2 null mouse model, characterise its genotype and phenotype, and use it as an *in vitro* model to study the role of DDAH2 in inflammation.

3. Identify DDAH2-dependent genes and pathways involved in atherosclerosis from RNA sequencing data on peritoneal macrophages and validate the *in silico* findings *in vitro*.

4. Investigate and validate hypotheses from the *in silico* data in a bone marrow-derived macrophages (BMDM) model.

6.3 Summary of salient findings

These aims have been tested in the presented results chapters, and the key findings are:

1. The candidate models to study the role of DDAH2 in inflammation, the mouse cell line 264.7 and BMDM, have been confirmed to be suitable for the project as they express the critical genes in the DDAH-ADMA-NOS pathway and respond to LPS stimulation (figures 3-2, 3-5, 3-16 and 3-17).

2. RAW 264.7 cells express iNOS gene and protein in response to LPS (Figure 3-4), and the sensitivity to ADMA is arginine-dependent (Figure 3-8).

3. In line with previous literature, mRNA expression of the candidate genes *Ddah2*, *eNOS* and *iNOS* (Figure 3-16), the response to LPS activation, the inhibitory effect of ADMA (Figure 3-17), and iNOS protein expression in BMDM were validated (Figure 3-19). Also, this study extends to confirm the expression of DDAH2 protein in BMDM by western blot (figure 3-18).

4. In line with previous literature, this study shows the positive effect of pyruvate on BMDM differentiation (Figure 3-12). Further, it extends this finding by quantifying the increased yield (Figure 3-13), which was highly statistically significant and validated the phenotype of the surplus cells by flow cytometry (Figure 3-14).

5. The Leiper novel macrophage-specific DDAH2 null mouse model was rederived (Figure 3-20). In line with previous observations using this approach, this study shows a significant decrease in *Ddah2* in peritoneal macrophages at the mRNA level (Figure 3-21.B). This study extends these findings to show that this approach also reduces DDAH2 in BMDMs at the mRNA level (Figure 3-21.A) and, for the first time, also shows its decrease at the protein level (Figure 3-22). Also, this study shows for the first time the ability of Cre to delete DDAH2 in these cells at both the mRNA and protein levels (Figures 3-21.A and 3-22). Therefore, this study demonstrates that and establishes this mouse as a suitable model to look at the role of DDAH2 in circulating immune cells.

6. Splenomegaly was a striking phenotype observed in the macrophage-specific *Ddah2* null mouse model in the KO mice, suggesting evidence of an immune-regulatory role for DDAH2 (Figure 3-24).

7. The RNA Sequencing experiment conducted on samples from the original model nearly ten years ago was reanalysed (Figures 4-2 to 4-7 and Tables 4-1 to 4-3) and then validated by RT-qPCR and showed a degree of concordance similar to that shown in previous literature. The *in silico* analysis suggests a role for DDAH2 in regulating *Cxcl1, Cxcl2, Ccrl2, Il6 and Il1b* (Table 4-4). However, this was not reproducible *in vitro* (Figures 4-8 and 4-9).

8. In line with previous literature, this study shows the expression of IL17A by peritoneal macrophages and further extends this finding to suggest a role for DDAH2 in regulating IL17A (Table 4-4 and Figures 4-9 and 4-10).

9. From the *in silico* analysis on peritoneal macrophages, it was inferred that *Olr1* and *Arg1* are DDAH2-dependent genes (Table 5-1). However, *in vitro* in BMDMs, *Olr1* and *Arg1* expression increased in response to 1 µg/mL LPS stimulation with no altered effect due to DDAH2 knockdown or pre-treatment with 100 µM ADMA (Figures 5-1 and 5-2).

10. From the *in silico* analysis on peritoneal macrophages, it was inferred that the apoptosis pathway is highly altered in the absence of DDAH2 (Table 5-

2). In BMDM, all the selected gene expressions were altered in response to LPS stimulation, but there was no modified effect due to either knocking DDAH2 out or treating it with ADMA (Figures 5-3 to 5-5).

11. No evidence of a role for DDAH2 in regulating *Il17a* gene expression was seen in BMDMs (Figures 5-6 and 5-7).

6.4 Thesis insights and implications

The individual results chapters contain a discussion of the specific results presented in those chapters, and it is not the intention to repeat those discussions here. The purpose of this general discussion is to discuss the overall findings of this thesis in the context of the previously published research, to illustrate areas where novel findings have been made, and to discuss their implications.

6.4.1 The *in silico* analysis indicates that a substantial number of genes are regulated by DDAH2

In the *in silico* analysis of this project, DDAH2 was found to regulate a large number of genes. Although it may be surprising that DDAH2 regulates such a large number of genes as its functions have been controversial and still being under investigation, nitric oxide has been described as a potent second messenger (Antosova *et al.*, 2012; Kerwin, Lancaster and Feldman, 1995; Murad, 2011). If we think of DDAH2 regulating nitric oxide synthase and the critical role NO has been demonstrated to have in the inflammatory response, then maybe it is not as surprising (Clancy and Abramson, 1995; Lambden, 2019; Sharma, Al-Omran and Parvathy, 2007). It is plausible that many of the gene changes are due to a NO-related response. On the other hand, some people have questioned whether DDAH2 regulates NO at all (Altmann *et al.*, 2012; Ragavan *et al.*, 2023). If these effects were completely independent of NO, it would make the ability of DDAH2 to regulate thousands of genes even more surprising. So maybe this data indirectly supports that DDAH2 works, at least in part through NO.

Those genes regulated by DDAH2 fall into many categories. Some of those genes are known targets for nitric oxide. So, it is plausible from the evidence in this project that DDAH2 is working through NO because it regulates genes known to

be NO-dependent. One example is the transcription factor NF-κB, which upregulates iNOS leading to the production of NO, the released NO inhibits the NF-κB pathway by altering its DNA binding activity to iNOS (Colasanti and Persichini, 2000; Matthews *et al.*, 1996; Moormann, Koenig and Meshnick, 1996). Furthermore, a potential binding site has been identified for NF-κB on the DDAH2 promotor (Li, Sun and Li, 2021). The acetylation of NF-κB has been associated with increased binding ability and a subsequent increase in DDAH2 promotor activity and DDAH2 upregulation (Li, Sun and Li, 2021).

Furthermore, within the literature, other researchers have shown that changing DDAH2 can regulate the expression levels of certain genes, some of which look like they are NO-dependent, such as evidence presented towards the role of DDAH2 in the regulation of viral immunity in a NO-dependent mechanism (Huang *et al.*, 2021). By using a combination of genetic modification techniques and the iNOS inhibitor N-(3-(Aminomethyl)benzyl)acetamidine (1400W), Huang *et al.* demonstrated evidence of viral infection leading to stimulation of RIG-I-like receptor (RLR)-signalling subsequently leading to the translocation of DDAH2 from the cytosol to mitochondria and resulting in increased NO production (Huang *et al.*, 2021).The NO messenger activated dynamin-related protein 1 (DRP1) which increased mitochondrial fission thus blocking mitochondrial anti-viral signalling (MAVS) aggregation which is necessary for subsequent signalling and continuation of the viral response (Huang *et al.*, 2021).

6.4.2 Inflammation regulation is a crucial function of DDAH2

Another exciting point demonstrated in this project is that many of the top differentially expressed genes, when looking at the effect of DDAH2 deletion at baseline and after LPS stimulation, are genes involved in inflammation and the immune response. Previously, our group demonstrated that the top pathway affected by DDAH2 deletion at baseline is the inflammatory pathway (Ahmetaj-Shala, 2013). In this project, when looking at the top pathway affected by DDAH2-dependent genes per the described analysis, it was the apoptotic pathway. Apoptosis is a method of controlled cell death to modulate the cell's response, and many of the genes functioning in apoptosis have inflammatory non-classic functions, such as caspases (Van Opdenbosch and Lamkanfi, 2019). The finding of altered inflammatory genes is not unexpected because we looked

at the difference in the cell's response to an inflammatory stimulus, so we, in a way, biased it towards that.

As mentioned, that is not really surprising, but it is also consistent with the fact that the *Ddah2* gene is localised in the MHC-III Locus. Several genes involved in inflammation are located in the locus, also called the "inflammatory region", including the tumour necrosis factor family and complement cascades (Deakin *et al.*, 2006). Variants in the MHC class III region have also been linked to autoimmune diseases such as systemic lupus erythematosus and multiple sclerosis (Fernando *et al.*, 2007; Morris *et al.*, 2012; Patsopoulos *et al.*, 2013).

Some pathways such as apoptosis are not classical inflammatory pathways that it seems to regulate, and that was perhaps an unexpected finding. Moreover, there may be other NO-independent mechanisms by which DDAH2 regulates these pathways. For example, recently our group has shown in a study on adipocytes that ADMA at pathophysiological concentrations can function in a NO-independent mechanism, mediated through the Calcium sensing receptor (CaSR) (Dowsett *et al.*, 2023). CaSR is universally expressed in many cell types including myeloid cells (Thrum *et al.*, 2022; Yamaguchi *et al.*, 1998). Furthermore, CaSR has been implicated in the development of inflammatory diseases including atherosclerosis (Malecki *et al.*, 2013). This may be another potential NO-independent mechanism by which DDAH2 might regulate these genes.

6.4.3 Unmasking the uniqueness: bone marrow-derived vs. peritoneal macrophages

An equally interesting finding in this project was how some of the data from the *in silico* analysis could not be validated *in vitro*. Factors regarding gene concordance when validating in the same cell type were discussed in the relevant chapter. Here, I wanted to look closer at the section of the project (chapter 5) where the *in silico* data was generated in peritoneal macrophages (a resident macrophage model) and the *in vitro* validation of the inferred hypotheses via qPCR was tested on Bone marrow-derived macrophages (a more naïve form of macrophages). This decision was made due to the availability of the *in silico* analysis from the same mouse model in conjunction with the aim to test the hypotheses in an atherosclerosis-related model.

However, differences between the two macrophage cell types have been documented and were expected. Moreover, the dose of LPS used in the *in silico* analysis was 10 µg/mL, aiming to achieve maximal stimulation and simulate a septic environment. However, it was reduced to 1 µg/mL in BMDM, as a lower grade of inflammation is expected in an atherosclerotic environment.

Although this project does not aim specifically to compare peritoneal macrophages to BMDM, a discussion and an overview here of the documented differences in the literature may help explain some of the results obtained *in vitro* using BMDM, in addition to the factors influencing gene concordance (Everaert *et al.*, 2017) and the LPS dose used. In the reviewed studies, which will be compared below, the different mouse strains used and variations in isolation methods of the peritoneal macrophages or differentiation of BMDM might influence the differences between the studies and render pooling them more complex. However, they all show a final consensus of difference between peritoneal and bone marrow-derived macrophages. Different isolation or differentiation methods and stimulatory factors will be highlighted as possible.

BMDMs are commonly differentiated *in vitro* using M-CSF or L-929 conditioned media. Peritoneal macrophages may be extracted directly from peritoneal exudate or by first injecting the mice with thioglycolate to increase the yield (elicited peritoneal macrophages) (Misharin, Saber and Perlman, 2012). In flow cytometry, M-CSF-differentiated BMDM were more clustered in their size and granularity, forming one population. Meanwhile, peritoneal macrophages had at least two populations (Zhao *et al.*, 2017). However, L-929-differentiated BMDM showed two populations almost overlapping with those formed by post-adherent elicited peritoneal macrophages (Zajd *et al.*, 2020). The increased homogeneity seen in M-CSF differentiated BMDM may be attributed to its purity, while L-929 media contains other factors besides M-CSF. Also, elicited peritoneal cells have been documented to be contaminated by other cells (Misharin, Saber and Perlman, 2012), which may be removed from the population by selective adhesion (Zajd *et al.*, 2020) or depletion by sorting (Misharin, Saber and Perlman, 2012).

MHC-II and cluster of differentiation 86 (CD86), which are co-stimulatory molecules usually expressed on the surface of fully functioning macrophages,

were found to be more highly expressed in peritoneal macrophages than BMDM (Wang *et al.*, 2013; Zhao *et al.*, 2017). Thus, peritoneal macrophages were described as more mature than BMDMs, which aligns with their *in vivo* maturation (Wang *et al.*, 2013).

The comparison of surface marker expression and polarisation markers was complicated by the variety of markers tested, strain background and isolation technique. However, the cumulative phenotype at steady state for M-CSF-differentiated BMDM was M2 skewed (Zhao *et al.*, 2017; Wang *et al.*, 2013), while L929 differentiated was M1 skewed (Zajd *et al.*, 2020). Although those studies did not each include both types of differentiation, they are backed up by studies supporting that differentiation using M-CSF results in skewing towards an M2 phenotype (Fleetwood *et al.*, 2007). On an mRNA level, Bisgaard et al. showed M2-skewed supportive evidence for M-CSF differentiated BMDM. However, peritoneal macrophages showed an overall increased expression of all markers rather than a distinctive M1/M2 profile (Bisgaard *et al.*, 2016). This data again supports inherent differences between BMDM and peritoneal macrophages.

Functional studies have shown that M-CSF and L929-differentiated BMDMs were more phagocytic than peritoneal macrophages (elicited or not) (Wang *et al.*, 2013; Zajd *et al.*, 2020), while Hu et al. demonstrated a higher phagocytic ability in peritoneal macrophages than GM-CSF-differentiated BMDM (Hu *et al.*, 2012). This highlights again the differences between the different cell types and differentiation methods.

Interestingly BMDM and peritoneal macrophages have been shown to express similar mRNA expression levels of TNF-α during rest and respond similarly to each other to a variety of stimuli such as LPS only, LPS and IFNy or IL-4 (Wang *et al.*, 2013; Zajd *et al.*, 2020; Zhao *et al.*, 2017). On the other hand, Bisgaard et al. showed that in response to 25 μg/mL oxLDL stimulation for 24 hours, TNF-α levels decreased only in peritoneal macrophages and not BMDM (Bisgaard *et al.*, 2016). That raises the question, could DDAH2 knockdown cause a different response with respect to TNF- α levels between peritoneal and BMDMs? Moreover, could that explain the other gene profiles? TNF-α mRNA levels were not measured during this project and would be an interesting lead to follow up. Especially as mentioned in (section 5.6.2), previous evidence has shown that

LPS-induced early apoptosis in BMDMs occurs through TNFα activation (Jia *et al.*, 2013).

It would be interesting to have a general comparative study between the two cell types within our model, specifically looking at the baseline expression level of DDAH2 per cell type, as that may affect the functional result of DDAH2 knockout under the same experimental conditions.

As for choosing the best model to study atherosclerosis in general, each has its advantages. Although less responsive to *in vitro* stimulation, peritoneal macrophages would have already been modified in response to the environment, which has its advantage, especially in a gene knockout model. BMDMs, on the other hand, have a much higher yield and, although they did not mature under the "gene knock-out" effect, can be helpful in mechanistic studies due to their higher responsiveness. Notably, one needs to remember the high plasticity of macrophages, heterogeneity of cells and stimuli *in vivo* and evidence of atherosclerotic plaques expressing a mixture of M1 and M2 markers (Bisgaard *et al.*, 2016).

Macrophages in plaques are circulating macrophages that have been stimulated to home to the plaque and transmigrate, and then they have been stimulated by the environment of the plaque. So again, there are reasons to think why a plaque macrophage may have acquired a phenotype that is somewhat distinct from either BMDM or peritoneal macrophages.

6.4.4 DDAH2 regulates IL17A production in peritoneal macrophages

This project has also confirmed, in line with previous literature, the production of IL17A by peritoneal macrophages and extended this finding to suggest a role for DDAH2 in regulating IL17A. To our knowledge, this is the first time this connection has been reported. Although there have been reports of IL17A being produced in peritoneal macrophages (details in chapter 4), generally, in literature, peritoneal macrophages are more described as responders rather than producers of IL17A (Cua and Tato, 2010). Therefore, peritoneal macrophages

may be a vital source of IL17A in peritonitis, and targeting DDAH2 to regulate it can be a valuable therapeutic strategy to investigate further.

Anti-IL17A therapy is already in motion for other inflammatory disorders. One example is secukinumab, approved by The Medicines and Healthcare Products Regulatory Agency (MHRA) and The Food and Drug Administration (FDA) as an anti-IL17A treatment for psoriasis (Papp *et al.*, 2013; Rich *et al.*, 2013). Psoriasis is a chronic systemic inflammatory disorder associated with cardiovascular disease, including atherosclerosis (Balci *et al.*, 2008). Interestingly, Elnabawi *et al.*, in a prospective observational study, showed that treating psoriasis with anti-IL-7a was associated with reduced plaque formation (Elnabawi *et al.*, 2019). Rheumatoid arthritis is a chronic inflammatory autoimmune disease where increased IL17A has been connected with increased bone damage and cardiovascular events (Robert *et al.*, 2020) and the effects of different anti-IL17A biologic treatments is under investigation (Chao *et al.*, 2011; Qi *et al.*, 2012). IL17A biologic treatments are also being trialled in systemic lupus erythematosus (SLE) with positive therapeutic indications (Costa *et al.*, 2021; Koriyama *et al.*, 2020; Li *et al.*, 2015). Interestingly, the downregulation of DDAH2 has been described in psoriatic skin lesions (Roberson *et al.*, 2012). This association may be a plausible indicator that IL17A may mediate psoriasis inflammation.

Furthermore, peritonitis affects many people. Spontaneous bacterial peritonitis, for example, occurs frequently in patients with cirrhosis and greatly increases morbidity (Marciano *et al.*, 2019), and sterile peritonitis occurs commonly in patients on peritoneal dialysis (Brown *et al.*, 2011; de Freitas and Gokal, 2005). Ageing increases the risk of peritonitis in dialysis patients (Gadola *et al.*, 2019; Wu *et al.*, 2020). IL17A plays a pivotal role in inflammatory damage in dialysis patients, and anti-IL17A has been suggested as a therapeutic target (Marchant *et al.*, 2020; Rodrigues-Díez *et al.*, 2014). Thus, a deeper understanding of the regulatory role of DDAH2 of IL17A may provide insight into the effect of DDAH2 in peritonitis.

The data in this project and other literature have shown the production of IL17A by resident peritoneal macrophages, and IL17A has been implicated in damage

occurring in peritonitis. IL17A produced by other resident macrophages may play a role in inflammation occurring in other anatomical sites, such as myocarditis.

6.5 Future perspectives

Looking ahead, there are several intriguing avenues for further exploration. It would be beneficial to investigate IL17A neutralising approaches in models of peritonitis, which could provide valuable insights into the therapeutic potentials of these approaches. Furthermore, the generality of the observation that DDAH2 regulates IL17A warrants investigation across multiple tissues. This could help us understand the broader implications of DDAH2's regulatory role. Lastly, to ensure the relevance and applicability of the findings in this thesis, it is crucial to validate the project outcomes in human peritoneal macrophages. This step will bridge the gap between this research and its potential clinical implications.

6.6 Summary

The enzyme Dimethylarginine dimethylaminohydrolase 2 (DDAH2) is the DDAH isoform found in macrophages. Studies suggest that DDAH2 plays a role in the hydrolysis of ADMA, a competitive inhibitor of nitric oxide. This suggests that DDAH2 could regulate the production of nitric oxide (NO) in the immune system via ADMA hydrolysis. On the other hand, DDAH2 has been shown to have roles beyond ADMA hydrolysis and to affect cellular functions in a NO-independent manner.

This thesis initially aimed to explore the role of DDAH2 in regulating NO production and inflammation in experimental atherosclerosis, using a combination of *in vitro* and *in vivo* studies in a macrophage-specific *Ddah2* null mouse model with atherosclerosis. However, due to the Covid-19 pandemic, this work was halted. To make the best use of available resources and time, the focus shifted to reanalysing RNA sequencing data previously produced by our group, rederiving the macrophage-specific *Ddah2* null mouse model, and conducting *in vitro* studies using a combination of cell lines and primary cells.

The suggested models were validated for the study of the DDAH-ADMA-NOS pathway. ADMA, as expected, inhibited the enzymatic activity of iNOS, and the inhibition was arginine-dependent. The previously documented positive effect of pyruvate on BMDM differentiation was reproduced and further extended by quantification of the increased yield and validation of the phenotype of the surplus cells. The Leiper macrophage-specific *Ddah2* null mouse model was successfully re-derived and validated. This model's validation was extended beyond our group's previous observations by showing a reduction of DDAH2 expression in BMDMs at the mRNA and protein levels. The RNA Sequencing experiment was reanalysed and then validated by RT-qPCR in peritoneal macrophages. Not all the investigated results suggested by the *in silico* data were reproducible *in vitro* in peritoneal and BMDMs. However, both RT-qPCR and ELISA validated the *in silico*-suggested role of DDAH2 in regulating IL17A production in peritoneal macrophages (Figure 6-1).

This study demonstrates that DDAH2 has important cellular regulatory functions and is a potential therapeutic target for inflammatory diseases. As targeting IL-17A is a current therapeutic modality in inflammatory diseases, exploring extending its use in atherosclerosis treatment is compelling.

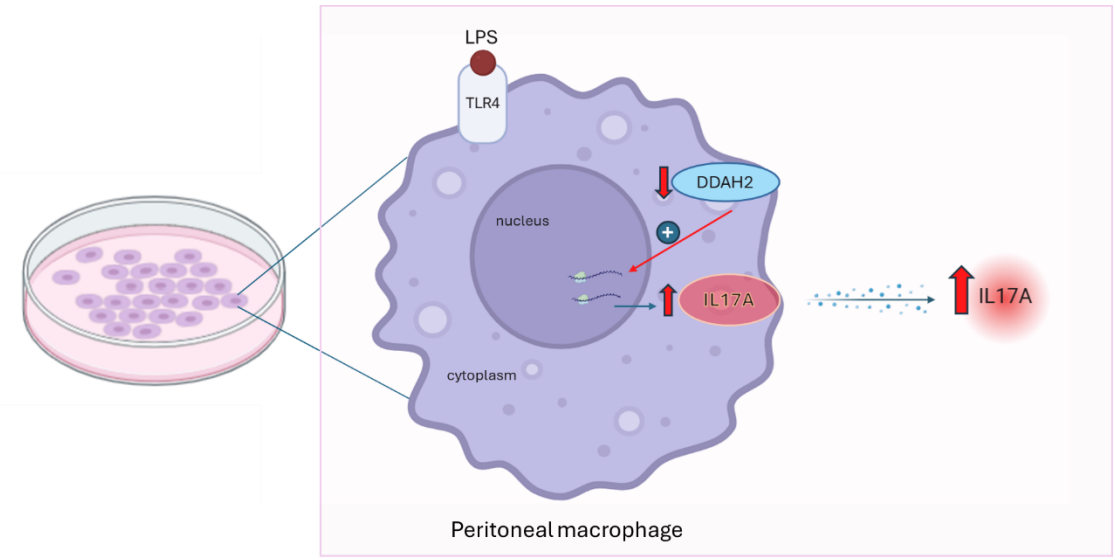

Figure 6-1 DDAH2 has an inhibitory role in the regulation of IL17A release in LPS-stimulated peritoneal macrophages

The knockdown of DDAH2 leads to increased expression of the *Il17a* gene and increased release of IL17A into the culture media. The illustration was created with BioRender.com.

List of References

Abdelouhab, K., Rafa, H., Toumi, R., Bouaziz, S., Medjeber, O. and Touil-Boukoffa, C. (2012) 'Mucosal intestinal alteration in experimental colitis correlates with nitric oxide production by peritoneal macrophages: effect of probiotics and prebiotics', *Immunopharmacol Immunotoxicol,* 34(4), pp. 590-7.

Abdolmaleki, F., Gheibi Hayat, S. M., Bianconi, V., Johnston, T. P. and Sahebkar, A. (2019) 'Atherosclerosis and immunity: A perspective', *Trends in Cardiovascular Medicine,* 29(6), pp. 363-371.

Abhary, S., Burdon, K. P., Kuot, A., Javadiyan, S., Whiting, M. J., Kasmeridis, N., Petrovsky, N. and Craig, J. E. (2010) 'Sequence variation in DDAH1 and DDAH2 genes is strongly and additively associated with serum ADMA concentrations in individuals with type 2 diabetes', *PLoS One,* 5(3), pp. e9462.

Ahmetaj-Shala, B. (2013) *The Role of Nitric Oxide Synthase Inhibitors on Macrophage Function.* Ph.D. Thesis, Kingston University with collaboration at Imperial College London.

Alexopoulou, L., Holt, A. C., Medzhitov, R. and Flavell, R. A. (2001) 'Recognition of double-stranded RNA and activation of NF-κB by Toll-like receptor 3', *Nature,* 413(6857), pp. 732-738.

Allahverdian, S., Chehroudi, A. C., McManus, B. M., Abraham, T. and Francis, G. A. (2014) 'Contribution of intimal smooth muscle cells to cholesterol accumulation and macrophage-like cells in human atherosclerosis', *Circulation,* 129(15), pp. 1551-1559.

Altmann, K. S., Havemeyer, A., Beitz, E. and Clement, B. J. C. V. (2012) 'Dimethylarginine-Dimethylaminohydrolase-2 (DDAH-2) Does Not Metabolize Methylarginines', (17), pp. 2599-2604.

Amir, M., Hassanein, S. I., Abdel Rahman, M. F. and Gad, M. Z. (2018) 'AGXT2 and DDAH-1 genetic variants are highly correlated with serum ADMA and SDMA levels and with incidence of coronary artery disease in Egyptians', *Molecular biology reports,* 45(6), pp. 2411-2419.

Anderssohn, M., Rosenberg, M., Schwedhelm, E., Zugck, C., Lutz, M., Lüneburg, N., Frey, N. and Böger, R. H. J. J. o. c. f. (2012) 'The L-arginine–asymmetric dimethylarginine ratio is an independent predictor of mortality in dilated cardiomyopathy', 18(12), pp. 904-911.

Andreozzi, F., Presta, I., Mannino, G. C., Scarpelli, D., Di Silvestre, S., Di Pietro, N., Succurro, E., Sciacqua, A., Pandolfi, A., Consoli, A., Hribal, M. L., Perticone, F. and Sesti, G. (2012) 'A Functional Variant of the Dimethylarginine Dimethylaminohydrolase-2 Gene Is Associated with Insulin Sensitivity', *PLOS ONE,* 7(4), pp. e36224.

Antoniades, C., Shirodaria, C., Leeson, P., Antonopoulos, A., Warrick, N., Van-Assche, T., Cunnington, C., Tousoulis, D., Pillai, R., Ratnatunga, C., Stefanadis, C. and Channon, K. M. (2009) 'Association of plasma asymmetrical dimethylarginine (ADMA) with elevated vascular superoxide production and endothelial nitric oxide synthase uncoupling: implications for endothelial function in human atherosclerosis', *European Heart Journal,* 30(9), pp. 1142-1150.

Antosova, M., Plevkova, J., Strapkova, A. and Buday, T. (2012) 'Nitric oxide¡ªImportant messenger in human body', *Open Journal of Molecular and Integrative Physiology,* Vol.02No.03, pp. 9.

Anzinger, J. J., Chang, J., Xu, Q., Barthwal, M. K., Bohnacker, T., Wymann, M. P. and Kruth, H. S. (2012) 'Murine bone marrow-derived macrophages differentiated with GM-CSF become foam cells by PI3Kγ-dependent fluid-phase pinocytosis of native LDL', *J Lipid Res,* 53(1), pp. 34-42.

Argmann, C. A. and Auwerx, J. (2006) 'Collection of Blood and Plasma from the Mouse', *Current Protocols in Molecular Biology,* 75(1), pp. 29A.3.1-29A.3.4.

Arrigoni, F., Ahmetaj, B. and Leiper, J. (2010) 'The biology and therapeutic potential of the DDAH/ADMA pathway', *Current pharmaceutical design,* 16(37), pp. 4089-4102.

Auffray, C., Fogg, D., Garfa, M., Elain, G., Join-Lambert, O., Kayal, S., Sarnacki, S., Cumano, A., Lauvau, G. and Geissmann, F. (2007) 'Monitoring of blood vessels and tissues by a population of monocytes with patrolling behavior', *Science,* 317(5838), pp. 666-670.

Averta, C., Mancuso, E., Spiga, R., Miceli, S., Succurro, E., Fiorentino, T. V., Perticone, M., Mannino, G. C., Thamtarana, P. J. and Sciacqua, A. (2022) 'The Functional Polymorphism of DDAH2 rs9267551 Is an Independent Determinant of Arterial Stiffness', *Frontiers in Cardiovascular Medicine,* 8, pp. 811431.

Babamale, A. O. and Chen, S.-T. (2021) 'Nod-like receptors: critical intracellular sensors for host protection and cell death in microbial and parasitic infections', *International Journal of Molecular Sciences,* 22(21), pp. 11398.

Babu, B. R. and Griffith, O. W. J. C. o. i. c. b. (1998) 'Design of isoform-selective inhibitors of nitric oxide synthase', 2(4), pp. 491-500.

Bahadoran, Z., Norouzirad, R., Mirmiran, P., Gaeini, Z., Jeddi, S., Shokri, M., Azizi, F. and Ghasemi, A. (2021) 'Effect of inorganic nitrate on metabolic parameters in patients with type 2 diabetes: A 24-week randomized double-blind placebo-controlled clinical trial', *Nitric Oxide,* 107, pp. 58-65.

Bailey, J. D., Shaw, A., McNeill, E., Nicol, T., Diotallevi, M., Chuaiphichai, S., Patel, J., Hale, A., Channon, K. M. and Crabtree, M. J. (2020) 'Isolation and culture of murine bone marrow-derived macrophages for nitric oxide and redox biology', *Nitric Oxide,* 100-101, pp. 17-29.

Balci, D., Balci, A., Karazincir, S., Ucar, E., Iyigun, U., Yalcin, F., Seyfeli, E., Inandi, T. and Egilmez, E. (2008) 'Increased carotid artery intima-media thickness and impaired endothelial function in psoriasis', *Journal of the European Academy of Dermatology and Venereology: JEADV,* 23(1), pp. 1-6.

Barish, G. D., Atkins, A. R., Downes, M., Olson, P., Chong, L.-W., Nelson, M., Zou, Y., Hwang, H., Kang, H. and Curtiss, L. (2008) 'PPARδ regulates multiple proinflammatory pathways to suppress atherosclerosis', *Proceedings of the National Academy of Sciences,* 105(11), pp. 4271-4276.

Bedford, M. T. and Richard, S. J. M. c. (2005) 'Arginine methylation: an emerging regulatorof protein function', 18(3), pp. 263-272.

Benjamin, E. J., Muntner, P., Alonso, A., Bittencourt, M. S., Callaway, C. W., Carson, A. P., Chamberlain, A. M., Chang, A. R., Cheng, S., Das, S. R., Delling, F. N., Djousse, L., Elkind, M. S. V., Ferguson, J. F., Fornage, M., Jordan, L. C., Khan, S. S., Kissela, B. M., Knutson, K. L., Kwan, T. W., Lackland, D. T., Lewis, T. T., Lichtman, J. H., Longenecker, C. T., Loop, M. S., Lutsey, P. L., Martin, S. S., Matsushita, K., Moran, A. E., Mussolino, M. E., O'Flaherty, M., Pandey, A., Perak, A. M., Rosamond, W. D., Roth, G. A., Sampson, U. K. A., Satou, G. M., Schroeder, E. B., Shah, S. H., Spartano, N. L., Stokes, A., Tirschwell, D. L., Tsao, C. W., Turakhia, M. P., VanWagner, L. B., Wilkins, J. T., Wong, S. S. and Virani, S. S. (2019) 'Heart Disease and Stroke Statistics—2019 Update: A Report From the American Heart Association', *Circulation,* 139(10), pp. e56-e528.

Benjamin, N., O'Driscoll, F., Dougall, H., Duncan, C., Smith, L., Golden, M. and McKenzie, H. (1994) 'Stomach NO synthesis', *Nature,* 368(6471), pp. 502-502.

Bi, Y., Chen, J., Hu, F., Liu, J., Li, M. and Zhao, L. (2019) 'M2 macrophages as a potential target for antiatherosclerosis treatment', *Neural plasticity,* 2019.

Bisgaard, L. S., Mogensen, C. K., Rosendahl, A., Cucak, H., Nielsen, L. B., Rasmussen, S. E. and Pedersen, T. X. (2016) 'Bone marrow-derived and peritoneal macrophages have different inflammatory response to oxLDL and M1/M2 marker expression–implications for atherosclerosis research', *Scientific reports,* 6(1), pp. 35234.

Bobryshev, Y. V. (2010) 'Dendritic cells and their role in atherogenesis', *Laboratory Investigation,* 90(7), pp. 970-984.

Boger, R., Mallamaci, F., Benedetto, F., Malatino, L., Cataliotti, A., Bellanuova, I., Bode-Boger, S. and Zoccali, C. 'Asymmetric dimethylarginine (ADMA): An endogenous inhibitor of NO synthase predicts mortality in patients with end-stage renal disease'. *Circulation*: LIPPINCOTT WILLIAMS & WILKINS 530 WALNUT ST, PHILADELPHIA, PA 19106-3621 USA, 179-179.

Bots, M. L., Hofman, A., De Jong, P. T. and Grobbee, D. E. (1996) 'Common carotid intima-media thickness as an indicator of atherosclerosis at other sites of the carotid artery the Rotterdam Study', *Annals of epidemiology,* 6(2), pp. 147-153.

Bredt, D. S., Hwang, P. M. and Snyder, S. H. (1990) 'Localization of nitric oxide synthase indicating a neural role for nitric oxide', *Nature,* 347(6295), pp. 768-770.

Bredt, D. S. and Snyder, S. H. (1990) 'Isolation of nitric oxide synthetase, a calmodulin-requiring enzyme', *Proceedings of the National Academy of Sciences,* 87(2), pp. 682-685.

Brochériou, I., Maouche, S., Durand, H., Braunersreuther, V., Le Naour, G., Gratchev, A., Koskas, F., Mach, F., Kzhyshkowska, J. and Ninio, E. (2011) 'Antagonistic regulation of macrophage phenotype by M-CSF and GM-CSF: implication in atherosclerosis', *Atherosclerosis,* 214(2), pp. 316-324.

Brown, M. C., Simpson, K., Kerssens, J. J. and Registry, R. A. (2011) 'Peritoneal dialysis–associated peritonitis rates and outcomes in a national cohort are not improving in the post-millennium (2000–2007)', *Peritoneal Dialysis International,* 31(6), pp. 639-650.

Busse, R. and Mülsch, A. (1990) 'Calcium-dependent nitric oxide synthesis in endothelial cytosol is mediated by calmodulin', *FEBS Letters,* 265(1-2), pp. 133-136.

Böger, R. H., Bode-Böger, S. M., Szuba, A., Tsao, P. S., Chan, J. R., Tangphao, O., Blaschke, T. F. and Cooke, J. P. (1998) 'Asymmetric dimethylarginine

(ADMA): a novel risk factor for endothelial dysfunction: its role in hypercholesterolemia', *Circulation,* 98(18), pp. 1842-7.

Caro, C., Fitz-Gerald, J. and Schroter, R. (1971) 'Atheroma and arterial wall shear-observation, correlation and proposal of a shear dependent mass transfer mechanism for atherogenesis', *Proceedings of the Royal Society of London. Series B. Biological Sciences,* 177(1046), pp. 109-133.

Chang, C. P., Su, Y. C., Hu, C. W. and Lei, H. Y. (2013) 'TLR2-dependent selective autophagy regulates NF-κB lysosomal degradation in hepatoma-derived M2 macrophage differentiation', *Cell Death & Differentiation,* 20(3), pp. 515-523.

Chanteux, H., Guisset, A. C., Pilette, C. and Sibille, Y. (2007) 'LPS induces IL-10 production by human alveolar macrophages via MAPKinases- and Sp1-dependent mechanisms', *Respiratory Research,* 8(1), pp. 71.

Chao, C.-C., Chen, S.-J., Adamopoulos, I. E., Davis, N., Hong, K., Vu, A., Kwan, S., Fayadat-Dilman, L., Asio, A. and Bowman, E. P. (2011) 'Anti-IL-17A therapy protects against bone erosion in experimental models of rheumatoid arthritis', *Autoimmunity,* 44(3), pp. 243-252.

Chauhan, S. D., Seggara, G., Vo, P. A., MacAllister, R. J., Hobbs, A. J. and Ahluwalia, A. J. T. F. j. (2003) 'Protection against lipopolysaccharide-induced endothelial dysfunction in resistance and conduit vasculature of iNOS knockout mice', 17(6), pp. 773-775.

Chen, K., Fan, W., Wang, X., Ke, X., Wu, G. and Hu, C. (2012) 'MicroRNA-101 mediates the suppressive effect of laminar shear stress on mTOR expression in vascular endothelial cells', *Biochemical and biophysical research communications,* 427(1), pp. 138-142.

Chen, W., Wang, H., Liu, J. and Li, K. (2022) 'Interference of KLF9 relieved the development of gestational diabetes mellitus by upregulating DDAH2', *Bioengineered,* 13(1), pp. 395-406.

Chinetti, G., Lestavel, S., Bocher, V., Remaley, A. T., Neve, B., Torra, I. P., Teissier, E., Minnich, A., Jaye, M., Duverger, N., Brewer, H. B., Fruchart, J. C., Clavey, V. and Staels, B. (2001) 'PPAR-alpha and PPAR-gamma activators induce cholesterol removal from human macrophage foam cells through stimulation of the ABCA1 pathway', *Nat Med,* 7(1), pp. 53-8.

Ciesielska, A., Matyjek, M. and Kwiatkowska, K. (2021) 'TLR4 and CD14 trafficking and its influence on LPS-induced pro-inflammatory signaling', *Cellular and Molecular Life Sciences,* 78(4), pp. 1233-1261.

Clancy, R. M. and Abramson, S. B. (1995) 'Nitric oxide: a novel mediator of inflammation', *Proceedings of the Society for Experimental Biology and Medicine,* 210(2), pp. 93-101.

Clarke, E. M., Thompson, R. C., Allam, A. H., Wann, L. S., Lombardi, G. P., Sutherland, M. L., Sutherland, J. D., Cox, S. L., Soliman, M. A.-T., Abd el-Maksoud, G., Badr, I., Miyamoto, M. I., Frohlich, B., Nur el-din, A.-H., Stewart, A. F. R., Narula, J., Zink, A. R., Finch, C. E., Michalik, D. E. and Thomas, G. S. (2014) 'Is atherosclerosis fundamental to human aging? Lessons from ancient mummies', *Journal of Cardiology,* 63(5), pp. 329-334.

Clausen, B. E., Burkhardt, C., Reith, W., Renkawitz, R. and Förster, I. (1999) 'Conditional gene targeting in macrophages and granulocytes using LysMcre mice', *Transgenic Research,* 8(4), pp. 265-277.

Cleeter, M. W. J., Cooper, J. M., Darley-Usmar, V. M., Moncada, S. and Schapira, A. H. V. (1994) 'Reversible inhibition of cytochrome c oxidase, the terminal enzyme of the mitochondrial respiratory chain, by nitric oxide: Implications for neurodegenerative diseases', *FEBS Letters,* 345(1), pp. 50-54.

Coenye, T. (2021) 'Do results obtained with RNA-sequencing require independent verification?', *Biofilm,* 3.

Colasanti, M. and Persichini, T. (2000) 'Nitric oxide: an inhibitor of NF-κB/Rel system in glial cells', *Brain research bulletin,* 52(3), pp. 155-161.

Colin, S., Chinetti-Gbaguidi, G. and Staels, B. (2014) 'Macrophage phenotypes in atherosclerosis', 262(1), pp. 153-166.

Connelly, L., Jacobs, A. T., Palacios-Callender, M., Moncada, S. and Hobbs, A. J. J. J. o. B. C. (2003) 'Macrophage endothelial nitric-oxide synthase autoregulates cellular activation and pro-inflammatory protein expression', 278(29), pp. 26480-26487.

Connelly, L., Madhani, M. and Hobbs, A. J. (2005) 'Resistance to Endotoxic Shock in Endothelial Nitric-oxide Synthase (eNOS) Knock-out Mice: A PRO-INFLAMMATORY ROLE FOR eNOS-DERIVED NO IN VIVO*♦', *Journal of Biological Chemistry,* 280(11), pp. 10040-10046.

Cooke, J. P. J. A., thrombosis, and biology, v. (2000) 'Does ADMA cause endothelial dysfunction?', 20(9), pp. 2032-2037.

Cooper, B. 'The origins of bone marrow as the seedbed of our blood: from antiquity to the time of Osler'. *Baylor University Medical Center Proceedings*: Taylor & Francis, 115-118.

Corraliza, I. M., Soler, G., Eichmann, K. and Modolell, M. (1995) 'Arginase induction by suppressors of nitric oxide synthesis (IL-4, IL-10 and PGE2) in murine bone-marrow-derived macrophages', *Biochemical and biophysical research communications,* 206(2), pp. 667-673.

Cossrow, N. and Falkner, B. (2004) 'Race/ethnic issues in obesity and obesity-related comorbidities', *The Journal of Clinical Endocrinology & Metabolism,* 89(6), pp. 2590-2594.

Costa, R., Antunes, P., Salvador, P., Oliveira, P. and Marinho, A. (2021) 'Secukinumab on Refractory Lupus Nephritis', *Cureus,* 13(8), pp. e17198.

Cross, M. and Renkawitz, R. (1990) 'Repetitive sequence involvement in the duplication and divergence of mouse lysozyme genes', *The EMBO journal,* 9(4), pp. 1283-1288.

Cua, D. J. and Tato, C. M. (2010) 'Innate IL-17-producing cells: the sentinels of the immune system', *Nature Reviews Immunology,* 10(7), pp. 479-489.

Das, H., Kumar, A., Lin, Z., Patino, W. D., Hwang, P. M., Feinberg, M. W., Majumder, P. K. and Jain, M. K. (2006) 'Kruppel-like factor 2 (KLF2) regulates proinflammatory activation of monocytes', *Proceedings of the National Academy of Sciences,* 103(17), pp. 6653-6658.

Das, P., van de Berg Bentz, D., Becker, A. J. L. i., methods, a. j. o. t. and pathology (1989) 'Atherosclerotic lesions in humans. In situ immunophenotypic analysis suggesting an immune mediated response', 61(2), pp. 166-170.

Davids, M. and Teerlink, T. (2013) 'Plasma concentrations of arginine and asymmetric dimethylarginine do not reflect their intracellular concentrations in peripheral blood mononuclear cells', *Metabolism,* 62(10), pp. 1455-61.

Davies, J. Q. and Gordon, S. (2005) 'Isolation and culture of murine macrophages', *Basic cell culture protocols*, pp. 91-103.

de Freitas, D. G. and Gokal, R. (2005) 'Sterile Peritonitis in the Peritoneal Dialysis Patient', *Peritoneal Dialysis International,* 25(2), pp. 146-151.

De Gaetano, M., Crean, D., Barry, M. and Belton, O. (2016) 'M1-and M2-type macrophage responses are predictive of adverse outcomes in human atherosclerosis', *Frontiers in immunology,* 7, pp. 275.

de Jonge, H. J., Fehrmann, R. S., de Bont, E. S., Hofstra, R. M., Gerbens, F., Kamps, W. A., de Vries, E. G., van der Zee, A. G., te Meerman, G. J. and ter Elst, A. (2007) 'Evidence based selection of housekeeping genes', *PloS one,* 2(9), pp. e898.

Deakin, J. E., Papenfuss, A. T., Belov, K., Cross, J. G. R., Coggill, P., Palmer, S., Sims, S., Speed, T. P., Beck, S. and Graves, J. A. M. (2006) 'Evolution and comparative analysis of the MHC Class III inflammatory region', *BMC Genomics,* 7(1), pp. 281.

Degboé, Y., Rauwel, B., Baron, M., Boyer, J. F., Ruyssen-Witrand, A., Constantin, A. and Davignon, J. L. (2019) 'Polarization of Rheumatoid Macrophages by TNF Targeting Through an IL-10/STAT3 Mechanism', *Front Immunol,* 10, pp. 3.

Dekker, R. J., Van Soest, S., Fontijn, R. D., Salamanca, S., De Groot, P. G., VanBavel, E., Pannekoek, H. and Horrevoets, A. J. (2002) 'Prolonged fluid shear stress induces a distinct set of endothelial cell genes, most specifically lung Kruppel-like factor (KLF2)', *Blood, The Journal of the American Society of Hematology,* 100(5), pp. 1689-1698.

Derbyshire, E. R. and Marletta, M. A. (2012) 'Structure and regulation of soluble guanylate cyclase', *Annual review of biochemistry,* 81, pp. 533-559.

Ding, H., Wu, B., Wang, H., Lu, Z., Yan, J., Wang, X., Shaffer, J. R., Hui, R. and Wang, D. W. (2010) 'A novel loss-of-function DDAH1 promoter polymorphism is associated with increased susceptibility to thrombosis stroke and coronary heart disease', *Circulation research,* 106(6), pp. 1145-1152.

Diotallevi, M., Nicol, T., Ayaz, F., Bailey, J., Shaw, A., McNeill, E., Davies, B., Channon, K. M. and Crabtree, M. J. (2022) 'Isolation and In vitro Culture of Bone Marrow-Derived Macrophages for the Study of NO-Redox Biology', *J Vis Exp,* (183).

Dowsett, L., Duluc, L., Higgins, E., Alghamdi, F., Fast, W., Salt, I. P. and Leiper, J. (2023) 'Asymmetric dimethylarginine positively modulates calcium-sensing receptor signalling to promote lipid accumulation', *Cellular Signalling,* 107, pp. 110676.

Dowsett, L., Higgins, E., Alanazi, S., Alshuwayer, N. A., Leiper, F. C. and Leiper, J. (2020) 'ADMA: a key player in the relationship between vascular dysfunction and inflammation in atherosclerosis', *Journal of Clinical Medicine,* 9(9), pp. 3026.

Dunham, D., Garcia, M., Shafqat, E., Williams, C. and Andrews, W. (2023) 'Comparing Immune Profiles of Two Cell Lines: The Response to LPS of Murine RAW 264.7 and J774A. 1 Macrophages'.

Dunn, J., Thabet, S. and Jo, H. (2015) 'Flow-dependent epigenetic DNA methylation in endothelial gene expression and atherosclerosis', *Arteriosclerosis, thrombosis, and vascular biology,* 35(7), pp. 1562-1569.

El Assar, M., Angulo, J., Santos-Ruiz, M., Ruiz de Adana, J. C., Pindado, M. L., Sánchez-Ferrer, A., Hernández, A. and Rodríguez-Mañas, L. (2016) 'Asymmetric dimethylarginine (ADMA) elevation and arginase up-regulation contribute to endothelial dysfunction related to insulin resistance in rats and morbidly obese humans', *The Journal of physiology,* 594(11), pp. 3045-3060.

El Bouhassani, M., Gilibert, S., Moreau, M., Saint-Charles, F., Tréguier, M., Poti, F., Chapman, M. J., Le Goff, W., Lesnik, P. and Huby, T. (2011) 'Cholesteryl ester transfer protein expression partially attenuates the adverse effects of SR-BI receptor deficiency on cholesterol metabolism and atherosclerosis', *Journal of Biological Chemistry,* 286(19), pp. 17227-17238.

Elnabawi, Y. A., Dey, A. K., Goyal, A., Groenendyk, J. W., Chung, J. H., Belur, A. D., Rodante, J., Harrington, C. L., Teague, H. L. and Baumer, Y. (2019) 'Coronary artery plaque characteristics and treatment with biologic therapy in severe psoriasis: results from a prospective observational study', *Cardiovascular research,* 115(4), pp. 721-728.

Emrich, S. J., Barbazuk, W. B., Li, L. and Schnable, P. S. (2007) 'Gene discovery and annotation using LCM-454 transcriptome sequencing', *Genome research,* 17(1), pp. 69-73.

Endo, A., Kuroda, M. and Tanzawa, K. (1976) 'Competitive inhibition of 3-hydroxy-3-methylglutaryl coenzyme A reductase by ML-236A and ML-236B fungal metabolites, having hypocholesterolemic activity', *FEBS letters,* 72(2), pp. 323-326.

Engelen, S. E., Robinson, A. J., Zurke, Y.-X. and Monaco, C. (2022) 'Therapeutic strategies targeting inflammation and immunity in atherosclerosis: how to proceed?', *Nature Reviews Cardiology,* 19(8), pp. 522-542.

Erwig, L. P. and Gow, N. A. (2016) 'Interactions of fungal pathogens with phagocytes', *Nature Reviews Microbiology,* 14(3), pp. 163-176.

Everaert, C., Luypaert, M., Maag, J. L., Cheng, Q. X., Dinger, M. E., Hellemans, J. and Mestdagh, P. (2017) 'Benchmarking of RNA-sequencing analysis workflows using whole-transcriptome RT-qPCR expression data', *Scientific reports,* 7(1), pp. 1559.

Falcone, F. H., Haas, H. and Gibbs, B. F. (2000) 'The human basophil: a new appreciation of its role in immune responses', *Blood,* 96(13), pp. 4028-4038.

Fernando, M. M. A., Stevens, C. R., Sabeti, P. C., Walsh, E. C., McWhinnie, A. J. M., Shah, A., Green, T., Rioux, J. D. and Vyse, T. J. (2007) 'Identification of two independent risk factors for lupus within the MHC in United Kingdom families', *PLoS genetics,* 3(11), pp. e192.

Fleetwood, A. J., Lawrence, T., Hamilton, J. A. and Cook, A. D. (2007) 'Granulocyte-macrophage colony-stimulating factor (CSF) and macrophage CSF-dependent macrophage phenotypes display differences in cytokine profiles and transcription factor activities: implications for CSF blockade in inflammation', *The Journal of immunology,* 178(8), pp. 5245-5252.

Flierl, M. A., Rittirsch, D., Gao, H., Hoesel, L. M., Nadeau, B. A., Day, D. E., Zetoune, F. S., Sarma, J. V., Huber-Lang, M. S. and Ferrara, J. L. (2008) 'Adverse functions of IL-17A in experimental sepsis'.

Fliser, D., Kronenberg, F., Kielstein, J. T., Morath, C., Bode-Bo, S. M., Haller, H. and Ritz, E. (2005) 'Asymmetric dimethylarginine and progression of chronic kidney disease: the mild to moderate kidney disease study', *Journal of the American Society of Nephrology,* 16(8), pp. 2456-2461.

Frąk, W., Wojtasińska, A., Lisińska, W., Młynarska, E., Franczyk, B. and Rysz, J. (2022) 'Pathophysiology of Cardiovascular Diseases: New Insights into Molecular Mechanisms of Atherosclerosis, Arterial Hypertension, and Coronary Artery Disease', *Biomedicines,* 10(8), pp. 1938.

Fujiwara, Y., Hama, K., Tsukahara, M., Izumi-Tsuzuki, R., Nagai, T., Ohe-Yamada, M., Inoue, K. and Yokoyama, K. (2018) 'Acyl Chain Preference in Foam Cell Formation from Mouse Peritoneal Macrophages', *Biol Pharm Bull,* 41(1), pp. 86-91.

Furfine, E. S., Harmon, M. F., Paith, J. E. and Garvey, E. P. (1993) 'Selective inhibition of constitutive nitric oxide synthase by L-NG-nitroarginine', *Biochemistry,* 32(33), pp. 8512-8517.

Furuki, K., Adachi, H., Matsuoka, H., Enomoto, M., Satoh, A., Hino, A., Hirai, Y. and Imaizumi, T. (2007) 'Plasma levels of asymmetric dimethylarginine (ADMA) are related to intima-media thickness of the carotid artery: An epidemiological study', *Atherosclerosis,* 191(1), pp. 206-210.

Förstermann, U., Gath, I., Schwarz, P., Closs, E. I. and Kleinert, H. (1995) 'Isoforms of nitric oxide synthase. Properties, cellular distribution and expressional control', *Biochem Pharmacol,* 50(9), pp. 1321-32.

Förstermann, U. and Sessa, W. C. (2012) 'Nitric oxide synthases: regulation and function', *Eur Heart J,* 33(7), pp. 829-37, 837a-837d.

Gadola, L., Poggi, C., Dominguez, P., Poggio, M. V., Lungo, E. and Cardozo, C. (2019) 'Risk Factors And Prevention of Peritoneal Dialysis-Related Peritonitis', *Perit Dial Int,* 39(2), pp. 119-125.

Garthwaite, J. (2019) 'NO as a multimodal transmitter in the brain: discovery and current status', *British Journal of Pharmacology,* 176(2), pp. 197-211.

Gary, J. D. and Clarke, S. (1998) 'RNA and protein interactions modulated by protein arginine methylation', *Progress in nucleic acid research and molecular biology*: Elsevier, pp. 65-131.

Gasperini, S., Calzetti, F., Bazzoni, F. and Cassatella, M. A. (2000) 'The neutrophil as a cellular source of chemokines', *Immunological reviews,* 177, pp. 195-203.

Gautier, E. L., Huby, T., Witztum, J. L., Ouzilleau, B., Miller, E. R., Saint-Charles, F., Aucouturier, P., Chapman, M. J. and Lesnik, P. (2009) 'Macrophage apoptosis exerts divergent effects on atherogenesis as a function of lesion stage', *Circulation,* 119(13), pp. 1795-1804.

Geissmann, F., Jung, S. and Littman, D. R. (2003) 'Blood monocytes consist of two principal subsets with distinct migratory properties', *Immunity,* 19(1), pp. 71-82.

Gimbrone, M. A., Nagel, T. and Topper, J. N. (1997) 'Biomechanical activation: an emerging paradigm in endothelial adhesion biology', *The Journal of clinical investigation,* 99(8), pp. 1809-1813.

Glagov, S., Weisenberg, E., Zarins, C. K., Stankunavicius, R. and Kolettis, G. J. (1987) 'Compensatory Enlargement of Human Atherosclerotic Coronary Arteries', 316(22), pp. 1371-1375.

Glagov, S., Zarins, C., Giddens, D. P. and Ku, D. N. (1988) 'Hemodynamics and atherosclerosis. Insights and perspectives gained from studies of human arteries', *Archives of pathology & laboratory medicine,* 112(10), pp. 1018-1031.

Goldstein, J. L. and Brown, M. S. (1973) 'Familial hypercholesterolemia: identification of a defect in the regulation of 3-hydroxy-3-methylglutaryl coenzyme A reductase activity associated with overproduction of cholesterol', *Proceedings of the National Academy of Sciences,* 70(10), pp. 2804-2808.

Gong, C., Qi, Y., Xu, Y., Tang, X., Liang, F. and Chen, L. (2021) 'Parecoxib improves atherosclerotic plaque stability by suppressing inflammation and inhibiting matrix metalloproteinases production', *Biomedicine & Pharmacotherapy,* 138, pp. 111423.

Griess, P. (1858) 'Preliminary notice of the reaction of nitrous acid with picramic acid and aminonitrophenol', *Ann. Chem. Pharm,* 106, pp. 123-125.

Griffith, M., Griffith, O. L., Mwenifumbo, J., Goya, R., Morrissy, A. S., Morin, R. D., Corbett, R., Tang, M. J., Hou, Y.-C., Pugh, T. J., Robertson, G., Chittaranjan, S., Ally, A., Asano, J. K., Chan, S. Y., Li, H. I., McDonald, H., Teague, K., Zhao, Y., Zeng, T., Delaney, A., Hirst, M., Morin, G. B., Jones, S. J. M., Tai, I. T. and Marra, M. A. (2010) 'Alternative expression analysis by RNA sequencing', *Nature Methods,* 7(10), pp. 843-847.

Grundy, S. M., Cleeman, J. I., Daniels, S. R., Donato, K. A., Eckel, R. H., Franklin, B. A., Gordon, D. J., Krauss, R. M., Savage, P. J. and Smith Jr, S. C. (2005) 'Diagnosis and management of the metabolic syndrome: an American Heart Association/National Heart, Lung, and Blood Institute scientific statement', *Circulation,* 112(17), pp. 2735-2752.

Gui, Y., Zheng, H. and Cao, R. Y. (2022) 'Foam Cells in Atherosclerosis: Novel Insights Into Its Origins, Consequences, and Molecular Mechanisms', *Front Cardiovasc Med,* 9, pp. 845942.

Guo, X., Li, B., Wen, C., Zhang, F., Xiang, X., Nie, L., Chen, J. and Mao, L. (2023) 'TREM2 promotes cholesterol uptake and foam cell formation in atherosclerosis', *Cell Mol Life Sci,* 80(5), pp. 137.

Haghighat, A., Weiss, D., Whalin, M. K., Cowan, D. P. and Taylor, W. R. (2007) 'Granulocyte Colony-Stimulating Factor and Granulocyte Macrophage Colony-Stimulating Factor Exacerbate Atherosclerosis in Apolipoprotein E–Deficient Mice', *Circulation,* 115(15), pp. 2049-2054.

Hansson, G. K. and Hermansson, A. J. N. i. (2011) 'The immune system in atherosclerosis', 12(3), pp. 204.

Hasegawa, K., Wakino, S., Kimoto, M., Minakuchi, H., Fujimura, K., Hosoya, K., Komatsu, M., Kaneko, Y., Kanda, T. and Tokuyama, H. (2013) 'The hydrolase DDAH2 enhances pancreatic insulin secretion by transcriptional regulation of

secretagogin through a Sirt1-dependent mechanism in mice', *The FASEB Journal*, 27(6), pp. 2301-2315.

Hasegawa, K., Wakino, S., Tatematsu, S., Yoshioka, K., Homma, K., Sugano, N., Kimoto, M., Hayashi, K. and Itoh, H. (2007) 'Role of asymmetric dimethylarginine in vascular injury in transgenic mice overexpressing dimethylarginie dimethylaminohydrolase 2', *Circulation Research,* 101(2), pp. e2-e10.

Hashimoto, D., Chow, A., Noizat, C., Teo, P., Beasley, M. B., Leboeuf, M., Becker, C. D., See, P., Price, J. and Lucas, D. (2013) 'Tissue-resident macrophages self-maintain locally throughout adult life with minimal contribution from circulating monocytes', *Immunity,* 38(4), pp. 792-804.

Hevel, J. M., White, K. A. and Marletta, M. A. (1991) 'Purification of the inducible murine macrophage nitric oxide synthase. Identification as a flavoprotein', *Journal of biological chemistry,* 266(34), pp. 22789-22791.

Hirsch, J. G. (1956) 'Phagocytin: a bactericidal substance from polymorphonuclear leucocytes', *J Exp Med,* 103(5), pp. 589-611.

Hong, D., Gao, H.-C., Wang, X., Li, L.-F., Li, C.-C., Luo, Y., Wang, K.-K., Bai, Y.-P. and Zhang, G.-G. (2015) 'Asymmetric dimethylarginine triggers macrophage apoptosis via the endoplasmic reticulum stress pathway', *Molecular and Cellular Biochemistry,* 398(1), pp. 31-38.

Hong, L. and Fast, W. (2007) 'Inhibition of human dimethylarginine dimethylaminohydrolase-1 by S-nitroso-L-homocysteine and hydrogen peroxide', *Journal of Biological Chemistry,* 282(48), pp. 34684-34692.

Horowitz, J. D. and Heresztyn, T. (2007) 'An overview of plasma concentrations of asymmetric dimethylarginine (ADMA) in health and disease and in clinical studies: methodological considerations', *Journal of Chromatography B,* 851(1-2), pp. 42-50.

Hossain, E., Ota, A., Karnan, S., Takahashi, M., Mannan, S. B., Konishi, H. and Hosokawa, Y. (2015) 'Lipopolysaccharide augments the uptake of oxidized LDL by

up-regulating lectin-like oxidized LDL receptor-1 in macrophages', *Molecular and cellular biochemistry,* 400, pp. 29-40.

Houthuys, E., Movahedi, K., De Baetselier, P., Van Ginderachter, J. A. and Brouckaert, P. (2010) 'A method for the isolation and purification of mouse peripheral blood monocytes', *Journal of Immunological Methods,* 359(1), pp. 1-10.

Hrabák, A., Bögel, G., Murányi, J., Tamási, V., Németh, K., Szokol, B., Kukor, Z., Kardon, T. and Őrfi, L. (2023) 'Decreasing effects of protein kinase inhibitors on the expression of NOS2 and inflammatory cytokines and on phagocytosis in rat peritoneal macrophages is partly related to repolarization', *Mol Immunol,* 153, pp. 10-24.

Hu, M., Pan, Z., Yang, Y., Meng, C., Geng, S., You, M. and Jiao, X. (2012) 'Different antigen presentation tendencies of granulocyte-macrophage colony-stimulating factor-induced bone marrow-derived macrophages and peritoneal macrophages', *In Vitro Cellular & Developmental Biology-Animal,* 48, pp. 434-440.

Hu, X., Atzler, D., Xu, X., Zhang, P., Guo, H., Lu, Z., Fassett, J., Schwedhelm, E., Böger, R. H. and Bache, R. J. (2011) 'Dimethylarginine dimethylaminohydrolase-1 is the critical enzyme for degrading the cardiovascular risk factor asymmetrical dimethylarginine', *Arteriosclerosis, thrombosis, and vascular biology,* 31(7), pp. 1540-1546.

Huan, W., Yandong, L., Chao, W., Sili, Z., Jun, B., Mingfang, L., Yu, C. and Lefeng, Q. (2021) 'YKL-40 aggravates early-stage atherosclerosis by inhibiting macrophage apoptosis in an aven-dependent way', *Frontiers in Cell and Developmental Biology,* 9, pp. 752773.

Huang, D. W., Sherman, B. T. and Lempicki, R. A. (2009) 'Bioinformatics enrichment tools: paths toward the comprehensive functional analysis of large gene lists', *Nucleic acids research,* 37(1), pp. 1-13.

Huang, S., Li, Z., Wu, Z., Liu, C., Yu, M., Wen, M., Zhang, L. and Wang, X. (2021) 'DDAH2 suppresses RLR-MAVS–mediated innate antiviral immunity by stimulating nitric oxide–activated, Drp1-induced mitochondrial fission', *Science Signaling,* 14(678), pp. eabc7931.

Huang, Z., Shiva, S., Kim-Shapiro, D. B., Patel, R. P., Ringwood, L. A., Irby, C. E., Huang, K. T., Ho, C., Hogg, N. and Schechter, A. N. (2005) 'Enzymatic function of hemoglobin as a nitrite reductase that produces NO under allosteric control', *The Journal of clinical investigation,* 115(8), pp. 2099-2107.

Huemer, M., Carvalho, D. R., Brum, J. M., Ünal, Ö., Coskun, T., Weisfeld-Adams, J. D., Schrager, N. L., Scholl-Bürgi, S., Schlune, A. and Donner, M. G. (2016) 'Clinical phenotype, biochemical profile, and treatment in 19 patients with arginase 1 deficiency', *Journal of inherited metabolic disease,* 39, pp. 331-340.

Hughes, M. N. (2008) 'Chapter One - Chemistry of Nitric Oxide and Related Species', in Poole, R.K. (ed.) *Methods in Enzymology*: Academic Press, pp. 3-19.

Hung, M.-J., Cherng, W.-J., Hung, M.-Y., Wu, H.-T. and Pang, J.-H. S. (2010) 'Interleukin-6 inhibits endothelial nitric oxide synthase activation and increases endothelial nitric oxide synthase binding to stabilized caveolin-1 in human vascular endothelial cells', *Journal of Hypertension,* 28(5).

Husebye, H., Halaas, Ø., Stenmark, H., Tunheim, G., Sandanger, Ø., Bogen, B., Brech, A., Latz, E. and Espevik, T. (2006) 'Endocytic pathways regulate Toll-like receptor 4 signaling and link innate and adaptive immunity', *The EMBO Journal,* 25(4), pp. 683-692.

Ignatowski, A. (1908) 'Influence of animal food on the organsim of rabbits', *Izvest Imper Voennomed Akad St Petersburg,* 16, pp. 154-173.

Ingersoll, M. A., Platt, A. M., Potteaux, S. and Randolph, G. J. (2011) 'Monocyte trafficking in acute and chronic inflammation', *Trends in immunology,* 32(10), pp. 470-477.

Ischiropoulos, H. and Al-Mehdi, A. B. (1995) 'Peroxynitrite-mediated oxidative protein modifications', *FEBS letters,* 364(3), pp. 279-282.

Isomäki, H., Koivisto, O. and Kiviniitty, K. (1971) 'Splenomegaly in Rheumatoid Arthritis', *Acta Rheumatologica Scandinavica,* 17(1-4), pp. 23-26.

Ito, A., Tsao, P. S., Adimoolam, S., Kimoto, M., Ogawa, T. and Cooke, J. P. (1999) 'Novel mechanism for endothelial dysfunction: dysregulation of dimethylarginine dimethylaminohydrolase', *Circulation,* 99(24), pp. 3092-3095.

Jacobi, J., Maas, R., Cardounel, A. J., Arend, M., Pope, A. J., Cordasic, N., Heusinger-Ribeiro, J., Atzler, D., Strobel, J. and Schwedhelm, E. (2010) 'Dimethylarginine dimethylaminohydrolase overexpression ameliorates atherosclerosis in apolipoprotein E-deficient mice by lowering asymmetric dimethylarginine', *The American journal of pathology,* 176(5), pp. 2559-2570.

Jia, S.-J., Lai, Y.-Q., Zhao, M., Gong, T. and Zhang, B.-K. (2013) 'Homocysteine-induced hypermethylation of DDAH2 promoter contributes to apoptosis of endothelial cells', *Die Pharmazie - An International Journal of Pharmaceutical Sciences,* 68(4), pp. 282-286.

John MacMicking, Qiao-wen Xie, a. and Nathan, C. (1997) 'NITRIC OXIDE AND MACROPHAGE FUNCTION', 15(1), pp. 323-350.

Jonasson, L., Holm, J., Skalli, O., Bondjers, G. and Hansson, G. K. J. A. A. O. J. o. t. A. H. A., Inc. (1986) 'Regional accumulations of T cells, macrophages, and smooth muscle cells in the human atherosclerotic plaque', 6(2), pp. 131-138.

Jones, L. C., Tran, C. T. L., Leiper, J. M., Hingorani, A. D. and Vallance, P. (2003) 'Common genetic variation in a basal promoter element alters DDAH2 expression in endothelial cells', *Biochemical and Biophysical Research Communications,* 310(3), pp. 836-843.

Junprung, W., Supungul, P., Sangklai, N. and Tassanakajon, A. (2022) 'Heat Shock Protein 70 Is a Damage-Associated Molecular Pattern That by Binding to Lipopolysaccharide and ß-1, 3-Glucan–Binding Protein Activates the

Prophenoloxidase System in Shrimp', *The Journal of Immunology,* 209(3), pp. 582-592.

Kakimoto, Y. and Akazawa, S. (1970) 'Isolation and identification of N-G,N-G- and N-G,N'-G-dimethyl-arginine, N-epsilon-mono-, di-, and trimethyllysine, and glucosylgalactosyl- and galactosyl-delta-hydroxylysine from human urine', *J Biol Chem,* 245(21), pp. 5751-8.

Kang, Y., Liu, R., Wu, J.-X. and Chen, L. (2019) 'Structural insights into the mechanism of human soluble guanylate cyclase', *Nature,* 574(7777), pp. 206-210.

Kaparakis, M., Turnbull, L., Carneiro, L., Firth, S., Coleman, H. A., Parkington, H. C., Le Bourhis, L., Karrar, A., Viala, J., Mak, J., Hutton, M. L., Davies, J. K., Crack, P. J., Hertzog, P. J., Philpott, D. J., Girardin, S. E., Whitchurch, C. B. and Ferrero, R. L. (2010) 'Bacterial membrane vesicles deliver peptidoglycan to NOD1 in epithelial cells', *Cellular Microbiology,* 12(3), pp. 372-385.

Kashgarian, M. (1985) 'Pathology of small blood vessel disease in hypertension', *American Journal of Kidney Diseases,* 5(4), pp. A104-A110.

Kattoor, A. J., Goel, A. and Mehta, J. L. (2019) 'LOX-1: regulation, signaling and its role in atherosclerosis', *Antioxidants,* 8(7), pp. 218.

Kawasaki, T. and Kawai, T. (2014) 'Toll-like receptor signaling pathways', *Frontiers in immunology,* 5, pp. 461.

Kazama, H., Ricci, J.-E., Herndon, J. M., Hoppe, G., Green, D. R. and Ferguson, T. A. (2008) 'Induction of immunological tolerance by apoptotic cells requires caspase-dependent oxidation of high-mobility group box-1 protein', *Immunity,* 29(1), pp. 21-32.

Kerwin, J. F., Jr., Lancaster, J. R. and Feldman, P. L. (1995) 'Nitric Oxide: A New Paradigm for Second Messengers', *Journal of Medicinal Chemistry,* 38(22), pp. 4343-4362.

Khallou-Laschet, J., Varthaman, A., Fornasa, G., Compain, C., Gaston, A.-T., Clement, M., Dussiot, M., Levillain, O., Graff-Dubois, S. and Nicoletti, A. (2010) 'Macrophage plasticity in experimental atherosclerosis', *PloS one,* 5(1), pp. e8852.

Kielstein, J. T., Bo, R. H., Bode-Bo, S. M., Haller, H., Ritz, E. and Fliser, D. (2002) 'Marked increase of asymmetric dimethylarginine in patients with incipient primary chronic renal disease', *Journal of the American Society of Nephrology,* 13(1), pp. 170-176.

Kielstein, J. T., Boger, R. H., Bode-Boger, S. M., Schaffer, J., Barbey, M., Koch, K. M. and Frolich, J. C. J. J. o. t. A. S. o. N. (1999) 'Asymmetric dimethylarginine plasma concentrations differ in patients with end-stage renal disease: relationship to treatment method and atherosclerotic disease', 10(3), pp. 594-600.

Kim, H., Kim, M., Im, S. K. and Fang, S. (2018) 'Mouse Cre-LoxP system: general principles to determine tissue-specific roles of target genes', *Lab Anim Res,* 34(4), pp. 147-159.

Knipp, M., Braun, O., Gehrig, P. M., Sack, R. and Vašák, M. (2003) 'Zn (II)-free dimethylargininase-1 (DDAH-1) is inhibited upon specific Cys-S-nitrosylation', *Journal of Biological Chemistry,* 278(5), pp. 3410-3416.

Kobayashi, S., Hamashima, S., Homma, T., Sato, M., Kusumi, R., Bannai, S., Fujii, J. and Sato, H. (2018) 'Cystine/glutamate transporter, system x(c)(-), is involved in nitric oxide production in mouse peritoneal macrophages', *Nitric Oxide,* 78, pp. 32-40.

Koch, C. M., Chiu, S. F., Akbarpour, M., Bharat, A., Ridge, K. M., Bartom, E. T. and Winter, D. R. (2018) 'A beginner's guide to analysis of RNA sequencing data', *American journal of respiratory cell and molecular biology,* 59(2), pp. 145-157.

Konstantinov, I. E., Mejevoi, N. and Anichkov, N. M. (2006) 'Nikolai N. Anichkov and his theory of atherosclerosis', *Texas Heart Institute Journal,* 33(4), pp. 417.

Koriyama, H., Ikeda, Y., Nakagami, H., Shimamura, M., Yoshida, S., Rakugi, H. and Morishita, R. (2020) 'Development of an IL-17A DNA Vaccine to Treat Systemic Lupus Erythematosus in Mice', *Vaccines (Basel),* 8(1).

Kresinsky, A., Schneble, N., Schmidt, C., Frister, A., Bauer, R., Wetzker, R. and Müller, J. P. (2016) 'Phagocytosis of bone marrow derived macrophages is controlled by phosphoinositide 3-kinase γ', *Immunol Lett,* 180, pp. 9-16.

Kubes, P., Suzuki, M. and Granger, D. (1991) 'Nitric oxide: an endogenous modulator of leukocyte adhesion', *Proceedings of the National Academy of Sciences,* 88(11), pp. 4651-4655.

Kume, N., MORIWAKI, H., KATAOKA, H., MINAMI, M., MURASE, T., SAWAMURA, T., MASAKI, T. and KITA, T. (2000) 'Inducible Expression of LOX-1, a Novel Receptor for Oxidized LDL, in Macrophages and Vascular Smooth Muscle Cells', 902(1), pp. 323-327.

Lambden, S. (2019) 'Bench to bedside review: therapeutic modulation of nitric oxide in sepsis—an update', *Intensive Care Medicine Experimental,* 7(1), pp. 64.

Lambden, S., Kelly, P., Ahmetaj-Shala, B., Wang, Z., Lee, B., Nandi, M., Torondel, B., Delahaye, M., Dowsett, L., Piper, S., Tomlinson, J., Caplin, B., Colman, L., Boruc, O., Slaviero, A., Zhao, L., Oliver, E., Khadayate, S., Singer, M., Arrigoni, F. and Leiper, J. (2015) 'Dimethylarginine Dimethylaminohydrolase 2 Regulates Nitric Oxide Synthesis and Hemodynamics and Determines Outcome in Polymicrobial Sepsis', 35(6), pp. 1382-1392.

Lange, C., Mowat, F., Sayed, H., Mehad, M., Duluc, L., Piper, S., Luhmann, U., Nandi, M., Kelly, P. and Smith, A. (2016) 'Dimethylarginine dimethylaminohydrolase-2 deficiency promotes vascular regeneration and attenuates pathological angiogenesis', *Experimental Eye Research,* 147, pp. 148-155.

Lanktree, M. B. and Hegele, R. A. (2017) 'Chapter 15 - Metabolic Syndrome', in David, S.P. (ed.) *Genomic and Precision Medicine (Third Edition)*. Boston: Academic Press, pp. 283-299.

Leiper, J., Murray-Rust, J., McDonald, N. and Vallance, P. (2002) 'S-nitrosylation of dimethylarginine dimethylaminohydrolase regulates enzyme activity: further interactions between nitric oxide synthase and dimethylarginine dimethylaminohydrolase', *Proceedings of the National Academy of Sciences,* 99(21), pp. 13527-13532.

Leiper, J., Nandi, M., Torondel, B., Murray-Rust, J., Malaki, M., O'Hara, B., Rossiter, S., Anthony, S., Madhani, M. and Selwood, D. J. N. m. (2007) 'Disruption of methylarginine metabolism impairs vascular homeostasis', 13(2), pp. 198.

Leiper, J. and Nandi, M. J. N. R. D. D. (2011) 'The therapeutic potential of targeting endogenous inhibitors of nitric oxide synthesis', 10(4), pp. 277-291.

Leiper, J. M., MARIA, J. S., CHUBB, A., MACALLISTER, R. J., CHARLES, I. G., WHITLEY, G. S. J. and VALLANCE, P. J. B. J. (1999) 'Identification of two human dimethylarginine dimethylaminohydrolases with distinct tissue distributions and homology with microbial arginine deiminases', 343(1), pp. 209-214.

Leone, A., Moncada, S., Vallance, P., Calver, A. and Collier, J. (1992) 'Accumulation of an endogenous inhibitor of nitric oxide synthesis in chronic renal failure', *The Lancet,* 339(8793), pp. 572-575.

Li, D., Guo, B., Wu, H., Tan, L., Chang, C. and Lu, Q. (2015) 'Interleukin-17 in systemic lupus erythematosus: A comprehensive review', *Autoimmunity,* 48(6), pp. 353-61.

Li, H., Samouilov, A., Liu, X. and Zweier, J. L. (2001) 'Characterization of the magnitude and kinetics of xanthine oxidase-catalyzed nitrite reduction: evaluation of its role in nitric oxide generation in anoxic tissues', *Journal of Biological Chemistry,* 276(27), pp. 24482-24489.

Li, J., Sun, L. and Li, Y. (2021) 'Regulation of dimethylarginine dimethylaminohydrolase 2 expression by NF-κB acetylation', *Exp Ther Med,* 21(2), pp. 114.

Libby, P. (2021) 'The changing landscape of atherosclerosis', *Nature,* 592(7855), pp. 524-533.

Libby, P., Buring, J. E., Badimon, L., Hansson, G. K., Deanfield, J., Bittencourt, M. S., Tokgözoğlu, L. and Lewis, E. F. (2019) 'Atherosclerosis', *Nat Rev Dis Primers,* 5(1), pp. 56.

Lin, K. Y., Ito, A., Asagami, T., Tsao, P. S., Adimoolam, S., Kimoto, M., Tsuji, H., Reaven, G. M. and Cooke, J. P. J. C. (2002) 'Impaired nitric oxide synthase pathway in diabetes mellitus: role of asymmetric dimethylarginine and dimethylarginine dimethylaminohydrolase', 106(8), pp. 987-992.

Lin, Z., Kumar, A., SenBanerjee, S., Staniszewski, K., Parmar, K., Vaughan, D. E., Gimbrone, M. A., Balasubramanian, V., García-Cardeña, G. and Jain, M. K. (2005) 'Kruppel-Like Factor 2 (KLF2) Regulates Endothelial Thrombotic Function', *Circulation Research,* 96(5), pp. e48-e57.

Lin, Z., Natesan, V., Shi, H., Dong, F., Kawanami, D., Mahabeleshwar, G. H., Atkins, G. B., Nayak, L., Cui, Y. and Finigan, J. H. (2010) 'Kruppel-like factor 2 regulates endothelial barrier function', *Arteriosclerosis, thrombosis, and vascular biology,* 30(10), pp. 1952-1959.

Linton, M. F., Babaev, V. R., Huang, J., Linton, E. F., Tao, H. and Yancey, P. G. (2016) 'Macrophage apoptosis and efferocytosis in the pathogenesis of atherosclerosis', *Circulation Journal,* 80(11), pp. 2259-2268.

Linton MRF, Y. P., Davies SS, et al. (2019) *The Role of Lipids and Lipoproteins in Atherosclerosis*. 2000- edn.

Lister, R., O'Malley, R. C., Tonti-Filippini, J., Gregory, B. D., Berry, C. C., Millar, A. H. and Ecker, J. R. (2008) 'Highly integrated single-base resolution maps of the epigenome in Arabidopsis', *Cell,* 133(3), pp. 523-536.

Liu, J., Thewke, D. P., Su, Y. R., Linton, M. F., Fazio, S. and Sinensky, M. S. (2005) 'Reduced Macrophage Apoptosis Is Associated With Accelerated

Atherosclerosis in Low-Density Lipoprotein Receptor-Null Mice', *Arteriosclerosis, Thrombosis, and Vascular Biology,* 25(1), pp. 174-179.

Liu, T., Liu, F., Peng, L. W., Chang, L. and Jiang, Y. M. (2018) 'The Peritoneal Macrophages in Inflammatory Diseases and Abdominal Cancers', *Oncol Res,* 26(5), pp. 817-826.

Liu, X., Fassett, J., Wei, Y. and Chen, Y. (2013) 'Regulation of DDAH1 as a potential therapeutic target for treating cardiovascular diseases', *Evidence-Based Complementary and Alternative Medicine,* 2013.

Liu, Y., Geng, L. and Suo, Z. (2009) 'Differentiation Effect of Pyruvate and Uridine on Cultured U937-ρ° Cells', *Ultrastructural Pathology,* 33(4), pp. 160-164.

Livak, K. J. and Schmittgen, T. D. (2001) 'Analysis of relative gene expression data using real-time quantitative PCR and the 2(-Delta Delta C(T)) Method', *Methods,* 25(4), pp. 402-8.

Lovren, F., Teoh, H. and Verma, S. (2015) 'Obesity and Atherosclerosis: Mechanistic Insights', *Canadian Journal of Cardiology,* 31(2), pp. 177-183.

Lu, Y.-C., Yeh, W.-C. and Ohashi, P. S. (2008) 'LPS/TLR4 signal transduction pathway', *Cytokine,* 42(2), pp. 145-151.

Ludwig, J. M., Zhang, Y., Chamulitrat, W., Stremmel, W. and Pathil, A. (2018) 'Anti-inflammatory properties of ursodeoxycholyl lysophosphatidylethanolamide in endotoxin-mediated inflammatory liver injury', *PLOS ONE,* 13(5), pp. e0197836.

Ludwig, L. M., Maxcy, K. L. and LaBelle, J. L. (2019) 'Flow Cytometry-Based Detection and Analysis of BCL-2 Family Proteins and Mitochondrial Outer Membrane Permeabilization (MOMP)', *Methods Mol Biol,* 1877, pp. 77-91.

Lundberg, J. O. N., Carlsson, S., Engstrand, L., Morcos, E., Wiklund, N. P. and Weitzberg, E. (1997) 'Urinary nitrite: More than a marker of infection', *Urology,* 50(2), pp. 189-191.

Luo, X., Chen, O., Wang, Z., Bang, S., Ji, J., Lee, S. H., Huh, Y., Furutani, K., He, Q. and Tao, X. (2021) 'IL-23/IL-17A/TRPV1 axis produces mechanical pain via macrophage-sensory neuron crosstalk in female mice', *Neuron,* 109(17), pp. 2691-2706. e5.

Ma, X. and Xu, S. (2013) 'TNF inhibitor therapy for rheumatoid arthritis', *Biomedical reports,* 1(2), pp. 177-184.

MacAllister, R. J., Parry, H., Kimoto, M., Ogawa, T., Russell, R. J., Hodson, H., Whitley, G. S. and Vallance, P. (1996) 'Regulation of nitric oxide synthesis by dimethylarginine dimethylaminohydrolase', *Br J Pharmacol,* 119(8), pp. 1533-40.

Maitra, U. and Li, L. (2013) 'Molecular mechanisms responsible for the reduced expression of cholesterol transporters from macrophages by low-dose endotoxin', *Arteriosclerosis, thrombosis, and vascular biology,* 33(1), pp. 24-33.

Malecki, R., Fiodorenko-Dumas, Z., Jakobsche-Policht, U., Malodobra, M. and Adamiec, R. (2013) 'Altered monocyte calcium-sensing receptor expression in patients with type 2 diabetes mellitus and atherosclerosis', *J Physiol Pharmacol,* 64(4), pp. 521-7.

Mannino, G. C., Pezzilli, S., Averta, C., Fuoco, A., Spiga, R., Mancuso, E., Di Fatta, C., Perticone, F., Prudente, S., Trischitta, V., Andreozzi, F. and Sesti, G. (2019) 'A functional variant of the dimethylarginine dimethylaminohydrolase-2 gene is associated with myocardial infarction in type 2 diabetic patients', *Cardiovascular Diabetology,* 18(1), pp. 102.

Marchant, V., Tejera-Muñoz, A., Marquez-Expósito, L., Rayego-Mateos, S., Rodrigues-Diez, R. R., Tejedor, L., Santos-Sanchez, L., Egido, J., Ortiz, A., Valdivielso, J. M., Fraser, D. J., López-Cabrera, M., Selgas, R. and Ruiz-Ortega, M. (2020) 'IL-17A as a Potential Therapeutic Target for Patients on Peritoneal Dialysis', *Biomolecules,* 10(10), pp. 1361.

Marciano, S., Díaz, J. M., Dirchwolf, M. and Gadano, A. (2019) 'Spontaneous bacterial peritonitis in patients with cirrhosis: incidence, outcomes, and treatment strategies', *Hepatic Medicine: Evidence and Research,* 11(null), pp. 13-22.

Marim, F. M., Silveira, T. N., Lima Jr, D. S. and Zamboni, D. S. (2010) 'A method for generation of bone marrow-derived macrophages from cryopreserved mouse bone marrow cells', *PloS one,* 5(12), pp. e15263.

Marshall, J. S. and Jawdat, D. M. (2004) 'Mast cells in innate immunity', *Journal of Allergy and Clinical Immunology,* 114(1), pp. 21-27.

Martin, F. J., Amode, M. R., Aneja, A., Austine-Orimoloye, O., Azov, Andrey G., Barnes, I., Becker, A., Bennett, R., Berry, A., Bhai, J., Bhurji, Simarpreet K., Bignell, A., Boddu, S., Branco Lins, P. R., Brooks, L., Ramaraju, S. B., Charkhchi, M., Cockburn, A., Da Rin Fiorretto, L., Davidson, C., Dodiya, K., Donaldson, S., El Houdaigui, B., El Naboulsi, T., Fatima, R., Giron, C. G., Genez, T., Ghattaoraya, G. S., Martinez, J. G., Guijarro, C., Hardy, M., Hollis, Z., Hourlier, T., Hunt, T., Kay, M., Kaykala, V., Le, T., Lemos, D., Marques-Coelho, D., Marugán, J. C., Merino, Gabriela A., Mirabueno, Louisse P., Mushtaq, A., Hossain, Syed N., Ogeh, D. N., Sakthivel, M. P., Parker, A., Perry, M., Piližota, I., Prosovetskaia, I., Pérez-Silva, J. G., Salam, Ahamed Imran A., Saraiva-Agostinho, N., Schuilenburg, H., Sheppard, D., Sinha, S., Sipos, B., Stark, W., Steed, E., Sukumaran, R., Sumathipala, D., Suner, M.-M., Surapaneni, L., Sutinen, K., Szpak, M., Tricomi, Francesca F., Urbina-Gómez, D., Veidenberg, A., Walsh, Thomas A., Walts, B., Wass, E., Willhoft, N., Allen, J., Alvarez-Jarreta, J., Chakiachvili, M., Flint, B., Giorgetti, S., Haggerty, L., Ilsley, Garth R., Loveland, Jane E., Moore, B., Mudge, Jonathan M., Tate, J., Thybert, D., Trevanion, Stephen J., Winterbottom, A., Frankish, A., Hunt, S. E., Ruffier, M., Cunningham, F., Dyer, S., Finn, Robert D., Howe, Kevin L., Harrison, P. W., Yates, A. D. and Flicek, P. (2022) 'Ensembl 2023', *Nucleic Acids Research,* 51(D1), pp. D933-D941.

Martinet, W., Coornaert, I., Puylaert, P. and De Meyer, G. R. Y. (2019) 'Macrophage Death as a Pharmacological Target in Atherosclerosis', *Front Pharmacol,* 10, pp. 306.

Masuda, H., Goto, M., Tamaoki, S. and Azuma, H. (1999) 'Accelerated intimal hyperplasia and increased endogenous inhibitors for NO synthesis in rabbits with alloxan-induced hyperglycaemia', *Br J Pharmacol,* 126(1), pp. 211-8.

Matthews, J. R., Botting, C. H., Panico, M., Morris, H. R. and Hay, R. T. (1996) 'Inhibition of NF-κB DNA binding by nitric oxide', *Nucleic acids research,* 24(12), pp. 2236-2242.

McMillan, G. C. (1995) 'Historical Review of Research on Atherosclerosis', in Longenecker, J.B., Kritchevsky, D. and Drezner, M.K. (eds.) *Nutrition and Biotechnology in Heart Disease and Cancer*. Boston, MA: Springer US, pp. 1-6.

Medina, E. (2009) 'Neutrophil extracellular traps: a strategic tactic to defeat pathogens with potential consequences for the host', *Journal of innate immunity,* 1(3), pp. 176-180.

Medzhitov, R., Preston-Hurlburt, P. and Janeway Jr, C. A. (1997) 'A human homologue of the Drosophila Toll protein signals activation of adaptive immunity', *Nature,* 388(6640), pp. 394-397.

Meinitzer, A., Seelhorst, U., Wellnitz, B., Halwachs-Baumann, G., Boehm, B. O., Winkelmann, B. R. and Marz, W. (2007) 'Asymmetrical dimethylarginine independently predicts total and cardiovascular mortality in individuals with angiographic coronary artery disease (the Ludwigshafen Risk and Cardiovascular Health study)', *Clinical chemistry,* 53(2), pp. 273-283.

Millar, T. M., Stevens, C. R., Benjamin, N., Eisenthal, R., Harrison, R. and Blake, D. R. (1998) 'Xanthine oxidoreductase catalyses the reduction of nitrates and nitrite to nitric oxide under hypoxic conditions', *FEBS Letters,* 427(2), pp. 225-228.

Min, K.-j., Cho, K.-H. and Kwon, T. K. (2012) 'The effect of oxidized low density lipoprotein (oxLDL)-induced heme oxygenase-1 on LPS-induced inflammation in RAW 264.7 macrophage cells', *Cellular signalling,* 24(6), pp. 1215-1221.

Misharin, A. V., Saber, R. and Perlman, H. (2012) 'Eosinophil contamination of thioglycollate-elicited peritoneal macrophage cultures skews the functional readouts of in vitro assays', *Journal of leukocyte biology,* 92(2), pp. 325-331.

Miwa, H., Fujii, J., Kanno, H., Taniguchi, N. and Aozasa, K. (2000) 'Pyruvate secreted by human lymphoid cell lines protects cells from hydrogen peroxide mediated cell death', *Free Radical Research,* 33(1), pp. 45-56.

Miyazaki, H., Matsuoka, H., Cooke, J. P., Usui, M., Ueda, S., Okuda, S. and Imaizumi, T. J. C. (1999) 'Endogenous nitric oxide synthase inhibitor: a novel marker of atherosclerosis', 99(9), pp. 1141-1146.

Moelants, E. A., Mortier, A., Van Damme, J. and Proost, P. (2013) 'Regulation of TNF-α with a focus on rheumatoid arthritis', *Immunology and cell biology,* 91(6), pp. 393-401.

Moore, K. J. and Tabas, I. J. C. (2011) 'Macrophages in the pathogenesis of atherosclerosis', 145(3), pp. 341-355.

Moormann, A., Koenig, R. and Meshnick, S. (1996) 'Effects of hydrogen peroxide, nitric oxide and antioxidants on NF-κB', *Redox Report,* 2(4), pp. 249-256.

Morales, Y., Cáceres, T., May, K., Hevel, J. M. J. A. o. b. and biophysics (2016) 'Biochemistry and regulation of the protein arginine methyltransferases (PRMTs)', 590, pp. 138-152.

Morris, D. L., Taylor, K. E., Fernando, M. M., Nititham, J., Alarcón-Riquelme, M. E., Barcellos, L. F., Behrens, T. W., Cotsapas, C., Gaffney, P. M. and Graham, R. R. (2012) 'Unraveling multiple MHC gene associations with systemic lupus erythematosus: model choice indicates a role for HLA alleles and non-HLA genes in Europeans', *The American Journal of Human Genetics,* 91(5), pp. 778-793.

Morris Jr, S. M. (2009) 'Recent advances in arginine metabolism: roles and regulation of the arginases', *British journal of pharmacology,* 157(6), pp. 922-930.

Mortazavi, A., Williams, B. A., McCue, K., Schaeffer, L. and Wold, B. (2008) 'Mapping and quantifying mammalian transcriptomes by RNA-Seq', *Nature methods,* 5(7), pp. 621-628.

Munder, M. (2009) 'Arginase: an emerging key player in the mammalian immune system', *British journal of pharmacology,* 158(3), pp. 638-651.

Munder, M., Eichmann, K., Morán, J. M., Centeno, F., Soler, G. and Modolell, M. (1999) 'Th1/Th2-regulated expression of arginase isoforms in murine macrophages and dendritic cells', *The Journal of Immunology,* 163(7), pp. 3771-3777.

Murad, F. (2011) 'Nitric oxide: the coming of the second messenger', *Rambam Maimonides Med J,* 2(2), pp. e0038.

Murakami, T., Mizuno, S. and Kaku, B. J. J. o. t. A. C. o. C. (1998) 'Clinical morbidities in subjects with Doppler-evaluated endothelial dysfunction of coronary artery', 31(2SA), pp. 419A-419A.

Murray-Rust, J., Leiper, J., McAlister, M., Phelan, J., Tilley, S., Maria, J. S., Vallance, P. and McDonald, N. (2001) 'Structural insights into the hydrolysis of cellular nitric oxide synthase inhibitors by dimethylarginine dimethylaminohydrolase', *Nature structural biology,* 8(8), pp. 679-683.

Mönckeberg, J. (1903) 'Über die reine Mediaverkalkung der', *Virchows Archiv für pathologische Anatomie und Physiologie und für klinische Medizin,* 171, pp. 141.

Nagalakshmi, U., Wang, Z., Waern, K., Shou, C., Raha, D., Gerstein, M. and Snyder, M. (2008) 'The transcriptional landscape of the yeast genome defined by RNA sequencing', *Science,* 320(5881), pp. 1344-1349.

Nagy, A. (2000) 'Cre recombinase: the universal reagent for genome tailoring', *genesis,* 26(2), pp. 99-109.

Napoli, C., D'Armiento, F. P., Mancini, F. P., Postiglione, A., Witztum, J. L., Palumbo, G. and Palinski, W. (1997) 'Fatty streak formation occurs in human

fetal aortas and is greatly enhanced by maternal hypercholesterolemia - Intimal accumulation of low density lipoprotein and its oxidation precede monocyte recruitment into early atherosclerotic lesions', *Journal of Clinical Investigation,* 100(11), pp. 2680-2690.

Newby, A. C. (2000) 'An overview of the vascular response to injury: a tribute to the late Russell Ross', *Toxicol Lett,* 112-113, pp. 519-29.

Nguyen, H., Chiasson, V. L., Chatterjee, P., Kopriva, S. E., Young, K. J. and Mitchell, B. M. (2013) 'Interleukin-17 causes Rho-kinase-mediated endothelial dysfunction and hypertension', *Cardiovascular research,* 97(4), pp. 696-704.

Noh, E. J., Ahn, K. S., Shin, E. M., Jung, S. H. and Kim, Y. S. (2006) 'Inhibition of lipopolysaccharide-induced iNOS and COX-2 expression by dehydroevodiamine through suppression of NF-κB activation in RAW 264.7 macrophages', *Life Sciences,* 79(7), pp. 695-701.

Nomura, M., Liu, J., Yu, Z.-X., Yamazaki, T., Yan, Y., Kawagishi, H., Rovira, I. I., Liu, C., Wolfgang, M. J. and Mukouyama, Y.-s. (2019) 'Macrophage fatty acid oxidation inhibits atherosclerosis progression', *Journal of molecular and cellular cardiology,* 127, pp. 270-276.

Nordlohne, J. and von Vietinghoff, S. (2019) 'Interleukin 17A in atherosclerosis–regulation and pathophysiologic effector function', *Cytokine,* 122, pp. 154089.

Notsu, Y., Yano, S., Shibata, H., Nagai, A. and Nabika, T. (2015) 'Plasma arginine/ADMA ratio as a sensitive risk marker for atherosclerosis: Shimane CoHRE study', *Atherosclerosis,* 239(1), pp. 61-66.

O'Donnell-Tormey, J., Nathan, C. F., Lanks, K., DeBoer, C. J. and de la Harpe, J. (1987) 'Secretion of pyruvate. An antioxidant defense of mammalian cells', *Journal of Experimental Medicine,* 165(2), pp. 500-514.

O'Dwyer, M. J., Dempsey, F., Crowley, V., Kelleher, D. P., McManus, R. and Ryan, T. J. C. c. (2006) 'Septic shock is correlated with asymmetrical dimethyl arginine levels, which may be influenced by a polymorphism in the

dimethylarginine dimethylaminohydrolase II gene: a prospective observational study', 10(5), pp. R139.

O'Neil, K. T., Hoess, R. H. and DeGrado, W. F. (1990) 'Design of DNA-binding peptides based on the leucine zipper motif', *Science,* 249(4970), pp. 774-778.

O'Shea, J. J., Gadina, M. and Siegel, R. M. (2019) '9 - Cytokines and Cytokine Receptors', in Rich, R.R., Fleisher, T.A., Shearer, W.T., Schroeder, H.W., Frew, A.J. and Weyand, C.M. (eds.) *Clinical Immunology (Fifth Edition)*. London: Elsevier, pp. 127-155.e1.

Ogawa, T., Kimoto, M. and Sasaoka, K. (1989) 'Purification and properties of a new enzyme, NG, NG-dimethylarginine dimethylaminohydrolase, from rat kidney', *Journal of Biological Chemistry,* 264(17), pp. 10205-10209.

Ogawa, T., Kimoto, M., Sasaoka, K. J. B. and communications, b. r. (1987) 'Occurrence of a new enzyme catalyzing the direct conversion of NG, NG-dimethyl-L-arginine to L-citrulline in rats', 148(2), pp. 671-677.

Ogawa, T., Kimoto, M. and Sasaoka, K. J. J. o. B. C. (1990) 'Dimethylarginine: pyruvate aminotransferase in rats. Purification, properties, and identity with alanine: glyoxylate aminotransferase 2', 265(34), pp. 20938-20945.

O'Brien, K. D., McDonald, T. O., Chait, A., Allen, M. D. and Alpers, C. E. (1996) 'Neovascular Expression of E-Selectin, Intercellular Adhesion Molecule-1, and Vascular Cell Adhesion Molecule-1 in Human Atherosclerosis and Their Relation to Intimal Leukocyte Content', *Circulation,* 93(4), pp. 672-682.

Pan, Y., Yu, C., Huang, J., Rong, Y., Chen, J. and Chen, M. (2020) 'Bioinformatics analysis of vascular RNA-seq data revealed hub genes and pathways in a novel Tibetan minipig atherosclerosis model induced by a high fat/cholesterol diet', *Lipids in Health and Disease,* 19, pp. 1-15.

Papp, K., Langley, R., Sigurgeirsson, B., Abe, M., Baker, D., Konno, P., Haemmerle, S., Thurston, H., Papavassilis, C. and Richards, H. (2013) 'Efficacy and safety of secukinumab in the treatment of moderate-to-severe plaque

psoriasis: a randomized, double-blind, placebo-controlled phase II dose-ranging study', *British Journal of Dermatology,* 168(2), pp. 412-421.

Parmar, K. M., Larman, H. B., Dai, G., Zhang, Y., Wang, E. T., Moorthy, S. N., Kratz, J. R., Lin, Z., Jain, M. K. and Gimbrone Jr, M. A. (2006) 'Integration of flow-dependent endothelial phenotypes by Kruppel-like factor 2', *The Journal of clinical investigation,* 116(1), pp. 49-58.

Patsopoulos, N. A., Barcellos, L. F., Hintzen, R. Q., Schaefer, C., van Duijn, C. M., Noble, J. A., Raj, T., Gourraud, P. A., Stranger, B. E., Oksenberg, J., Olsson, T., Taylor, B. V., Sawcer, S., Hafler, D. A., Carrington, M., De Jager, P. L. and de Bakker, P. I. (2013) 'Fine-mapping the genetic association of the major histocompatibility complex in multiple sclerosis: HLA and non-HLA effects', *PLoS Genet,* 9(11), pp. e1003926.

Pavlou, S., Lindsay, J., Ingram, R., Xu, H. and Chen, M. (2018) 'Sustained high glucose exposure sensitizes macrophage responses to cytokine stimuli but reduces their phagocytic activity', *BMC Immunology,* 19(1), pp. 24.

Pavlou, S., Wang, L., Xu, H. and Chen, M. (2017) 'Higher phagocytic activity of thioglycollate-elicited peritoneal macrophages is related to metabolic status of the cells', *Journal of Inflammation,* 14(1), pp. 4.

Pekarova, M., Kubala, L., Martiskova, H., Bino, L., Twarogova, M., Klinke, A., Rudolph, T. K., Kuchtova, Z., Kolarova, H., Ambrozova, G., Kuchta, R., Kadlec, J. and Lojek, A. (2013) 'Asymmetric dimethylarginine regulates the lipopolysaccharide-induced nitric oxide production in macrophages by suppressing the activation of NF-kappaB and iNOS expression', *European Journal of Pharmacology,* 713(1), pp. 68-77.

Perticone, F., Sciacqua, A., Maio, R., Perticone, M., Maas, R., Boger, R. H., Tripepi, G., Sesti, G. and Zoccali, C. (2005) 'Asymmetric Dimethylarginine, L-Arginine, and Endothelial Dysfunction in Essential Hypertension', *Journal of the American College of Cardiology,* 46(3), pp. 518-523.

Piazza, M., Guillemette, J. G. and Dieckmann, T. (2015) 'Dynamics of Nitric Oxide Synthase–Calmodulin Interactions at Physiological Calcium Concentrations', *Biochemistry,* 54(11), pp. 1989-2000.

Pirro, M., Schillaci, G., Savarese, G., Gemelli, F., Mannarino, M. R., Siepi, D., Bagaglia, F., Mannarino, E. J. E. J. o. C. P. and Rehabilitation (2004) 'Attenuation of inflammation with short-term dietary intervention is associated with a reduction of arterial stiffness in subjects with hypercholesterolaemia', 11(6), pp. 497-502.

Pollock, J. S., Förstermann, U., Mitchell, J. A., Warner, T. D., Schmidt, H. H., Nakane, M. and Murad, F. (1991) 'Purification and characterization of particulate endothelium-derived relaxing factor synthase from cultured and native bovine aortic endothelial cells', *Proceedings of the National Academy of Sciences,* 88(23), pp. 10480-10484.

Poltorak, A., He, X., Smirnova, I., Liu, M.-Y., Huffel, C. V., Du, X., Birdwell, D., Alejos, E., Silva, M. and Galanos, C. (1998) 'Defective LPS signaling in C3H/HeJ and C57BL/10ScCr mice: mutations in Tlr4 gene', *Science,* 282(5396), pp. 2085-2088.

Pope, A. J., Karuppiah, K. and Cardounel, A. J. (2009) 'Role of the PRMT–DDAH-ADMA axis in the regulation of endothelial nitric oxide production', *Pharmacological Research,* 60(6), pp. 461-465.

Potteaux, S., Gautier, E. L., Hutchison, S. B., Van Rooijen, N., Rader, D. J., Thomas, M. J., Sorci-Thomas, M. G. and Randolph, G. J. (2011) 'Suppressed monocyte recruitment drives macrophage removal from atherosclerotic plaques of Apoe−/−mice during disease regression', *The Journal of clinical investigation,* 121(5), pp. 2025-2036.

Pourcet, B., Feig, J. E., Vengrenyuk, Y., Hobbs, A. J., Kepka-Lenhart, D., Garabedian, M. J., Morris Jr, S. M., Fisher, E. A. and Pineda-Torra, I. (2011) 'LXRα regulates macrophage arginase 1 through PU. 1 and interferon regulatory factor 8', *Circulation research,* 109(5), pp. 492-501.

Poznyak, A. V., Sadykhov, N. K., Kartuesov, A. G., Borisov, E. E., Melnichenko, A. A., Grechko, A. V. and Orekhov, A. N. (2022) 'Hypertension as a risk factor for atherosclerosis: Cardiovascular risk assessment', *Front Cardiovasc Med,* 9, pp. 959285.

Puylaert, P., Zurek, M., Rayner, K. J., Meyer, G. R. Y. D. and Martinet, W. (2022) 'Regulated Necrosis in Atherosclerosis', *Arteriosclerosis, Thrombosis, and Vascular Biology,* 42(11), pp. 1283-1306.

Päivä, H., Laakso, J., Laine, H., Laaksonen, R., Knuuti, J. and Raitakari, O. T. (2002) 'Plasma asymmetric dimethylarginine and hyperemic myocardial blood flow in young subjects with borderline hypertension or familial hypercholesterolemia', *Journal of the American College of Cardiology,* 40(7), pp. 1241-1247.

Qi, J., Kan, F., Ye, X., Guo, M., Zhang, Y., Ren, G. and Li, D. (2012) 'A bispecific antibody against IL-1ß and IL-17A is beneficial for experimental rheumatoid arthritis', *Int Immunopharmacol,* 14(4), pp. 770-8.

Radomski, M., Palmer, R. and Moncada, S. (1987) 'Endogenous nitric oxide inhibits human platelet adhesion to vascular endothelium', *The Lancet,* 330(8567), pp. 1057-1058.

Ragavan, V. N., Nair, P. C., Jarzebska, N., Angom, R. S., Ruta, L., Bianconi, E., Grottelli, S., Tararova, N. D., Ryazanskiy, D. and Lentz, S. R. (2023) 'A multicentric consortium study demonstrates that dimethylarginine dimethylaminohydrolase 2 is not a dimethylarginine dimethylaminohydrolase', *Nature communications,* 14(1), pp. 3392.

Raschke, W. C. 'Transformation by Abelson murine leukemia virus: properties of the transformed cells'. *Cold Spring Harbor Symposia on Quantitative Biology*: Citeseer, 1187-1194.

Raschke, W. C., Baird, S., Ralph, P. and Nakoinz, I. (1978) 'Functional macrophage cell lines transformed by Abelson leukemia virus', *Cell,* 15(1), pp. 261-7.

Rath, M., Müller, I., Kropf, P., Closs, E. I. and Munder, M. (2014) 'Metabolism via Arginase or Nitric Oxide Synthase: Two Competing Arginine Pathways in Macrophages', *Frontiers in Immunology,* 5.

Ravin, K. A. and Loy, M. (2016) 'The Eosinophil in Infection', *Clinical Reviews in Allergy & Immunology,* 50(2), pp. 214-227.

Reece, S. W., Varikuti, S., Kilburg-Basnyat, B., Dunigan-Russell, K., Hodge, M. X., Luo, B., Madenspacher, J. H., Thomas, S. Y., Tokarz, D. A. and Tighe, R. M. (2021) 'Scavenger receptor BI attenuates IL-17A–dependent neutrophilic inflammation in asthma', *American Journal of Respiratory Cell and Molecular Biology,* 64(6), pp. 698-708.

Rich, P., Sigurgeirsson, B., Thaci, D., Ortonne, J. P., Paul, C., Schopf, R., Morita, A., Roseau, K., Harfst, E. and Guettner, A. (2013) 'Secukinumab induction and maintenance therapy in moderate-to-severe plaque psoriasis: a randomized, double-blind, placebo-controlled, phase II regimen-finding study', *British Journal of Dermatology,* 168(2), pp. 402-411.

Ridker, P. M., Danielson, E., Fonseca, F. A., Genest, J., Gotto Jr, A. M., Kastelein, J. J., Koenig, W., Libby, P., Lorenzatti, A. J. and MacFadyen, J. G. J. T. L. (2009) 'Reduction in C-reactive protein and LDL cholesterol and cardiovascular event rates after initiation of rosuvastatin: a prospective study of the JUPITER trial', 373(9670), pp. 1175-1182.

Rios, F. J., Ferracini, M., Pecenin, M., Koga, M. M., Wang, Y., Ketelhuth, D. F. and Jancar, S. (2013) 'Uptake of oxLDL and IL-10 production by macrophages requires PAFR and CD36 recruitment into the same lipid rafts', *Plos one,* 8(10), pp. e76893.

Rios, F. J., Touyz, R. M. and Montezano, A. C. (2017) 'Isolation and Differentiation of Murine Macrophages', *Hypertension*: Springer New York, pp. 297-309.

Robbins, C. S., Hilgendorf, I., Weber, G. F., Theurl, I., Iwamoto, Y., Figueiredo, J.-L., Gorbatov, R., Sukhova, G. K., Gerhardt, L. M. S., Smyth, D., Zavitz, C. C.

J., Shikatani, E. A., Parsons, M., van Rooijen, N., Lin, H. Y., Husain, M., Libby, P., Nahrendorf, M., Weissleder, R. and Swirski, F. K. (2013) 'Local proliferation dominates lesional macrophage accumulation in atherosclerosis', *Nature Medicine,* 19(9), pp. 1166-1172.

Roberson, E. D. O., Liu, Y., Ryan, C., Joyce, C. E., Duan, S., Cao, L., Martin, A., Liao, W., Menter, A. and Bowcock, A. M. (2012) 'A Subset of Methylated CpG Sites Differentiate Psoriatic from Normal Skin', *Journal of Investigative Dermatology,* 132(3, Part 1), pp. 583-592.

Robert, M., Hot, A., Mifsud, F., Ndongo-Thiam, N. and Miossec, P. (2020) 'Synergistic Interaction Between High Bioactive IL-17A and Joint Destruction for the Occurrence of Cardiovascular Events in Rheumatoid Arthritis', *Front Immunol,* 11, pp. 1998.

Robichaux III, W. G., Mei, F. C., Yang, W., Wang, H., Sun, H., Zhou, Z., Milewicz, D. M., Teng, B.-B. and Cheng, X. (2020) 'Epac1 (exchange protein directly activated by cAMP 1) upregulates LOX-1 (oxidized low-density lipoprotein receptor 1) to promote foam cell formation and atherosclerosis development', *Arteriosclerosis, thrombosis, and vascular biology,* 40(12), pp. e322-e335.

Rodionov, R. N., Murry, D. J., Vaulman, S. F., Stevens, J. W. and Lentz, S. R. (2010) 'Human alanine-glyoxylate aminotransferase 2 lowers asymmetric dimethylarginine and protects from inhibition of nitric oxide production', *Journal of Biological Chemistry,* 285(8), pp. 5385-5391.

Rodrigues-Díez, R., Aroeira, L. S., Orejudo, M., Bajo, M. A., Heffernan, J. J., Rodrigues-Díez, R. R., Rayego-Mateos, S., Ortiz, A., Gonzalez-Mateo, G., López-Cabrera, M., Selgas, R., Egido, J. and Ruiz-Ortega, M. (2014) 'IL-17A is a novel player in dialysis-induced peritoneal damage', *Kidney International,* 86(2), pp. 303-315.

Ross, R. (1993) 'ATHEROSCLEROSIS - A DEFENSE-MECHANISM GONE', *American Journal of Pathology,* 143(4), pp. 987-1002.

Ross, R. (1999) 'Atherosclerosis — An Inflammatory Disease', 340(2), pp. 115-126.

Ross, R., Glomset, J. and Harker, L. (1977) 'Response to injury and atherogenesis', *Am J Pathol,* 86(3), pp. 675-84.

Roy, P., Orecchioni, M. and Ley, K. (2022) 'How the immune system shapes atherosclerosis: roles of innate and adaptive immunity', *Nature Reviews Immunology,* 22(4), pp. 251-265.

Ryan, R., Thornton, J., Duggan, E., McGovern, E., O'Dwyer, M. J., Ryan, A. W., Kelleher, D., McManus, R. and Ryan, T. (2006) 'Gene polymorphism and requirement for vasopressor infusion after cardiac surgery', *The Annals of thoracic surgery,* 82(3), pp. 895-901.

Salvayre, R., Auge, N., Benoist, H. and Negre-Salvayre, A. (2002) 'Oxidized low-density lipoprotein-induced apoptosis', *Biochimica et Biophysica Acta (BBA) - Molecular and Cell Biology of Lipids,* 1585(2), pp. 213-221.

Sasaki, T. and Matano, K. (1979) 'Formation of nitrite from nitrate at the dorsum linguae studies on nitrite formation in the human oral cavity (I)', *Food Hygiene and Safety Science (Shokuhin Eiseigaku Zasshi),* 20(5), pp. 363-369.

Sauer, B. (1998) 'Inducible gene targeting in mice using the Cre/loxSystem', *Methods,* 14(4), pp. 381-392.

Sauer, B. and Henderson, N. (1988) 'Site-specific DNA recombination in mammalian cells by the Cre recombinase of bacteriophage P1', *Proceedings of the National Academy of Sciences,* 85(14), pp. 5166-5170.

Schillaci, G., Pucci, G., Pirro, M., Monacelli, M., Scarponi, A. M., Manfredelli, M. R., Rondelli, F., Avenia, N. and Mannarino, E. J. A. (2011) 'Large-artery stiffness: a reversible marker of cardiovascular risk in primary hyperparathyroidism', 218(1), pp. 96-101.

Schlesinger, S., Sonntag, S. R., Lieb, W. and Maas, R. J. P. O. (2016) 'Asymmetric and symmetric dimethylarginine as risk markers for total mortality and

cardiovascular outcomes: a systematic review and meta-analysis of prospective studies', 11(11).

Schmidt, H., Pollock, J. S., Nakane, M., Gorsky, L. D., Förstermann, U. and Murad, F. (1991) 'Purification of a soluble isoform of guanylyl cyclase-activating-factor synthase', *Proceedings of the National Academy of Sciences,* 88(2), pp. 365-369.

Schulze, F., Maas, R., Freese, R., Schwedhelm, E., Silberhorn, E. and Böger, R. J. E. j. o. c. i. (2005) 'Determination of a reference value for NG, NG-dimethyl-L-arginine in 500 subjects', 35(10), pp. 622-626.

Schwartz, D., Mendonca, M., Schwartz, I., Xia, Y., Satriano, J., Wilson, C. B. and Blantz, R. C. J. T. J. o. c. i. (1997) 'Inhibition of constitutive nitric oxide synthase (NOS) by nitric oxide generated by inducible NOS after lipopolysaccharide administration provokes renal dysfunction in rats', 100(2), pp. 439-448.

Seimon, T. and Tabas, I. (2009) 'Mechanisms and consequences of macrophage apoptosis in atherosclerosis', *Journal of lipid research,* 50, pp. S382-S387.

Seo, D., Wang, T., Dressman, H., Herderick, E. E., Iversen, E. S., Dong, C., Vata, K., Milano, C. A., Rigat, F. and Pittman, J. (2004) 'Gene expression phenotypes of atherosclerosis', *Arteriosclerosis, thrombosis, and vascular biology,* 24(10), pp. 1922-1927.

Seo, H.-A., Kim, S.-W., Jeon, E.-J., Jeong, J.-Y., Moon, S.-S., Lee, W.-K., Kim, J.-G., Lee, I.-K. and Park, K.-G. (2012) 'Association of the DDAH2 gene polymorphism with type 2 diabetes and hypertension', *Diabetes Research and Clinical Practice,* 98(1), pp. 125-131.

Sesti, G., Mannino, G. C., De Lorenzo, C., Greco, A., Sciacqua, A., Marini, M. A., Andreozzi, F. and Perticone, F. (2013) 'A functional variant of the dimethylarginine dimethylaminohydrolase-2 gene is associated with chronic kidney disease', *Atherosclerosis,* 231(1), pp. 141-144.

Shah, A. M., Spurgeon, H. A., Sollott, S. J., Talo, A. and Lakatta, E. G. (1994) '8-Bromo-cGMP reduces the myofilament response to Ca2+ in intact cardiac myocytes', *Circulation Research,* 74(5), pp. 970-978.

Shapouri-Moghaddam, A., Mohammadian, S., Vazini, H., Taghadosi, M., Esmaeili, S. A., Mardani, F., Seifi, B., Mohammadi, A., Afshari, J. T. and Sahebkar, A. J. J. o. c. p. (2018) 'Macrophage plasticity, polarization, and function in health and disease', 233(9), pp. 6425-6440.

Sharma, J., Al-Omran, A. and Parvathy, S. (2007) 'Role of nitric oxide in inflammatory diseases', *Inflammopharmacology,* 15, pp. 252-259.

Sharma, T., Romeo, F. and Mehta, J. L. (2022) 'LOX-1: Implications in atherosclerosis and myocardial ischemia', *EXCLI journal,* 21, pp. 273.

Shi, J., Hua, L., Harmer, D., Li, P. and Ren, G. (2018) 'Cre Driver Mice Targeting Macrophages', *Methods Mol Biol,* 1784, pp. 263-275.

Shi, Y., Evans, J. E. and Rock, K. L. (2003) 'Molecular identification of a danger signal that alerts the immune system to dying cells', *Nature,* 425(6957), pp. 516-521.

Shi, Y. and He, M. (2014) 'Differential gene expression identified by RNA-Seq and qPCR in two sizes of pearl oyster (Pinctada fucata)', *Gene,* 538(2), pp. 313-322.

Shimada, K. J. C. J. (2009) 'Immune system and atherosclerotic disease', 73(6), pp. 994-1001.

Shin, J., Edelberg, J. E. and Hong, M. K. (2003) 'Vulnerable atherosclerotic plaque: clinical implications', *Current vascular pharmacology,* 1(2), pp. 183-204.

Shiva, S., Huang, Z., Grubina, R., Sun, J., Ringwood, L. A., MacArthur, P. H., Xu, X., Murphy, E., Darley-Usmar, V. M. and Gladwin, M. T. (2007) 'Deoxymyoglobin is a nitrite reductase that generates nitric oxide and regulates mitochondrial respiration', *Circulation research,* 100(5), pp. 654-661.

Shivkar, R. R. and Abhang, S. A. (2014) 'Ratio of serum asymmetric dimethyl arginine (ADMA)/nitric oxide in coronary artery disease patients', *Journal of Clinical and Diagnostic Research: JCDR,* 8(8), pp. CC04.

Sica, A. and Mantovani, A. (2012) 'Macrophage plasticity and polarization: in vivo veritas', *J Clin Invest,* 122(3), pp. 787-95.

Silveira Rossi, J. L., Barbalho, S. M., Reverete de Araujo, R., Bechara, M. D., Sloan, K. P. and Sloan, L. A. (2022) 'Metabolic syndrome and cardiovascular diseases: Going beyond traditional risk factors', *Diabetes Metab Res Rev,* 38(3), pp. e3502.

Simionescu, N., Vasile, E., Lupu, F., Popescu, G. and Simionescu, M. (1986) 'PRELESIONAL EVENTS IN ATHEROGENESIS - ACCUMULATION OF EXTRACELLULAR CHOLESTEROL-RICH LIPOSOMES IN THE ARTERIAL INTIMA AND CARDIAC VALVES OF THE HYPERLIPIDEMIC RABBIT', *American Journal of Pathology,* 123(1), pp. 109-125.

Singh, R. K., Haka, A. S., Asmal, A., Barbosa-Lorenzi, V. C., Grosheva, I., Chin, H. F., Xiong, Y., Hla, T. and Maxfield, F. R. (2020) 'TLR4 (Toll-Like Receptor 4)-Dependent Signaling Drives Extracellular Catabolism of LDL (Low-Density Lipoprotein) Aggregates', *Arteriosclerosis, Thrombosis, and Vascular Biology,* 40(1), pp. 86-102.

Sinha, S. K., Miikeda, A., Fouladian, Z., Mehrabian, M., Edillor, C., Shih, D., Zhou, Z., Paul, M. K., Charugundla, S. and Davis, R. C. (2021) 'Local M-CSF (macrophage colony-stimulating factor) expression regulates macrophage proliferation and apoptosis in atherosclerosis', *Arteriosclerosis, thrombosis, and vascular biology,* 41(1), pp. 220-233.

Smirnova, I., Kajstura, M., Sawamura, T. and Goligorsky, M. (2004) 'Asymmetric dimethylarginine upregulates LOX-1 in activated macrophages: role in foam cell formation', *American Journal of Physiology-Heart and Circulatory Physiology,* 287(2), pp. H782-H790.

Smirnova, I. V., Sawamura, T. and Goligorsky, M. S. (2004) 'Upregulation of lectin-like oxidized low-density lipoprotein receptor-1 (LOX-1) in endothelial cells by nitric oxide deficiency', *American Journal of Physiology-Renal Physiology,* 287(1), pp. F25-F32.

Son, D. J., Kumar, S., Takabe, W., Woo Kim, C., Ni, C.-W., Alberts-Grill, N., Jang, I.-H., Kim, S., Kim, W. and Won Kang, S. (2013) 'The atypical mechanosensitive microRNA-712 derived from pre-ribosomal RNA induces endothelial inflammation and atherosclerosis', *Nature communications,* 4(1), pp. 3000.

Song, C., Luo, L., Lei, Z., Li, B., Liang, Z., Liu, G., Li, D., Zhang, G., Huang, B. and Feng, Z.-H. (2008) 'IL-17-producing alveolar macrophages mediate allergic lung inflammation related to asthma', *The Journal of Immunology,* 181(9), pp. 6117-6124.

Soudi, S., Zavaran-Hosseini, A., Hassan, Z. M., Soleimani, M., Adegani, F. J. and Hashemi, S. M. (2013) 'Comparative study of the effect of LPS on the function of BALB/c and C57BL/6 peritoneal macrophages', *Cell Journal (Yakhteh),* 15(1), pp. 45.

Spanjaard, R. A., Lee, P. J., Sarkar, S., Goedegebuure, P. S. and Eberlein, T. J. (1997) 'Clone 10d/BM28 (CDCL1), an early S-phase protein, is an important growth regulator of melanoma', *Cancer Res,* 57(22), pp. 5122-8.

Stark, R., Grzelak, M. and Hadfield, J. (2019) 'RNA sequencing: the teenage years', *Nature Reviews Genetics,* 20(11), pp. 631-656.

Steffen, Y., Vuillaume, G., Stolle, K., Roewer, K., Lietz, M., Schueller, J., Lebrun, S. and Wallerath, T. (2012) 'Cigarette smoke and LDL cooperate in reducing nitric oxide bioavailability in endothelial cells via effects on both eNOS and NADPH oxidase', *Nitric Oxide,* 27(3), pp. 176-184.

Stepp, D. W., Ou, J., Ackerman, A. W., Welak, S., Klick, D. and Pritchard Jr, K. A. (2002) 'Native LDL and minimally oxidized LDL differentially regulate

superoxide anion in vascular endothelium in situ', *American Journal of Physiology-Heart and Circulatory Physiology,* 283(2), pp. H750-H759.

Sternberg, N., Austin, S., Hamilton, D. and Yarmolinsky, M. (1978) 'Analysis of bacteriophage P1 immunity by using lambda-P1 recombinants constructed in vitro', *Proceedings of the National Academy of Sciences,* 75(11), pp. 5594-5598.

Stuehr, D. J., Cho, H. J., Kwon, N. S., Weise, M. F. and Nathan, C. F. (1991a) 'Purification and characterization of the cytokine-induced macrophage nitric oxide synthase: an FAD-and FMN-containing flavoprotein', *Proceedings of the National Academy of Sciences,* 88(17), pp. 7773-7777.

Stuehr, D. J., Kwon, N. S., Nathan, C. F., Griffith, O. W., Feldman, P. L. and Wiseman, J. (1991b) 'N omega-hydroxy-L-arginine is an intermediate in the biosynthesis of nitric oxide from L-arginine', *Journal of Biological Chemistry,* 266(10), pp. 6259-6263.

Stühlinger, M. C., Tsao, P. S., Her, J.-H., Kimoto, M., Balint, R. F. and Cooke, J. P. (2001) 'Homocysteine impairs the nitric oxide synthase pathway: role of asymmetric dimethylarginine', *Circulation,* 104(21), pp. 2569-2575.

Sydow, K. and Münzel, T. (2003) 'ADMA and oxidative stress', *Atherosclerosis Supplements,* 4(4), pp. 41-51.

Taciak, B., Białasek, M., Braniewska, A., Sas, Z., Sawicka, P., Kiraga, Ł., Rygiel, T. and Król, M. (2018) 'Evaluation of phenotypic and functional stability of RAW 264.7 cell line through serial passages', *PLOS ONE,* 13(6), pp. e0198943.

Tain, Y.-L. and Hsu, C.-N. (2017) 'Toxic dimethylarginines: asymmetric dimethylarginine (ADMA) and symmetric dimethylarginine (SDMA)', *Toxins,* 9(3), pp. 92.

Takada, Y. and Noguchi, T. (1982) 'Subcellular distribution, and physical and immunological properties of hepatic alanine: glyoxylate aminotransferase isoenzymes in different mammalian species', *Comparative Biochemistry and physiology. B, Comparative Biochemistry,* 72(4), pp. 597-604.

Takahashi, M., Ishida, T., Traub, O., Corson, M. A. and Berk, B. C. (1997) 'Mechanotransduction in endothelial cells: temporal signaling events in response to shear stress', *Journal of vascular research,* 34(3), pp. 212-219.

Tan, L., Wang, Z. and Li, Y. (2018) 'Rabbit models provide insights into bone formation related biological process in atherosclerotic vascular calcification', *Biochemical and biophysical research communications,* 496(4), pp. 1369-1375.

Teerlink, T. J. J. o. C. B. (2007) 'HPLC analysis of ADMA and other methylated L-arginine analogs in biological fluids', 851(1-2), pp. 21-29.

Teerlink, T. J. V. m. (2005) 'ADMA metabolism and clearance', 10(1_suppl), pp. S73-S81.

Teupser, D., Burkhardt, R., Wilfert, W., Haffner, I., Nebendahl, K. and Thiery, J. (2006) 'Identification of macrophage arginase I as a new candidate gene of atherosclerosis resistance', *Arteriosclerosis, thrombosis, and vascular biology,* 26(2), pp. 365-371.

Thomas, A. C., Sala-Newby, G. B., Ismail, Y., Johnson, J. L., Pasterkamp, G. and Newby, A. C. (2007) 'Genomics of foam cells and nonfoamy macrophages from rabbits identifies arginase-I as a differential regulator of nitric oxide production', *Arteriosclerosis, thrombosis, and vascular biology,* 27(3), pp. 571-577.

Thomas, G. S., Wann, L. S., Allam, A. H., Thompson, R. C., Michalik, D. E., Sutherland, M. L., Sutherland, J. D., Lombardi, G. P., Watson, L., Cox, S. L., Valladolid, C. M., Abd el-Maksoud, G., Al-Tohamy Soliman, M., Badr, I., el-Halim Nur el-din, A., Clarke, E. M., Thomas, I. G., Miyamoto, M. I., Kaplan, H. S., Frohlich, B., Narula, J., Stewart, A. F. R., Zink, A. and Finch, C. E. (2014) 'Why Did Ancient People Have Atherosclerosis?: From Autopsies to Computed Tomography to Potential Causes', *Global Heart,* 9(2), pp. 229-237.

Thompson, R. C., Allam, A. H., Lombardi, G. P., Wann, L. S., Sutherland, M. L., Sutherland, J. D., Soliman, M. A.-T., Frohlich, B., Mininberg, D. T. and Monge, J. M. (2013) 'Atherosclerosis across 4000 years of human history: the Horus study of four ancient populations', *The lancet,* 381(9873), pp. 1211-1222.

Thorp, E., Cui, D., Schrijvers, D. M., Kuriakose, G. and Tabas, I. (2008) 'Mertk receptor mutation reduces efferocytosis efficiency and promotes apoptotic cell accumulation and plaque necrosis in atherosclerotic lesions of apoe−/− mice', *Arteriosclerosis, thrombosis, and vascular biology,* 28(8), pp. 1421-1428.

Thrum, S., Sommer, M., Raulien, N., Gericke, M., Massier, L., Kovacs, P., Krasselt, M., Landgraf, K., Körner, A., Dietrich, A., Blüher, M., Rossol, M. and Wagner, U. (2022) 'Macrophages in obesity are characterised by increased IL-1ß response to calcium-sensing receptor signals', *International Journal of Obesity,* 46(10), pp. 1883-1891.

Toda, G., Yamauchi, T., Kadowaki, T. and Ueki, K. (2021) 'Preparation and culture of bone marrow-derived macrophages from mice for functional analysis', *STAR Protocols,* 2(1), pp. 100246.

Tojo, A., Welch, W. J., Bremer, V., Kimoto, M., Kimura, K., Omata, M., Ogawa, T., Vallance, P. and Wilcox, C. S. (1997) 'Colocalization of demethylating enzymes and NOS and functional effects of methylarginines in rat kidney', *Kidney international,* 52(6), pp. 1593-1601.

Topper, J. N. and Gimbrone Jr, M. A. (1999) 'Blood flow and vascular gene expression: fluid shear stress as a modulator of endothelial phenotype', *Molecular medicine today,* 5(1), pp. 40-46.

Torchia, E. C., Boyd, K., Rehg, J. E., Qu, C. and Baker, S. J. (2007) 'EWS/FLI-1 induces rapid onset of myeloid/erythroid leukemia in mice', *Mol Cell Biol,* 27(22), pp. 7918-34.

Tran, C. T. L., Fox, M. F., Vallance, P. and Leiper, J. M. (2000) 'Chromosomal Localization, Gene Structure, and Expression Pattern of DDAH1: Comparison with DDAH2 and Implications for Evolutionary Origins', *Genomics,* 68(1), pp. 101-105.

Traub, O. and Berk, B. C. (1998) 'Laminar shear stress: mechanisms by which endothelial cells transduce an atheroprotective force', *Arteriosclerosis, thrombosis, and vascular biology,* 18(5), pp. 677-685.

Trogan, E., Feig, J. E., Dogan, S., Rothblat, G. H., Angeli, V., Tacke, F., Randolph, G. J. and Fisher, E. A. (2006) 'Gene expression changes in foam cells and the role of chemokine receptor CCR7 during atherosclerosis regression in ApoE-deficient mice', *Proceedings of the National Academy of Sciences,* 103(10), pp. 3781-3786.

Trus, E., Basta, S. and Gee, K. (2020) 'Who's in charge here? Macrophage colony stimulating factor and granulocyte macrophage colony stimulating factor: Competing factors in macrophage polarization', *Cytokine,* 127, pp. 154939.

Untergasser, A., Cutcutache, I., Koressaar, T., Ye, J., Faircloth, B. C., Remm, M. and Rozen, S. G. (2012) 'Primer3--new capabilities and interfaces', *Nucleic Acids Res,* 40(15), pp. e115.

Vallance, P., Leone, A., Calver, A., Collier, J. and Moncada, S. (1992) 'Endogenous dimethylarginine as an inhibitor of nitric oxide synthesis', *Journal of cardiovascular pharmacology,* 20, pp. S60-2.

van den Berg, M. P. M., Meurs, H. and Gosens, R. (2018) 'Targeting arginase and nitric oxide metabolism in chronic airway diseases and their co-morbidities', *Current Opinion in Pharmacology,* 40, pp. 126-133.

Van Opdenbosch, N. and Lamkanfi, M. (2019) 'Caspases in Cell Death, Inflammation, and Disease', *Immunity,* 50(6), pp. 1352-1364.

Vieira, O., Escargueil-Blanc, I., Jurgens, G., Borner, C., Almeida, L., Salvayre, R. and Negre-salvayre, A. (2000) 'Oxidized LDLs alter the activity of the ubiquitin-proteasome pathway: potential role in oxidized LDL-induced apoptosis', *The FASEB Journal,* 14(3), pp. 532-542.

Vincent, J.-L., Zhang, H., Szabo, C. and Preiser, J.-C. (2000) 'Effects of Nitric Oxide in Septic Shock', *American Journal of Respiratory and Critical Care Medicine,* 161(6), pp. 1781-1785.

Virmani, R., Kolodgie, F. D., Burke, A. P., Farb, A. and Schwartz, S. M. (2000) 'Lessons From Sudden Coronary Death', *Arteriosclerosis, Thrombosis, and Vascular Biology,* 20(5), pp. 1262-1275.

Vivier, E., Tomasello, E., Baratin, M., Walzer, T. and Ugolini, S. (2008) 'Functions of natural killer cells', *Nature Immunology,* 9(5), pp. 503-510.

Vodovotz, Y., Kwon, N., Pospischil, M., Manning, J., Paik, J. and Nathan, C. J. T. J. o. I. (1994) 'Inactivation of nitric oxide synthase after prolonged incubation of mouse macrophages with IFN-gamma and bacterial lipopolysaccharide', 152(8), pp. 4110-4118.

Voehringer, D. (2017) 'Recent advances in understanding basophil functions in vivo', *F1000Research,* 6.

Wamhoff, B., Hoofnagle, M., Burns, A., Sinha, S., McDonald, O. and Owens, G. (2004) 'AG/C element mediates repression of the SM22α promoter within phenotypically modulated smooth muscle cells in experimental atherosclerosis', *Circulation research,* 95(10), pp. 981-988.

Wang, C., Yu, X., Cao, Q., Wang, Y., Zheng, G., Tan, T. K., Zhao, H., Zhao, Y., Wang, Y. and Harris, D. C. H. (2013) 'Characterization of murine macrophages from bone marrow, spleen and peritoneum', *BMC Immunology,* 14(1), pp. 6.

Wang, D., Gill, P. S., Chabrashvili, T., Onozato, M. L., Raggio, J., Mendonca, M., Dennehy, K., Li, M., Modlinger, P., Leiper, J., Vallance, P., Adler, O., Leone, A., Tojo, A., Welch, W. J. and Wilcox, C. S. (2007) 'Isoform-specific regulation by NG,NG-dimethylarginine dimethylaminohydrolase of rat serum asymmetric dimethylarginine and vascular endothelium-derived relaxing factor/NO', *Circulation Research,* 101(6), pp. 627-635.

Wang, J., Cheng, X. and Shi, G.-P. 2011. Immunoglobulin E promotes vascular wall cell inflammatory molecule expression, apoptosis, and atherogenesis. Am Heart Assoc.

Wann, L. S., Narula, J., Blankstein, R., Thompson, R. C., Frohlich, B., Finch, C. E. and Thomas, G. S. (2019) 'Atherosclerosis in 16th-Century Greenlandic Inuit Mummies', *JAMA Network Open,* 2(12), pp. e1918270-e1918270.

Weinberg, J. B., Granger, D. L., Pisetsky, D. S., Seldin, M. F., Misukonis, M. A., Mason, S. N., Pippen, A. M., Ruiz, P., Wood, E. R. and Gilkeson, G. S. J. T. J. o. e. m. (1994) 'The role of nitric oxide in the pathogenesis of spontaneous murine autoimmune disease: increased nitric oxide production and nitric oxide synthase expression in MRL-lpr/lpr mice, and reduction of spontaneous glomerulonephritis and arthritis by orally administered NG-monomethyl-L-arginine', 179(2), pp. 651-660.

Weis, M., Kledal, T. N., Lin, K. Y., Panchal, S. N., Gao, S., Valantine, H. A., Mocarski, E. S. and Cooke, J. P. (2004) 'Cytomegalovirus infection impairs the nitric oxide synthase pathway: role of asymmetric dimethylarginine in transplant arteriosclerosis', *Circulation,* 109(4), pp. 500-505.

Windaus, A. (1910) 'Über den Gehalt normaler und atheromatöser Aorten an Cholesterin und Cholesterinestern', 67(2), pp. 174-176.

Wink, D. A., Hanbauer, I., Grisham, M. B., Laval, F., Nims, R. W., Laval, J., Cook, J., Pacelli, R., Liebmann, J., Krishna, M., Ford, P. C. and Mitchell, J. B. (1996) 'Chemical biology of nitric oxide: Regulation and protective and toxic mechanisms', in Stadtman, E.R. and Chock, P.B. (eds.) *Current Topics in Cellular Regulation*: Academic Press, pp. 159-187.

Winkler, M. S., Kluge, S., Holzmann, M., Moritz, E., Robbe, L., Bauer, A., Zahrte, C., Priefler, M., Schwedhelm, E., Böger, R. H., Goetz, A. E., Nierhaus, A. and Zoellner, C. (2017) 'Markers of nitric oxide are associated with sepsis severity: an observational study', *Critical Care,* 21(1), pp. 189.

Wintergerst, E. S., Jelk, J., Rahner, C. and Asmis, R. (2000) 'Apoptosis induced by oxidized low density lipoprotein in human monocyte-derived macrophages involves CD36 and activation of caspase-3', *European Journal of Biochemistry,* 267(19), pp. 6050-6059.

Wu, G. and Morris Jr, S. M. (1998) 'Arginine metabolism: nitric oxide and beyond', *Biochemical Journal,* 336(1), pp. 1-17.

Wu, H., Ye, H., Huang, R., Yi, C., Wu, J., Yu, X. and Yang, X. (2020) 'Incidence and risk factors of peritoneal dialysis-related peritonitis in elderly patients: A retrospective clinical study', *Peritoneal Dialysis International,* 40(1), pp. 26-33.

Wu, W., Geng, P., Zhu, J., Li, J., Zhang, L., Chen, W., Zhang, D., Lu, Y. and Xu, X. (2019) 'KLF2 regulates eNOS uncoupling via Nrf2/HO-1 in endothelial cells under hypoxia and reoxygenation', *Chem Biol Interact,* 305, pp. 105-111.

Xaus, J., Comalada, M., Valledor, A. F., Lloberas, J., López-Soriano, F., Argilés, J. M., Bogdan, C. and Celada, A. (2000) 'LPS induces apoptosis in macrophages mostly through the autocrine production of TNF-alpha', *Blood,* 95(12), pp. 3823-31.

Xiao, L., Ornatowska, M., Zhao, G., Cao, H., Yu, R., Deng, J., Li, Y., Zhao, Q., Sadikot, R. T. and Christman, J. W. (2012) 'Lipopolysaccharide-induced expression of microsomal prostaglandin E synthase-1 mediates late-phase PGE2 production in bone marrow derived macrophages', *PloS one,* 7(11), pp. e50244.

Xie, Y., Chen, H., Qu, P., Qiao, X., Guo, L. and Liu, L. (2022) 'Novel insight on the role of Macrophages in atherosclerosis: Focus on polarization, apoptosis and efferocytosis', *International Immunopharmacology,* 113, pp. 109260.

Xuan, C., Tian, Q.-W., Li, H., Zhang, B.-B., He, G.-W. and Lun, L.-M. J. E. j. o. p. c. (2016) 'Levels of asymmetric dimethylarginine (ADMA), an endogenous nitric oxide synthase inhibitor, and risk of coronary artery disease: A meta-analysis based on 4713 participants', 23(5), pp. 502-510.

Yamaguchi, T., Olozak, I., Chattopadhyay, N., Butters, R. R., Kifor, O., Scadden, D. T. and Brown, E. M. (1998) 'Expression of extracellular calcium (Ca2+ o)-sensing receptor in human peripheral blood monocytes', *Biochemical and biophysical research communications,* 246(2), pp. 501-506.

Yamanishi, Y. and Karasuyama, H. (2016) 'Basophils and mast cells in immunity and inflammation', *Seminars in Immunopathology,* 38(5), pp. 535-537.

Yang, H. Y., Bian, Y. F., Zhang, H. P., Gao, F., Xiao, C. S., Liang, B., Li, J., Zhang, N. N. and Yang, Z. M. (2015) 'LOX-1 is implicated in oxidized low-density lipoprotein-induced oxidative stress of macrophages in atherosclerosis', *Molecular Medicine Reports,* 12(4), pp. 5335-5341.

Ye, J., Coulouris, G., Zaretskaya, I., Cutcutache, I., Rozen, S. and Madden, T. L. (2012) 'Primer-BLAST: a tool to design target-specific primers for polymerase chain reaction', *BMC Bioinformatics,* 13, pp. 134.

Yona, S., Kim, K.-W., Wolf, Y., Mildner, A., Varol, D., Breker, M., Strauss-Ayali, D., Viukov, S., Guilliams, M. and Misharin, A. (2013) 'Fate mapping reveals origins and dynamics of monocytes and tissue macrophages under homeostasis', *Immunity,* 38(1), pp. 79-91.

Yurdagul, A., Jr., Doran, A. C., Cai, B., Fredman, G. and Tabas, I. A. (2017) 'Mechanisms and Consequences of Defective Efferocytosis in Atherosclerosis', *Front Cardiovasc Med,* 4, pp. 86.

Zajd, C. M., Ziemba, A. M., Miralles, G. M., Nguyen, T., Feustel, P. J., Dunn, S. M., Gilbert, R. J. and Lennartz, M. R. (2020) 'Bone marrow-derived and elicited peritoneal macrophages are not created equal: the questions asked dictate the cell type used', *Frontiers in Immunology,* 11, pp. 269.

Zanoni, I., Ostuni, R., Marek, L. R., Barresi, S., Barbalat, R., Barton, G. M., Granucci, F. and Kagan, J. C. (2011) 'CD14 controls the LPS-induced endocytosis of Toll-like receptor 4', *Cell,* 147(4), pp. 868-880.

Zhang, P., Xu, X., Hu, X., Wang, H., Fassett, J., Huo, Y., Chen, Y. and Bache, R. J. (2013) 'DDAH1 deficiency attenuates endothelial cell cycle progression and angiogenesis', *PLoS One,* 8(11), pp. e79444.

Zhang, Q., Xiang, L., Zaman, M. H., Dong, W., He, G. and Deng, G.-M. (2020) 'Predominant role of immunoglobulin G in the pathogenesis of splenomegaly in murine lupus', *Frontiers in immunology,* 10, pp. 3020.

Zhang, X., Zhang, M., Li, L., Chen, W., Zhou, W. and Gao, J. (2021) 'IRAK-M knockout promotes allergic airway inflammation, but not airway hyperresponsiveness, in house dust mite-induced experimental asthma model', *Journal of Thoracic Disease,* 13(3), pp. 1413.

Zhang, Y., Wang, J., Wang, W., Tian, J., Yin, K., Tang, X., Ma, J., Xu, H. and Wang, S. (2016) 'IL-17A produced by peritoneal macrophages promote the accumulation and function of granulocytic myeloid-derived suppressor cells in the development of colitis-associated cancer', *Tumor Biology,* 37(12), pp. 15883-15891.

Zhao, Y.-l., Tian, P.-x., Han, F., Zheng, J., Xia, X.-x., Xue, W.-j., Ding, X.-m. and Ding, C.-g. (2017) 'Comparison of the characteristics of macrophages derived from murine spleen, peritoneal cavity, and bone marrow', *Journal of Zhejiang University. Science. B,* 18(12), pp. 1055.

Zhu, Z. D., Ye, J. M., Fu, X. M., Wang, X. C., Ye, J. Y., Wu, X. R., Hua, P., Liao, Y. Q., Xuan, W. and Duan, J. L. (2019) 'DDAH2 alleviates myocardial fibrosis in diabetic cardiomyopathy through activation of the DDAH/ADMA/NOS/NO pathway in rats', *International Journal of Molecular Medicine,* 43(2), pp. 749-760.

Zsuga, J., Török, J., Magyar, M. T., Valikovics, A., Gesztelyi, R., Kéki, S., Csiba, L., Zsuga, M. and Bereczki, D. J. C. d. (2007) 'Serum asymmetric dimethylarginine negatively correlates with intima-media thickness in early-onset atherosclerosis', 23(5-6), pp. 388-394.

Zweier, J. L., Wang, P., Samouilov, A. and Kuppusamy, P. (1995) 'Enzyme-independent formation of nitric oxide in biological tissues', *Nat Med,* 1(8), pp. 804-9.